Asymmetric localization of Gurken protein and mRNA in the oocyte of *Drosophila melanogaster*

Door B.H.A Herpers

Asymmetric localization of Gurken protein and mRNA in the oocyte of *Drosophila melanogaster*
Herpers, Bram H.A.
Utrecht, Universiteit Utrecht, Faculteit Geneeskunde
Proefschrift Universiteit Utrecht, met een samenvatting in het Nederlands.

Printed by Digital Printing Partners Utrecht BV.

Asymmetric localization of Gurken protein and mRNA in the oocyte of *Drosophila melanogaster*

Asymmetrische lokalisatie van Gurken eiwit en mRNA in de oocyt van *Drosophila melanogaster*

(met een samenvatting in het Nederlands)

Proefschrift

ter verkrijging van de graad van doctor aan de Universiteit Utrecht
op gezag van de rector magnificus, prof.dr. W.H. Gispen,
ingevolge het besluit van het college voor promoties
in het openbaar te verdedigen op
dinsdag 12 december 2006 des ochtends te 10.30 uur

door

Bram Hubertus Anne Herpers
geboren op 4 april 1979 te Urmond

Asymmetric localization of Gurken protein and mRNA in the oocyte of *Drosophila melanogaster*
B.H.A. Herpers

Promotor:

Prof. Dr. J. Klumperman

Co-promotor:

Dr. C. Rabouille

Het verschijnen van dit proefschrift werd mogelijk gemaakt met financiële steun van ZonMw en de Dr. Ir. van de Laar Stichting.

You cannot
depend on your eyes
when your imagination
is out of focus

- Mark Twain

Asymmetric localization of Gurken protein and mRNA in the oocyte of *Drosophila melanogaster*
B.H.A. Herpers

Contents

Abbreviations

AP:	anterior-posterior
ATP:	adenosine triphosphate
BFA:	Brefeldin A
bcd:	*bicoid*
CGN:	cis Golgi network
COP (I or II):	coat protein complex
CPEB:	cytoplasmic polyadenylation element binding protein
DA:	dorso-anterior
DIG:	digoxygenin
DNA:	deoxyribonucleic acid
DV:	dorsal-ventral
eIF:	eukaryotic initiation factor
EM:	electron microscopy
ER:	endoplasmic reticulum
ERGIC:	ER to Golgi intermediate compartment (IC)
FISH:	fluorescent in situ hybridization
FRAP:	fluorescence recovery after photobleaching
GA:	glutaraldehyde
GDP:	guanosine diphosphate
GEF:	guanine exchange factor
GFP:	green fluorescent protein
grk:	*gurken*
GTP:	guanosine triphosphate
hnRNP:	heterogeneous nuclear ribonucleoprotein
IC:	intermediate compartment (VTC)
IEM:	immuno-electron microscopy
ISH:	in situ hybridization
ISH-IEM:	in situ hybridization combined with immuno-electron microscopy
LatA:	Latrunculin A
LE:	localization element
mRNA:	messenger RNA
MT:	microtubule
MTOC:	microtubule organizing centre
osk:	*oskar*
P-bodies:	Processing bodies
PABP:	poly(A) binding protein
PAG:	protein A gold complex
PFA:	paraformaldehyde
PP:	posterior pole

RNA:	ribonucleic acid
SB:	sponge bodies
SG:	stress granules
SRP:	signal recognition particle
tER:	transitional endoplasmic reticulum (ER exit site)
tER-Golgi unit:	unit composed of a transitional endoplasmic reticulum site and a Golgi stack
TGN:	trans Golgi network
TP:	transport particles
UTR:	untranslated region
VA:	ventral-anterior
VTC:	vesicular tubular cluster (IC)

CHAPTER 1

General Introduction

Outline:

1. The oogenesis in *Drosophila melanogaster*

Drosophila melanogaster is one of the major model organisms for development. Its short generation time (two weeks at 25°C), its limited number of chromosomes (4), and its well-described body pattern formation has allowed characterization of many genes required for its development (Struhl, 1989; Nusslein-Volhard, 1991; Wolpert, 1994). The sequencing of the whole *Drosophila* genome in 2000 (Adams et al., 2000), revealed that the 165 million bases making up the genome encode for roughly 13,000 genes. As my target in research, I will focus here on some of the genes that are important for the early stages in *Drosophila* development: the oogenesis.

1.1 The 14 developmental stages of the oocyte

Oogenesis takes place in the female gonads, called the ovaries. The ovaries harbour ovarioles that are strings of egg chambers of various developmental stages. Inside the egg chambers, the oocytes develop into the mature egg. This development has been divided into 14 developmental stages: stages 1-7 are called pre-vitellogenic, and 8-14 vitellogenic (Lasko, 1999).

1.1.1 Oocyte specification in the germarium: stage 1

The birthplace of an egg chamber is the germarium; here the germline is generated from the stem cell centre, where one stem cell divides four times by incomplete meiotic divisions to generate sixteen germ cells. These cells stay interconnected via cytoplasmic bridges, called ring canals (Spradling, 1993). Due to the way the germ cells have undergone division, two cells in the sixteen-cell cluster have four ring canals and will become the pro-oocytes.

These start to accumulate cytoplasmic factors, such as centrioles, from where microtubules nucleate and extend through the ring canals into the other fourteen cells. This organization of the microtubule cytoskeleton allows accumulation of other cellular components like mitochondria, mRNA and proteins into the pro-oocytes. This process is mediated by the action of the proteins Egalitarian (Egl) and Bicaudal D (BicD), which are cofactors of the Dynein motor complex (see part 3.4.2). They regulate the transport of the cellular components by accumulating in the pro-oocytes.

The pro-oocyte with the largest ring canal, ultimately receives most of BicD, Egl, and Orb (a cytoplasmic polyadenylation element binding protein that regulates mRNA translation). This pro-oocyte becomes the oocyte while the other reverts to the same fate as the other 14 germ cells, which become the nurse cells. The newly specified oocyte forms a clear microtubule organizing centre from where microtubules extend into the cytoplasm of all the nurse cells (Huynh and St Johnston, 2000).

Soon after oocyte specification, this oocyte starts to migrate to what will become the posterior of the egg chamber. In this posterior region of the germarium, the sixteen interconnected germ cells are enveloped by a monolayer of somatic follicle cells and the formation of a proper egg chamber is achieved (Figure 1A, Germarium).

1.1.2 Egg chamber formation: stage 2

At stage 2, the envelopment of the fifteen nurse cells and the specified oocyte by the follicle cells is completed. The resulting eggchamber stays attached with its anterior side to the posterior side of the germarium through a few stalk cells (Xi et al., 2003), derived from the follicle cells. This stalk (Figure 1A) is thought to be an other oocyte specifying factor (Torres et al., 2003).

From this stage on, the egg chamber starts to grow and the fifteen nurse cells begin

to replicate their DNA by repetitive S phases without intervening M phases (endoreplication), making them polyploid. They become very active in producing cellular components and sending them into the oocyte (Royzman et al., 2002). This delivery is mostly dependent on microtubule mediated transport through the ring canals (Theurkauf et al., 1992; Spradling, 1993). Some of the cargo that is delivered are the *bicoid*, *oskar* and *gurken* transcripts, encoding crucial factors for the further development of the oocyte (see parts 3.2, 3.2.2 and 1.2.1, respectively) (Lasko, 1999).

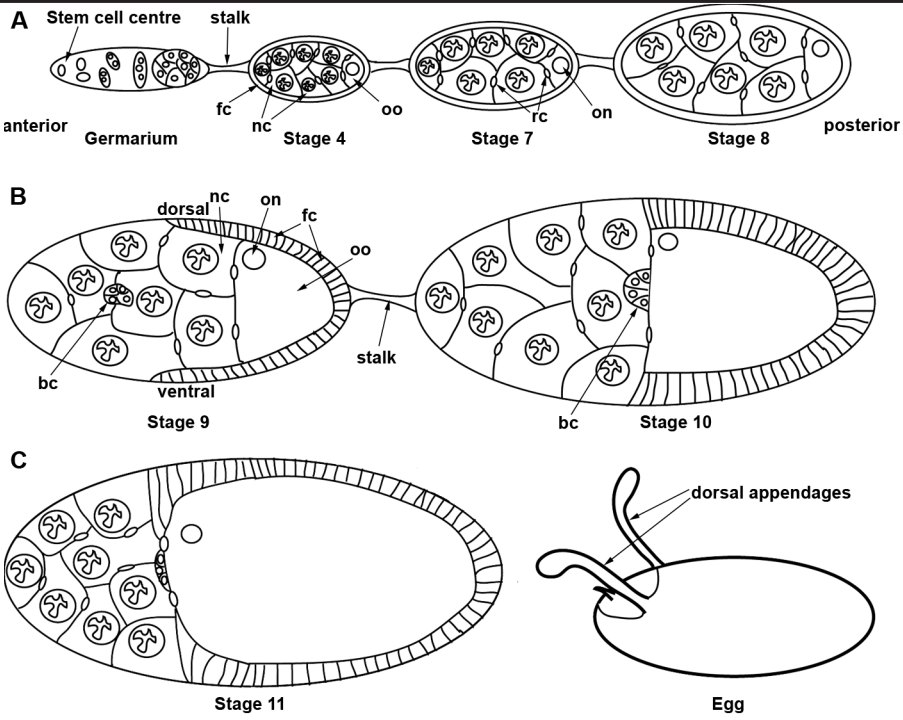

Figure 1. The 14 developmental stages of Drosophila oocytes.
*After oocyte specification at the end of the germarium **(A)**, the oocyte (oo) is located at the posterior of the egg chamber, connected via ring canals (rc) to the other 15 germ cells, the nurse cells (nc). These feed the oocyte during the developmental stages while being enveloped by a monolayer of somatic follicle cells (fc) that also interconnect the different stages via the formation of a stalk. The oocyte nucleus (on) is initially located at the posterior of the oocyte, but after anterior-posterior axis formation by Gurken secretion at the posterior, the oocyte nucleus moves towards the dorso-anterior corner, from where Gurken will signal for the second time **(B)**. This sets up the dorso-ventral axis. The follicle cells and the border cells (bc) start to migrate towards the posterior at stage 9 and will finally only surround the oocyte at stage 10. From stage 11 **(C)** the nurse cells massively empty their cytoplasmic contents into the oocyte and degenerate, while the follicle cells form a protective layer around the oocyte (chorion) and form the dorsal respiratory appendages. Redrawn from (Lasko, 1999).*

1.1.3 Anterior-Posterior body axis formation at stage 6-7

The eggchamber starts to grow and at stage 6 the oocyte nucleus is localized at the posterior of the oocyte (see Figure 2). This is also where *gurken* mRNA accumulates capping the oocyte nucleus and facing the plasma membrane, just underneath what will become the posterior follicle cells. From this posterior position, the oocyte secretes Gurken protein, a transforming growth factor alpha like peptide (Neuman-Silberberg and Schupbach, 1993) that binds to the *Drosophila* EGF-receptor Torpedo in the plasma membrane of the most adjacent follicle cells (Figure 2) where it induces a signalling cascade that leads to their adoption of a posterior (or terminal) follicle cell fate. This initiates the setting up of the anterior-posterior (AP) axis.

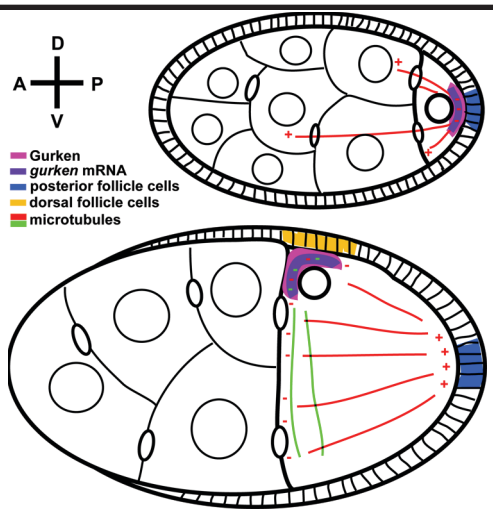

Figure 2: Gurken signaling.
At stage 6-7 Gurken is produced from the posterior localized gurken *mRNA. This specifies the overlying follicle cells to adopt a posterior fate, which initiates the setting up the anterior-posterior axis. At stage 9, Gurken is secreted at the dorso-anterior corner, where* gurken *mRNA is localized as a cap around the oocyte nucleus. The adjacent follicle cells become dorsal and this sets up the dorsal-ventral axis. D: dorsal, P: posterior, V: ventral, A: anterior.*

1.1.4 Dorsal-Ventral body axis formation at stage 8-10

As a consequence, these posterior cells produce of an unknown signal to the oocyte which leads to the depolymerization of the microtubule cytoskeleton and its repolymerization with a reverse orientation: Microtubules begin to nucleate from the anterior (Theurkauf et al., 1992). This new microtubule polarity results, at stage 8, in the migration of the oocyte nucleus from a posterior position towards the dorsal-anterior corner of the oocyte (Schupbach and Roth, 1994; Gavis, 1995) (Figure 1A, stage 8). It also affects the intracellular localization of several other transcripts: *bicoid* mRNA starts to accumulate at the anterior side of the oocyte, while *oskar* mRNA first localizes at the anterior before being restricted to the posterior pole. The localization of these two transcripts to opposite sides of the oocyte contributes to the establishment and maintenance of the anterior-posterior axis throughout oogenesis and embryogenesis (Huynh and St Johnston, 2004).

gurken mRNA, in contast, accumulates at the same site as the oocyte nucleus. This is followed by the secretion of Gurken protein, this time in the intercellular space between the oocyte plasma membrane and that of the follicle cells overlying the dorso-anterior corner where it induces their dorsal fate (Figure 2, stage 9). The detection of Gurken by the EGF-R in the follicle cells leads to a repression of Pipe, a sulfotransferase that leads to preventing the nuclear entry of Dorsal, a NF-kappaB-like transcription factor. In turn, this prevents the follicle cells from entering their default ventral fate (Roth, 2003). The dorsalized follicle cells will ultimately form the dorsal respiratory appendages at the final stages of oocyte development (see section 1.1.5).

This setting up of the dorsal side of the oocyte by Gurken during stage 8-10 (with a peak at stage 10a) leads therefore to the formation of the second body axis: the dorso-ventral (DV) axis (Neuman-Silberberg and Schupbach, 1993; Neuman-Silberberg and Schupbach, 1996).

1.1.5 Completion of oogenesis: stage 10-14

At stage 8, the eggchamber has entered the vitellogenic stages during which the follicle cells secrete yolk in the intercellular space between the oocyte and the follicle cells. The oocyte takes up the yolk via endocytosis and stores it in large yolk granules in its cytoplasm until utilization during embryogenesis, to allow growth.

During stage 9, follicle cells start to migrate posteriorly over the surface of the germ cells and finally at stage 10, most face the oocyte. A small group of border cells pass through three nurse cell junctions to arrive at the anterior end of the oocyte at stage 10 (Figure 1B). The anterior localized follicle cells at the oocyte-nurse cell transition then migrate inwards to meet the anterior localized border cells (centripetal migration) (Horne-Badovinac and Bilder, 2005).

Around stage 11, the nurse cells, that get separated from the oocyte, quickly empty their cytoplasmic content into the oocyte, so the oocyte undergoes a rapid ten-fold increase in size (Figure 1C). At stage 12, the follicle cells have covered the entire oocyte and the nurse cells degenerate, and by stage 13, the follicle cells have completed the secretion a protective layer around the oocyte, the chorion. The chorion is made up out of three layers: the vitelline envelope, the endochorion, and the exochorion (French et al., 2003). A subset of these follicle cells undergoes morphogenesis to generate the dorsal appendages, specialized structures that facilitate gas exchange in the developing embryo. With this the egg formation is complete at stage 14 (Figure 1C, Egg).

1.2 The role of Gurken in the oocyte development

1.2.1 Identification of the *gurken* gene

As I have described above, Gurken protein secretion is essential for the setup of both the AP and the DV axes. The identification of Gurken started with an ethyl-methanesulfonate (EMS) mutagenic screen on the second chromosome for genes affecting the patterning of the follicular and embryonic epithelium. EMS is an alkylating agent that creates deletions and mutations in the DNA, leading to random mutations along the length of the chromosome (Schupbach, 1987).

Mutations in the *gurken* gene resulted in eggs that lacked the dorsal respiratory appendages and embryos showed a reduction of the cells specified to become the dorsal side. It was therefore proposed that *gurken* encodes a factor that induces a dorsal fate, and loss of Gurken leads to ventralization.

The ventralization phenotype was phenocopied by mutations in the *torpedo* gene. However, meticulous comparison of the *gurken* and *torpedo* mutant phenotypes revealed that *gurken* was not required in the somatic cells, while *torpedo* was not required in the germ cells. This suggested that Gurken was expressed in the germline whereas Torpedo was expressed in the somatic follicle cells during oogenesis (Neuman-Silberberg and Schupbach, 1993).

Cloning and sequence comparison of these two proteins showed that Gurken encodes a TGF-alpha like protein, whereas Torpedo encodes an EGF-like-receptor. Data suggested that Gurken could be the ligand for Torpedo. Gurken was ultimately shown to be secreted by the oocyte and to bind to Torpedo in the follicle cells (Neuman-Silberberg and Schupbach, 1994).

The function of the *gurken* gene in the induction of the dorsal side of the future embryo was analysed at both RNA and protein level. By cloning the *gurken* mRNA and producing an antisense nucleotide sequence, an RNA *in situ* hybridization could be performed to detect the transcript that exhibited a specific and restricted location in the oocyte. It was exclusively found

at the dorso-anterior (DA) corner of the oocyte, as a cap over the oocyte nucleus (Neuman-Silberberg and Schupbach, 1993), thus confirming that *gurken* mRNA is exclusively expressed by the oocyte.

This was validated by the production of a Gurken specific antibody, which showed that Gurken protein was also restricted to the DA corner at the intercellular space between the oocyte plasma membrane and this of the follicle cells covering the DA corner (Neuman-Silberberg and Schupbach, 1996), where it can be received by the EGF receptor, Torpedo.

1.2.2 Gurken is a secreted protein and requires processing in the exocytic pathway

Gurken showed homology to TGF-alpha and it was predicted to harbour a transmembrane domain, therefore involving the exocytic pathway in the *Drosophila* oocyte for its deposition at its final destination.

Although the transmembrane domain is present in the newly synthesized Gurken (the ER form), it is not present in the final secreted peptide, because Gurken is proteolytically processed during its transport through the exocytic pathway. Analogous to Spitz, a second EGF-R ligand in *Drosophila*, which is cleaved by the serine protease Rhomboid-1 in the Golgi, Gurken was also shown to be cleaved, but by Rhomboid-2 (Guichard et al., 2000; Urban et al., 2001; Ghiglione et al., 2002; Urban et al., 2002). Recently, it was elegantly shown that this cleavage takes place in the ER, not in the Golgi, as previously anticipated (Bokel et al., 2006).

The function of a transmembrane domain (that is cleaved just after synthesis) in Gurken secretion was tested by stably expressing a construct that lacked both the cytoplasmic tail and the transmembrane domain. This produces only a luminal fragment, mimicking, at least theorically, the secreted Gurken peptide (Queenan et al., 1999). However, the expression of this luminal peptide did not rescue the loss of Gurken function in a *gurken* null mutant. Although the mRNA was still properly localized to the DA corner, the synthesis of this Gurken peptide was not restricted to the DA corner and it was present all over the oocyte, later shown to be the ER pervading the entire cell. The transmembrane domain is therefore required for proper exit of the newly synthesized Gurken protein out of the endoplasmic reticulum (ER, see part 2) (Queenan et al., 1999). This ER exit involves the cargo receptor Cornichon (Roth et al., 1995; Bokel et al., 2006). It was shown that without functional Cornichon, Gurken is unable to reach the plasma membrane (see part 2.4.1). This indicated that sorting events in the exocytic pathway mediate the correct asymmetric secretion of Gurken at the DA corner.

However, in the case of Gurken, these sorting events have to be coupled to its RNA localization. The first question I address in this thesis related to Gurken protein is to understand how a transmembrane/secreted protein can be deposited in an asymmetric fashion from its asymmetric mRNA, taken into account that it must utilize the cellular exocytic pathway. In other words, I will examine how a cell couples the mRNA localization to the organization of its exocytic pathway. For this, I need to describe this organization in the *Drosophila* oocyte. Therefore, I will introduce what is known on this pathway in the context of my question.

2. The exocytic pathway

2.1 Introduction

The exocytic (or secretory) pathway comprises a series of distinct membrane-bound compartments that functions to synthesize, modify, process and sort luminal and transmembrane proteins and lipids destined to the plasma membrane, the extracellular medium and the compartments of the exocytic and endocytic pathway.

In the early exocytic pathway, which is composed of the endoplasmic reticulum (ER), the transitional ER (tER), the ER-to-Golgi intermediate compartment (ERGIC or IC) and the Golgi apparatus (Allan and Balch, 1999), newly synthesized proteins enter the secretory route. Here proteins are glycosylated, some get cleaved or lipid modified, which will/can enhance their sorting and function (Guy, 2000; Lee et al., 2001; Anderson et al., 2002; Gusarova et al., 2003). By default, this pathway mediates the trafficking of proteins from intracellular to extracellular (anterograde transport), and by doing so, proteins finally arrive at the trans Golgi network (TGN), which makes up the late exocytic pathway (Orci et al., 1987; Tekirian, 2002). Here, proteins are sorted to the correct intracellular compartments or extracellular regions.

Along this exocytic pathway, some transmembrane and luminal proteins are ensured that these are retained or recycled in the correct compartment (retrograde transport). These retention/recycling sites are the tER and IC, the Golgi and the TGN. The sorting of anterograde from retrograde cargo in the early exocytic pathway is mediated by COPII and COPI coated vesicles, for instance at the tER, where anterograde cargo receptors select their cargo for packaging into COPII coated vesicles and COPI coated vesicles fuse to re-target retrograde cargo into the ER.

At the late exocytic pathway, cargo is targeted to the endocytic compartments (endosomes and lysosomes) dependent or independently of the mannose-6-phosphate receptor (MPR) (Ni et al., 2006) and recycled via the retromer (Seaman, 2004). The targeting to the endocytic compartments is out of the scope of this thesis and will not be discussed further. Other anterograde cargo that is destined to the plasma membrane, is sorted at the TGN into pleiomorphic vesicles that require the exocyst complex to finally fuse with the plasma membrane (Hsu et al., 2004; Ponnambalam and Baldwin, 2003).

2.1.1 The entry site for proteins into the exocytic pathway: the Endoplasmic Reticulum (ER)

The ER is a single-lumen membrane-bound organelle that pervades in a maze-like fashion the entire cell (Bobinnec et al., 2003; Levine and Rabouille, 2005). This vast organelle comprises discrete subdomains, that are morphologically distinct but continuous: the rough ER (RER), the smooth ER (SER) and the nuclear envelope (Voeltz *et al*., 2002). The attachment of ribosomes in progress of translation determines the morphology of the RER, this is where synthesis of transmembrane and luminal proteins takes place (Figure 3).

All protein translation initially starts in the cytoplasm, but proteins destined for the exocytic pathway contain a signal sequence (Blobel and Dobberstein, 1975). This is recognized by the signal recognition particle (SRP) (Walter and Blobel, 1980; Martoglio and Dobberstein, 1998). This targets the nascent peptide via the SRP receptor (Meyer and Dobberstein, 1980; Walter and Blobel, 1981) to the translocon complex or Sec61 complex that functions as a gate for newly synthesised transmembrane and lumenal proteins into the secretory pathway.

The nascent protein translocates into the ER lumen (Deshaies and Schekman, 1987;

Rothblatt et al., 1989; Swanton and Bulleid, 2003), is immediately bound by chaperones such as BiP (Alder et al., 2005; Wickner and Schekman, 2005), starts to fold and undergoes O- and N-linked glycosylation by ER resident enzymes (Ernst and Prill, 2001; Dempski and Imperiali, 2002; Helenius and Aebi, 2004).

C-tail anchored proteins are the few exceptions to the translocon-mediated membrane insertion. These proteins are synthesized and released in the cytosol before being inserted into the ER membranes via a hydrophobic C-terminal domain. These proteins will mostly function at the cytosolic face of the membranes they are bound to (Borgese *et al*., 2003). A couple of the best examples are the SNAREs (soluble N-ethyl maleimide sensitive factor attachment protein receptors) involved in vesicle fusion (Rothman, 1994; Salaun et al., 2004) and the Golgi localized protein Giantin (Linstedt et al., 1995).

2.1.2 The exit from the ER: the transitional ER (tER) sites

After the folding and ER-related modifications have been completed, the newly synthesized proteins leave the ER (Feldman et al., 1987; Swanton and Bulleid, 2003; Helenius and Aebi, 2004; van Anken and Braakman, 2005). The exit from the ER occurs at specific subdomains, which are known as ER exit sites (Cole et al., 1996; Tang et al., 2005) or transitional ER (tER) sites (Bevis et al., 2002; Kondylis and Rabouille, 2003). By morphology, these tER sites were defined by the absence of ribosomes (Orci *et al*., 1991) and by the formation of COPII-coated vesicles (Barlowe et al., 1994; Barlowe, 1995) that carry proteins from the ER towards the Golgi (Figure 3, green vesicle coat).

The COPII coat complex was initially described in yeast cells in a screen for proteins that affected protein secretion (Novick *et al*., 1980). This screen revealed a core complex composed of one transmembrane component (Sec12) and a set of at least 5 cytosolic components, which is conserved from yeast through man (Sar1, Sec23, Sec24, Sec13 and Sec31). The components of the COPII coat complex can be used as molecular markers to define the tER sites (Klumperman, 2000). This revealed that cargo, which started its life in the ER, gets concentrated in these sites, and gets packaged into a ~60nm wide COPII coated vesicle that buds from the ER (Zeuschner et al., 2006).

The formation of a COPII coat occurs in a stepwise fashion: first, the transmembrane Guanine Exchange Factor (GEF) Sec12 concentrates at the tER sites where it converts cytosolic Sar1-GDP to Sar1-GTP to promote tER-association of Sar1. This in turn recruits the hetero-dimeric complex Sec23-Sec24. This recruitment is mediated by binding of Sar1-GTP to Sec23, while Sec24 serves as a cargo-selector for different transmembrane proteins. Through the subsequent recruitment of the other hetero-dimeric complex Sec13-Sec31, polymerization of the coat and membrane curvature is induced and vesicle budding can occur. Subsequent COPII coat disassembly is then induced by the GTPase-activation function of Sec23. This is promoted by membrane curvature by the binding of the Sec13-Sec31 complex and leads to the hydrolysis of Sar1-GTP by Sec23, leaving uncoated transport vesicles (Antonny and Schekman, 2001; Bonifacino and Glick, 2004).

Although the components for COPII coat formation are conserved in evolution, the number of tER sites differs per species. For instance, tissue cultured mammalian cells such as HeLa cells can display about 200 small tER sites (Hammond and Glick, 2000). In contrast, the yeast *Pichia pastoris* has only 2-5 tER sites at steady state (Rossanese et al., 1999) and there are about 20 in *Drosophila* S2 cells (Kondylis and Rabouille, 2003).

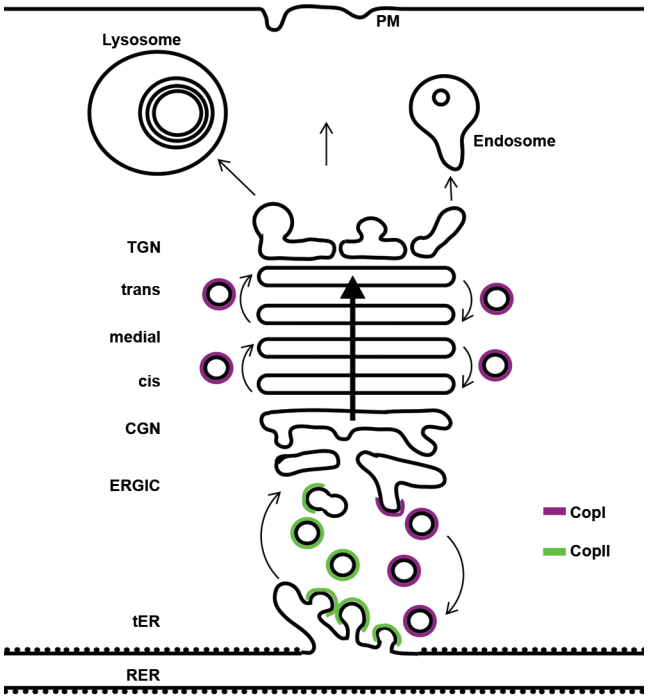

Figure 3: The exocytic pathway.
Upon synthesis by ribosomes attached to the ER, transmembrane and luminal proteins can be selectively sorted into transitional ER sites (tER). Here, the secretory cargo is packaged into COPII coated vesicles (green) which transport the cargo anterograde into the ER-to-Golgi intermediate compartment (ERGIC). Here function COPI coated vesicles (purple) to redirect mislocalized proteins back to the ER. The ERGIC forms or fuses with the cis-Golgi network (CGN). The cargo is further transported in the Golgi via the cis-, medial-, and trans-cisternae, while guided by COPI vesicles, towards the trans-Golgi network (TGN), where the cargo is selectively recruited into carriers that take the cargo to its destination, which can be for instance lysosomes, endosomes and plasma membrane (PM). Redrawn from various manuscripts.

2.1.3 The ER to Golgi intermediate compartment (ERGIC)

Once packaged into COPII vesicles, the cargo moves to the next compartment of the exocytic pathway, a separate compartment between the ER and the Golgi (Martinez-Menarguez et al., 1999), called the ER-to-Golgi intermediate compartment (ERGIC), reflecting its morphology and its position in the exocytic pathway. The ERGIC forms from the COPII buds from the ER, either by homotypic fusion of uncoated COPII vesicles or by fusion to an existing ERGIC (Figure 3) (Rabouille and Klumperman, 2005).

The ERGIC is very closely opposed to the tER sites, and is thought to be the place where COPII vesicles are replaced by COPI vesicles (Figure 3, purple coated vesicles) (Aridor et al., 1995; Bannykh et al., 1998; Klumperman et al., 1998; Appenzeller et al., 1999; Klumperman, 2000; Ben Tekaya et al., 2005; Appenzeller-Herzog and Hauri, 2006). While COPII coated vesicles function in the anterograde transport, COPI coated vesicles function in the retrograde transport of proteins (Lavoie et al., 1999; Lee et al., 2004; Antonny et al., 2005).

The small GTPase Arf1 (ADP ribosylation factor 1) mediates initiation of the COPI coat. When this protein is associated with the membrane it recruits seven other coat subunits (α-, β-, β′-, γ-, δ-, ε- and ζ-COP) (Duden, 2003). This type of vesicular transport allows retrograde transport from the IC back to the ER of misplaced ER-targeted proteins, like for instance the

KDEL-receptor or proteins containing a di-lysine motif (Cosson and Letourneur, 1994; Orci et al., 1997). By bringing the ER-destined cargo selectively back to the ER, the IC actually becomes concentrated with anterograde cargo.

The ERGIC shows a similar intracellular distribution as the many tER-sites in mammalian cells (Hammond and Glick, 2000; Stephens et al., 2000). However, unlike the tER-sites, intermediate compartments show fast microtubule-dependent movement within the cell (Presley et al., 1997; Scales et al., 1997) to take cargo from peripheral tER-sites to the centrally localized Golgi apparatus. Therefore the intermediate compartment has not been identified in cells with no central Golgi organization (Rossanese et al., 1999; Glick, 2000; Kondylis and Rabouille, 2003). In these cells, the tER sites are closely opposed by the Golgi stacks and therefore have no need for long ER to Golgi transport and moving intermediate compartments (see part 2.5.1).

2.1.4 The Golgi apparatus: a polarized stack

From the intermediate compartment, the newly synthesized proteins reach the Golgi apparatus. The Golgi apparatus consists of a series of flattened membrane-bound compartments, the cisternae, that are closely apposed to each other and aligned in parallel to form a stack (Rabouille et al., 1995; Farquhar and Palade, 1998; Ladinsky et al., 1999; Shorter and Warren, 2002). Each side of the Golgi stack is apposed by a tubular-vesicular network. The cis-Golgi network (CGN) is closest to the tER sites and this is where the anterograde cargo will enter the Golgi (Figure 3). At the other end lies the trans Golgi network (TGN), the site where the exocytic cargoes will be sorted to their final destination (Traub and Kornfeld, 1997). Each of the cisternae contains a different set of enzymes and proteins (Nilsson et al., 1993). The existence of these functionally distinct cisternae gives a polarized organization to the Golgi, allowing the distinction of cis-, medial- and trans-Golgi cisternae (Figure 3) (Ladinsky et al., 1999).

In mammalian cells, the multiple Golgi stacks are laterally interconnected, resulting in a single-copy reticulum, the Golgi ribbon (Novikoff et al., 1971; Rambourg et al., 1974). The Golgi ribbon has a very characteristic subcellular localization. It is capping the nucleus with its most *trans* cisternae close to the microtubule organizing centre (MTOC). This relationship is highly relevant as drug-mediated depolymerization of microtubules showed that the organization of the Golgi ribbon is dependent on microtubules (Sandoval et al., 1984; Kreis, 1990; Cole et al., 1996).

Although the stacked Golgi organization has been conserved throughout eukaryotic evolution, the Golgi ribbon seems to be a unique feature of the mammalian cells. In plants, yeast and *Drosophila* the Golgi appears in discrete Golgi stacks dispersed throughout the cytoplasm (Rossanese et al., 1999; Kondylis and Rabouille, 2003; Neumann et al., 2003) and there is no particular spatial relationship with the MTOC (Kondylis et al., 2006).

2.2 Protein modification in the exocytic pathway

Upon entry of the secretory pathway proteins start to undergo modifications that influence their folding, transport and function. One of the most characteristic modifications that occur in the secretory pathway is glycosylation. Mono- or oligo-saccharides can be attached to asparagine (N-linked glycosylation) or to serine/threonine residues (O-linked glycosylation). N-linked glycosylation starts upon translocation in the ER lumen and continues in the Golgi, and O-linked glycosylation occurs post-translationally by sequential addition of sugar residues

in different levels of the secretory pathway (Kornfeld and Kornfeld, 1985; Verbert et al., 1987; Parodi, 2000; Ernst and Prill, 2001; Munro, 2001).

Another type of modification that influences the function of transmembrane and luminal proteins is cleavage. Cleavage by proprotein convertases, such as rhomboids (serine proteases), or furin (a paired basic amino acid cleaving enzyme) is important as the cleaved product might be involved in many crucial cellular processes (Stawowy and Fleck, 2005). Cleavage is often used to activate precursor proteins. For instance, early in the secretory pathway, pro-insulin is produced by cleavage of prepro-insulin (Halban, 1991) by signal peptide peptidases (Okun and Shields, 1992; Martoglio, 2003). The finally secreted insulin must be cleaved from pro-insulin by PC2 (Furuta et al., 1998), which starts in the TGN and is completed in the secretory granules (Steiner and James, 1992).

The rhomboids are intramembrane proteases that have been shown to cleave all the TGF-alpha homologues, Spitz, Keren and Gurken in *Drosophila* (Urban et al., 2002). These transmembrane proteins are cleaved in the exocytic pathway, releasing a bioactive luminal peptide that is finally secreted in the extracellular medium.

Other types of modification are sulfation and lipid modification. Respectively, these represent the permanent addition of a sulphate group to newly synthesized proteins that influences the biological activity (Huttner, 1988; Luders et al., 2003) and the addition of hydrophobic moieties to proteins. Lipid modifications are required to increase or restrict the range of Hedgehog, Wnt and EGF-R ligands, proteins that induce concentration-dependent responses (Miura and Treisman, 2006).

2.3 Transport through the early exocytic pathway

The modifications are taking place while the proteins are transported from one compartment to the next, including the different cisternae of the Golgi. However, it is still a debate on how proteins move through the early exocytic pathway in an anterograde direction. Two models have been proposed: the cisternal maturation model and the stable compartments model (Glick and Malhotra, 1998; Pelham and Rothman, 2000; Kartberg et al., 2005; Rabouille and Klumperman, 2005).

The maturation model predicts that the cargo moves in an anterograde fashion by remaining within the same cisterna that matures from cis to trans while resident enzymes move in a retrograde fashion (Bonfanti et al., 1998; Mironov et al., 2001). The stable compartments model states that the cisternae are stable compartments containing a stable set of resident proteins and receive cargo by COPI vesicle-mediated transport (Orci et al., 1989; Rothman and Orci, 1990) moving from cisterna to cisterna in an anterograde fashion.

At the heart of this debate are the COPI vesicles. There is no definitive answer to which direction these vesicles carry their cargo, from cis to trans, the reverse or both (Figure 3) (Rabouille and Klumperman, 2005). However, recently two studies strongly indicated that the maturation of Golgi citernae is taking place, at least, in yeast (Losev et al., 2006; Matsuura-Tokita et al., 2006). By following in time early and late cisternae by tagging the one with green markers and the other with red, both groups found that the early cisternae at some point turned from green to yellow and finally red, indicating that the early cisterna had matured into a late cisterna by acquiring the late cisternal marker.

Although this maturation model seems to be the most likely way for cargo transport through the Golgi, this debate has also raised the question of how the Golgi apparatus acquires and maintains its complex stacked organization. Two models exist: the *de novo* formation model and the Golgi matrix model (Wells, 2001; Lowe, 2002; Shorter and Warren, 2002).

The *de novo* formation model is the direct outcome from the cisternal maturation model and proposes that COPII coated vesicles that bud from the tER sites have the capacity to fuse and self-assemble into the new cisterna. This new cisterna would stack to the cis cisterna that would in turn mature into the medial, etc.

All the cargo derived from the ER then cooperates to determine the functional and architectural features of the Golgi (Glick, 2002; Altan-Bonnet et al., 2004; Altan-Bonnet et al., 2006). This model is supported by the fact the Golgi enzymes recycle to the ER. This is clearly evidenced after treatment with the fungal metabolite Brefeldin A (BFA) (Lippincott-Schwartz et al., 1989; Puri and Linstedt, 2003), or by the block of ER export by dominant-negative mutants of Sar1 (Seemann et al., 2000; Prescott et al., 2001). In both cases, the stacked Golgi architecture disappeared. By allowing the cargo to exit the ER (for instance by BFA washout) the Golgi recovers its typical architecture. This therefore suggested that ER export is essential for Golgi biogenesis, suggesting that ER-derived vesicles have the capacity to form a Golgi apparatus.

The Golgi matrix model proposes that a template or matrix exists to guide the assembly of the Golgi. This model is supported by the discovery of the Golgi matrix proteins (Cluett and Brown, 1992; Slusarewicz et al., 1994). These proteins peripherally interact with the Golgi membranes and each other, this interaction is important to maintain the stacked Golgi morphology (Short et al., 2001; Shorter and Warren, 2002; Diao et al., 2003; Kondylis et al., 2005). The matrix model is supported by the fate of the Golgi during mitosis: it disassembles into clusters of tubules and vesicles that contain Golgi enzymes and matrix proteins that do not redirect to the ER during mitosis (Seemann et al., 2002; Pecot and Malhotra, 2004). These clusters are thought to facilitate the inheritance of the Golgi, and upon completion of mitosis the Golgi can regain its stacked organization by the presence of the matrix proteins that serve as a scaffold (Shima et al., 1997; Shorter and Warren, 2002).

2.4 Protein sorting in the exocytic pathway

Although very interesting, the way by which cargo moves through the exocytic pathway and the mode of Golgi assembly are out of the scope of this thesis and will not be discussed further. Instead, I focus here on the function of the exocytic pathway to sort and transport transmembrane and luminal proteins to the plasma membrane or the intercellular space, while sending others to other destinations such as the endocytic system and retaining the exocytic pathway-resident proteins in their proper compartments.

2.4.1 Sorting at tER sites

There are multiple sorting stations along this pathway, the first one being at the tER sites where anterograde cargo is recruited into the COPII coated vesicles. In general, the COPII component Sec24 itself initiates the sorting. It has three cargo-binding domains, each with its own cargo preference (Miller et al., 2005a; Mossessova et al., 2003). Furthermore, four Sec24 isoforms exist in mammalian cells (Roberg et al., 1999; Tang et al., 1999; Kurihara et al., 2000).

The specific sorting of anterograde cargo is reinforced by the multitude of different cargo receptors interacting with the COPII machinery (Bonifacino and Glick, 2004). These are for instance (soluble) cargo selectors such as ERGIC-53 (a lectin, recognizes high mannose sugar structures) (Schweizer et al., 1990; Appenzeller et al., 1999), members of the p24 family EMP24p and ERV25p (Barlowe, 1998), the multiple-span protein Erv29p (Belden and Barlowe, 2001; Otte et al., 2001), and many more, reviewed in (Otte et al., 2001). The specificity of these cargo receptors is mediated by their recognition of ER export signals encoded by the cargo. These export signals are found in the cytoplasmic portion of the cargo proteins, which are either di-acidic motifs or di-hydrophobic motifs (Barlowe, 2003).

An important cargo receptor to sort Gurken out of the ER is Cornichon (Roth et al., 1995; Bokel et al., 2006). Its yeast homologue, Erv14p, specifically recruits Axl2p from the ER into COPII vesicles (Powers and Barlowe, 1998). In *Drosophila*, Cornichon interacts with a domain at the end of the luminal portion of Gurken (towards the N terminus). Cornichon is recruited in the COPII complex and Gurken is efficiently exported. This export to the Golgi occurs after the transmembrane domain has been removed by rhomboid-mediated cleavage (Bokel et al., 2006).

2.4.2 Sorting at the Golgi apparatus

This wide array of cargo selectors allows the specific recruitment of anterograde cargo into the ERGIC. Here, ER resident proteins are recycled to the ER via COPI (Stephens et al., 2000) and anterograde cargo is targeted to the Golgi. Once at the Golgi, the sorting of different groups of anterograde and retrograde cargo continues. The CGN and the cis-Golgi cisternae display similar functions to the ERGIC: sorting retrograde cargo and cargo receptors back for recycling. While cargo moves anterograde, the COPI vesicles mediate the recycling of cargo receptors and Golgi enzymes between the Golgi stacks (Short and Barr, 2000; Duden, 2003).

2.4.3 Sorting at the TGN

When the cargo has finally arrived at the trans-Golgi cisternae and the TGN, active sorting mechanisms sort lysosomal enzymes from plasma membrane targeted proteins and sort constitutively secreted proteins from regulated proteins (Rodriguez-Boulan and Musch, 2005). The sorting takes effect by packaging into distinct vesicular or tubular carriers by recruiting distinct coats and adaptor molecules that allow specific transport to the final destination (Gu et al., 2001; Gleeson et al., 2004).

In polarized cells that display an apical/basolateral polarity such as Madine-Darby canine kidney (MDCK) cells (cultured mammalian epithelial cells very often used as a model system), the TGN functions to sort apical from basolateral targeted plasma membrane proteins. The specificity for either destination is determined by factors, such as a polarized cytoskeleton and sorting signals, amongst which tyrosine- or dileucine-based amino acid motifs, lipid affinities and cytosolic protein interactions (Ikonen and Simons, 1998).

In this apico-basal specific sorting, the different lipid composition of the apical and basal membrane domains also plays an important role. This is based on the observation that many apically destined proteins accumulated in microdomains composed of glycosphingolipids and cholesterol (lipid rafts) in the Golgi complex. These rafts might then serve as sorting platforms to be incorporated into the transport intermediates that shuttle these apical destined proteins to the apical plasma membrane (van Meer and Simons, 1988; Ikonen and Simons, 1998; Rodriguez-Boulan and Musch, 2005).

2.5 The exocytic pathway in *Drosophila*

2.5.1 The organization of the exocytic pathway

The Golgi apparatus is only a single copy organelle in mammalian cells. In *Drosophila*, the Golgi stacks remain discrete in the cytoplasm but they are always found in close proximity to a tER site (Kondylis and Rabouille, 2003) thus forming a tER-Golgi unit, a name that has been proposed for a similar organization in *Pichia pastoris* (Mogelsvang et al., 2003). In *Drosophila* S2 cells, the number of tER sites is restricted and constant (around 20).

There is a close resemblance of the organization of the *Drosophila* exocytic pathway with this of mammalian cells treated with microtubule-depolymerizing drugs. This treatment leads to disassembly of the Golgi ribbon and redistribution of Golgi stacks throughout the cytoplasm but directly opposing a tER-site (Rogalski and Singer, 1984; Cole et al., 1996; Hammond and Glick, 2000), thus mimicking tER-Golgi units.

In contrast, microtubule-depolymerizing drugs do not affect the Golgi function and organization in *Drosophila* S2 cells (Kondylis et al., 2006). In the developing *Drosophila* embryo, nevertheless, the microtubule network seems to be very important for cellularization, which is the individualization process of the nuclei in the late syncitial embryo. This happens by membrane addition at the apical side of the syncitial cells. The newly formed plasma membrane will finally enclose each individual nucleus. The embryo achieves this by actively moving the tER-Golgi units from the core of the embryo to the apical side where these will contribute to the cellularization process (Papoulas et al., 2005).

The exocytic pathway in the oocyte has a similar setup as in the S2 cells. The Golgi stacks are found in close proximity to tER-sites. These tER-Golgi units are dispersed throughout the cytoplasm of the oocyte (Figure 4), and their number has been estimated to one thousand, which gives a similar density per volume of cytoplasm as in S2 cells. This study is part of **chapter 2**, in which we investigated the restricted deposition of Gurken into the intercellular space between the oocyte and the overlying follicle cells at the dorso-anterior corner and investigated how this restricted secretion is achieved by the exocytic pathway of the oocyte.

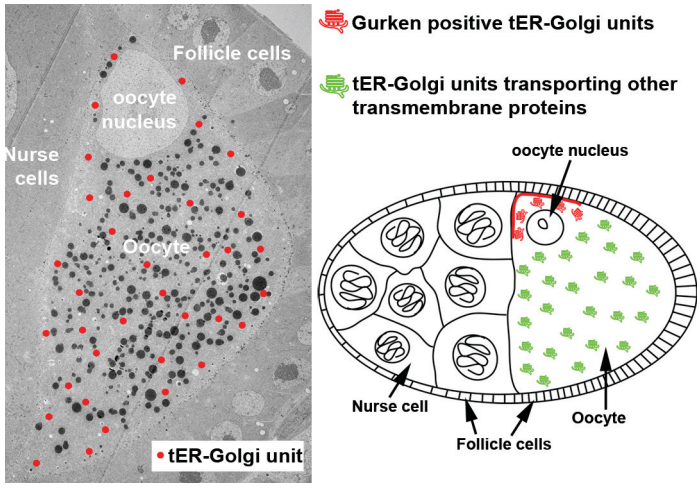

Figure 4: The organization of the exocytic pathway in the Drosophila oocyte.
The exocytic pathway in the stage 9 oocyte is composed of about one thousand tER-Golgi units that are scattered throughout the oocyte. Only those at the dorso-anterior corner as a cap over the oocyte nucleus are positive for Gurken (red), while all tER-Golgi units (red and green) are capable to transport transmembrane proteins.

2.5.2 How is the polarized deposition of Gurken achieved in such an exocytic pathway?

The question left pending at the end of part 1 of my introduction was to understand how a transmembrane/secreted protein can be deposited in an asymmetric fashion from the translation of its asymmetric mRNA, while requiring an exocytic pathway.

In polarized cells, the apico-basolateral sorting of plasma membrane proteins occurs post-translationally. Analogous to other polarized cells, the DA corner should then be considered as the apical side of the oocyte, which is supported by the presence of the microtubule organizing centre (MTOC) at this corner (Januschke et al., 2006). We have seen earlier (part 2.4.1) that Gurken sorting to the DA corner in the oocyte indeed occurs in the exocytic pathway, however mainly at the ER and the tER sites (**chapter 2**) and not at the TGN as polarized proteins in MDCK cells.

Considering the organization of the exocytic pathway in the oocyte, comprising many dispersed tER-Golgi units, it is difficult to reconcile the restricted Gurken deposition with this scattered organization if we would not take into account that its mRNA is also localized. So I propose that in addition to post-translational sorting of Gurken, a pre-translational sorting mechanism exists that relies on the localization of *gurken* mRNA at the DA corner. In **chapter 2**, we demonstrate that the *gurken* mRNA localization allows the utilization of only a subset of tER-Golgi units for Gurken transport, the nearest to the mRNA wherever the mRNA is localized in the oocyte, thus coupling mRNA localization and anterograde transport in the exocytic pathway.

We also conclude that the tER-Golgi units function independently of each other; while some, those at the DA corner, sort and transport Gurken, others, situated at different locations in the oocyte, transport different transmembrane proteins such as Yolkless.

3. RNA localization

We have discussed above that the site of Gurken synthesis and deposition relies on where its mRNA is localized. In the third part of the introduction, I will introduce different aspects of the RNA biology that are important to understand the localization of *gurken* mRNA.

Research into the nature, function and localization of mRNAs is a well-studied topic. Why there is so much interest in RNA can be explained from its characteristics and functions within the cell. Messenger RNAs are the information shuttling from nucleus to cytoplasm, the means to initiate and control gene expression. The expression of a given mRNA in a tissue or cell can reveal the function of that tissue. mRNA expression is often linked to protein expression, since the primary fate of most mRNAs is to be translated. But in certain cases, the mRNA is localized, stored, repressed or even degraded and sometimes never translated.

Here, I will describe these different aspects and I will focus on the different factors that influence mRNA localization and regulation processes, which are often linked to the formation of different cytoplasmic structures that function to control these alternative fates (see part 4).

3.1 Birth and use of mRNA

3.1.1 Transcription

mRNAs are the transcription products of genes in the nucleus. The onset of RNA production is mediated by the recruitment of RNA polymerase to the activated gene, which makes a transcript (mRNA) of the DNA sequence. After transcription, this RNA sequence is edited. This means that the introns in the gene sequence that were transcribed into the RNA sequence are cleaved out and the exons are connected (by the Exon Junction Complex) to produce the mRNA sequence that can be translated into a protein sequence (Aguilera, 2005). Translation always starts at the start codon (the triplet sequence AUG, coding for a Methionine). The RNA sequence upstream the AUG sequence is called the 5′ untranslated region (5′UTR) and the RNA sequence downstream of the stop codon is called the 3′UTR. Furthermore, all newly produced mRNAs are equipped with a poly(A)-tail at the 3′end of the transcript and with a 7-methyl-guanosine (m^7GpppN) (or analogous) cap structure at its 5′end (Mignone *et al.*, 2002). The poly(A)-tail and the cap structure influence the stability and fate of the mRNA in the cytoplasm (Drummond et al., 1985; Piccioni et al., 2005). After completion, the mRNA is exported into the cytoplasm via the nuclear pore complex (Cole and Scarcelli, 2006), a multifaceted process that I will not describe here.

3.1.2 Translation and regulation

The primary fate of a given mRNA is to be translated. Translation is initiated by the binding of eukaryotic initation factor 4E (eIF4E) to the cap structure at the 5′end of the mRNA. This recuits eIF4G, that in turn recruits a translation complex composed of translation factors (eukaryotic initation factors), poly(A) binding protein (PABP) and the ribosomal subunits (Pelletier and Sonenberg, 1987; Hershey, 1990; Gebauer and Hentze, 2004). These factors allow translation by circularization of the mRNA (Figure 5A) (Wells et al., 1998).

For translation to be initiated, the transcript must be circularized. Impairment of this circularization or the formation of the translation complex can lead to translation repression. In many cases, eIF4E-binding proteins (4E-BPs) are inhibitory proteins that downregulate the availability of eIF4E for binding to the cap structure (Figure 5C) (Raught and Gingras, 1999).

Whether an mRNA is translated is also dependent on the length of the polyA-tail.

Some mRNAs contain a cytoplasmic polyadenylation element (CPE) (Mendez and Richter, 2001). The CPE is bound by phosphorylated CPEB, a protein that recruits CPSF (cleavage and polyadenylation specificity factor), which initiates binding of poly(A) polymerase required to elongate the polyA tail at the 3'end of the transcript. This long polyA tail is then bound by PABP, which can interact with eIF4G. Together with eIF4E, this leads to the circularization of the transcript (Figure 5B) (Piccioni et al., 2005). However, when CPEB is not phosphorylated, it still binds to the CPE and then acts as a repressor of translation by its interaction with Maskin. Maskin then binds to eIF4E and inhibits binding of eIF4G, leading to translation repression (Figure 5D) (Stebbins-Boaz et al., 1999).

Similar translation regulating principles are found in *Drosophila*. For instance Bicoid protein acts as a repressor for *caudal* mRNA in the embryo. By binding to sequences in the 3'UTR of *caudal* and to eIF4E, formation of the translation complex is inhibited, and anterior expression of Caudal prevented (Figure 5E) (Niessing et al., 2002). *oskar* mRNA is regulated by the binding of Cup to eIF4E, and of Bruno, which binds to the Bruno recognition elements (BRE) in its 3'UTR (Figure 5F) (Chekulaeva et al., 2006).

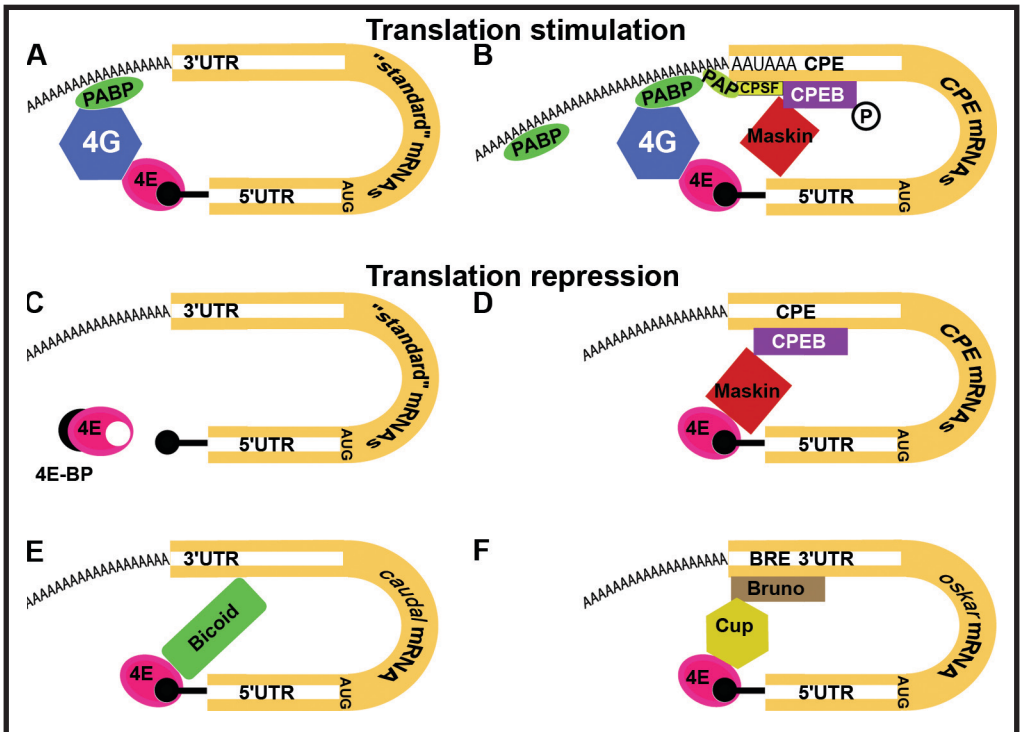

Figure 5: Modes of translational regulation.
(A-B) *The interaction of eIF4E with eIF4G that binds to the poly(A) binding protein (PABP) promotes circularization and translation of eukaryotic mRNAs.* ***(B)*** *Translation in cytoplasmic polyadenlyation element (CPE) containing mRNAs is regulated by the binding of CPEB, which, when phosphorylated, allows the binding of cleavage and polyadenylation specificity factor (CPSF). This factor recruits the poly(A) polymerase (PAP) that elongates the poly(A) tail and thereby allows PABP to bind the mRNA.*
(C) *"Standard" mRNAs can be repressed by the inhibitory proteins eIF4E-binding proteins (4E-BP).*
(D) *Translation of CPE containing mRNAs is not only stimulated by CPEB, but also repressed, when CPEB is not phosphorylated. This then interacts through Maskin with eIF4E, and this blocks translation initiation.*
(E) *Bicoid interacts with the 3'UTR of the* caudal *mRNA sequence and with eIF4E to inhibit translation initiation.*
(F) oskar *mRNA is regulated by the binding of Cup to eIF4E and to Bruno that recognizes the Bruno Response Elements (BRE) in the 3'UTR of* oskar *mRNA. Redrawn after (Piccioni et al., 2005).*

3.1.3 Degradation

After being translated, the transcript can enter another (delayed) round of translation, or it is degraded. In eukaryotes, degradation takes place in cytoplasmic structures called processing bodies (P-bodies) (see also part 4.3 of this introduction) (Coller and Parker, 2005). The onset of degradation is the removal of the translation complex and shortening of the poly(A)-tail by poly(A) ribonuclease activity. Thereby PABP is unable to bind to the poly(A) tail and the eIF4E-eIF4G complex is destabilized. This allows the binding of eIF4E-transporter to eIF4E, which targets the mRNA to the P-bodies (Andrei et al., 2005).

This eIF4E-eIF4E-transporter complex interacts in the P-bodies with decapping enzymes (Parker and Song, 2004) that act to cleave the 5'end cap structure, so the RNA sequence becomes available for 5'-> 3' exonucleases to degrade the mRNA.

3.2 Mechanisms of RNA localization

Among the many RNAs synthesized, a number of them are localized in a restricted fashion to contribute to efficient protein sorting and localization. In mammalian neurons for instance, ~400 mRNAs are specifically localized to the dendrites (Eberwine et al., 2001) and in *Drosophila* about 10% of randomly selected mRNAs localize anteriorly in the oocyte (Dubowy and Macdonald, 1998). There are two important reasons for a cell to localize its proteins through mRNA localization:

1. to ensure that a protein can be expressed at the correct site, and
2. to control protein expression at specific regions of its cytoplasm (St Johnston, 2005).

The asymmetric localization of *actin* mRNA in migrating fibroblasts is one of the best examples. The localization of this mRNA contributes to polarization of the actin cytoskeleton (Condeelis and Singer, 2005). In the *Drosophila* embryo, restricting cytoplasmic determinants such as Bicoid protein through localizing the *bicoid* mRNA to the anterior, ensures head development (Ephrussi and St Johnston, 2004). Signal transduction in neurons is also dependent on asymmetric mRNA localization (Palacios and St Johnston, 2001). And as we have seen above, *gurken* mRNA localization dictates Gurken protein secretion to the proper site in the *Drosophila* oocyte (Neuman-Silberberg and Schupbach, 1993).

Asymmetric mRNA localization is achieved by one of the four generalized mechanisms: 1. Local RNA synthesis from the nucleus; 2. Diffusion and anchoring; 3. Local protection from degradation and 4. Active transport (St Johnston, 2005). The cell might however not strictly follow one of these mechanisms and use any combination, in place or time.

3.2.1 Local RNA synthesis from the nucleus

Localization of the mRNA can be regulated by the local synthesis by the nucleus. When the nucleus is asymmetrically localized in a cell, it can contribute to the transcript synthesis in a restricted region of the cell and create a local pool of these mRNAs.

When a cell is multinucleated such as mammalian myofibres, multiple nuclei are dispersed in its cytoplasm. In the myotubes, some nuclei are located just underneath the synapse where the neuronal bouton makes contact to the myotube (Burden, 1993). Only these nuclei produce transcripts that encode proteins that are involved in the signal transduction cascade, in particular plasma membrane targeted receptors.

In the *Drosophila* oocyte, the nucleus is asymmetrically localized. It would be tempting to think that *gurken* mRNA achieves its asymmetric distribution because it is synthesized by

this nucleus. However, this is not likely to be the case since the oocyte nucleus is in profase I of meiosis and therefore thought transcriptionally inactive (Spradling, 1993), plus that the accumulation of *gurken* mRNA at the DA corner is independent of the ability of the oocyte nucleus to produce *gurken* mRNA. This was elucidated by germline clones of eggchambers composed of nurse cells bearing the wildtype *gurken* gene and a *gurken* null mutant oocyte (Caceres and Nilson, 2005).

The nucleus itself might also be polarized. For example, in the unicellular flagellated alga *Chlamydomonas reinhardtii* the nucleus is located close to the attachment site of the two flagellae (Colon-Ramos *et al*., 2003). When this alga looses its flagellae, it initiates their regrowth by localizing the *alpha-2-tubulin* mRNA into the main cell body, where the ribosomes are located. To achieve this specific localization, the alga closes all the nuclear pores other than those facing the ribosome pool.

3.2.2 Diffusion and anchoring

As explained above, after release from the nucleus, mRNAs can diffuse through the cytoplasm. By trapping these diffusing transcripts by a localized anchor, these mRNAs can become localized. This trapping, or anchoring, is mostly mediated by a protein that recognizes the mRNA (an RNA binding protein) that has somehow achieved an asymmetric distribution within the cell. The anchoring can also be mediated by cytoskeletal elements and proteins, such as Dynein that can bind to the microtubule cytoskeleton (Claussen and Suter, 2005). For instance, the formation of the pole plasm in *Drosophila* (that will define the germline in the future embryo) relies on the trapping of the transcripts for *nanos*, *germ cell-less* and *Cyclin B* at the posterior of the late oocyte. This trapping is achieved by the actin cytoskeleton or by polar granules (Raff et al., 1990; Jongens et al., 1992; Forrest and Gavis, 2003) that are formed earlier during oocyte development, through local translation of *oskar* mRNA at the posterior pole (Ephrussi et al., 1991). Cytoplasmic flows induced by other intracellular transport mechanisms might facilitate the diffusion and anchoring of these transcripts to the pole plasm (Forrest and Gavis, 2003).

3.2.3 Local protection from degradation

mRNA binding proteins do not only mediate mRNA anchoring or mRNA translation, but proteins might also specifically bind to mRNA to target it for degradation (Fillman and Lykke-Andersen, 2005). By activating the degradation mechanism at all sites within the cell where a given mRNA is not required or wanted, while protecting this mRNA from degradation at the site where it is required, a cell can ensure the local availability of that mRNA. This mechanism has been shown for restricting the localization of *hsp83* mRNA to the posterior pole of the *Drosophila* egg (Ding *et al*., 1993). This dual protection/degradation mechanism is mediated by two distinct sequences in the 3'UTR of the transcript: one to protect and stabilize the *hsp83* mRNA at the posterior pole, and one to specifically degrade the transcript in other regions of the embryo.

3.2.4 Active transport: Cytoskeleton mediated transport and anchoring

The cytoskeleton mediated RNA localization has been the most studied so far. This mechanism is dependent on an intact microtubule or actin cytoskeleton, along which the RNA is actively transported via specific motors and finally anchored at the target sites.

Movement can occur in different directions, via different motors. The three main classes of motors are myosins, dyneins and kinesins. Myosins move along actin filaments, dyneins move towards the minus-end of microtubules and kinesins towards the plus-end of microtubules. This active transport of mRNAs via motors along cytoskeletal filaments has been implicated as the major localization mechanism in most cells (Lopez and Jansen, 2004) and is detailed below.

3.3 Actin based mRNA localization

Actin based mRNA localization is dependent on the myosin motor complex. This motor moves along the actin microfilaments in an ATP dependent fashion at speeds around 0.4μm/sec and is used to transport RNA-protein complexes (comprising mRNA, effector proteins and RNA binding proteins) (Lopez and Jansen, 2004).

The best described example is found in budding yeast *S. cerevisiae* with the localization of *ASH1* mRNA into the bud tip via the She1p/She2p/She3p complex (Bertrand et al., 1998; Bohl et al., 2000; Long et al., 2000; Niessing et al., 2004). The RNA binding protein She2p binds to *ASH1* mRNA in the nucleus, which docks via the adaptor protein She3p onto She1p, the yeast myosin-V (Myo4p), which sorts it to the bud tip. This motor complex is involved in the localization of at least 22 different mRNAs into the bud (Shepard et al., 2003).

Interestingly, the cargo bound to the yeast myosin-V, acts as a modulator of the motor activity and its retention at the bud tip (Kruse et al., 2002). This suggests that the motor does not transport its cargo at random, but that the nature of the RNA-protein complexes regulates it.

Myosin II has been shown to transport *beta-actin* mRNA to the leading edge of fibroblasts and in neuronal cells (Latham et al., 2001). In the nucleus, ZBP1 (zipcode-binding protein-1) specifically binds to two target sequences in the *beta-actin* mRNA, called the zipcode (Kislauskis et al., 1994; Zhang et al., 2001). This complex is exported to the nucleus, where it recruits Myosin II, that transports the *beta-actin* mRNA to the newly forming protrusions at speeds up to 0.6 μm/sec (Oleynikov and Singer, 2003). During this transport, the translation of *beta-actin* mRNA is inhibited. At the destination, ZBP1 is phosphorylated by the protein kinase Src. This allows spatial and temporal control of *beta-actin* mRNA translation (Huttelmaier et al., 2005).

3.4 Microtubule based mRNA localization

Microtubules form a polarized network within the cell emanating from the microtubule organizing centre: the MTOC. Here, the minus-ends of the microtubules concentrate, and the plus-ends of the microtubules grow outwards. In polarized epithelial cells for instance, the microtubules align along the plasma membrane with the minus-ends at the apical site where the MTOC is found, and the plus-ends toward the basal domain (Musch, 2004). This organization is implicated in the maintenance of the apico-basal polarity.

The MTOCs in syncitial blastoderm embryos of *Drosophila* are also localized apically. From here microtubules nucleate and extend around the nuclei into the cytoplasm. This apical localization of the MTOCs allows microtubule minus-end directed transport of pair-rule transcripts to the apical cytoplasm (Davis and Ish-Horowicz, 1991; Wilkie and Davis, 2001). In neuronal cells, the minus ends are focused in the soma (cell body) and the plus-ends extend into the axon and the dendrites, allowing directional transport from the soma into the dendrites and axons (Job and Eberwine, 2001; Smith, 2004).

The transport of intracellular organelles, proteins and mRNAs along the microtubule network requires two distinct motor complexes: kinesins and dyneins. Kinesins are preferential plus-end directed motors, while dyneins move cargo towards the minus-end of microtubules and the MTOC (Goldstein and Yang, 2000).

3.4.1 The Kinesins

In mammals more than 40 kinesin-related proteins have been identified (Miki et al., 2001). Kinesins are composed of two heavy chains (KHC) and two light chains (KLC), which generate force via ATP-hydrolysis (Vale et al., 1985; Brady, 1985).

Kinesin-mediated transport of mRNAs is especially important in neurons, where the dendritic localization of the mRNAs require plus-end directed transport along microtubules. This is the case for myelin basic protein (*MBP*) mRNA (Smith, 2004; Carson et al., 1997), calcium/calmodulin-dependent kinase-2α (*CamKIIα*) mRNA (Blichenberg et al., 2001), microtubule associated protein 2 (*MAP2*) (Blichenberg et al., 1999) and also *beta-actin* mRNA (Bassell et al., 1998). By localizing mRNAs in the dendrites, kinesin can contribute to synaptic plasticity (Huang et al., 2003) and to synaptic strength (Giustetto et al., 2003; Miller et al., 2005b) by controlling the amount of mRNA localized and thereby controlling the availability of mRNAs to be translated upon extracellular cues.

Kinesin-mediated transport is also used in the *Drosophila* oocyte to localize *oskar* mRNA to the posterior pole of the oocyte (Brendza et al., 2002; Januschke et al., 2002).

3.4.2 Dynein

Cytoplasmic dynein is a large, mega-dalton-sized multicomponent motor complex that moves towards the minus-end of microtubules in an ATP hydrolysis dependent fashion (Mizuno *et al*., 2004). The Dynein motor complex is composed of two ~520 kDa subunits, Dynein heavy chains (Dhc), which have a globular head structure, a stalk and a stem. The stalk binds to the microtubules, while the stem is bound to the other components of the motor complex. These are Dynein intermediate chain (Dic), Dynein light intermediate chain (Dlic), and a number of different homologues of Dynein light chain (Dlc), such as Roadblock, LC8 and Tctex-1 (Figure 6A) (Sakato and King, 2004). The nature of the light chains seems to be tissue specific (Susalka et al., 2000).

The activity of the Dynein motor complex is regulated by the multi-subunit complex dynactin (Figure 6B). For instance, the dynactin subunit p150^{Glued} can induce long-range movement of cytoplasmic Dynein along microtubules (Schroer, 2004). The activity of the motor complex is furthermore regulated by Lissencephaly-1 (Lis-1), a WD40-domain containing protein that is required for neuronal migration, nuclear postitioning and regulation of the ATPase activity of Dhc (Swan et al., 1999; Faulkner et al., 2000; Claussen and Suter, 2005; Mesngon et al., 2006). Bicaudal D (BicD) and Egalitarian (Egl) also function to control the activity of the Dynein motor. Egl binds with its C-terminus to Dlc and its N-terminus to BicD (Navarro et al., 2004), which in turn can bind to the dynactin subunit dynamitin (Hoogenraad et al., 2001; Hoogenraad et al., 2003). This connection of the Dynein motor complex to dynactin is thought not only to influence cargo selectivity, but also the functionality of the Dynein motor.

Dhc, BicD and Egl are required for apical localization of *wingless* and the pair-rule transcripts in the embryo, and accumulate apically together with these mRNAs when injected into the embryos (Bullock and Ish-Horowicz, 2001; Wilkie and Davis, 2001; Navarro et al., 2004;

Delanoue and Davis, 2005). These mRNAs move apically at speeds of 0.5µm/sec, a speed that is reduced by injection of inactivating anti-Dhc antibodies, and in *Dhc* hypomorphic mutants (Wilkie and Davis, 2001). Similar to the activity of the Myo4p/She1p motor in yeast, the activity of the Dynein motor is postulated to be regulated by the nature of its cargo (Bullock et al., 2003). That is, as was shown for *hairy* mRNA localization in the embryo, mRNAs containing a localization sequence more efficiently recruit the Dynein motor complex than RNAs in which the localization sequence is mutated, and surprisingly, also move faster.

RNA transport by the Dynein motor complex is also important in the *Drosophila* oocyte. The organization of the microtubule cytoskeleton in the germ cells in the previtellogenic eggchamber is organized by the MTOC which is situated near the oocyte nucleus. From here, microtubules extend through the ring canals into the nurse cells with their plus-ends (Figure 2). A number of mRNAs, such as *bicoid*, *K10* and *gurken* mRNA are produced in the nurse cells and transported into the oocyte, a process that, similar to the pair-rule transcripts, requires the function of BicD, Egl and Dhc (Huynh and St Johnston, 2000; MacDougall et al., 2003).

Recently, Dynein was also found to be involved in the anchoring of mRNAs at its destination. Dhc, Egl and BicD not only just move together with pair-rule transcripts to the apical side, but their localization there perdures, suggesting a role in anchoring (Bullock and Ish-Horowicz, 2001; Bullock et al., 2003; Delanoue and Davis, 2005). Furthermore, interference with anti-Dhc antibodies leads to the loss of RNA anchoring. However, this anchoring appeared to be independent of the motor activity of Dhc and inactivation of Egl after anchoring did not lead to loss of anchoring (Delanoue and Davis, 2005). Therefore their model proposed that Dhc makes a switch from a molecular motor to a stable anchor upon delivery of its cargo at the end of microtubules.

The proposed functional switch of Dhc also seems to be happening for *gurken* mRNA localization in the oocyte. The role of Dynein in the transport and the anchoring of *gurken* RNA within the oocyte is the subject of **chapter 4** of my thesis.

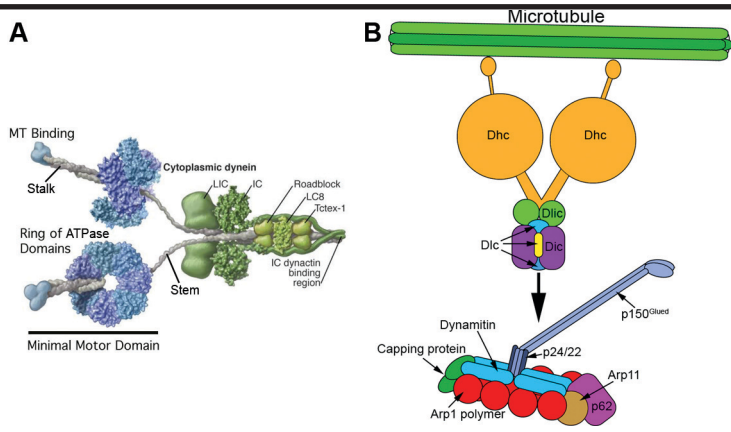

Figure 6: Cytoplasmic dynein and dynactin.
(A) *Structural representation of cytoplasmic dynein. The globular head domain of Dhc is composed of are ring of ATPase domains that connect via the stalk to the microtubule (MT) binding domain and via the stem to the other components of the motor: Dlic (LIC), Dic (IC) and the different Dlc homologues such as Roadblock, LC8 and Tctex-1. Picture originates from* valelab.ucsf.edu/research/ res_mec_dynein.html.
(B) *Schematic representation of the interaction of cytoplasmic dynein with the dynactin complex. While Dynein binds with one end to the microtubules, the Dic subunit interacts with the dynactin subunit p150Glued, which connects via p24/22 to Dynamitin. This connects to the Arp1 rod of the dynactin complex, which is composed of the Arp1 polymer, capping proteins, Arp11 and p62 and other proteins that function together in cargo binding. Composed from* ***(A)*** *and (Schroer, 2004).*

3.5 Factors that determine the intracellular localization of transcripts

The way an mRNA is sorted by one of the above-described mechanisms depends on localization signals intrinsic to the mRNA, the *cis*-acting factors, and on the proteins that interact with the mRNA, the *trans*-acting factors. Together these function as "zipcodes" and "postage stamps" to get the message delivered (Chabanon et al., 2004).

3.5.1 Cis-acting factors: specific RNA sequences

The cis-acting factors can be stretches of sequences within the mRNA itself, and a secondary structure adopted by the mRNA. The 3' untranslated region (3'UTR) is found between the stop-codon and the 3'end of the mRNA sequence. In many localized transcripts, the 3'UTR defines or influences the intracellular fate of the mRNA. For instance, adding the 3'UTR of *beta-actin* mRNA to a normally non-localized reporter leads to localization of that reporter identical to where the *beta-actin* RNA normally localizes to (Kislauskis et al., 1993). The 3'UTR of *oskar* mRNA contains several 100-200 nucleotide regions that act in different steps in its posterior localization in the *Drosophila* oocyte (Kim-Ha et al., 1993). In neurons, *MBP* mRNA also contains multiple regions within its 3'UTR to determine its final localization, an RNA transport sequence and an RNA localization region (Ainger et al., 1997).

However, not all transcripts localize via the 3'UTR. The localization element (LE) for *gurken*, *yemanuclein-α* and *ASH1* mRNA for instance, involves also their 5'UTR or the coding region itself (Capri et al., 1997; Gonzalez et al., 1999; Thio et al., 2000). These localization elements can either be specific nucleotide sequences that are recognized by specialized proteins (trans acting factors) or structural elements like stem-loop structures, which are recognized by other trans acting factors. The stem-loop structures are formed by base-pairing of intrinsic complementary nucleotide sequences of the mRNA, which produces stretches of double stranded mRNA. The formation of stem-loop structures has been implicated in the localization of many *Drosophila* transcripts (Van de Bor and Davis, 2004). One of the first stem-loop sequences identified were these of *K10* and *orb* mRNA, that form a similar hairpin structure that is interchangeable and indispensable for the sorting of these mRNAs (Cohen et al., 2005).

Similarly important are the stem-loop sequences found in *hairy* mRNA for apical localization in the *Drosophila* embryo and the anterior localization of transcript for *bicoid* in the oocyte; their localization was shown not only to be sequence specific, but also dependent on the secondary structure imposed by that sequence (Ferrandon et al., 1997; Bullock et al., 2003). These LE define the region of the cell where a transcript is localized: for instance *oskar* mRNA that is normally sorted to the posterior pole of the oocyte, gets localized anteriorly when it is fused to the 3'UTR of *bicoid* mRNA (Ephrussi and Lehmann, 1992).

Furthermore, localization sequences may converge during evolution and thereby use the same localization machinery: the *Drosophila* specific retrotransposon called *I-factor*, follows the exact same transport route as *gurken* mRNA to the DA corner, due to structural similarity of the *I-factor* and *gurken* localization sequences (Van De Bor *et al*., 2005).

3.5.2 Trans acting factors: proteins that bind mRNAs

In the part 3.1, I have introduced the translation initiation and regulation machinery for mRNAs. It is now clear from experimental evidences that while certain mRNAs are being localized, their translation is en route being regulated by some of these proteins that act as trans acting factors (Kindler *et al*., 2005).

The transport process itself and the final anchoring of mRNAs is regulated by other trans acting factors. These factors bind to the cis-acting elements and these interactions often start in the nucleus. A large family of these nuclear-acquired factors are the hnRNPs (heterogeneous nuclear ribonucleoproteins), proteins that bind to mRNA sequences and can shuttle between the nucleus and the cytoplasm (Shyu and Wilkinson, 2000).

Once in the cytoplasm, these hnRNPs control the localization of the bound mRNA. For instance, the *X. laevis* hnRNP I, VgRBP60, binds to the 3'UTR of *Vg1* mRNA and moves together with it and finally colocalizes with it at the vegetal pole of the oocyte (Cote et al., 1999). The mammalian hnRNP-A2 mediates the localization of *MBP* mRNA in neurons via binding to specific A2 response elements (A2RE) in the *MBP* sequence and thereby specifies this mRNA to be localized into the dendrites (Munro et al., 1999). In *Drosophila*, Squid, a homologue of hnRNP-A1, is involved in the localization of *gurken* and *oskar* mRNA to the DA corner and the posterior pole respectively (Norvell et al., 1999; Norvell et al., 2005).

Staufen, a double-stranded RNA binding protein (dsRBP), shows affinity for stem-loop sequences in transcripts (Ramos et al., 2000). It has initially been identified to play a role in the localization of transcripts such as *bicoid* and *oskar* in *Drosophila* (St Johnston et al., 1991; Ferrandon et al., 1997; Li et al., 1997). Staufen homologs have also been described in neurons, *X. laevis* and zebrafish (Krichevsky and Kosik, 2001; Allison et al., 2004; Bateman et al., 2004). Staufen has been shown to travel together with localized mRNAs. The function of Staufen is to control the localization of mRNAs in two ways. It targets the recognized mRNA to microtubules for transport (Ferrandon et al., 1994), and it mediates in the anchoring of its target mRNAs at their specific destination (Micklem et al., 2000; Allison et al., 2004).

CamKIIα mRNA and *BC1* RNA are two examples of neuronal transcripts that are Staufen-dependent for their dendritic localization (Krichevsky and Kosik, 2001; Thomas et al., 2005). This localization takes place in large Staufen and mRNA positive macromolecular complexes that are transported along microtubules by kinesins, the neuronal granules (see part 4.2) (Hirokawa, 2006). During transport, the present mRNAs are kept translationally inactive. This is aided by *BC1* RNA, which is a special type of RNA that does not code for a protein but it is involved in translation regulation of other mRNAs during transport. This function of *BC1* mRNA is conveyed by the interaction with Fragile X mental retardation protein (FMRP), which is an RNA binding protein that targets *BC1* RNA onto target mRNAs. The formation of this complex then leads to inhibition of the assembly of the translation initiation complex (Wang et al., 2002; Zalfa et al., 2005). This shows that also RNAs can function as trans acting factors to regulate the fate of other mRNAs.

Another example of a translation regulator in neuronal granules is Zipcode Binding Protein 1 (ZBP1) which binds to *beta-actin* mRNA via specific sequences at the 3'UTR (Ross et al., 1997; Huttelmaier et al., 2005). During transport to the peripheral sites of actin polymerization, ZBP1 represses the translation of its associated transcripts. When *beta-actin* mRNA reaches the periphery of the cell, ZBP1 is phosphorylated by Src, which destabilizes ZBP1 binding to *beta-actin* mRNA, and this allows synthesis of beta-actin protein (Huttelmaier et al., 2005).

This shows that trans acting factors not only control the fate of mRNAs, but may also act to gather more mRNAs together in particles to increase the efficiency of transport or to create a local mRNA pool. This is for instance exemplified by Bruno, a translation repressor for *gurken* and *oskar* mRNA. Bruno has been shown to be able to oligomerize into large 50S-80S silencing particles (Chekulaeva et al., 2006) that mediate *oskar* mRNA transport.

4. RNA particles, granules and bodies: function and formation

The research on RNA localization has not only led to the identification many of the factors described above, but also to the understanding that RNAs do not move as single molecules or in small complexes, but in large particles that are indentifiable by light microscopy (Anderson and Kedersha, 2006). RNA has been shown to be localized in cytoplasmic granules, made up of mRNAs and proteins. This has become a large topic of research, as these granules were not only related to mRNA transport, but also in other regulation mechanisms, such as posttranscriptional silencing, protection and decay. Here I will introduce the various RNA granules found in eukaryotic cells, together with what is known or thought about their function.

4.1 RNA granules

RNA granules are found in many types of organisms and tissues where they are given different names. In germ cells, they are called germinal granules in *X. laevis*, polar granules in *Drosophila* or P-granules in *C. elegans*. In somatic cells RNA granules are called stress granules and processing (P-) bodies. In neurons they are termed neuronal granules.

RNA granules differ in size, from small (100nm) to very large (several microns). Furthermore, different types of RNA granules might exist next to each other, and the composition of a granule may even change during the lifetime of the RNA granules (Kress *et al*., 2004).

Generally speaking, these granules are important for transport and posttranscriptional regulation of gene expression. RNA granules can contain ribosomal subunits, translation factors, helicases, decay enzymes and RNA binding proteins (Anderson and Kedersha, 2006), depending on their function. Some types of granules are mobile, other remain at their site of formation. Some form *de novo* in the cytoplasm, whereas others start their lifetime in the nucleus and then end up in the cytoplasm. There is therefore a large variability that I will describe below.

4.2 Neuronal granules: mRNA transport

Neurons use neuronal granules to transport mRNAs from the soma into the dendrites. Inside these granules the mRNAs are kept translationally silent until their deposition at the destination or stimulation by exogenous stimuli (Krichevsky and Kosik, 2001). In addition to mRNAs, these granules contain small and large ribosomal subunits, translation initiation factors and mRNA binding proteins that regulate the mRNA, suggesting that at some point the mRNAs are translationally active, and they move into the dendrites via kinesins (Kanai et al., 2004; Hirokawa and Takemura, 2005).

More than 20 dendrite-localized mRNAs have been identified to be localized and transported in neuronal granules (Smith, 2004), among which *CamKIIα*, *MAP2*, *beta-actin* and *BC1* mRNA. *CamKIIα* and *MAP2* mRNA are translationally regulated by CPEB (cytoplasmic polyadenylation element binding protein, see 3.1.2). This translational regulation is important for the dendritic localization. Overexpression of CPEB enhances this localization and loss-of-function mutations reduce it. CPEB furthermore co-immuno-precipitates with both Dynein and Kinesin, which shows the potential bi-directional movement of the RNA granules (Wu et al., 1998; Mendez and Richter, 2001; Huang et al., 2003). These opposite directed motors cause oscillatory movement of the particles, although a fraction also shows unidirectional movement at speeds up to 0.2μm/sec (Rook et al., 2000; Kanai et al., 2004). This direct link between translation regulation and transport proves that change inducing environmental cues (for instance phosphorylation of CPEB) can control the site of mRNA localization and thus protein

expression.

4.3 Processing bodies: storage and degradation

Stress induces the formation of two types of granules, stress granules (see next section) and processing bodies. To relieve stress situations, mRNAs might be temporarily stored or specifically degraded. mRNA degradation is mediated by exonucleases. These RNA degrading enzymes are not present throughout the cytoplasm, but show a focal distribution in the cell. These focal areas are the processing (P-) bodies (Bashkirov et al., 1997; Eystathioy et al., 2003; Sheth and Parker, 2003), uniform spheroid particles that increase in size and number in response to stress (Kedersha et al., 2005; Teixeira et al., 2005; Wilczynska et al., 2005).

P-bodies have been implicated in three ways that lead to mRNA degradation. Degradation of common mRNAs is preceded by deadenylation of the poly(A)-tail and remodelling of the RNA molecule by RNA helicases and the removal of the 5′ cap structure by decapping enzymes and enhancers of the decapping process (Coller and Parker, 2004). The decapping then allows 5′ to 3′ exonucleases to access and degrade the mRNA. More specific degradation occurs for mRNAs targeted for nonsense-mediated decay (Sheth and Parker, 2006) and mRNAs that are specifically silenced by short nucleotide sequences via the RNA-induced silencing complex (RISC) (Liu et al., 2005a; Liu et al., 2005b; Anderson and Kedersha, 2006).

P-bodies not only function to degrade mRNAs, but can also protect mRNAs during stress conditions (Brengues et al., 2005; Anderson and Kedersha, 2006). Furthermore, P-bodies are also thought to regulate and repress mRNA translation under different conditions by functioning as a buffer between the translating and non-translating pool of mRNAs (Coller and Parker, 2004). For instance, when excess mRNA is present, the mRNAs are moved into the P-bodies and when mRNAs levels are dropping, the mRNAs inside the P-bodies move out to contribute to the translating pool. This implies that P-bodies are not only sites for decay, but also for temporary storage and upon demand or upon stress relief they release their RNA contents so the temporarily stored mRNAs can re-enter translation (Brengues et al., 2005). However, this translation does not occur inside the P-bodies because they do not contain ribosomal subunits or initiation factors, which implies that mRNAs have to move out of the P-bodies to enter translation (Sheth and Parker, 2003; Wickens and Goldstrohm, 2003; Kedersha et al., 2005).

4.4 Stress granules: mRNA protection

Eukaryotic cells form stress granules (SG) under environmental stress. These can be heat shock, hypoxia, oxidative conditions and UV irradiation. Upon stress, most cellular mRNAs move into SG, but not the mRNAs encoding heat shock proteins (Nover et al., 1989). This is because the translation of heat-shock proteins is increased to do their work in damage repair, while the cell protects its 'housekeeping' mRNAs in the SG (Kedersha and Anderson, 2002). These SG show stalled transcript-ribosome complexes, the presence of the helicase p54/Rck, the exonuclease XRN1 and the RNA binding proteins Staufen, CPEB, Fragile X mental retardation protein (FMRP) and many others (Anderson and Kedersha, 2006). These proteins all point at a role to store and protect mRNAs in process of translation, and when necessary, these mRNAs might be targeted for specified decay.

The stress granules are however not stable storage compartments of untranslated mRNAs, since drugs that stabilize polysomes (like cycloheximide) inhibit SG formation and drugs that destabilize polysomes (like puromycin) enhance SG formation.

SG and P-bodies share many components, but differ in size and fine composition: stress granules can be rather large (several microns), and seem to exchange material and components with the surrounding cytoplasm, while staying rather immobile (Kedersha et al., 2005). P-bodies in contrast are mobile but seem to be able to interact with SG, which suggests the upkeep of a balance between degradation and translational regulation (Coller and Parker, 2005).

4.5 Germ cell granules: storage and regulation

Germ cell granules play a role during organism development. The P-granules, polar granules and the germinal granules in *C. elegans*, *Drosophila* and *X. laevis*, respectively, share the ability to store translationally silent mRNAs for later embryonic development (Navarro and Blackwell, 2005).

The P-granules, for instance, do not only contain polyadenylated maternal transcripts (which points at translational activation) (Schisa et al., 2001), but contain RNA helicases, decapping enzymes and translation initiation factors. All these components point at a role of these P-granules in maternal mRNA translation initiation, translation control and mRNA degradation, to regulate expression levels during development (Stebbins-Boaz and Richter, 1997; Anderson and Kedersha, 2006).

4.6 RNA granules: a diversity that controls the fate of mRNAs

Although the content of each type of RNA granule is distinct, many proteins are found in more than one type of granules. This points at a dynamic use of the proteins that can regulate mRNA localization, translation and degradation. The dynamics of these granules (to form upon extracellular influences, to exchange contents with the cytoplasm and each other) suggests that these RNA granules serve to meet the spatial and temporal demands for regulating the translational silencing of mRNAs (Anderson and Kedersha, 2006).

5. Techniques to visualize mRNA

The discovery of asymmetrically localized mRNAs has been made possible by the development of RNA visualization techniques. These techniques make use of the intrinsic property of nucleotides, of basepairing. Four basic methods are used to visualize the expression of an mRNA in the tissue by microscopy. These are *in situ* hybridization, molecular beacons, MS2-GFP tagging and RNA injection. These have been used to reveal the location of an mRNA and even the localization process of an mRNA *in vivo*. The next challenge in mRNA localization is to couple these *in vivo* data with ultrastructural analysis.

5.1 *in situ* hybridization

One of the first techniques that has been developed to visualize mRNA directly in tissues is the RNA *in situ* hybridization (ISH) technique. It makes use of labeled antisense nucleotide sequences, the antisense probes, that are incubated with the fixed tissue in a hybridization buffer, at the annealing temperature optimal for the RNA of interest, usually between 40 and 65 degrees Celsius. The tissue is then washed to remove the unbound probe, followed by the necessary detection method for light microscopy.

The technique was initially applied to radioactively-labeled probes and followed by visualization by autoradiography (Hafen et al., 1983; Fillman and Lykke-Andersen, 2005), a process that has to be perfomed with care and patience because of the radioactivity and the lengthy detection.

The safety and speed of the technique was enhanced by the use of non-radioactive probes. These are labeled with Biotin or Digoxigenin, small moieties that do not interfere with the nucleotide sequence of the RNA, and can easily be detected by specific antibodies (Tautz and Pfeifle, 1989; Kiyama et al., 1990). Fluorescent nucleotides or fluorescent enzyme-substrates have also been used to visualize the mRNA (Swiger and Tucker, 1996).

In situ hybridizations are used to map genes on chromosomes, to study mRNA expression profiles and to study pathogenic infection like viruses and microbes. Furthermore, ISH is used in pathological studies, cancer research and developmental biology to study changes in mRNA expression and localization (Speel, 1999). The disadvantage of ISH is that it can only be used to study mRNA after fixation, and it is therefore not applicable for life cell imaging.

5.2 Molecular beacons

The capacity of antisense RNA sequences to bind to the target mRNA is further exploited by molecular beacons. The molecular beacons are hybridization probes that generate fluorescent signals only when they are bound to the target sequence. They are composed of a fluorophore placed on one end of the oligonucleotide sequence and a quencher at the other end. Upon injection, the beacon that is free in the cytoplasm, does not fluoresce because the quencher is in proximity of the fluorophore due to the hairpin structure the beacon forms. But when the probe detects its target mRNA, this structure unwinds and the fluorophore is no longer quenched and becomes active. This way the disadvantage of ISH, which is that ISH only allows visualization of mRNAs in fixed material, is overcome and therefore the site of mRNA production, its way through the nuclear pores, its cytoplasmic residence, transport and anchoring may be monitored *in vivo* (Bratu *et al*., 2003). The difficulty with this technique lies in the weak signal of the beacon as only one fluorophore will bind to the mRNA of interest.

5.3 MS2-GFP tagging and GFP tagging of other RNA binding proteins

Another technique to visualize mRNA is to exploit the characteristics of the protein MS2, which has binding properties for specific RNA sequences with very high affinity. The bacteriophage *ms2 replicase* mRNA has a specific stem-loop sequence which can be bound by the RNA binding protein MS2 to package it into newly forming phages (Nagai, 1996). The characteristics of this phage are used by fusing this MS2 capsid protein to GFP and introducing this stably in the cell line of interest. To visualize the mRNA of interest, the *ms2* stem-loop sequences then need to be inserted into the target mRNA. By placing the gene or the MS2-GFP protein under an inducible promoter, transcript transport can then be followed by life cell imaging (Bertrand et al., 1998; Beach et al., 1999; Rook et al., 2000; Hamada et al., 2003).

To study the endogenous localization processes of mRNAs, also other RNA binding proteins can be tagged with GFP. This is a non-invasive technique that will then reveal the localization of the target mRNA, without the requirement to add specific localization elements to that mRNA (Martin et al., 2003; Wang and Hazelrigg, 1994). However, the disadvantage of this is that RNA binding proteins mostly do not have a single target mRNA and it is therefore necessary to show that the moving particles contain the mRNA of interest (St Johnston, 2005).

5.4 Injection of *in vitro* produced mRNA

Antisense and sense RNA sequences can be made in vitro. Antisense RNAs are used as probe in ISH to detect the mRNA (see 5.1). Sense RNAs, on the other hand are similar to mRNAs, and can therefore be used to mimic the characteristics of the endogenous mRNA in the living tissue upon injection.

To protect the injected RNA from the endogenous exonucleases in the cell, the RNA requires a 5′ cap analog and a 3′UTR (the polyadenylation site, see 3.1.1), so it resembles endogenous mRNAs (Wilkie and Davis, 2001). By labeling the synthetic RNA with fluorescent nucleotides, it is possible to visualize the RNA upon injection and to follow its path in the living cell (Carson et al., 1997; Wilkie and Davis, 2001; Bullock et al., 2003).

This technique has created a league of possibilities, such as understanding how RNAs move in the cell, where this movement is directed to and what factors are required for its movement (MacDougall et al., 2003; Delanoue and Davis, 2005). Furthermore, since the RNA can also directly be labeled with a tag, antibodies can also be used to detect the tagged RNA. This is where the exciting possibilities have come in. Injected samples can be fixed at the time at which an interesting event is observed by life cell imaging and processed for electron microscopy to have a detailed view on the location, structure and composition of the structure underlying the event.

5.5 Visualization of endogenous RNA by ISH combined with immuno-electron microscopy (ISH-IEM).

Although injection of RNA can mimic the localization processes of the endogenous mRNA in the tissue, at least at the light microscopy level, it is necessary to confirm whether the endogenous mRNA indeed behaves similarly. In particular, the ultrastructural information gathered with injected RNA needs to be confirmed and examined with endogenous transcripts.

The detection of endogenous mRNA by EM is a challenge. Multiple protocols have been proposed to detect mRNA at the EM level. These were either based on standard ISH methods followed by embedding for EM (pre-embedding ISH), or embedding for EM, followed

by sectioning and then ISH (post-embedding ISH). For post-embedding ISH it is imperative to either embed the tissue or cells in hydrophilic resins or to make frozen thin sections, since ISH is a technique that requires an aqueous milieu to allow the antisense probe to bind to the target mRNA. Performing ISH on ultrathin cryosections has been explored previously (Dirks et al., 1992; van Minnen, 1994; Dirks, 1996; Macville et al., 1996) in axons and cultured cells. These reports convincingly showed the possibility to use ultrathin cryosections for mRNA studies at EM level. However, our attempts to use the reported protocols to investigate *gurken* mRNA localization in the oocyte led to loss of the quality of the ultrastructure and the specificity of the labeling pattern found was questionable.

To overcome this, we have based the development of a new protocol for RNA detection at EM level on the immuno-labeling protocol for protein detection and combined it with the knowledge coming from the existing ones for ISH on cryosections. In **chapter 3**, I will describe the resulting ISH-IEM (RNA *in situ* hybridization coupled to immunoelectron microscopy) technique we developed to detect endogenous mRNA on ultrathin cryosections of *Drosophila* oocytes. This method allows direct ISH on cryosections, so the antisense probe detects the endogenous mRNA in the tissue sections. This method is independent of mild fixations or protein digestions, and therefore preserves the ultrastructure. With this novel immuno-electron microscopy technique, it is not only possible to identify structures that mediate mRNA localization, but also perform double immunolabeling for RNA and proteins.

6. The localization of *gurken* mRNA

From previous studies, it is clear that the accumulation of *gurken* mRNA in the previtellogenic oocyte, its localization to the posterior pole during stage 6-7 and its localization to the dorso-anterior corner at stages 8-10 is microtubule-dependent. At this final destination, *gurken* mRNA needs to be anchored. To achieve the asymmetric localization and anchoring, a number of *cis*- and *trans*- acting factors have been shown to be important and this will be detailed below.

6.1 Transport of *gurken* mRNA in the oocyte

The first evidence that Dynein was involved in the localization of *gurken* mRNA to the DA corner was established by overexpression of dynamitin, this inhibits Dynein function (Duncan and Warrior, 2002; Januschke et al., 2002). Later, injection of fluorescently labeled *gurken* RNA in stage 9 oocytes revealed that this injected RNA moved rapidly in particles in a two-step fashion to the DA corner (MacDougall et al., 2003). In this assay, the injected *gurken* RNA initially accumulates at the anterior of the oocyte and then moves along the anterior to the oocyte nucleus. This movement could be abolished by disruption of the microtubule cytoskeleton or co-injection of inactivating anti-Dhc antibodies, and slowed down in Dhc hypomorphic alleles. Taken together, these results showed that *gurken* localization to the DA corner occurs in particles that are transported by Dynein on microtubules (MacDougall et al., 2003).

Few of the questions are whether these moving particles are hitchhiking on vesicles, on ER membranes, or directly on microtubules, and how many RNA molecules could be transported together in one particle. In **chapter 4**, I describe these particles as observed by IEM. Their diameter is in the range of 300nm, they seem to move directly on microtubules and are estimated to contain hundreds of RNA molecules associated to Dynein. These transport particles might function similarly to the neuronal granules (see above, part 4.2), which is to transport mRNAs in dense particles together with RNA binding proteins and motor molecules.

We immuno-localized the molecular motor Dhc in the transport particles together with its cofactors Egl and BicD, pointing towards their role in minus end directed transport. This fits with the movement observed in the oocyte since the minus ends accumulate around the oocyte nucleus. In addition, live imaging of the microtubule-binding protein Tau coupled to GFP and microtubule regrowth experiments after cold-shock showed that two distinct populations of microtubules nucleate in the vicinity of the oocyte nucleus (MacDougall et al., 2003; Januschke et al., 2006). The existence of these two populations creates the possibility for Dynein to sequentially transport its cargo, first to the anterior, then to the DA corner.

The second step in *gurken* mRNA transport is specifically disrupted in *K10* and *squid* mutants (Neuman-Silberberg and Schupbach, 1993), while the anterior localization step seems unaffected. The effect of these mutants might be due to an effector of Dynein mediated transport, such as a signal that in wild-type oocytes specifies the transport particles to change microtubule tracks at the anterior side to those that can deliver the mRNA at the dorso-anterior corner. This effector is hypothesized to be the Squid protein. When this protein is absent, *gurken* mRNA stays anterior. In **chapter 4** the anterior localization of *gurken* mRNA is recapitulated by *gurken* RNA injection in the *squid* mutant and by Squid inhibition after *gurken* mRNA anchoring at the dorso-anterior corner. It is shown that the mRNA is in fact continuously transported in transport particles to the anterior side in this mutant.

6.2 *gurken* mRNA anchoring

Once localized at the DA corner, the *gurken* transcript is anchored to ensure the proper local synthesis of Gurken and signaling to the overlying follicle cells during stages 8-10, of a total duration of ~20 hours (Horne-Badovinac and Bilder, 2005).

As mentioned in part 3.4.2, the anchoring of pair-rule transcripts in the syncitial embryo depends on microtubules and Dynein but the ATPase activity of Dynein is not required (Delanoue and Davis, 2005). It was therefore concluded that Dynein makes a switch from being a motor to a static anchor upon arrival at the end of the microtubules at the apical side.

In **chapter 4**, we investigated the anchoring of *gurken* mRNA and we found that it was mediated by large cytoplasmic structures, the sponge bodies. Sponge bodies were first described at EM level by the group of Christiane Nüsslein-Volhard (Wilsch-Brauninger *et al*., 1997), to be present in the nurse cells and the whole oocyte cytoplasm during stages 8 to 10. Our analysis showed that the sponge bodies found at the DA corner are specifically populated by *gurken* mRNA, a feature observed for both the injected *gurken* RNA and the endogenous mRNA that we have detected by the novel technique introduced in part 5.5 of the introduction and described in **chapter 3**.

In **chapter 4**, we have further characterized the anchoring properties by FRAP experiments, by microtubule depolymerization and anti-Dhc injection and show that anchoring depends on an intact microtubule network and on Dynein that, as in the case of the embryo, has switched from a motor to an anchor.

As was mentioned above, in *squid* mutants, *gurken* mRNA is localized along the anterior side of the oocyte and does not reach the DA corner (Norvell et al., 1999; Kelley, 1993). This led to the notion that Squid is required for the second step of transport. An additional role for Squid is described in **chapter 4**, not only its role in transport but also in anchoring that we have identified by a combination of mutants, RNA injections and antibody injection. We found that Squid mediates the coalescence/ self association of the transport particles described above, into sponge bodies, a process under which Dynein undergoes the switch from a motor to an anchor.

6.3 *gurken* mRNA in RNA granules: how do these form?

We have characterized two types of RNA granules, the transport particles and the sponge bodies, in which *gurken* mRNA resides together with Dynein and Squid during transport and anchoring. The sponge bodies, however, are not only found at the DA corner together with *gurken* RNA, but throughout the cytoplasm of the oocyte. Furthermore, all sponge bodies contain Dynein. The questions we asked in **chapter 5** are how Dynein becomes localized in these sponge bodies and what its role is there.

We found that inactivation of Dynein heavy chain (Dhc) leads to the disappearance of all the sponge bodies throughout the oocyte. This pointed at a function in the structural maintenance of the sponge bodies. We also found that *dhc* mRNA itself is present in the sponge bodies and that Dhc transports its own mRNA into the sponge bodies.

This suggests that Dhc could be synthesized directly in the sponge bodies to contribute to their structure. However, no evidence was found for translation processes happening in the sponge bodies. Sponge bodies do not have ribosomes and are concentrated in the translational repressor Bruno and the RNA helicase Me31B (Nakamura et al., 2001), as well as the regulator Orb. This points to a role in mRNA storage and translational silencing. Based on this, we propose

a functional relatedness of sponge bodies and P-bodies.

Instead of being synthesized locally in the sponge bodies, we conclude that Dynein becomes localized there via the transport of mRNAs (including its own) and that it contributes to their structure by undergoing a functional switch upon cargo delivery.

Scope of this thesis

The local synthesis and secretion of Gurken occurs where its asymmetrically localized mRNA is situated. The mechanisms underlying the asymmetric localization of *gurken* mRNA and local Gurken protein secretion are the topic of this thesis.
Two fundamental aspects will be examined:
I. The relationship between Gurken secretion and *gurken* mRNA localization, or how a transmembrane protein can achieve an asymmetric localization from its localized mRNA;
II. The mechanism underlying the asymmetric localization of *gurken* mRNA.

In **chapter 2,** we will show that restricted deposition of Gurken depends on two aspects: *gurken* mRNA localization and efficient transport mechanisms through the exocytic pathway.

In **chapter 3,** I will present the novel technique that I have developed, the ISH-IEM, *in situ* hybridization combined with immuno-electron microscopy, with which we show that *gurken* mRNA is localized in sponge bodies.

In **chapter 4,** the journey of *gurken* mRNA is described: its transport in transport particles and how it finally anchors in the sponge bodies, highlighting new roles for Squid and Dynein.

In **chapter 5,** I will present a novel role for Dynein: that it is involved in the structural integrity of the sponge bodies. In fact, these are likely the P-bodies for the *Drosophila* oocyte and their function in translational regulation is explored further.

In the Summarizing Discussion (**chapter 6**), the results of this thesis are explored into a broader context.

References

Adams,M.D., Celniker,S.E., Holt,R.A., Evans,C.A., Gocayne,J.D., et al. (2000). The genome sequence of Drosophila melanogaster. Science 287, 2185-2195.

Aguilera,A. (2005). Cotranscriptional mRNP assembly: from the DNA to the nuclear pore. Curr. Opin. Cell Biol. 17, 242-250.

Ainger,K., Avossa,D., Diana,A.S., Barry,C., Barbarese,E., and Carson,J.H. (1997). Transport and localization elements in myelin basic protein mRNA. J. Cell Biol. 138, 1077-1087.

Alder,N.N., Shen,Y., Brodsky,J.L., Hendershot,L.M., and Johnson,A.E. (2005). The molecular mechanisms underlying BiP-mediated gating of the Sec61 translocon of the endoplasmic reticulum. J. Cell Biol. 168, 389-399.

Allan,B.B. and Balch,W.E. (1999). Protein sorting by directed maturation of Golgi compartments. Science 285, 63-66.

Allison,R., Czaplinski,K., Git,A., Adegbenro,E., Stennard,F., Houliston,E., and Standart,N. (2004). Two distinct Staufen isoforms in Xenopus are vegetally localized during oogenesis. RNA. 10, 1751-1763.

Altan-Bonnet,N., Sougrat,R., and Lippincott-Schwartz,J. (2004). Molecular basis for Golgi maintenance and biogenesis. Curr. Opin. Cell Biol. 16, 364-372.

Altan-Bonnet,N., Sougrat,R., Liu,W., Snapp,E.L., Ward,T., and Lippincott-Schwartz,J. (2006). Golgi inheritance in mammalian cells is mediated through endoplasmic reticulum export activities. Mol. Biol. Cell 17, 990-1005.

Anderson,E.D., Molloy,S.S., Jean,F., Fei,H., Shimamura,S., and Thomas,G. (2002). The ordered and compartment-specfific autoproteolytic removal of the furin intramolecular chaperone is required for enzyme activation. J. Biol. Chem. 277, 12879-12890.

Anderson,P. and Kedersha,N. (2006). RNA granules. J. Cell Biol. 172, 803-808.

Andrei,M.A., Ingelfinger,D., Heintzmann,R., Achsel,T., Rivera-Pomar,R., and Luhrmann,R. (2005). A role for eIF4E and eIF4E-transporter in targeting mRNPs to mammalian processing bodies. RNA. 11, 717-727.

Antonny,B., Bigay,J., Casella,J.F., Drin,G., Mesmin,B., and Gounon,P. (2005). Membrane curvature and the control of GTP hydrolysis in Arf1 during COPI vesicle formation. Biochem. Soc. Trans. 33, 619-622.

Antonny,B. and Schekman,R. (2001). ER export: public transportation by the COPII coach. Curr. Opin. Cell Biol. 13, 438-443.

Appenzeller,C., Andersson,H., Kappeler,F., and Hauri,H.P. (1999). The lectin ERGIC-53 is a cargo transport receptor for glycoproteins. Nat. Cell Biol. 1, 330-334.

Appenzeller-Herzog,C. and Hauri,H.P. (2006). The ER-Golgi intermediate compartment (ERGIC): in search of its identity and function. J. Cell Sci. 119, 2173-2183.

Aridor,M., Bannykh,S.I., Rowe,T., and Balch,W.E. (1995). Sequential coupling between COPII and COPI vesicle coats in endoplasmic reticulum to Golgi transport. J. Cell Biol. 131, 875-893.

Bannykh,S.I., Nishimura,N., and Balch,W.E. (1998). Getting into the Golgi. Trends Cell Biol. 8, 21-25.

Barlowe,C. (1995). COPII: a membrane coat that forms endoplasmic reticulum-derived vesicles. FEBS Lett. 369, 93-96.

Barlowe,C. (1998). COPII and selective export from the endoplasmic reticulum. Biochim. Biophys. Acta 1404, 67-76.

Barlowe,C. (2003). Signals for COPII-dependent export from the ER: what's the ticket out? Trends Cell Biol. 13, 295-300.

Barlowe,C., Orci,L., Yeung,T., Hosobuchi,M., Hamamoto,S., Salama,N., Rexach,M.F., Ravazzola,M., Amherdt,M., and Schekman,R. (1994). COPII: a membrane coat formed by Sec proteins that drive vesicle budding from the endoplasmic reticulum. Cell 77, 895-907.

Bashkirov,V.I., Scherthan,H., Solinger,J.A., Buerstedde,J.M., and Heyer,W.D. (1997). A mouse cytoplasmic exoribonuclease (mXRN1p) with preference for G4 tetraplex substrates. J. Cell Biol. 136, 761-773.

Bassell,G.J., Zhang,H., Byrd,A.L., Femino,A.M., Singer,R.H., Taneja,K.L., Lifshitz,L.M., Herman,I.M., and Kosik,K.S. (1998). Sorting of beta-actin mRNA and protein to neurites and growth cones in culture. J. Neurosci. 18, 251-265.

Bateman,M.J., Cornell,R., d'Alencon,C., and Sandra,A. (2004). Expression of the zebrafish Staufen gene in the embryo and adult. Gene Expr. Patterns. 5, 273-278.

Beach,D.L., Salmon,E.D., and Bloom,K. (1999). Localization and anchoring of mRNA in budding yeast. Curr. Biol. 9, 569-578.

Belden,W.J. and Barlowe,C. (2001). Role of Erv29p in collecting soluble secretory proteins into ER-derived transport vesicles. Science 294, 1528-1531.

Ben Tekaya,H., Miura,K., Pepperkok,R., and Hauri,H.P. (2005). Live imaging of bidirectional traffic from the ERGIC. J. Cell Sci. 118, 357-367.

Bertrand,E., Chartrand,P., Schaefer,M., Shenoy,S.M., Singer,R.H., and Long,R.M. (1998). Localization of ASH1 mRNA particles in living yeast. Mol. Cell 2, 437-445.

Bevis,B.J., Hammond,A.T., Reinke,C.A., and Glick,B.S. (2002). De novo formation of transitional ER sites and

Golgi structures in Pichia pastoris. Nat. Cell Biol. 4, 750-756.
Blichenberg,A., Rehbein,M., Muller,R., Garner,C.C., Richter,D., and Kindler,S. (2001). Identification of a cis-acting dendritic targeting element in the mRNA encoding the alpha subunit of Ca2+/calmodulin-dependent protein kinase II. Eur. J. Neurosci. 13, 1881-1888.
Blichenberg,A., Schwanke,B., Rehbein,M., Garner,C.C., Richter,D., and Kindler,S. (1999). Identification of a cis-acting dendritic targeting element in MAP2 mRNAs. J. Neurosci. 19, 8818-8829.
Blobel,G. and Dobberstein,B. (1975). Transfer of proteins across membranes. I. Presence of proteolytically processed and unprocessed nascent immunoglobulin light chains on membrane-bound ribosomes of murine myeloma. J. Cell Biol. 67, 835-851.
Bobinnec,Y., Marcaillou,C., Morin,X., and Debec,A. (2003). Dynamics of the endoplasmic reticulum during early development of Drosophila melanogaster. Cell Motil. Cytoskeleton 54, 217-225.
Bohl,F., Kruse,C., Frank,A., Ferring,D., and Jansen,R.P. (2000). She2p, a novel RNA-binding protein tethers ASH1 mRNA to the Myo4p myosin motor via She3p. EMBO J. 19, 5514-5524.
Bokel,C., Dass,S., Wilsch-Brauninger,M., and Roth,S. (2006). Drosophila Cornichon acts as cargo receptor for ER export of the TGFalpha-like growth factor Gurken. Development 133, 459-470.
Bonfanti,L., Mironov,A.A., Jr., Martinez-Menarguez,J.A., Martella,O., Fusella,A., Baldassarre,M., Buccione,R., Geuze,H.J., Mironov,A.A., and Luini,A. (1998). Procollagen traverses the Golgi stack without leaving the lumen of cisternae: evidence for cisternal maturation. Cell 95, 993-1003.
Bonifacino,J.S. and Glick,B.S. (2004). The mechanisms of vesicle budding and fusion. Cell 116, 153-166.
Borgese,N., Colombo,S., and Pedrazzini,E. (2003). The tale of tail-anchored proteins: coming from the cytosol and looking for a membrane. J. Cell Biol. 161, 1013-1019.
Brady,S.T. (1985). A novel brain ATPase with properties expected for the fast axonal transport motor. Nature 317, 73-75.
Bratu,D.P., Cha,B.J., Mhlanga,M.M., Kramer,F.R., and Tyagi,S. (2003). Visualizing the distribution and transport of mRNAs in living cells. Proc. Natl. Acad. Sci. U. S. A 100, 13308-13313.
Brendza,R.P., Serbus,L.R., Saxton,W.M., and Duffy,J.B. (2002). Posterior localization of dynein and dorsal-ventral axis formation depend on kinesin in Drosophila oocytes. Curr. Biol. 12, 1541-1545.
Brengues,M., Teixeira,D., and Parker,R. (2005). Movement of eukaryotic mRNAs between polysomes and cytoplasmic processing bodies. Science 310, 486-489.
Bullock,S.L. and Ish-Horowicz,D. (2001). Conserved signals and machinery for RNA transport in Drosophila oogenesis and embryogenesis. Nature 414, 611-616.
Bullock,S.L., Zicha,D., and Ish-Horowicz,D. (2003). The Drosophila hairy RNA localization signal modulates the kinetics of cytoplasmic mRNA transport. EMBO J. 22, 2484-2494.
Burden,S.J. (1993). Synapse-specific gene expression. Trends Genet. 9, 12-16.
Caceres,L. and Nilson,L.A. (2005). Production of gurken in the nurse cells is sufficient for axis determination in the Drosophila oocyte. Development 132, 2345-2353.
Capri,M., Santoni,M.J., Thomas-Delaage,M., and Ait-Ahmed,O. (1997). Implication of a 5' coding sequence in targeting maternal mRNA to the Drosophila oocyte. Mech. Dev. 68, 91-100.
Carson,J.H., Worboys,K., Ainger,K., and Barbarese,E. (1997). Translocation of myelin basic protein mRNA in oligodendrocytes requires microtubules and kinesin. Cell Motil. Cytoskeleton 38, 318-328.
Chabanon,H., Mickleburgh,I., and Hesketh,J. (2004). Zipcodes and postage stamps: mRNA localisation signals and their trans-acting binding proteins. Brief. Funct. Genomic. Proteomic. 3, 240-256.
Chekulaeva,M., Hentze,M.W., and Ephrussi,A. (2006). Bruno acts as a dual repressor of oskar translation, promoting mRNA oligomerization and formation of silencing particles. Cell 124, 521-533.
Claussen,M. and Suter,B. (2005). BicD-dependent localization processes: from Drosophilia development to human cell biology. Ann. Anat. 187, 539-553.
Cluett,E.B. and Brown,W.J. (1992). Adhesion of Golgi cisternae by proteinaceous interactions: intercisternal bridges as putative adhesive structures. J. Cell Sci. 103 (Pt 3), 773-784.
Cohen,R.S., Zhang,S., and Dollar,G.L. (2005). The positional, structural, and sequence requirements of the Drosophila TLS RNA localization element. RNA. 11, 1017-1029.
Cole,C.N. and Scarcelli,J.J. (2006). Transport of messenger RNA from the nucleus to the cytoplasm. Curr. Opin. Cell Biol. 18, 299-306.
Cole,N.B., Sciaky,N., Marotta,A., Song,J., and Lippincott-Schwartz,J. (1996). Golgi dispersal during microtubule disruption: regeneration of Golgi stacks at peripheral endoplasmic reticulum exit sites. Mol. Biol. Cell 7, 631-650.
Coller,J. and Parker,R. (2004). Eukaryotic mRNA decapping. Annu. Rev. Biochem. 73, 861-890.
Coller,J. and Parker,R. (2005). General translational repression by activators of mRNA decapping. Cell 122, 875-886.
Colon-Ramos,D.A., Salisbury,J.L., Sanders,M.A., Shenoy,S.M., Singer,R.H., and Garcia-Blanco,M.A. (2003). Asymmetric distribution of nuclear pore complexes and the cytoplasmic localization of beta2-tubulin mRNA in Chlamydomonas reinhardtii. Dev. Cell 4, 941-952.
Condeelis,J. and Singer,R.H. (2005). How and why does beta-actin mRNA target? Biol. Cell 97, 97-110.

Cosson,P. and Letourneur,F. (1994). Coatomer interaction with di-lysine endoplasmic reticulum retention motifs. Science 263, 1629-1631.
Cote,C.A., Gautreau,D., Denegre,J.M., Kress,T.L., Terry,N.A., and Mowry,K.L. (1999). A Xenopus protein related to hnRNP I has a role in cytoplasmic RNA localization. Mol. Cell 4, 431-437.
Davis,I. and Ish-Horowicz,D. (1991). Apical localization of pair-rule transcripts requires 3' sequences and limits protein diffusion in the Drosophila blastoderm embryo. Cell 67, 927-940.
Delanoue,R. and Davis,I. (2005). Dynein anchors its mRNA cargo after apical transport in the Drosophila blastoderm embryo. Cell 122, 97-106.
Dempski,R.E., Jr. and Imperiali,B. (2002). Oligosaccharyl transferase: gatekeeper to the secretory pathway. Curr. Opin. Chem. Biol. 6, 844-850.
Deshaies,R.J. and Schekman,R. (1987). A yeast mutant defective at an early stage in import of secretory protein precursors into the endoplasmic reticulum. J. Cell Biol. 105, 633-645.
Diao,A., Rahman,D., Pappin,D.J., Lucocq,J., and Lowe,M. (2003). The coiled-coil membrane protein golgin-84 is a novel rab effector required for Golgi ribbon formation. J. Cell Biol. 160, 201-212.
Ding,D., Parkhurst,S.M., Halsell,S.R., and Lipshitz,H.D. (1993). Dynamic Hsp83 RNA localization during Drosophila oogenesis and embryogenesis. Mol. Cell Biol. 13, 3773-3781.
Dirks,R.W. (1996). RNA molecules lighting up under the microscope. Histochem. Cell Biol. 106, 151-166.
Dirks,R.W., Van Dorp,A.G., van Minnen,J., Fransen,J.A., Van der,P.M., and Raap,A.K. (1992). Electron microscopic detection of RNA sequences by non-radioactive in situ hybridization in the mollusk Lymnaea stagnalis. J. Histochem. Cytochem. 40, 1647-1657.
Drummond,D.R., Armstrong,J., and Colman,A. (1985). The effect of capping and polyadenylation on the stability, movement and translation of synthetic messenger RNAs in Xenopus oocytes. Nucleic Acids Res. 13, 7375-7394.
Dubowy,J. and Macdonald,P.M. (1998). Localization of mRNAs to the oocyte is common in Drosophila ovaries. Mech. Dev. 70, 193-195.
Duden,R. (2003). ER-to-Golgi transport: COP I and COP II function (Review). Mol. Membr. Biol. 20, 197-207.
Duncan,J.E. and Warrior,R. (2002). The cytoplasmic dynein and kinesin motors have interdependent roles in patterning the Drosophila oocyte. Curr. Biol. 12, 1982-1991.
Eberwine,J., Miyashiro,K., Kacharmina,J.E., and Job,C. (2001). Local translation of classes of mRNAs that are targeted to neuronal dendrites. Proc. Natl. Acad. Sci. U. S. A 98, 7080-7085.
Ephrussi,A., Dickinson,L.K., and Lehmann,R. (1991). Oskar organizes the germ plasm and directs localization of the posterior determinant nanos. Cell 66, 37-50.
Ephrussi,A. and Lehmann,R. (1992). Induction of germ cell formation by oskar. Nature 358, 387-392.
Ephrussi,A. and St Johnston,D. (2004). Seeing is believing: the bicoid morphogen gradient matures. Cell 116, 143-152.
Ernst,J.F. and Prill,S.K. (2001). O-glycosylation. Med. Mycol. 39 Suppl 1, 67-74.
Eystathioy,T., Jakymiw,A., Chan,E.K., Seraphin,B., Cougot,N., and Fritzler,M.J. (2003). The GW182 protein colocalizes with mRNA degradation associated proteins hDcp1 and hLSm4 in cytoplasmic GW bodies. RNA. 9, 1171-1173.
Farquhar,M.G. and Palade,G.E. (1998). The Golgi apparatus: 100 years of progress and controversy. Trends Cell Biol. 8, 2-10.
Faulkner,N.E., Dujardin,D.L., Tai,C.Y., Vaughan,K.T., O'Connell,C.B., Wang,Y., and Vallee,R.B. (2000). A role for the lissencephaly gene LIS1 in mitosis and cytoplasmic dynein function. Nat. Cell Biol. 2, 784-791.
Feldman,R.I., Bernstein,M., and Schekman,R. (1987). Product of SEC53 is required for folding and glycosylation of secretory proteins in the lumen of the yeast endoplasmic reticulum. J. Biol. Chem. 262, 9332-9339.
Ferrandon,D., Elphick,L., Nusslein-Volhard,C., and St Johnston,D. (1994). Staufen protein associates with the 3'UTR of bicoid mRNA to form particles that move in a microtubule-dependent manner. Cell 79, 1221-1232.
Ferrandon,D., Koch,I., Westhof,E., and Nusslein-Volhard,C. (1997). RNA-RNA interaction is required for the formation of specific bicoid mRNA 3' UTR-STAUFEN ribonucleoprotein particles. EMBO J. 16, 1751-1758.
Fillman,C. and Lykke-Andersen,J. (2005). RNA decapping inside and outside of processing bodies. Curr. Opin. Cell Biol. 17, 326-331.
Forrest,K.M. and Gavis,E.R. (2003). Live imaging of endogenous RNA reveals a diffusion and entrapment mechanism for nanos mRNA localization in Drosophila. Curr. Biol. 13, 1159-1168.
French,R.L., Cosand,K.A., and Berg,C.A. (2003). The Drosophila female sterile mutation twin peaks is a novel allele of tramtrack and reveals a requirement for Ttk69 in epithelial morphogenesis. Dev. Biol. 253, 18-35.
Furuta,M., Carroll,R., Martin,S., Swift,H.H., Ravazzola,M., Orci,L., and Steiner,D.F. (1998). Incomplete processing of proinsulin to insulin accompanied by elevation of Des-31,32 proinsulin intermediates in islets of mice lacking active PC2. J. Biol. Chem. 273, 3431-3437.
Gavis,E.R. (1995). Pattern formation. Gurken meets torpedo for the first time. Curr. Biol. 5, 1252-1254.
Gebauer,F. and Hentze,M.W. (2004). Molecular mechanisms of translational control. Nat. Rev. Mol. Cell Biol.

5, 827-835.
Ghiglione,C., Bach,E.A., Paraiso,Y., Carraway,K.L., III, Noselli,S., and Perrimon,N. (2002). Mechanism of activation of the Drosophila EGF Receptor by the TGFalpha ligand Gurken during oogenesis. Development 129, 175-186.
Giustetto,M., Hegde,A.N., Si,K., Casadio,A., Inokuchi,K., Pei,W., Kandel,E.R., and Schwartz,J.H. (2003). Axonal transport of eukaryotic translation elongation factor 1alpha mRNA couples transcription in the nucleus to long-term facilitation at the synapse. Proc. Natl. Acad. Sci. U. S. A 100, 13680-13685.
Gleeson,P.A., Lock,J.G., Luke,M.R., and Stow,J.L. (2004). Domains of the TGN: coats, tethers and G proteins. Traffic. 5, 315-326.
Glick,B.S. (2000). Organization of the Golgi apparatus. Curr. Opin. Cell Biol. 12, 450-456.
Glick,B.S. (2002). Can the Golgi form de novo? Nat. Rev. Mol. Cell Biol. 3, 615-619.
Glick,B.S. and Malhotra,V. (1998). The curious status of the Golgi apparatus. Cell 95, 883-889.
Goldstein,L.S. and Yang,Z. (2000). Microtubule-based transport systems in neurons: the roles of kinesins and dyneins. Annu. Rev. Neurosci. 23, 39-71.
Gonzalez,I., Buonomo,S.B., Nasmyth,K., and von Ahsen,U. (1999). ASH1 mRNA localization in yeast involves multiple secondary structural elements and Ash1 protein translation. Curr. Biol. 9, 337-340.
Gu,F., Crump,C.M., and Thomas,G. (2001). Trans-Golgi network sorting. Cell Mol. Life Sci. 58, 1067-1084.
Guichard,A., Roark,M., Ronshaugen,M., and Bier,E. (2000). brother of rhomboid, a rhomboid-related gene expressed during early Drosophila oogenesis, promotes EGF-R/MAPK signaling. Dev. Biol. 226, 255-266.
Gusarova,V., Brodsky,J.L., and Fisher,E.A. (2003). Apolipoprotein B100 exit from the endoplasmic reticulum (ER) is COPII-dependent, and its lipidation to very low density lipoprotein occurs post-ER. J. Biol. Chem. 278, 48051-48058.
Guy,R.K. (2000). Inhibition of sonic hedgehog autoprocessing in cultured mammalian cells by sterol deprivation. Proc. Natl. Acad. Sci. U. S. A 97, 7307-7312.
Hafen,E., Levine,M., Garber,R.L., and Gehring,W.J. (1983). An improved in situ hybridization method for the detection of cellular RNAs in Drosophila tissue sections and its application for localizing transcripts of the homeotic Antennapedia gene complex. EMBO J. 2, 617-623.
Halban,P.A. (1991). Structural domains and molecular lifestyles of insulin and its precursors in the pancreatic beta cell. Diabetologia 34, 767-778.
Hamada,S., Ishiyama,K., Choi,S.B., Wang,C., Singh,S., Kawai,N., Franceschi,V.R., and Okita,T.W. (2003). The transport of prolamine RNAs to prolamine protein bodies in living rice endosperm cells. Plant Cell 15, 2253-2264.
Hammond,A.T. and Glick,B.S. (2000). Dynamics of transitional endoplasmic reticulum sites in vertebrate cells. Mol. Biol. Cell 11, 3013-3030.
Helenius,A. and Aebi,M. (2004). Roles of N-linked glycans in the endoplasmic reticulum. Annu. Rev. Biochem. 73, 1019-1049.
Hershey,J.W. (1990). Overview: phosphorylation and translation control. Enzyme 44, 17-27.
Hirokawa,N. (2006). mRNA transport in dendrites: RNA granules, motors, and tracks. J. Neurosci. 26, 7139-7142.
Hirokawa,N. and Takemura,R. (2005). Molecular motors and mechanisms of directional transport in neurons. Nat. Rev. Neurosci. 6, 201-214.
Hoogenraad,C.C., Akhmanova,A., Howell,S.A., Dortland,B.R., De Zeeuw,C.I., Willemsen,R., Visser,P., Grosveld,F., and Galjart,N. (2001). Mammalian Golgi-associated Bicaudal-D2 functions in the dynein-dynactin pathway by interacting with these complexes. EMBO J. 20, 4041-4054.
Hoogenraad,C.C., Wulf,P., Schiefermeier,N., Stepanova,T., Galjart,N., Small,J.V., Grosveld,F., De Zeeuw,C.I., and Akhmanova,A. (2003). Bicaudal D induces selective dynein-mediated microtubule minus end-directed transport. EMBO J. 22, 6004-6015.
Horne-Badovinac,S. and Bilder,D. (2005). Mass transit: epithelial morphogenesis in the Drosophila egg chamber. Dev. Dyn. 232, 559-574.
Hsu,S.C., TerBush,D., Abraham,M., and Guo,W. (2004). The exocyst complex in polarized exocytosis. Int. Rev. Cytol. 233, 243-265.
Huang,Y.S., Carson,J.H., Barbarese,E., and Richter,J.D. (2003). Facilitation of dendritic mRNA transport by CPEB. Genes Dev. 17, 638-653.
Huttelmaier,S., Zenklusen,D., Lederer,M., Dictenberg,J., Lorenz,M., Meng,X., Bassell,G.J., Condeelis,J., and Singer,R.H. (2005). Spatial regulation of beta-actin translation by Src-dependent phosphorylation of ZBP1. Nature 438, 512-515.
Huttner,W.B. (1988). Tyrosine sulfation and the secretory pathway. Annu. Rev. Physiol 50, 363-376.
Huynh,J.R. and St Johnston,D. (2000). The role of BicD, Egl, Orb and the microtubules in the restriction of meiosis to the Drosophila oocyte. Development 127, 2785-2794.
Huynh,J.R. and St Johnston,D. (2004). The origin of asymmetry: early polarisation of the Drosophila germline cyst and oocyte. Curr. Biol. 14, R438-R449.
Ikonen,E. and Simons,K. (1998). Protein and lipid sorting from the trans-Golgi network to the plasma

membrane in polarized cells. Semin. Cell Dev. Biol. 9, 503-509.
Januschke,J., Gervais,L., Dass,S., Kaltschmidt,J.A., Lopez-Schier,H., St Johnston,D., Brand,A.H., Roth,S., and Guichet,A. (2002). Polar transport in the Drosophila oocyte requires Dynein and Kinesin I cooperation. Curr. Biol. 12, 1971-1981.
Januschke,J., Gervais,L., Gillet,L., Keryer,G., Bornens,M., and Guichet,A. (2006). The centrosome-nucleus complex and microtubule organization in the Drosophila oocyte. Development 133, 129-139.
Job,C. and Eberwine,J. (2001). Localization and translation of mRNA in dendrites and axons. Nat. Rev. Neurosci. 2, 889-898.
Jongens,T.A., Hay,B., Jan,L.Y., and Jan,Y.N. (1992). The germ cell-less gene product: a posteriorly localized component necessary for germ cell development in Drosophila. Cell 70, 569-584.
Kanai,Y., Dohmae,N., and Hirokawa,N. (2004). Kinesin transports RNA: isolation and characterization of an RNA-transporting granule. Neuron 43, 513-525.
Kartberg,F., Elsner,M., Froderberg,L., Asp,L., and Nilsson,T. (2005). Commuting between Golgi cisternae--mind the GAP! Biochim. Biophys. Acta 1744, 351-363.
Kedersha,N. and Anderson,P. (2002). Stress granules: sites of mRNA triage that regulate mRNA stability and translatability. Biochem. Soc. Trans. 30, 963-969.
Kedersha,N., Stoecklin,G., Ayodele,M., Yacono,P., Lykke-Andersen,J., Fitzler,M.J., Scheuner,D., Kaufman,R. J., Golan,D.E., and Anderson,P. (2005). Stress granules and processing bodies are dynamically linked sites of mRNP remodeling. J. Cell Biol. 169, 871-884.
Kelley,R.L. (1993). Initial organization of the Drosophila dorsoventral axis depends on an RNA-binding protein encoded by the squid gene. Genes Dev. 7, 948-960.
Kim-Ha,J., Webster,P.J., Smith,J.L., and Macdonald,P.M. (1993). Multiple RNA regulatory elements mediate distinct steps in localization of oskar mRNA. Development 119, 169-178.
Kindler,S., Wang,H., Richter,D., and Tiedge,H. (2005). RNA transport and local control of translation. Annu. Rev. Cell Dev. Biol. 21, 223-245.
Kislauskis,E.H., Li,Z., Singer,R.H., and Taneja,K.L. (1993). Isoform-specific 3'-untranslated sequences sort alpha-cardiac and beta-cytoplasmic actin messenger RNAs to different cytoplasmic compartments. J. Cell Biol. 123, 165-172.
Kislauskis,E.H., Zhu,X., and Singer,R.H. (1994). Sequences responsible for intracellular localization of beta-actin messenger RNA also affect cell phenotype. J. Cell Biol. 127, 441-451.
Kiyama,H., Emson,P.C., and Tohyama,M. (1990). Recent progress in the use of the technique of non-radioactive in situ hybridization histochemistry: new tools for molecular neurobiology. Neurosci. Res. 9, 1-21.
Klumperman,J. (2000). Transport between ER and Golgi. Curr. Opin. Cell Biol. 12, 445-449.
Klumperman,J., Schweizer,A., Clausen,H., Tang,B.L., Hong,W., Oorschot,V., and Hauri,H.P. (1998). The recycling pathway of protein ERGIC-53 and dynamics of the ER-Golgi intermediate compartment. J. Cell Sci. 111 (Pt 22), 3411-3425.
Kondylis, V., Herpers, B., Xanthakis, D., Friggi-Grelin, F., and Rabouille, C. The Golgi comprises a paired stack that is separated at G2 by modulation of the actin cytoskeleton through Abi and Scar/WAVE. Submitted.
Kondylis,V. and Rabouille,C. (2003). A novel role for dp115 in the organization of tER sites in Drosophila. J. Cell Biol. 162, 185-198.
Kondylis,V., Spoorendonk,K.M., and Rabouille,C. (2005). dGRASP localization and function in the early exocytic pathway in Drosophila S2 cells. Mol. Biol. Cell 16, 4061-4072.
Kornfeld,R. and Kornfeld,S. (1985). Assembly of asparagine-linked oligosaccharides. Annu. Rev. Biochem. 54, 631-664.
Kreis,T.E. (1990). Role of microtubules in the organisation of the Golgi apparatus. Cell Motil. Cytoskeleton 15, 67-70.
Kress,T.L., Yoon,Y.J., and Mowry,K.L. (2004). Nuclear RNP complex assembly initiates cytoplasmic RNA localization. J. Cell Biol. 165, 203-211.
Krichevsky,A.M. and Kosik,K.S. (2001). Neuronal RNA granules: a link between RNA localization and stimulation-dependent translation. Neuron 32, 683-696.
Kruse,C., Jaedicke,A., Beaudouin,J., Bohl,F., Ferring,D., Guttler,T., Ellenberg,J., and Jansen,R.P. (2002). Ribonucleoprotein-dependent localization of the yeast class V myosin Myo4p. J. Cell Biol. 159, 971-982.
Kurihara,T., Hamamoto,S., Gimeno,R.E., Kaiser,C.A., Schekman,R., and Yoshihisa,T. (2000). Sec24p and Iss1p function interchangeably in transport vesicle formation from the endoplasmic reticulum in Saccharomyces cerevisiae. Mol. Biol. Cell 11, 983-998.
Ladinsky,M.S., Mastronarde,D.N., McIntosh,J.R., Howell,K.E., and Staehelin,L.A. (1999). Golgi structure in three dimensions: functional insights from the normal rat kidney cell. J. Cell Biol. 144, 1135-1149.
Lasko,P. (1999). RNA sorting in Drosophila oocytes and embryos. FASEB J. 13, 421-433.
Latham,V.M., Yu,E.H., Tullio,A.N., Adelstein,R.S., and Singer,R.H. (2001). A Rho-dependent signaling pathway operating through myosin localizes beta-actin mRNA in fibroblasts. Curr. Biol. 11, 1010-1016.
Lavoie,C., Paiement,J., Dominguez,M., Roy,L., Dahan,S., Gushue,J.N., and Bergeron,J.J. (1999). Roles for alpha(2)p24 and COPI in endoplasmic reticulum cargo exit site formation. J. Cell Biol. 146, 285-299.

Lee,J.R., Urban,S., Garvey,C.F., and Freeman,M. (2001). Regulated intracellular ligand transport and proteolysis control EGF signal activation in Drosophila. Cell 107, 161-171.

Lee,M.C., Miller,E.A., Goldberg,J., Orci,L., and Schekman,R. (2004). Bi-directional protein transport between the ER and Golgi. Annu. Rev. Cell Dev. Biol. 20, 87-123.

Levine,T. and Rabouille,C. (2005). Endoplasmic reticulum: one continuous network compartmentalized by extrinsic cues. Curr. Opin. Cell Biol. 17, 362-368.

Li,P., Yang,X., Wasser,M., Cai,Y., and Chia,W. (1997). Inscuteable and Staufen mediate asymmetric localization and segregation of prospero RNA during Drosophila neuroblast cell divisions. Cell 90, 437-447.

Linstedt,A.D., Foguet,M., Renz,M., Seelig,H.P., Glick,B.S., and Hauri,H.P. (1995). A C-terminally-anchored Golgi protein is inserted into the endoplasmic reticulum and then transported to the Golgi apparatus. Proc. Natl. Acad. Sci. U. S. A 92, 5102-5105.

Lippincott-Schwartz,J., Yuan,L.C., Bonifacino,J.S., and Klausner,R.D. (1989). Rapid redistribution of Golgi proteins into the ER in cells treated with brefeldin A: evidence for membrane cycling from Golgi to ER. Cell 56, 801-813.

Liu,J., Rivas,F.V., Wohlschlegel,J., Yates,J.R., III, Parker,R., and Hannon,G.J. (2005a). A role for the P-body component GW182 in microRNA function. Nat. Cell Biol. 7, 1261-1266.

Liu,J., Valencia-Sanchez,M.A., Hannon,G.J., and Parker,R. (2005b). MicroRNA-dependent localization of targeted mRNAs to mammalian P-bodies. Nat. Cell Biol. 7, 719-723.

Long,R.M., Gu,W., Lorimer,E., Singer,R.H., and Chartrand,P. (2000). She2p is a novel RNA-binding protein that recruits the Myo4p-She3p complex to ASH1 mRNA. EMBO J. 19, 6592-6601.

Lopez,d.H. and Jansen,R.P. (2004). mRNA localization and the cytoskeleton. Curr. Opin. Cell Biol. 16, 80-85.

Losev,E., Reinke,C.A., Jellen,J., Strongin,D.E., Bevis,B.J., and Glick,B.S. (2006). Golgi maturation visualized in living yeast. Nature.

Lowe,M. (2002). Golgi complex: biogenesis de novo? Curr. Biol. 12, R166-R167.

Luders,F., Segawa,H., Stein,D., Selva,E.M., Perrimon,N., Turco,S.J., and Hacker,U. (2003). Slalom encodes an adenosine 3'-phosphate 5'-phosphosulfate transporter essential for development in Drosophila. EMBO J. 22, 3635-3644.

MacDougall,N., Clark,A., MacDougall,E., and Davis,I. (2003). Drosophila gurken (TGFalpha) mRNA localizes as particles that move within the oocyte in two dynein-dependent steps. Dev. Cell 4, 307-319.

Macville,M.V., Van Dorp,A.G., Dirks,R.W., Fransen,J.A., and Raap,A.K. (1996). Evaluation of pepsin treatment for electron microscopic RNA in situ hybridization on ultra-thin cryosections of cultured cells. Histochem. Cell Biol. 105, 139-145.

Martin,S.G., Leclerc,V., Smith-Litiere,K., and St Johnston,D. (2003). The identification of novel genes required for Drosophila anteroposterior axis formation in a germline clone screen using GFP-Staufen. Development 130, 4201-4215.

Martinez-Menarguez,J.A., Geuze,H.J., Slot,J.W., and Klumperman,J. (1999). Vesicular tubular clusters between the ER and Golgi mediate concentration of soluble secretory proteins by exclusion from COPI-coated vesicles. Cell 98, 81-90.

Martoglio,B. (2003). Intramembrane proteolysis and post-targeting functions of signal peptides. Biochem. Soc. Trans. 31, 1243-1247.

Martoglio,B. and Dobberstein,B. (1998). Signal sequences: more than just greasy peptides. Trends Cell Biol. 8, 410-415.

Matsuura-Tokita,K., Takeuchi,M., Ichihara,A., Mikuriya,K., and Nakano,A. (2006). Live imaging of yeast Golgi cisternal maturation. Nature.

Mendez,R. and Richter,J.D. (2001). Translational control by CPEB: a means to the end. Nat. Rev. Mol. Cell Biol. 2, 521-529.

Mesngon,M.T., Tarricone,C., Hebbar,S., Guillotte,A.M., Schmitt,E.W., Lanier,L., Musacchio,A., King,S.J., and Smith,D.S. (2006). Regulation of cytoplasmic dynein ATPase by Lis1. J. Neurosci. 26, 2132-2139.

Meyer,D.I. and Dobberstein,B. (1980). Identification and characterization of a membrane component essential for the translocation of nascent proteins across the membrane of the endoplasmic reticulum. J. Cell Biol. 87, 503-508.

Micklem,D.R., Adams,J., Grunert,S., and St Johnston,D. (2000). Distinct roles of two conserved Staufen domains in oskar mRNA localization and translation. EMBO J. 19, 1366-1377.

Mignone,F., Gissi,C., Liuni,S., and Pesole,G. (2002). Untranslated regions of mRNAs. Genome Biol. 3, REVIEWS0004.

Miki,H., Setou,M., Kaneshiro,K., and Hirokawa,N. (2001). All kinesin superfamily protein, KIF, genes in mouse and human. Proc. Natl. Acad. Sci. U. S. A 98, 7004-7011.

Miller,E.A., Liu,Y., Barlowe,C., and Schekman,R. (2005a). ER-Golgi transport defects are associated with mutations in the Sed5p-binding domain of the COPII coat subunit, Sec24p. Mol. Biol. Cell 16, 3719-3726.

Miller,K.E., DeProto,J., Kaufmann,N., Patel,B.N., Duckworth,A., and Van Vactor,D. (2005b). Direct observation demonstrates that Liprin-alpha is required for trafficking of synaptic vesicles. Curr. Biol. 15, 684-689.

Mironov,A.A., Beznoussenko,G.V., Nicoziani,P., Martella,O., Trucco,A., Kweon,H.S., Di Giandomenico,D., Polishchuk,R.S., Fusella,A., Lupetti,P., Berger,E.G., Geerts,W.J., Koster,A.J., Burger,K.N., and Luini,A. (2001). Small cargo proteins and large aggregates can traverse the Golgi by a common mechanism without leaving the lumen of cisternae. J. Cell Biol. 155, 1225-1238.

Miura,G.I. and Treisman,J.E. (2006). Lipid modification of secreted signaling proteins. Cell Cycle 5, 1184-1188.

Mizuno,N., Toba,S., Edamatsu,M., Watai-Nishii,J., Hirokawa,N., Toyoshima,Y.Y., and Kikkawa,M. (2004). Dynein and kinesin share an overlapping microtubule-binding site. EMBO J. 23, 2459-2467.

Mogelsvang,S., Gomez-Ospina,N., Soderholm,J., Glick,B.S., and Staehelin,L.A. (2003). Tomographic evidence for continuous turnover of Golgi cisternae in Pichia pastoris. Mol. Biol. Cell 14, 2277-2291.

Mossessova,E., Bickford,L.C., and Goldberg,J. (2003). SNARE selectivity of the COPII coat. Cell 114, 483-495.

Munro,S. (2001). What can yeast tell us about N-linked glycosylation in the Golgi apparatus? FEBS Lett. 498, 223-227.

Munro,T.P., Magee,R.J., Kidd,G.J., Carson,J.H., Barbarese,E., Smith,L.M., and Smith,R. (1999). Mutational analysis of a heterogeneous nuclear ribonucleoprotein A2 response element for RNA trafficking. J. Biol. Chem. 274, 34389-34395.

Musch,A. (2004). Microtubule organization and function in epithelial cells. Traffic. 5, 1-9.

Nagai,K. (1996). RNA-protein complexes. Curr. Opin. Struct. Biol. 6, 53-61.

Nakamura,A., Amikura,R., Hanyu,K., and Kobayashi,S. (2001). Me31B silences translation of oocyte-localizing RNAs through the formation of cytoplasmic RNP complex during Drosophila oogenesis. Development 128, 3233-3242.

Navarro,C., Puthalakath,H., Adams,J.M., Strasser,A., and Lehmann,R. (2004). Egalitarian binds dynein light chain to establish oocyte polarity and maintain oocyte fate. Nat. Cell Biol. 6, 427-435.

Navarro,R.E. and Blackwell,T.K. (2005). Requirement for P granules and meiosis for accumulation of the germline RNA helicase CGH-1. Genesis. 42, 172-180.

Neuman-Silberberg,F.S. and Schupbach,T. (1993). The Drosophila dorsoventral patterning gene gurken produces a dorsally localized RNA and encodes a TGF alpha-like protein. Cell 75, 165-174.

Neuman-Silberberg,F.S. and Schupbach,T. (1994). Dorsoventral axis formation in Drosophila depends on the correct dosage of the gene gurken. Development 120, 2457-2463.

Neuman-Silberberg,F.S. and Schupbach,T. (1996). The Drosophila TGF-alpha-like protein Gurken: expression and cellular localization during Drosophila oogenesis. Mech. Dev. 59, 105-113.

Neumann,U., Brandizzi,F., and Hawes,C. (2003). Protein transport in plant cells: in and out of the Golgi. Ann. Bot. (Lond) 92, 167-180.

Ni,X., Canuel,M., and Morales,C.R. (2006). The sorting and trafficking of lysosomal proteins. Histol. Histopathol. 21, 899-913.

Niessing,D., Blanke,S., and Jackle,H. (2002). Bicoid associates with the 5'-cap-bound complex of caudal mRNA and represses translation. Genes Dev. 16, 2576-2582.

Niessing,D., Huttelmaier,S., Zenklusen,D., Singer,R.H., and Burley,S.K. (2004). She2p is a novel RNA binding protein with a basic helical hairpin motif. Cell 119, 491-502.

Nilsson,T., Slusarewicz,P., Hoe,M.H., and Warren,G. (1993). Kin recognition. A model for the retention of Golgi enzymes. FEBS Lett. 330, 1-4.

Norvell,A., Debec,A., Finch,D., Gibson,L., and Thoma,B. (2005). Squid is required for efficient posterior localization of oskar mRNA during Drosophila oogenesis. Dev. Genes Evol. 215, 340-349.

Norvell,A., Kelley,R.L., Wehr,K., and Schupbach,T. (1999). Specific isoforms of squid, a Drosophila hnRNP, perform distinct roles in Gurken localization during oogenesis. Genes Dev. 13, 864-876.

Nover,L., Scharf,K.D., and Neumann,D. (1989). Cytoplasmic heat shock granules are formed from precursor particles and are associated with a specific set of mRNAs. Mol. Cell Biol. 9, 1298-1308.

Novick,P., Field,C., and Schekman,R. (1980). Identification of 23 complementation groups required for post-translational events in the yeast secretory pathway. Cell 21, 205-215.

Novikoff,P.M., Novikoff,A.B., Quintana,N., and Hauw,J.J. (1971). Golgi apparatus, GERL, and lysosomes of neurons in rat dorsal root ganglia, studied by thick section and thin section cytochemistry. J. Cell Biol. 50, 859-886.

Nusslein-Volhard,C. (1991). Determination of the embryonic axes of Drosophila. Dev. Suppl 1, 1-10.

Okun,M.M. and Shields,D. (1992). Translocation of preproinsulin across the endoplasmic reticulum membrane. The relationship between nascent polypeptide size and extent of signal recognition particle-mediated inhibition of protein synthesis. J. Biol. Chem. 267, 11476-11482.

Oleynikov,Y. and Singer,R.H. (2003). Real-time visualization of ZBP1 association with beta-actin mRNA during transcription and localization. Curr. Biol. 13, 199-207.

Orci,L., Malhotra,V., Amherdt,M., Serafini,T., and Rothman,J.E. (1989). Dissection of a single round of vesicular transport: sequential intermediates for intercisternal movement in the Golgi stack. Cell 56, 357-368.

Orci,L., Ravazzola,M., Amherdt,M., Perrelet,A., Powell,S.K., Quinn,D.L., and Moore,H.P. (1987). The trans-most cisternae of the Golgi complex: a compartment for sorting of secretory and plasma membrane proteins. Cell 51, 1039-1051.

Orci,L., Ravazzola,M., Meda,P., Holcomb,C., Moore,H.P., Hicke,L., and Schekman,R. (1991). Mammalian Sec23p homologue is restricted to the endoplasmic reticulum transitional cytoplasm. Proc. Natl. Acad. Sci. U. S. A 88, 8611-8615.

Orci,L., Stamnes,M., Ravazzola,M., Amherdt,M., Perrelet,A., Sollner,T.H., and Rothman,J.E. (1997). Bidirectional transport by distinct populations of COPI-coated vesicles. Cell 90, 335-349.

Otte,S., Belden,W.J., Heidtman,M., Liu,J., Jensen,O.N., and Barlowe,C. (2001). Erv41p and Erv46p: new components of COPII vesicles involved in transport between the ER and Golgi complex. J. Cell Biol. 152, 503-518.

Palacios,I.M. and St Johnston,D. (2001). Getting the message across: the intracellular localization of mRNAs in higher eukaryotes. Annu. Rev. Cell Dev. Biol. 17, 569-614.

Papoulas,O., Hays,T.S., and Sisson,J.C. (2005). The golgin Lava lamp mediates dynein-based Golgi movements during Drosophila cellularization. Nat. Cell Biol. 7, 612-618.

Parker,R. and Song,H. (2004). The enzymes and control of eukaryotic mRNA turnover. Nat. Struct. Mol. Biol. 11, 121-127.

Parodi,A.J. (2000). Role of N-oligosaccharide endoplasmic reticulum processing reactions in glycoprotein folding and degradation. Biochem. J. 348 Pt 1, 1-13.

Pecot,M.Y. and Malhotra,V. (2004). Golgi membranes remain segregated from the endoplasmic reticulum during mitosis in mammalian cells. Cell 116, 99-107.

Pelham,H.R. and Rothman,J.E. (2000). The debate about transport in the Golgi--two sides of the same coin? Cell 102, 713-719.

Pelletier,J. and Sonenberg,N. (1987). The involvement of mRNA secondary structure in protein synthesis. Biochem. Cell Biol. 65, 576-581.

Piccioni,F., Zappavigna,V., and Verrotti,A.C. (2005). Translational regulation during oogenesis and early development: the cap-poly(A) tail relationship. C. R. Biol. 328, 863-881.

Ponnambalam,S. and Baldwin,S.A. (2003). Constitutive protein secretion from the trans-Golgi network to the plasma membrane. Mol. Membr. Biol. 20, 129-139.

Powers,J. and Barlowe,C. (1998). Transport of axl2p depends on erv14p, an ER-vesicle protein related to the Drosophila cornichon gene product. J. Cell Biol. 142, 1209-1222.

Prescott,A.R., Farmaki,T., Thomson,C., James,J., Paccaud,J.P., Tang,B.L., Hong,W., Quinn,M., Ponnambalam,S., and Lucocq,J. (2001). Evidence for prebudding arrest of ER export in animal cell mitosis and its role in generating Golgi partitioning intermediates. Traffic. 2, 321-335.

Presley,J.F., Cole,N.B., Schroer,T.A., Hirschberg,K., Zaal,K.J., and Lippincott-Schwartz,J. (1997). ER-to-Golgi transport visualized in living cells. Nature 389, 81-85.

Puri,S. and Linstedt,A.D. (2003). Capacity of the golgi apparatus for biogenesis from the endoplasmic reticulum. Mol. Biol. Cell 14, 5011-5018.

Queenan,A.M., Barcelo,G., Van Buskirk,C., and Schupbach,T. (1999). The transmembrane region of Gurken is not required for biological activity, but is necessary for transport to the oocyte membrane in Drosophila. Mech. Dev. 89, 35-42.

Rabouille,C. and Klumperman,J. (2005). Opinion: The maturing role of COPI vesicles in intra-Golgi transport. Nat. Rev. Mol. Cell Biol. 6, 812-817.

Rabouille,C., Misteli,T., Watson,R., and Warren,G. (1995). Reassembly of Golgi stacks from mitotic Golgi fragments in a cell-free system. J. Cell Biol. 129, 605-618.

Raff,J.W., Whitfield,W.G., and Glover,D.M. (1990). Two distinct mechanisms localise cyclin B transcripts in syncytial Drosophila embryos. Development 110, 1249-1261.

Rambourg,A., Clermont,Y., and Marraud,A. (1974). Three-dimensional structure of the osmium-impregnated Golgi apparatus as seen in the high voltage electron microscope. Am. J. Anat. 140, 27-45.

Ramos,A., Grunert,S., Adams,J., Micklem,D.R., Proctor,M.R., Freund,S., Bycroft,M., St Johnston,D., and Varani,G. (2000). RNA recognition by a Staufen double-stranded RNA-binding domain. EMBO J. 19, 997-1009.

Raught,B. and Gingras,A.C. (1999). eIF4E activity is regulated at multiple levels. Int. J. Biochem. Cell Biol. 31, 43-57.

Roberg,K.J., Crotwell,M., Espenshade,P., Gimeno,R., and Kaiser,C.A. (1999). LST1 is a SEC24 homologue used for selective export of the plasma membrane ATPase from the endoplasmic reticulum. J. Cell Biol. 145, 659-672.

Rodriguez-Boulan,E. and Musch,A. (2005). Protein sorting in the Golgi complex: shifting paradigms. Biochim. Biophys. Acta 1744, 455-464.

Rogalski,A.A. and Singer,S.J. (1984). Associations of elements of the Golgi apparatus with microtubules. J. Cell Biol. 99, 1092-1100.

Rook,M.S., Lu,M., and Kosik,K.S. (2000). CaMKIIalpha 3' untranslated region-directed mRNA translocation

in living neurons: visualization by GFP linkage. J. Neurosci. 20, 6385-6393.
Ross,A.F., Oleynikov,Y., Kislauskis,E.H., Taneja,K.L., and Singer,R.H. (1997). Characterization of a beta-actin mRNA zipcode-binding protein. Mol. Cell Biol. 17, 2158-2165.
Rossanese,O.W., Soderholm,J., Bevis,B.J., Sears,I.B., O'Connor,J., Williamson,E.K., and Glick,B.S. (1999). Golgi structure correlates with transitional endoplasmic reticulum organization in Pichia pastoris and Saccharomyces cerevisiae. J. Cell Biol. 145, 69-81.
Roth,S. (2003). The origin of dorsoventral polarity in Drosophila. Philos. Trans. R. Soc. Lond B Biol. Sci. 358, 1317-1329.
Roth,S., Neuman-Silberberg,F.S., Barcelo,G., and Schupbach,T. (1995). cornichon and the EGF receptor signaling process are necessary for both anterior-posterior and dorsal-ventral pattern formation in Drosophila. Cell 81, 967-978.
Rothblatt,J.A., Deshaies,R.J., Sanders,S.L., Daum,G., and Schekman,R. (1989). Multiple genes are required for proper insertion of secretory proteins into the endoplasmic reticulum in yeast. J. Cell Biol. 109, 2641-2652.
Rothman,J.E. (1994). Intracellular membrane fusion. Adv. Second Messenger Phosphoprotein Res. 29, 81-96.
Rothman,J.E. and Orci,L. (1990). Movement of proteins through the Golgi stack: a molecular dissection of vesicular transport. FASEB J. 4, 1460-1468.
Royzman,I., Hayashi-Hagihara,A., Dej,K.J., Bosco,G., Lee,J.Y., and Orr-Weaver,T.L. (2002). The E2F cell cycle regulator is required for Drosophila nurse cell DNA replication and apoptosis. Mech. Dev. 119, 225-237.
Sakato,M. and King,S.M. (2004). Design and regulation of the AAA+ microtubule motor dynein. J. Struct. Biol. 146, 58-71.
Salaun,C., James,D.J., Greaves,J., and Chamberlain,L.H. (2004). Plasma membrane targeting of exocytic SNARE proteins. Biochim. Biophys. Acta 1693, 81-89.
Sandoval,I.V., Bonifacino,J.S., Klausner,R.D., Henkart,M., and Wehland,J. (1984). Role of microtubules in the organization and localization of the Golgi apparatus. J. Cell Biol. 99, 113s-118s.
Scales,S.J., Pepperkok,R., and Kreis,T.E. (1997). Visualization of ER-to-Golgi transport in living cells reveals a sequential mode of action for COPII and COPI. Cell 90, 1137-1148.
Schisa,J.A., Pitt,J.N., and Priess,J.R. (2001). Analysis of RNA associated with P granules in germ cells of C. elegans adults. Development 128, 1287-1298.
Schroer,T.A. (2004). Dynactin. Annu. Rev. Cell Dev. Biol. 20, 759-779.
Schupbach,T. (1987). Germ line and soma cooperate during oogenesis to establish the dorsoventral pattern of egg shell and embryo in Drosophila melanogaster. Cell 49, 699-707.
Schupbach,T. and Roth,S. (1994). Dorsoventral patterning in Drosophila oogenesis. Curr. Opin. Genet. Dev. 4, 502-507.
Schweizer,A., Fransen,J.A., Matter,K., Kreis,T.E., Ginsel,L., and Hauri,H.P. (1990). Identification of an intermediate compartment involved in protein transport from endoplasmic reticulum to Golgi apparatus. Eur. J. Cell Biol. 53, 185-196.
Seaman,M.N. (2004). Cargo-selective endosomal sorting for retrieval to the Golgi requires retromer. J. Cell Biol. 165, 111-122.
Seemann,J., Jokitalo,E., Pypaert,M., and Warren,G. (2000). Matrix proteins can generate the higher order architecture of the Golgi apparatus. Nature 407, 1022-1026.
Seemann,J., Pypaert,M., Taguchi,T., Malsam,J., and Warren,G. (2002). Partitioning of the matrix fraction of the Golgi apparatus during mitosis in animal cells. Science 295, 848-851.
Shepard,K.A., Gerber,A.P., Jambhekar,A., Takizawa,P.A., Brown,P.O., Herschlag,D., DeRisi,J.L., and Vale,R. D. (2003). Widespread cytoplasmic mRNA transport in yeast: identification of 22 bud-localized transcripts using DNA microarray analysis. Proc. Natl. Acad. Sci. U. S. A 100, 11429-11434.
Sheth,U. and Parker,R. (2003). Decapping and decay of messenger RNA occur in cytoplasmic processing bodies. Science 300, 805-808.
Sheth,U. and Parker,R. (2006). Targeting of aberrant mRNAs to cytoplasmic processing bodies. Cell 125, 1095-1109.
Shima,D.T., Haldar,K., Pepperkok,R., Watson,R., and Warren,G. (1997). Partitioning of the Golgi apparatus during mitosis in living HeLa cells. J. Cell Biol. 137, 1211-1228.
Short,B. and Barr,F.A. (2000). The Golgi apparatus. Curr. Biol. 10, R583-R585.
Short,B., Preisinger,C., Korner,R., Kopajtich,R., Byron,O., and Barr,F.A. (2001). A GRASP55-rab2 effector complex linking Golgi structure to membrane traffic. J. Cell Biol. 155, 877-883.
Shorter,J. and Warren,G. (2002). Golgi architecture and inheritance. Annu. Rev. Cell Dev. Biol. 18, 379-420.
Shyu,A.B. and Wilkinson,M.F. (2000). The double lives of shuttling mRNA binding proteins. Cell 102, 135-138.
Slusarewicz,P., Nilsson,T., Hui,N., Watson,R., and Warren,G. (1994). Isolation of a matrix that binds medial Golgi enzymes. J. Cell Biol. 124, 405-413.
Smith,R. (2004). Moving molecules: mRNA trafficking in Mammalian oligodendrocytes and neurons.

Neuroscientist. 10, 495-500.
Speel,E.J. (1999). Robert Feulgen Prize Lecture 1999. Detection and amplification systems for sensitive, multiple-target DNA and RNA in situ hybridization: looking inside cells with a spectrum of colors. Histochem. Cell Biol. 112, 89-113.
Spradling,A.C. (1993). Germline cysts: communes that work. Cell 72, 649-651.
St Johnston,D. (2005). Moving messages: the intracellular localization of mRNAs. Nat. Rev. Mol. Cell Biol. 6, 363-375.
St Johnston,D., Beuchle,D., and Nusslein-Volhard,C. (1991). Staufen, a gene required to localize maternal RNAs in the Drosophila egg. Cell 66, 51-63.
Stawowy,P. and Fleck,E. (2005). Proprotein convertases furin and PC5: targeting atherosclerosis and restenosis at multiple levels. J. Mol. Med. 83, 865-875.
Stebbins-Boaz,B., Cao,Q., de Moor,C.H., Mendez,R., and Richter,J.D. (1999). Maskin is a CPEB-associated factor that transiently interacts with elF-4E. Mol. Cell 4, 1017-1027.
Stebbins-Boaz,B. and Richter,J.D. (1997). Translational control during early development. Crit Rev. Eukaryot. Gene Expr. 7, 73-94.
Steiner,D.F. and James,D.E. (1992). Cellular and molecular biology of the beta cell. Diabetologia 35 Suppl 2, S41-S48.
Stephens,D.J., Lin-Marq,N., Pagano,A., Pepperkok,R., and Paccaud,J.P. (2000). COPI-coated ER-to-Golgi transport complexes segregate from COPII in close proximity to ER exit sites. J. Cell Sci. 113 (Pt 12), 2177-2185.
Struhl,G. (1989). Morphogen gradients and the control of body pattern in insect embryos. Ciba Found. Symp. 144, 65-86.
Susalka,S.J., Hancock,W.O., and Pfister,K.K. (2000). Distinct cytoplasmic dynein complexes are transported by different mechanisms in axons. Biochim. Biophys. Acta 1496, 76-88.
Swan,A., Nguyen,T., and Suter,B. (1999). Drosophila Lissencephaly-1 functions with Bic-D and dynein in oocyte determination and nuclear positioning. Nat. Cell Biol. 1, 444-449.
Swanton,E. and Bulleid,N.J. (2003). Protein folding and translocation across the endoplasmic reticulum membrane. Mol. Membr. Biol. 20, 99-104.
Swiger,R.R. and Tucker,J.D. (1996). Fluorescence in situ hybridization: a brief review. Environ. Mol. Mutagen. 27, 245-254.
Tang,B.L., Kausalya,J., Low,D.Y., Lock,M.L., and Hong,W. (1999). A family of mammalian proteins homologous to yeast Sec24p. Biochem. Biophys. Res. Commun. 258, 679-684.
Tang,B.L., Wang,Y., Ong,Y.S., and Hong,W. (2005). COPII and exit from the endoplasmic reticulum. Biochim. Biophys. Acta 1744, 293-303.
Tautz,D. and Pfeifle,C. (1989). A non-radioactive in situ hybridization method for the localization of specific RNAs in Drosophila embryos reveals translational control of the segmentation gene hunchback. Chromosoma 98, 81-85.
Teixeira,D., Sheth,U., Valencia-Sanchez,M.A., Brengues,M., and Parker,R. (2005). Processing bodies require RNA for assembly and contain nontranslating mRNAs. RNA. 11, 371-382.
Tekirian,T.L. (2002). The central role of the trans-Golgi network as a gateway of the early secretory pathway: physiologic vs nonphysiologic protein transit. Exp. Cell Res. 281, 9-18.
Theurkauf,W.E., Smiley,S., Wong,M.L., and Alberts,B.M. (1992). Reorganization of the cytoskeleton during Drosophila oogenesis: implications for axis specification and intercellular transport. Development 115, 923-936.
Thio,G.L., Ray,R.P., Barcelo,G., and Schupbach,T. (2000). Localization of gurken RNA in Drosophila oogenesis requires elements in the 5' and 3' regions of the transcript. Dev. Biol. 221, 435-446.
Thomas,M.G., Martinez Tosar,L.J., Loschi,M., Pasquini,J.M., Correale,J., Kindler,S., and Boccaccio,G.L. (2005). Staufen recruitment into stress granules does not affect early mRNA transport in oligodendrocytes. Mol. Biol. Cell 16, 405-420.
Torres,I.L., Lopez-Schier,H., and St Johnston,D. (2003). A Notch/Delta-dependent relay mechanism establishes anterior-posterior polarity in Drosophila. Dev. Cell 5, 547-558.
Traub,L.M. and Kornfeld,S. (1997). The trans-Golgi network: a late secretory sorting station. Curr. Opin. Cell Biol. 9, 527-533.
Urban,S., Lee,J.R., and Freeman,M. (2001). Drosophila rhomboid-1 defines a family of putative intramembrane serine proteases. Cell 107, 173-182.
Urban,S., Lee,J.R., and Freeman,M. (2002). A family of Rhomboid intramembrane proteases activates all Drosophila membrane-tethered EGF ligands. EMBO J. 21, 4277-4286.
Vale,R.D., Reese,T.S., and Sheetz,M.P. (1985). Identification of a novel force-generating protein, kinesin, involved in microtubule-based motility. Cell 42, 39-50.
van Anken,E. and Braakman,I. (2005). Versatility of the endoplasmic reticulum protein folding factory. Crit Rev. Biochem. Mol. Biol. 40, 191-228.
Van de Bor,V. and Davis,I. (2004). mRNA localisation gets more complex. Curr. Opin. Cell Biol. 16, 300-307.

Van De Bor,V., Hartswood,E., Jones,C., Finnegan,D., and Davis,I. (2005). gurken and the I factor retrotransposon RNAs share common localization signals and machinery. Dev. Cell 9, 51-62.

van Meer,G. and Simons,K. (1988). Lipid polarity and sorting in epithelial cells. J. Cell Biochem. 36, 51-58.

van Minnen,J. (1994). Axonal localization of neuropeptide-encoding mRNA in identified neurons of the snail Lymnaea stagnalis. Cell Tissue Res. 276, 155-161.

Verbert,A., Cacan,R., and Cecchelli,R. (1987). Membrane transport of sugar donors to the glycosylation sites. Biochimie 69, 91-99.

Voeltz,G.K., Rolls,M.M., and Rapoport,T.A. (2002). Structural organization of the endoplasmic reticulum. EMBO Rep. 3, 944-950.

Walter,P. and Blobel,G. (1980). Purification of a membrane-associated protein complex required for protein translocation across the endoplasmic reticulum. Proc. Natl. Acad. Sci. U. S. A 77, 7112-7116.

Walter,P. and Blobel,G. (1981). Translocation of proteins across the endoplasmic reticulum III. Signal recognition protein (SRP) causes signal sequence-dependent and site-specific arrest of chain elongation that is released by microsomal membranes. J. Cell Biol. 91, 557-561.

Wang,H., Iacoangeli,A., Popp,S., Muslimov,I.A., Imataka,H., Sonenberg,N., Lomakin,I.B., and Tiedge,H. (2002). Dendritic BC1 RNA: functional role in regulation of translation initiation. J. Neurosci. 22, 10232-10241.

Wang,S. and Hazelrigg,T. (1994). Implications for bcd mRNA localization from spatial distribution of exu protein in Drosophila oogenesis. Nature 369, 400-403.

Wells,S.E., Hillner,P.E., Vale,R.D., and Sachs,A.B. (1998). Circularization of mRNA by eukaryotic translation initiation factors. Mol. Cell 2, 135-140.

Wells,W.A. (2001). Let's make Golgi. J. Cell Biol. 155, 498-499.

Wickens,M. and Goldstrohm,A. (2003). Molecular biology. A place to die, a place to sleep. Science 300, 753-755.

Wickner,W. and Schekman,R. (2005). Protein translocation across biological membranes. Science 310, 1452-1456.

Wilczynska,A., Aigueperse,C., Kress,M., Dautry,F., and Weil,D. (2005). The translational regulator CPEB1 provides a link between dcp1 bodies and stress granules. J. Cell Sci. 118, 981-992.

Wilkie,G.S. and Davis,I. (2001). Drosophila wingless and pair-rule transcripts localize apically by dynein-mediated transport of RNA particles. Cell 105, 209-219.

Wilsch-Brauninger,M., Schwarz,H., and Nusslein-Volhard,C. (1997). A sponge-like structure involved in the association and transport of maternal products during Drosophila oogenesis. J. Cell Biol. 139, 817-829.

Wolpert,L. (1994). Positional information and pattern formation in development. Dev. Genet. 15, 485-490.

Wu,L., Wells,D., Tay,J., Mendis,D., Abbott,M.A., Barnitt,A., Quinlan,E., Heynen,A., Fallon,J.R., and Richter,J. D. (1998). CPEB-mediated cytoplasmic polyadenylation and the regulation of experience-dependent translation of alpha-CaMKII mRNA at synapses. Neuron 21, 1129-1139.

Xi,R., McGregor,J.R., and Harrison,D.A. (2003). A gradient of JAK pathway activity patterns the anterior-posterior axis of the follicular epithelium. Dev. Cell 4, 167-177.

Zalfa,F., Adinolfi,S., Napoli,I., Kuhn-Holsken,E., Urlaub,H., Achsel,T., Pastore,A., and Bagni,C. (2005). Fragile X mental retardation protein (FMRP) binds specifically to the brain cytoplasmic RNAs BC1/BC200 via a novel RNA-binding motif. J. Biol. Chem. 280, 33403-33410.

Zeuschner,D., Geerts,W.J., van Donselaar,E., Humbel,B.M., Slot,J.W., Koster,A.J., and Klumperman,J. (2006). Immuno-electron tomography of ER exit sites reveals the existence of free COPII-coated transport carriers. Nat. Cell Biol. 8, 377-383.

Zhang,H.L., Eom,T., Oleynikov,Y., Shenoy,S.M., Liebelt,D.A., Dictenberg,J.B., Singer,R.H., and Bassell,G. J. (2001). Neurotrophin-induced transport of a beta-actin mRNP complex increases beta-actin levels and stimulates growth cone motility. Neuron 31, 261-275.

CHAPTER 2

mRNA localization and ER-based protein sorting mechanisms dictate the use of transitional Endoplasmic Reticulum-Golgi units involved in Gurken transport in *Drosophila* oocytes

Bram Herpers and Catherine Rabouille

The Cell Microscopy Centre, Dept. of Cell Biology, University Medical Centre Utrecht,
AZU Rm G02.525, Heidelberglaan 100, 3584 CX Utrecht, The Netherlands

MOL. BIOL. CELL, 2004. 15(12): P. 5306-17

Abstract

The anteroposterior and dorsoventral axes of the future embryo are specified within *Drosophila* oocytes by localizing *gurken* mRNA, which targets the secreted Gurken transforming growth factor-α synthesis and transport to the same site. A key question is whether *gurken* mRNA is targeted to a specialized exocytic pathway to achieve the polar deposition of the protein. Here, we show, by (immuno)electron microscopy, that the exocytic pathway in stage 9-10 *Drosophila* oocytes comprises a thousand evenly distributed transitional endoplasmic reticulum (tER)-Golgi units. Using *Drosophila* mutants, we show that it is the localization of *gurken* mRNA coupled to efficient sorting of Gurken out of the ER that determines which of the numerous equivalent tER-Golgi units are used for the protein transport and processing. The choice of tER-Golgi units by mRNA localization makes them independent of each other, and represents a non-conventional way, by which the oocyte implements polarized deposition of transmembrane/secreted proteins. We propose that this pre-translational mechanism could be a general way for targeted secretion in polarized cells, such as neurons.

Introduction

Polarized localization of proteins is achieved by at least two different mechanisms. The first one relies on restricted localization of mRNAs that encode cytosolic proteins, allowing local protein translation, thus creating differential protein activity and generating cell asymmetry and polarity (Bashirullah et al., 1998). This is, for instance, the case of *actin* mRNA localization in the nerve terminal of neurons (Lee and Hollenbeck, 2003), *oskar* localization at the posterior pole of *Drosophila* oocytes (Ephrussi et al., 1991), and *ASH1* localization in dividing yeast cells (Long et al., 1997). On the other hand, the mechanism ensuring the polarized deposition of transmembrane or secreted proteins is thought, in mammalian cells, to be achieved by post-translational sorting events in the t*rans*-Golgi network (TGN). There, signals in their cytoplasmic tail or lumenal domain are deciphered, resulting in the directed movement of specialized transport vesicles to allow specific deposition at the apical or basolateral plasma membrane of epithelial cells (Ikonen and Simons, 1998; Nelson and Yeaman, 2001).

However, there is a growing number of transmembrane and secreted proteins for which their transcript also exhibits a restricted localization. The transcript for the yeast plasma membrane protein Ist2 is actively transported along the acto-myosin network to the bud tip (Takizawa et al., 2000), and the protein is deposited locally (Juschke et al., 2004). *wingless* mRNA is localized apically in epithelial cells (Simmonds et al., 2001). In a stage 9-10 *Drosophila* oocyte, *gurken* mRNA is transported and deposited exclusively in the dorsal/anterior corner (D/A; (Neuman-Silberberg and Schupbach, 1993); Figure 1B). *gurken* encodes a protein that is synthesized in the endoplasmic reticulum (ER) as a 285-amino acid type I transmembrane protein precursor, and transported to the Golgi apparatus where it is cleaved off by a specific protease, Brother of Rhomboid (Guichard et al., 2000; Ghiglione et al., 2002; Urban et al., 2002), generating a lumenal fragment belonging to the transforming growth factor-α family. This fragment is transported and released by exocytosis at the D/A corner in the intercellular space between the oocyte and the overlying follicle cells. There, it binds the epidermal growth factor receptor Torpedo in the plasma membrane of these follicle cells and induces a signaling cascade, so that they adopt their dorsal fate (van Eeden and St Johnston, 1999; Roth, 2003).

A key question regarding the restricted localization of transcripts encoding transmembrane/secreted proteins is how synthesis and transport is achieved, and whether they are sustained by a specialized exocytic pathway, near to where the transcripts are localized. We focus here on Gurken in *Drosophila* oocytes to address this issue.

In mammalian cells, the exocytic pathway comprises the continuous membrane bound organelle comprising a single lumen, the ER, where proteins destined to the extracellular medium and all membrane compartments of the cell (except mitochondria) are synthesized. Newly synthesized proteins exit the ER at numerous specialized ER exit sites, characterized by the presence of COPII-coated structures (also called transitional ER sites, tER sites) (Barlowe et al., 1994; Bonifacino and Glick, 2004). The proteins reach the Golgi apparatus, a single copy organelle of striking morphology that comprises dozens of stacked Golgi cisternae, linked together by tubules to form a single large reticulum capping the nucleus (Mellman and Warren, 2000). It is the organelle where the newly synthesized proteins are post-translationally modified and processed before reaching the TGN, where they are dispatched toward their correct final destination. The exocytic pathway is believed to function synchronously, that is, all the ER exit sites and all the stacks of the Golgi reticulum are involved in the transport of all proteins newly synthesised in the ER. Even in polarized cells, transmembrane proteins destined for the apical

or basolateral plasma membrane are thought to be synthesised and transported together till they reach the TGN, where they are sorted from one another to their appropriate location.

In *Drosophila*, the Golgi apparatus does not always exhibit a morphology of stacked cisternae. For instance, in imaginal discs of third instars, follicle cells of egg chambers and syncitial embryos, it forms as a cluster of vesicles and tubules that are positive for several Golgi markers (Ripoche et al., 1994; Kondylis et al., 2001; Kondylis and Rabouille, 2003). Furthermore, the Golgi stacks when present are not linked together to form a single copy organelle. Instead, they are dispersed in the cytoplasm as it is in yeast (Rossanese et al., 1999) and plants (Boevink et al., 1998). Whatever the morphology of the Golgi apparatus, they are in very close proximity to tER sites marked by the COPII subunit, dSec23p. The resulting membrane structure (one tER site and one Golgi complex, found in the concavity of an ER cisterna, Figure 1C) is what we call a tER-Golgi unit, as it has been described in the yeast *Pichia pastoris* (Mogelsvang et al., 2003). In *Drosophila* S2 cells, their number is definite (~20) (Kondylis and Rabouille, 2003).

We show here that the organization of the exocytic pathway in a stage 9-10 *Drosophila* oocyte (see (King, 1970) for a description of the developmental stages) is the same as in *Drosophila* S2 cells, comprising multiple, seemingly identical tER-Golgi units (but now up to 1000) that are evenly distributed throughout the cell cytoplasm. We show that only a subset of them, situated at the D/A corner, are involved in the transport, processing and deposition of Gurken protein as described above. And we show, by using three *Drosophila* mutants in which *gurken* mRNA is mislocalized, that what controls the choice of the tER-Golgi units involved in Gurken transport, among the thousand present, is the localization of *gurken* mRNA. This pre-translational mechanism is coupled to post-translational sorting events involving Cornichon and the transmembrane domain of Gurken that prevent its diffusion in the ER away from the D/A corner, and ensures its efficient sorting to the tER-Golgi units at that same corner.

Together, these results suggest that tER-Golgi units can function independently from one another and that it is the mRNA localization coupled to sorting events in the ER that dictate their use to achieve polar distribution of transmembrane proteins.

Materials and Methods

Fly stocks

Oregon R and W^{1118} are wild-type *Drosophila melanogaster*. Mutant fly stocks used are dCOG5-GFP (w;GFP-Fws/Cyo) (Farkas *et al*., 2003); PDI-GFP (PDI::GFP/GFP-TM3,Sb) (Bobinnec *et al*., 2003); *K10* (y[1] fs(1)K10[4] cv[1] v[1] f[1]/FM0) (Bloomington *Drosophila* Stock Centre); *squid*^{1} (Sqd^{1}/TM3, Sb Ser) (Norvell *et al*., 1999); cni^{AR55} (b cni^{AR55} pr cn/Cyo), cni^{CF5} (b cni^{CF5} pr cn wx bw/Cyo) and cni^{AA12} (b cni^{AA12}/Cyo) (Roth *et al*., 1995); grk^{2B6} (grk[2B6]b cn s L bo/Cyo) and grk^{2E12} (w; grk[2E12]b/Cyo) (Neuman-Silberberg and Schupbach, 1993); and fly lines expressing Gurken lacking the transmembrane and the cytoplasmic domain, gΔTC4.1, and the cytoplasmic domain gΔC100 (Queenan *et al*., 1999). The stocks carrying the constructs encoding the truncated versions of Gurken proteins were crossed into the grk^{2B6} background and females from this cross were mated with male grk^{2E12} to yield orange-eyed black flies (gΔTC4.1; grk^{2B6}/grk^{2E12} and gΔC100; grk^{2B6}/grk^{2E12}). All are raised on normal cornmeal-agar medium at 25°C. The *merlin* thermosensitive mutant yw ts594 (*mer*^{ts1}, MacDougall *et al*., 2001) was induced by shifting virgin flies to 29°C for 3 d. Ovaries were prepared by dissecting 2- to 3-d-old females (fed with extra yeast) in *Drosophila* Ringer buffer. They were transferred to the appropriate fixatives as whole ovaries.

Antibodies

The antibodies used are the monoclonal mouse anti Gurken antibody 1D12 (Developmental Studies Hybridoma Bank, Iowa City, IA; Queenan *et al*., 1999); the anti mammalian Sec23p rabbit polyclonal

antibody (Affinity BioReagents, Golden, CO; Kondylis and Rabouille, 2003); the crude anti Yolkless rabbit polyclonal antibody 155 (gift from A. Mahowald, Chicago, IL); and the polyclonal anti-green fluorescent protein (GFP) antibody A6455 (Molecular Probes, Leiden, The Netherlands).

Electron microscopy
Ovaries were dissected and fixed with trialdehyde (5% Glutaraldehyde [GA], 2% Paraformaldehyde [PFA], 1% Acrolein, 2.5% DMSO in 0.08M cacodylate buffer pH7.4) for 3 h at room temperature. This was followed by post-fixation and embedding in Spurr's low viscosity resin. Ultrathin resin sections were cut on a Reichert Ultra Microtome. Ovaries were also fixed in 4% PFA in 0.1M phosphate buffer (PB) pH7.4 for 3 h at room temperature (RT) followed by overnight at 4°C, or in 2% PFA and 0.2% GA in the same buffer for 3h at RT, followed by overnight at 4°C, and stored in 1% PFA in PB at 4°C. The individual egg chambers were embedded in 12% gelatin (Liou et al., 1996) and mounted on aluminum pins and frozen in liquid nitrogen so that they could be cut along the long axis on a Reichert Ultracut S cryotome at -120°C.

Immunoelectron microscopy (IEM)
Sixty-nanometer-thick cryosections were incubated with antibodies described above. Rabbit antibodies were recognized by proteinA conjugated to 10- or 15-nm gold particles. Mouse antibodies were detected by a rabbit anti-mouse IgG (DakoCytomation Denmark A/S; Glostrup, Denmark) followed by either one of the proteinA gold complexes. Double labeling procedures were performed sequentially as described in (Slot et al., 1991).

***In situ* hybridization**
In situ hybridization on whole mount ovaries (fixed for 15 min in 4% PFA in phosphate buffered saline [PBS]) was carried out according to (Tautz and Pfeifle, 1989) with minor modifications. Digoxigenin labeled *gurken* RNA-probe was produced from the 1.7kb gurken cDNA (Neuman-Silberberg and Schupbach, 1993) using a DIG RNA labeling kit according to manufacturers recommendations (Roche Diagnostics, Mannheim, Germany).

Immunofluorescence
Ovaries were dissected and fixed in 4% PFA in PBS for 15 minutes at RT. After 3 washes in 0.3% TritonX100 in PBS (PBT), ovaries were first incubated in 1% TritonX100 in PBS for 30 minutes, followed by 1-h block in PBT with 2% bovine serum albumine (BSA) followed by the incubation with the primary antibodies in PBT supplemented by 0.5% BSA for 3 hours at RT or O/N at 4°C. Ovaries were washed in PBT 3 times in 1 h before incubation with the secondary IgG coupled to Alexa 488 for rabbit antibodies, or Alexa 568 for mouse antibodies (1:500; Molecular Probes) in 0.5%BSA in PBT for 2 hours at RT. Ovaries were washed in PBT, mounted in Vectashield, and viewed under a Leica TCS-NT confocal microscope.

Fluorescence Recovery after Photobleaching (FRAP) analysis
Protein disulfide isomerase (PDI)-GFP transgenic females were directly dissected in halocarbon oil series 95 on a glass slide. Ovarioles were separated and covered with a coverslip. The GFP-signal was analysed directly by using a Leica TCS-NT confocal microscope with a 40x objective and scanned at 2x zoom at 25% laser power (pre-bleach). The photobleaching was performed by scanning a distinct area at 32x zoom, (square box in Figure 7, A-D) at full laser power for 30 s. Recovery of the GFP signal was analysed at 2x zoom with 25% laser power, every 30 s.

Drug-treatments
WT or cni^{AR55}/cni^{CF5} ovaries were directly dissected in serum enriched Schneider insect medium supplemented with either 0.4% ethanol (control) or 90µM brefeldin A (BFA; dissolved in 80% ethanol; Sigma-Aldrich, St Louis, MO). The ovaries were incubated for 15 minutes at 37°C, followed by 90 minutes at 25°C (as described for *Drosophila* S2 cells, Kondylis and Rabouille, 2003), followed by immunofluorescence processing.

Quantitation

tER-Golgi units are described in the text and in Kondylis and Rabouille (2003). For estimating the total number of the tER-Golgi units in a stage 9 oocyte, the resin embedded oocytes were serial-sectioned. Only one 50nm section every 500nm of tissue was picked up. This is because a tER-Golgi unit is comprised within a sphere of 500nm in diameter, so the tER-Golgi units in each section selected should only be counted once. We counted the total number of tER-Golgi units through the stacks of selected sections for 2 oocytes, and estimated both their total number and their density. The density was verified on any other single section through at least 20 different oocytes. The labeling density of Gurken within the tER-Golgi units was estimated by point hit as previously described (Kondylis and Rabouille, 2003). We also measured the distance between the most D/A plasma membrane point and the Gurken positive tER-Golgi units. Pictures of the dorsal anterior corner of WT oocyte cryosections were taken at 6000X, printed and assembled, in order to visualize both the Gurken labeled tER-Golgi units and the non-labeled ones. Since *gurken* mRNA is localized between the nucleus and the plasma membrane at the D/A corner, we took the point representing this corner as the reference point and measured the distance between this point and the labeled tER-Golgi units. We verified the distance on immunofluorescence pictures where individual tER-Golgi units are visualized. We used a similar method for *merlin* mutants where the most posterior point of the oocyte was the point of reference. We also measured the area of cytoplasm where gurken mRNA is localized and where most of the labeled tER-Golgi units are situated. This area is described as a triangle where the point representing the D/A corner is the top angle opposite to the line crossing the nucleus in the middle minus the nucleus itself (Figure 1A, in black). The area of cytoplasm was estimated by point hit.

Results

The exocytic pathway in the Drosophila oocyte comprises multiple tER-Golgi units that are uniformly distributed throughout the ooplasm

To determine whether the exocytic pathway was restricted to a particular region of the ooplasm (for instance at the D/A corner), or present all over, we investigated the organization of this pathway in stage 9 oocytes by electron and immunofluorescence microscopy. At that stage, the oocyte is a cell with an anterior/posterior length of 30-40µm and a dorsoventral diameter of 50-70µm. We found that the oocyte, like other *Drosophila* cells, comprises multiple tER-Golgi units, some exhibiting a Golgi stack organization (Figures 1C and 2A), and others Golgi clusters (Figure 2C). They are comprised within a sphere of about 400 ± 100nm in diameter, and are positive for the Golgi tethering factor, COG5 (Figure 1E), a subunit of the COG complex, tethering ER derived vesicles to Golgi membranes (Whyte and Munro, 2001), that is also known in *Drosophila* as Four Way Stop or dCOG5 (Farkas et al., 2003), and positive for dSec23p (Figure 2), a COPII subunit marking the tER sites (Kondylis and Rabouille, 2003).

Figure 1: Examination of the exocytic pathway in *Drosophila* oocytes.
(A) Schematic representation of a stage 9-10 eggchamber with the oocyte abutting the 15 nurse cells and surrounded by a layer of somatic follicle cells. The dorsal/anterior corner is depicted in black (see Materials and Methods), and is where both Gurken protein and *gurken* RNA are known to localize. WT **(B-D)** and dCOG5-GFP **(E and F)** Drosophila eggchambers were processed for *gurken* RNA *in situ* hybridization **(B)**; immuno-electron microscopy **(C and E)**, conventional electron microscopy **(D)**, and immunofluorescence **(F)**.
(C) Representation of a tER-Golgi unit (in brackets), according to the criteria described in the text, exhibiting a portion of an ER cisterna, one ER exit site and a Golgi complex comprising a Golgi stack (G).
(D) All tER-Golgi units visualized on the ultrathin resin stage 9 oocyte section are marked by an asterisk (*).
(E) Ultrathin cryosections of dCOG5-GFP expressing eggchambers were labeled for GFP (10 nm gold). The tER-Golgi unit (in brackets) is positive for dCOG5-GFP as were all the other in the oocyte cryosection.
(F) Confocal section of a stage 9 dCOG5-GFP expressing eggchambers were labeled for GFP. The dots represent the tER-Golgi units in the oocyte, in the surrounding follicle cells and nurse cells. Note that the tER-Golgi units are randomly distributed within the ooplasm without concentration around the oocyte nucleus (N). The center of the oocyte shows a dimmer labeling intensity, due to penetration problems of the GFP antibody. Posterior, anterior, dorsal, ventral are indicated by P,A,D,V respectively. N, nucleus. Bars, 200nm (C and E); 5µm (D and F).

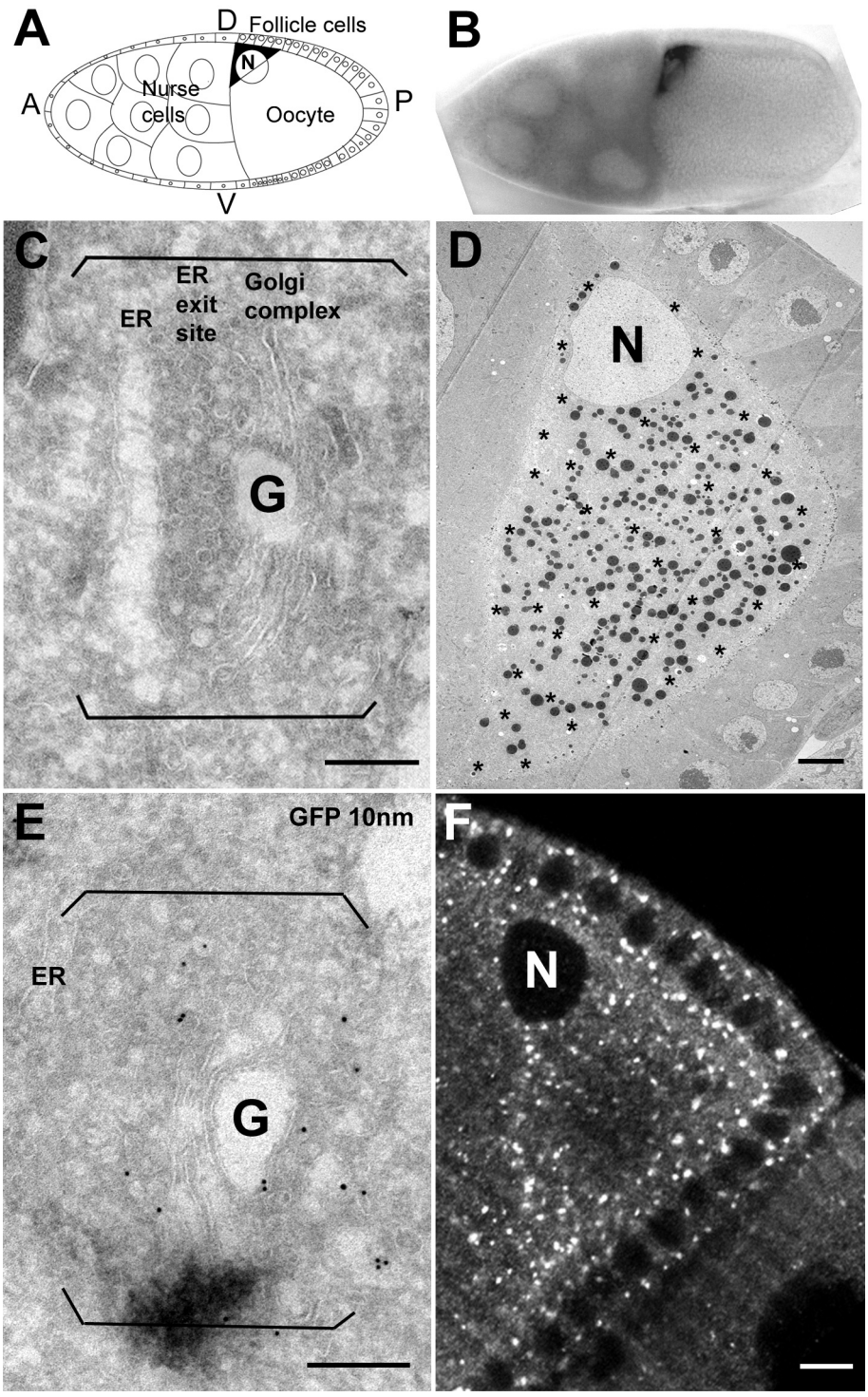
A
D
Follicle cells
N
A
Nurse cells
Oocyte
P
V
B
C
ER
ER exit site
Golgi complex
G
D
N
E
GFP 10nm
ER
G
F
N

We serial sectioned stage 9 oocytes along the long axis and estimated that they contain 1000±200 tER-Golgi units in total. They were randomly distributed throughout the ooplasm (Figure 1D, asterisks) with the same density near and around the nucleus, a landmark for the D/A corner (1unit / 26.6 ± 5.1μm^2 section), at the ventral, anterior and posterior sides (1unit / 22.2 ± 4.1μm^2 section). This random distribution was confirmed by examining confocal projections of stage 9 oocytes expressing dCOG5-GFP (that is present in all tER-Golgi units of the oocyte, Figure 1E) either live, or fixed and postlabeled with an anti GFP antibody (Figure 1F).

Gurken protein is only transported through the tER-Golgi units at the D/A corner

Gurken protein exhibits a restricted and polar localization at the D/A corner of a stage 9-10 oocyte (Neuman-Silberberg and Schupbach, 1996). The tER-Golgi units that make up the oocyte exocytic pathway are evenly distributed. Therefore, we predict that Gurken is transported and processed exclusively in the tER-Golgi units present at the D/A corner.

To test this hypothesis, we cryosectioned fixed stage 9 oocytes, and visualized Gurken by IEM. As expected, a fraction of gold particles corresponding to Gurken (ranging from 10 to 20%) was found in the space between the oocyte and the overlying follicle cells of the D/A corner. However, the bulk of Gurken was found within the oocyte at the D/A corner between the nucleus and plasma membrane. About 20% of intracellular Gurken was present in the local endoplasmic reticulum, consistent with its site of synthesis. The remainder was found in 10 ± 2 tER-Golgi units/section (Figure 2A), 95% of them situated in the region 1 of the cytoplasm encompassed within the triangle as shown in Figure 1A and 2A (see *Materials and Methods* for definition). This region has an area of 225 ± 50μm^2 and is where *gurken* mRNA is known to localize (Figure 1B). These Gurken-positive tER-Golgi units (comprising either a Golgi stack or a Golgi cluster) exhibited a labeling density for Gurken of 26 ± 12 gold/μm^2, and were situated not further than 20μm from the most D/A corner (see *Materials and Methods* for definition) with an average distance of 12.2 ± 3.0μm. We also found 5% of Gurken-positive units at longer distance (up to 30μm) but their labeling density was much weaker (3 ± 2gold/μm^2).

Away from the nucleus, at a distance higher than 30μm along the anterior or dorsal side, Gurken was mostly absent from the extracellular space, and the tER-Golgi units comprised within the considered areas were negative for Gurken (our unpublished data). So were the tER-Golgi units in the middle of the oocyte (Figure 2B; area 2), at the posterior pole (our unpublished data), and at the ventral/anterior corner (Figure 2C, area 3). However, all units were positive for dSec23p (Figure 2).

We also visualized Gurken by immunofluorescence in WT oocytes and were able to distinguish the tER-Golgi units involved in its transport (Figure 3A). These units were represented by dots around the nucleus, at the D/A corner, and were positive for dCOG5-GFP (Figure 3, B-D), and dSec23p (our unpublished data). As expected, Gurken was also observed at the plasma membrane (Figure 3, arrowheads) and in the ER at the D/A corner (arrows) where it does not colocalize with dCOG5-GFP. These results confirmed that only tER-Golgi units in the area of cytoplasm around the nucleus, at the distance not >20μm from the outmost D/A corner, were involved in Gurken transport and processing.

This result shows that within a single cell, proteins can be transported through a specific subset of tER-Golgi units, suggesting that the functioning of these units can be independent of each other.

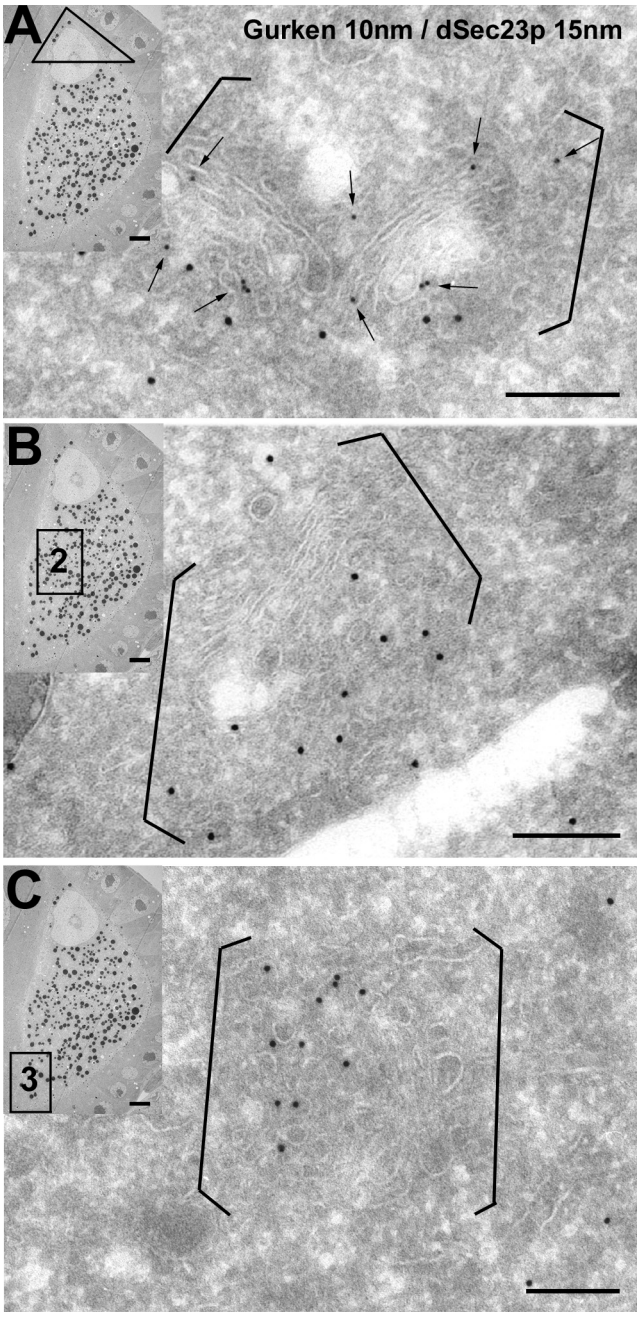

Figure 2: Gurken in the tER-Golgi units at the D/A corner.
WT eggchamber cryosections were double labeled for Gurken (10nm gold) and dSec23p (15nm gold). Different areas of the oocyte sections were examined. **(A)** Area 1 corresponds to the D/A corner (see Materials and Methods, inset; the nucleus serves as a landmark). Gurken protein (arrows) is present in all the tER-Golgi units in this area that are also labeled for dSec23p. **(B)** Area 2 corresponds to the anterior side of the oocyte (inset) toward the middle. **(C)** Area 3 corresponds to the V/A corner (inset). In areas 2 and 3, the tER-Golgi units are negative for Gurken protein but positive for dSec23p. Bar, 200nm (inset: 5µm).

All tER-Golgi units are functional and transport Yolkless

One way to explain this result, though, is to argue that the Gurken positive tER-Golgi units are the only functional ones in the oocyte. We therefore tested the transport of Yolkless, a transmembrane receptor present over the entire oocyte plasma membrane, and in the oocyte endosomal compartment, where it acts as the receptor for vitellogenin proteins synthesized by

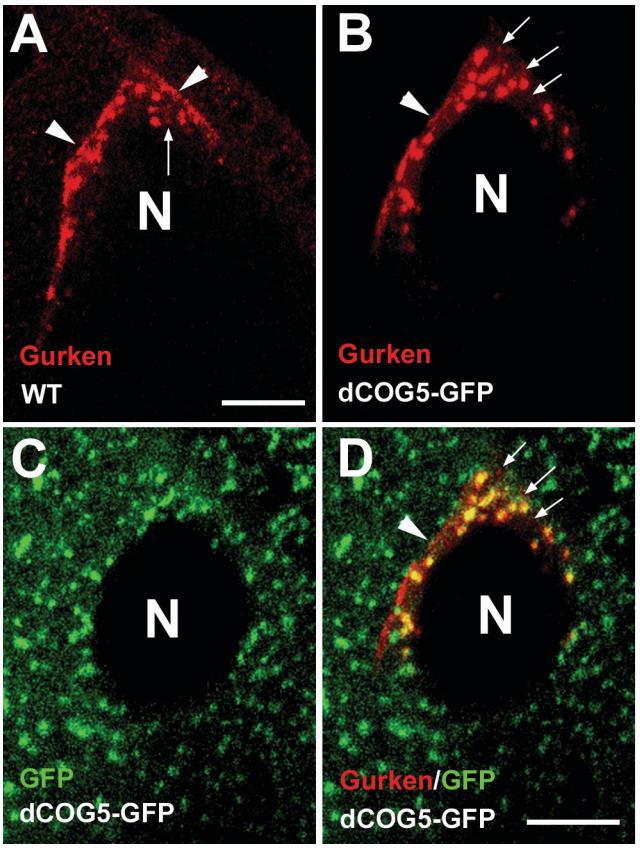

Figure 3: Gurken colocalizes with dCOG5-GFP at the D/A corner.
(A) Stage 9-10 WT egg chambers were processed for immunofluorescence and labeled for Gurken (red). Gurken is present in dots around the oocyte nucleus (N), in the ER at the D/A corner (white arrows), and in the intercellular space between the oocyte and the follicle cells at the D/A corner (white arrowheads). **(B-D)** dCOG5-GFP expressing egg chambers were double labeled for Gurken (**B**, red) and GFP (**C**, green). Note that the Gurken positive dots show complete overlap with dCOG5-GFP (**D**, merge), and therefore represent individual tER-Golgi units. Note that the Gurken in the ER (white arrows) does not overlap with dCOG5-GFP. The number of Gurken positive tER-Golgi units is higher than 10 (see Results), because the thickness of the confocal section presented here is 3 times higher than this of cryosections. The eggchambers are oriented as in Figure 1A. Bar, 5µm (A and D).

the follicle cells (Schonbaum et al., 1995; Schonbaum et al., 2000). These vitellogenin proteins, once endocytosed, are stored in yolk granules, on which the egg feeds once it is fertilized.

Yolkless is synthesised and transported to the plasma membrane through the oocyte exocytic pathway. In stage 9-10 eggchambers, Yolkless could be observed in transit in all tER-Golgi units observed in all areas of the oocyte, for instance at the ventral side (Figure 4B), at the posterior pole (Figure 4C), and at the D/A corner together with Gurken (Figure 4A). This shows that all tER-Golgi units present in the ooplasm are functional. It also reinforces the statement of independent functioning of the tER-Golgi units.

It is *gurken* mRNA localization that dictates the choice of tER-Golgi units used for Gurken transport

If, within an oocyte, functional tER-Golgi units are evenly distributed, how is the selection of those involved in Gurken transport achieved and implemented? Because *gurken* mRNA is localized at the D/A corner, we hypothesize that the choice of these tER-Golgi units is dictated by the restricted localization of *gurken* mRNA. If this is true, ectopically- or mislocalized *gurken* mRNA should recruit other tER-Golgi units away from the D/A corner.

To test this hypothesis, we first used *merlin* mutants in which *gurken* mRNA remains localized at the posterior pole till later stages (including 9 and 10, (MacDougall et al., 2001)). In WT, at the end of stage 7, Gurken signaling at the posterior pole follicle cells is answered by

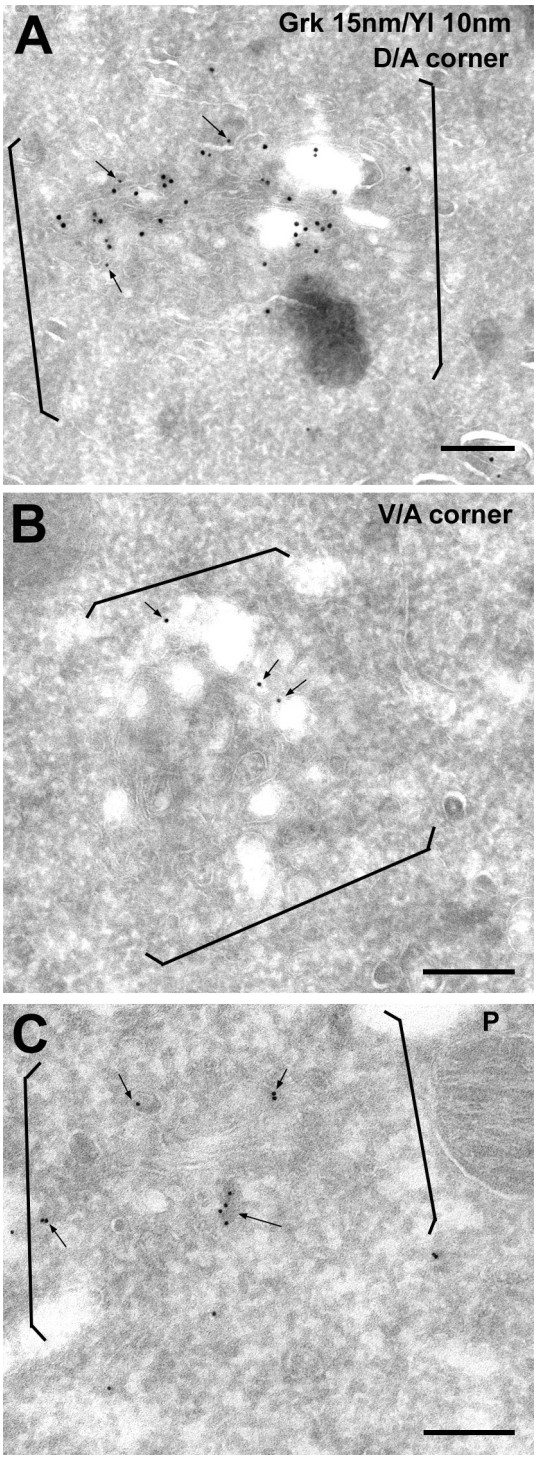

Figure 4: Yolkless is transported in all tER-Golgi units.
Cryosections of stage 9-10 WT eggchambers were labeled for the Gurken (15nm) and Yolkless (10 nm). Yolkless, on its way to the plasma membrane, passes through all the tER-Golgi units of the ooplasm, at the D/A corner (**A**, together with Gurken), at the V/A corner **(B)** and at the posterior pole (P) **(C)**. Arrows mark the specific Yolkless labeling. The 10nm gold in (A) that is not marked by arrows is an artefact due, in this instance, to the double labeling technique. Bar: 200nm

their sending a signal back to the oocyte, which leads to the change of microtubule polarity. As a consequence, the nucleus moves from the posterior pole toward the dorsal anterior corner, and *gurken* mRNA is also found localized at this corner (van Eeden and St Johnston, 1999; Roth, 2003). In *merlin* mutants, the posterior follicle cells do not send the signal back to the oocyte, the microtubules do not change their polarity, with the result that, in 55% of the cases, the nucleus and *gurken* mRNA remain at the posterior pole ((MacDougall et al., 2001), Figure 5A).

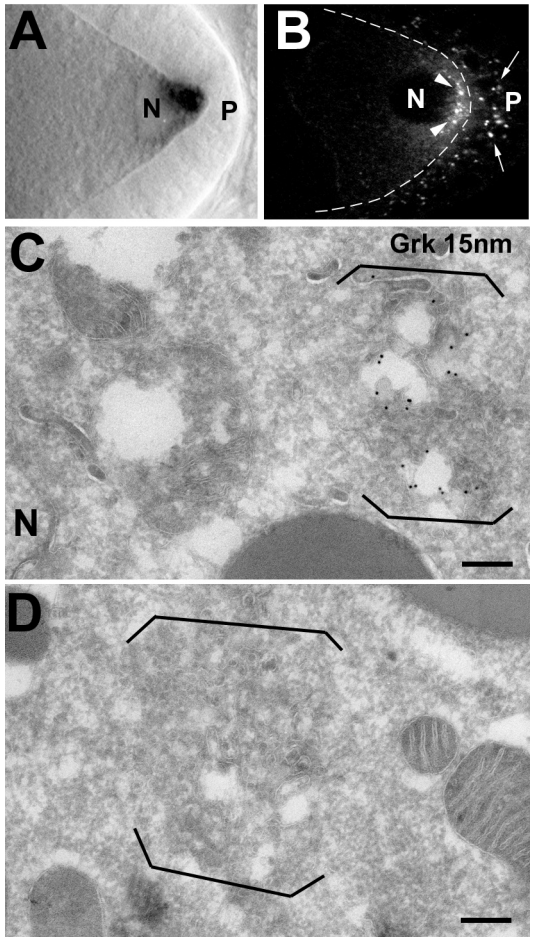

Figure 5: Gurken protein in the posterior tER-Golgi units of *merlin* mutants.
Homozygous stage 9-10 *merlin* egg chambers were processed for *gurken* mRNA *in situ* hybridization **(A)**, immunofluorescence of Gurken protein **(B)**, and cryosectioned and labeled for Gurken (15-nm gold) **(C and D)**. Note that only the tER-Golgi units next to the oocyte nucleus (N) at the posterior pole are Gurken positive **(C)**, whereas these of the anterior side are negative **(D)**. The white arrows in **B** point to Gurken positive structures in posterior follicle cells, representing presumably endosomes, and the white arrowheads point to tER-Golgi units at the oocyte posterior pole. The dashed white line represents the contours of the oocyte. The eggchambers are oriented as in Figure 1A. P, posterior pole. Bar, 200nm.

We localized Gurken protein in stage 9-10 *merlin* oocytes by immunofluorescence and IEM. Gurken was found in the space between the oocyte and the posterior follicle cells (our unpublished data) as well as in endosomes in follicle cells (Figure 5B, arrows), in agreement with its signaling. Furthermore, only the tER-Golgi units located at the posterior pole were positive for Gurken (Figure 5, B and C). They were located not further away than 20µm from the most posterior point, where the mRNA is located. Their labeling density for Gurken was 27.1 ± 11.0 gold/µm^2, in agreement with the WT situation at the D/A corner. The anterior tER-Golgi units were totally negative (Figure 5D). This suggests that mRNA localization can indeed dictate the usage of tER-Golgi units located next to it, in the D/A corner for a stage 9-10 WT oocyte, and at the posterior pole for an equivalent *merlin* oocyte.

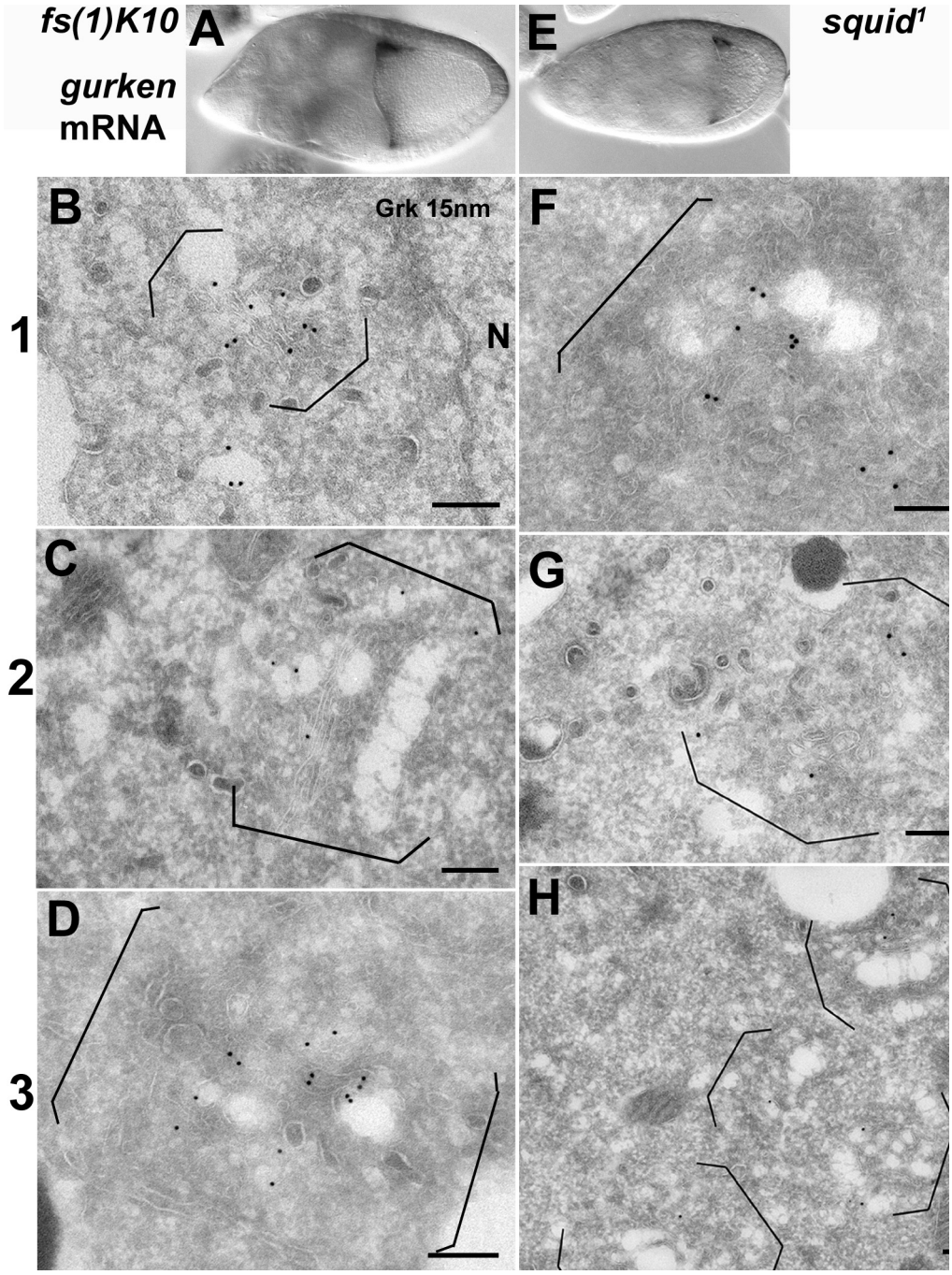

Figure 6: Gurken protein in the tER-Golgi units of *K10* and *squid*[1] mutants.
Homozygous *K10* **(A-D)** and *squid*[1] **(E-H)** eggchambers were processed for *gurken* mRNA *in situ* hybridization **(A and E)**, or cryosectioned and labeled for Gurken (15-nm gold) **(B-D, F-H)**. Different areas of the oocyte sections were examined. Area 1 **(B and F)** corresponds to the D/A corner (the oocyte nucleus (N) serves as a landmark), area 2 **(C and G)** corresponds to the anterior side of the oocyte, and area 3 **(D and H)** corresponds to the V/A corner (see legend for Figure 2). The tER-Golgi units (in brackets) were all positive for Gurken protein. Bar, 200nm.

To test this prediction further, we used the *fs(1)K10* and *squid*[1] mutants, where *gurken* mRNA is no longer restricted to the D/A corner, but delocalized along the anterior cortex and at the ventral/anterior corner ((Serano et al., 1995; Norvell et al., 1999); Figure 6, A and E). *gurken* mRNA localizes to an asymmetric ring along the anterior side of the oocyte with a weaker intensity toward the ventral side. The translation and deposition of Gurken protein is nevertheless sustained ((Norvell et al., 1999; Serano et al., 1995); Figure 6). As expected, Gurken labeling was present in the tER-Golgi units at the D/A corner (Figure 6, B and F) with a labeling density of 23.5 ± 11.0 gold/μm^2 for *K10* mutants, and 21.5 ± 10.0 gold/μm^2 for *squid*[1], comparable with WT (Figure 2). But in both mutants, Gurken was also present in the tER-Golgi units along the anterior side (Figure 6, C and G, with a Gurken labeling density of 8.5 ± 5.0 for *K10*, and 6.5 ± 2.5 for *squid*[1]), and at the ventral/anterior corner (Figure 6, D and H, with a Gurken labeling density of 8.5 ± 6.0 for *K10*, and 5.5 ± 3.5 for *squid*[1]), in a sharp contrast to WT (Figure 2, B and C). The slightly decreased Gurken labeling density along the anterior axis, and at the ventral/anterior corner is in agreement with the weaker RNA labeling observed (Figure 6, A and E). The space between the oocyte and the nurse cells was also weakly positive for Gurken (our unpublished data).

That mislocalized *gurken* mRNA was able to induce the local synthesis, transport and processing of full length Gurken protein was suggested by Serano *et al.* (1995) and Norvell *et al.* (1999). Our results show, here, that this is sustained by polarized exocytosis through selected tER-Golgi units (and post-Golgi compartments) situated in close proximity to, and chosen by, *gurken* mRNA. This suggests, then, that mRNA localization dictates the use of the machinery for processing and transport of transmembrane / secreted proteins.

A very active transport out of the ER

Additional mechanisms might ensure that local synthesis of Gurken is followed by local polarized delivery at the D/A intercellular space. To achieve this, diffusion of newly synthesized Gurken must be restricted, either because the ER is discontinuous and Gurken cannot go beyond the stretch of ER in which it has been synthesized (for instance around the nucleus at the D/A corner), or because Gurken is transported very efficiently out of the ER as soon as it is synthesized.

In eukaryotic cells, the ER is continuous throughout the entire cytoplasm. In *Drosophila* oocytes, the visualization of the ER resident protein protein disulfide isomerase tagged with GFP (PDI-GFP) shows that the ER pervades the entire oocyte (Bobinnec et al., 2003).

We show here that the ER does not only pervade the oocyte, but also comprises a single lumen. We first performed a FRAP (Nehls et al., 2000) experiment on the PDI-GFP expressing egg chambers (Figure 7, A-D). Since PDI-GFP is resident in the ER, it can be used as a marker for diffusion in this organelle. By bleaching a certain area in the oocyte (boxed area in Figure 7A), the GFP signal is initially lost (Figure 7B), but recovers (Figure 7C) and is restored completely (Figure 7D) in ~5 min. This result can only be explained by flow of not-bleached PDI-GFP into the bleached area, from the surrounding ER, showing the continuity. A similar result was obtained when bleaching any region of the oocyte ER, including the D/A corner.

We confirmed that the ER is continuous by using *cornichon (cni)* mutants. Cornichon is a protein of 144 aminoacids, is predicted to contain three transmembrane domains, has been described as the potential Gurken receptor at the tER sites (Roth et al., 1995), and is the putative orthologue of Erv14p (Powers and Barlowe, 1998). In the strong allelic combination of

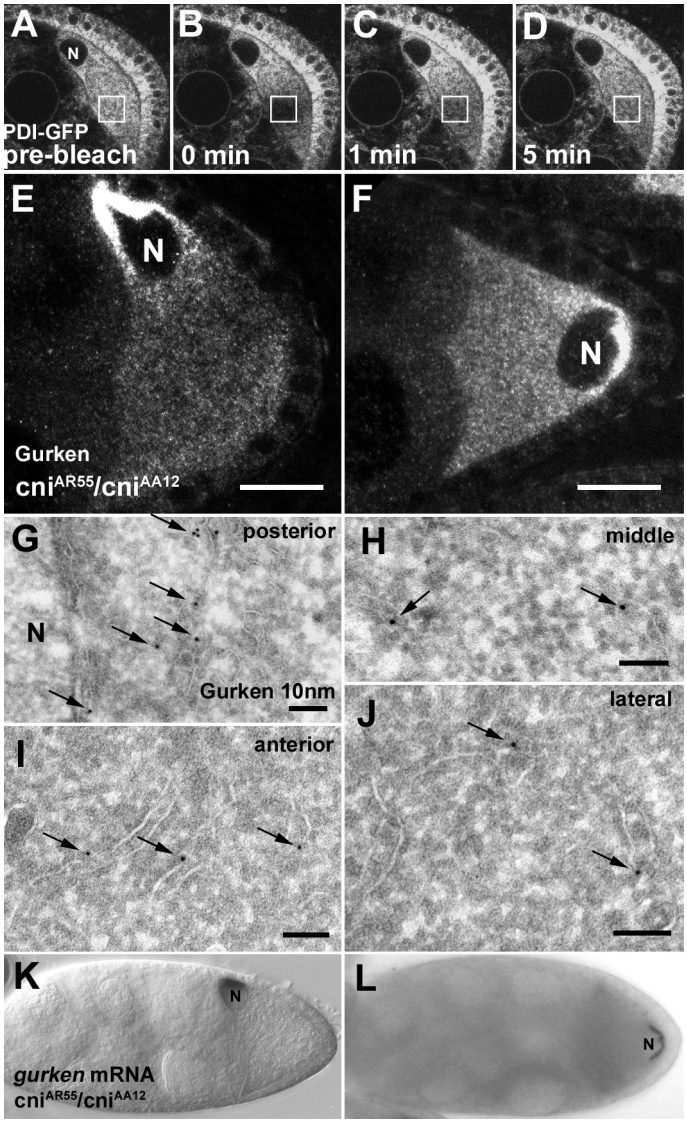

Figure 7: The ER is continuous in the *Drosophila* oocyte.
(A-D) FRAP experiment on PDI-GFP eggchambers shows that the ER pervades the oocyte and comprises a single lumen. Photobleaching was performed for 30 s at 100% laser power in a selected area (square box, **B**), but diffusion from the surrounding ER enables recovery of the GFP signal **(C)**, which is fully restored after 5 min **(D)**. Cornichon mutants (strong allelic combination cni^{AR55}/cni^{AA12}) were labeled for Gurken protein by immunofluorescence **(E and F)** or IEM (**G-J**, 10-nm gold, arrows) and for mRNA **(K and L)**. In this genetic background, the nucleus fails to move to the D/A corner in 70% of the oocytes and is localized at the posterior pole **(F and L)**. The IEM micrographs **(G-J)** were generated from such an oocyte, and Gurken is present throughout the ER in all areas, reaching the anterior side after being synthesized at the posterior pole **(L)**. The tER-Golgi units were not labeled. The eggchambers are oriented as in Figure 1A. N, oocyte nucleus. Bars, 10µm (E and F); 100nm (G-J).

cni^{AR55}/cni^{AA12} mutants (leading to truncated proteins), Gurken is retained intracellularly (Roth et al., 1995) and is observed throughout the entire oocyte (Figure 7, E and F). Though it is still concentrated near the nucleus at the D/A corner (Figure 7E), or at the posterior pole (Figure 7F) when oocyte development has been impaired due to the mutation (Roth et al., 1995), we show here that it exclusively labels the ER throughout the oocyte (Figure 7, G-J) and that the tER-Golgi units are not labeled, suggesting that Gurken sorting has not been achieved.

This ER-retained Gurken protein was produced from a single source of mRNA localized near the nucleus, at the D/A corner (Figure 7K), or at the posterior pole (Figure 7L). This shows that the ER can be filled up entirely by from a single localized source of translation, thus indicating that it is connected throughout the oocyte, including the D/A corner.

In this continuous ER, diffusion of newly synthesized Gurken protein within the plane of the organelle membrane is in principle expected before it is further transported toward the tER-Golgi units. However, Gurken does not seem to diffuse, and is possibly transported very efficiently out of the ER. We set out to investigate several mechanisms responsible for this efficient sorting.

First, as described above, Cornichon provides the first of such a mechanism; when its function is impaired, Gurken is present in the ER and not transported to the tER-Golgi units (Figure 7, E-J).

Second, different domains of Gurken protein provide information for its efficient sorting. Gurken transmembrane domain has been suggested to be necessary for the efficient transport of the protein. The truncated Gurken protein lacking its transmembrane and cytoplasmic domain (gΔTC) has been shown to be retained intracellularly (Queenan et al., 1999). When gΔTC is expressed in a Gurken protein null background (grk^{2E12}/grk^{2B6}), the truncated protein is present throughout the entire ER as seen by immunofluorescence (Figure 8, A and B) and by IEM (our unpublished data). As a result it cannot signal to the adjacent follicle cells, and rescue the *gurken* mutant phenotype. This result suggests that gΔTC is locally synthesized and diffuses throughout the oocyte ER, suggesting that the truncated domains are crucial for its efficient sorting at the D/A corner. A truncated version of Gurken lacking only its cytoplasmic domain (gΔC) does not show such a strong diffusion and fully rescues the grk^{2E12}/grk^{2B6} phenotype (Queenan et al., 1999). Its diffusion in the ER was nevertheless slightly broader than in the WT (our unpublished data). This shows that it is the transmembrane domain of Gurken that is mostly necessary for efficient exit from the ER.

We further investigated whether the diffusion of WT Gurken in the ER could be induced by chemically blocking its exit from the ER using the drug BFA. Under BFA treatment, transmembrane proteins that normally would be transported to the Golgi apparatus are trapped and diffuse in the ER (Lippincott-Schwartz et al., 1989; Altan-Bonnet et al., 2004). Treatment of WT oocytes with BFA had a moderate effect of retention and diffusion of Gurken in the ER, and was observed only in ~30% of the egg chambers, even when incubations with the drug were extended to 3h (Figure 8D). In 70% of the treated egg chambers, the pattern did not differ from the mock-treated ones (Figure 8C), and Gurken was present in tER-Golgi units and the ER in the D/A corner. We reasoned that perhaps, in WT oocytes, Cornichon was binding Gurken and trapped it at the tER sites, possibly in COPII coated vesicles, even though the movement of cargo to the Golgi apparatus is inhibited by the BFA treatment (Altan-Bonnet et al., 2004).

We tested this notion by performing the BFA treatment in a weak allelic combination of *cornichon*, cni^{AR55}/cni^{CF5}. The *CF5* allele produces a Cornichon protein that is 22 amino acids larger than the WT because of a mutation in the stop codon (Roth et al., 1995). In the absence of the drug, the intracellular Gurken pattern in this mutant is almost indistinguishable from the WT (compare Figure 8, C and E); Gurken is found in tER-Golgi units with a fraction also observed in the ER, but its secretion is moderately impaired, leading to a weak signaling to the D/A follicle cells and ventralization of the oocytes (our unpublished observation). In the presence of BFA, though, Gurken diffuses further in the ER in 75% of the observed egg chambers. This indicates the importance of Cornichon as a protein required for capturing newly synthesised Gurken in the ER, and directing it to the most proximal tER-Golgi units. This also suggests, as in mammalian cells, that BFA can be efficient at affecting the ER to Golgi dynamics and retrieving Golgi localized proteins (such as Gurken) in the ER.

Together, this suggests that the pre-translational mechanism (through *gurken* mRNA localization) that implements the polar synthesis of Gurken at the D/A corner is followed by strong sorting events of the protein from the ER, preventing its diffusion and ensuring its delivery at the D/A intercellular space where it can perform its biological function.

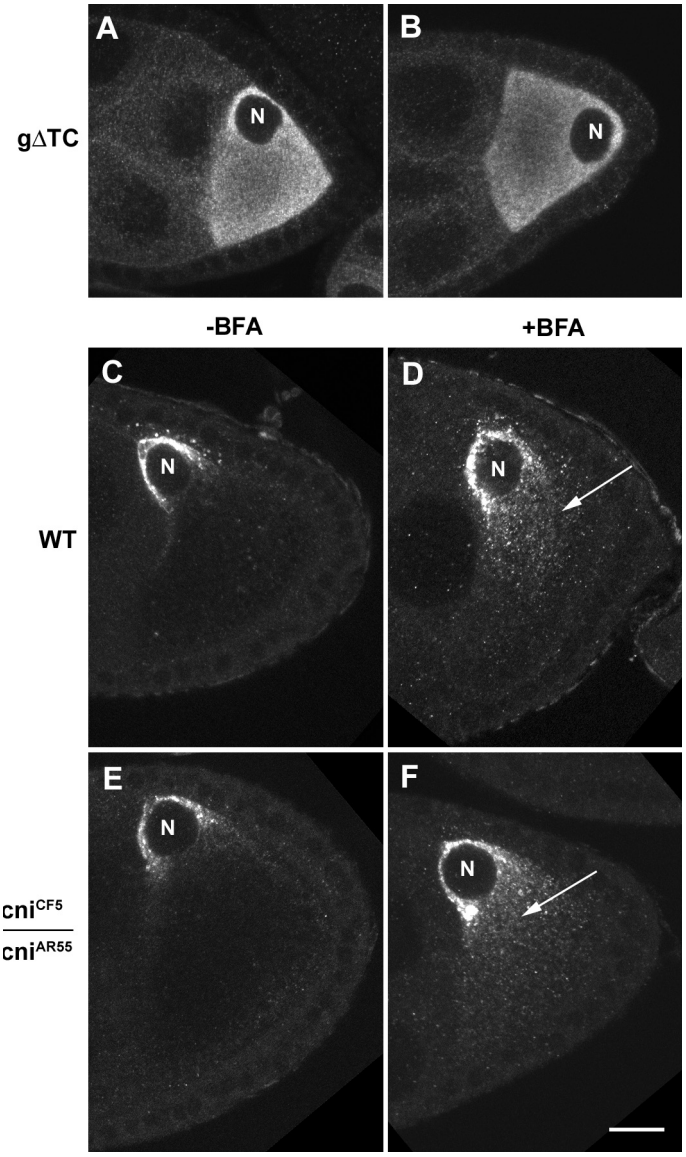

Figure 8: Gurken diffusion in the ER can be induced.
Gurken protein null background (grk^{2B6}/grk^{2E12}) eggchambers expressing the truncated form of Gurken lacking its transmembrane and cytoplasmic domain (gΔTC) **(A and B)**, WT eggchambers **(C and D)** and cni^{CF5}/cni^{AR55} **(E and F)**, mock- **(C and E)**, and brefeldin A-treated **(D and F)** were labeled for Gurken for immunofluorescence. Note that Gurken has diffused in the ER when it is truncated, and when the eggchambers are treated with BFA (arrows in **D** and **F**). The eggchambers are oriented as in Figure 1A. N, oocyte nucleus. Bar, 10μm.

Discussion

The tER-Golgi units at the D/A corner are seemingly identical to the others

To understand how Gurken, as a transmembrane protein, achieves its polar distribution, we elucidated the organization of the exocytic pathway in *Drosophila* oocytes. We found that it is similar to other *Drosophila* cells observed so far. Namely, it contains a continuous ER that pervades the entire ooplasm (Bobinnec *et al*., 2003; this study), from which a multitude of tER-

Golgi units arise. In the oocyte, like in S2 cells, the tER-Golgi units comprise an ER exit site (positive for dSec23p), closely apposed to a Golgi apparatus, either under the form of a cluster of vesicles and tubules, or a Golgi stack, both marked by the Golgi marker, dCOG5. S2 cells contain ~20 of these units, whereas the number is much greater in oocytes (~1000; this study) but with an equivalent density (S2 cells have about a 60-100 times smaller volume than a stage 9 oocyte).

One way to explain Gurken deposition at the D/A corner is to argue for a concentration of the tER-Golgi units at this corner. Recently, it has been shown (Preisinger et al., 2004) that cell migration in wound healing was accompanied by the redistribution and concentration of their Golgi complex to the part of the cell facing the injury, thus sustaining a polarized secretion which helps in the healing. We show, using immunofluorescence and electron microscopy, that the thousand tER-Golgi units in the *Drosophila* oocyte are evenly distributed throughout the ooplasm. This concentration is therefore unlikely to be the underlying mechanism for Gurken polarity.

Another way to explain that Gurken is only synthesized and transported in the tER-Golgi units localized at the D/A corner is to argue that they have a unique composition in regard to the known three proteins involved in its movement through the exocytic pathway, Star (Pickup and Banerjee, 1999), Cornichon (Roth et al., 1995), and Brother of Rhomboid (Brho; Guichard *et al*., 2002). Perhaps these three proteins only reside in the tER-Golgi units at the D/A corner, therefore rendering them, and only them, competent for Gurken transport. Star is thought to act as an ER chaperone helping in the exit from the ER (Ghiglione et al., 2002; Urban et al., 2002). Cornichon is a potential Gurken receptor at the ER exit sites (Roth *et al*., 1995). Brho is a specific endoprotease located in the Golgi apparatus (Ghiglione et al., 2002; Urban et al., 2002) that cleaves Gurken just after its transmembrane domain, thus generating the lumenal active ligand of Torpedo, and a C-terminal membrane bound fragment whose fate is undetermined.

Several lines of evidence, however, suggest that these proteins are not restricted to the tER-Golgi units of the D/A corner. First, *cornichon* and *brho* mRNAs do not have a polarized localization, but rather occupy the entire oocyte (Guichard *et al*., 2002; Roth *et al*., 1995). This suggests that the two proteins are expressed ubiquitously, as is Star protein in stage 6-10 oocytes (Pickup and Banerjee, 1999). Second, in an S2 cell assay, Gurken is only cleaved and secreted when cells are transfected with both Brho and Star. When transfected with Brho alone, Gurken is cleaved but not secreted, and with Star alone, Gurken is neither processed nor secreted (Ghiglione et al., 2002). Because both in *squid* and *K10* mutants, Gurken protein is transported all tER-Golgi units along the anterior side and at the ventral/anterior corner (our observations) and is found in the space between the oocyte and the nurse cells (Serano *et al*., 1995; Norvell *et al*., 1999, our observations), this suggests that at least Star and Brho are present in all tER-Golgi units, including these away from the D/A corner, and act in the processing and transport of Gurken. Along the same line, Star, Cornichon and Brho are also likely localized to the tER-Golgi units at the posterior pole, in WT stage 6-7 and stage 9-10 *merlin* oocytes where Gurken protein is synthesized, transported and processed, so it signals to the posterior follicle cells. Third, it was recently published that in stage 10 germ line clone of the sec5 exocyst complex subunit, Gurken protein was synthesized in the middle and at the posterior pole of the *Drosophila* oocyte (Murthy and Schwarz, 2004). This experiment, and those described above, shows that all tER-Golgi units have potentially the capacity of transporting and processing Gurken protein. Together, the tER-Golgi units at the D/A corner do not seemingly contain a different set of transport and processing proteins from the others.

It is *gurken* RNA localization that dictates the use of the tER-Golgi units

We show here, by using *K10*, *squid*, and *merlin* mutants, that what dictates the use of these numerous, seemingly identical and evenly distributed tER-Golgi units, is the restricted localization of *gurken* mRNA. This could also be the case for other transmembrane / secreted proteins.

gurken mRNA is localized in a restricted fashion at the D/A corner (MacDougall et al., 2003), where it is then anchored. The anchoring mechanism is not yet clear and is the subject of intense research, but we could envisage that an efficient recruitment of local tER-Golgi units would be achieved by anchoring the mRNA directly on their membrane. The ER was suggested as such an anchor by (Saunders and Cohen, 1999). Whatever the anchoring mechanism and wherever it is localized, *gurken* RNA diffuses locally (~20µm; this study), binds to ribosomes, is translated, and recognized by the signal recognition particle that targets it to the most proximal ER membrane, where the protein is synthesized and subsequently transported through the most adjacent tER-Golgi units.

Gurken protein is efficiently sorted from the ER, preventing its diffusion

Additional mechanisms also ensure that local synthesis is followed by local polarized delivery at the D/A intercellular space, where the activity of Gurken is necessary but also needs to be restricted for proper oocyte development (van Eeden and St Johnston, 1999; Roth, 2003).

In eukaryotic cells, the ER has been shown to be continuous throughout the entire cytoplasm. FRAP experiments on PDI-GFP expressing oocytes as well as the use of a strong allelic combination of Cornichon have shown that the ER comprises a single lumen throughout the oocyte, including at the D/A corner. Partial diffusion of the newly synthesized Gurken in the membrane of the ER is therefore expected. Such a diffusion over long distance (>0.5mm) within the ER has been shown for soluble proteins, such as the light and heavy chains of the immunoglobulins in frog oocytes (Colman et al., 1982). However, the maximum distance over which intracellular Gurken is found is 20µm.

Therefore, the diffusion of Gurken is likely to be prevented by efficient sorting mechanisms. Those rely primarily on the transmembrane domain of Gurken and Cornichon. Gurken lacking its transmembrane domain diffuses in the ER in a very similar way as WT Gurken does in a strong cornichon mutant (Roth *et al*., 1995; Queenan *et al*., 1999; our observations), except for the concentration observed at the D/A corner. This could be explained by the difference in diffusion between a transmembrane protein and a lumenal fragment. Nevertheless, this phenocopy suggests that Gurken binds Cornichon through its transmembrane domain. This interaction could mediate the efficient packaging of transmembrane Gurken in COPII transport vesicles. Cornichon presents homology to Erv14p, which is involved, in yeast, in the exit of the plasma membrane Axl2 transmembrane protein from the ER in COPII-coated vesicles. The interaction between Erv14p and Axl2p has been suggested to act via a novel mechanism that might be mediated by interactions of transmembrane segments (Powers and Barlowe, 2002). The binding of Gurken to Cornichon might rely on a similar mechanism, though it is not clear why a transmembrane cargo protein would need an extra transmembrane chaperone for its sorting and incorporation into COPII buds.

This is particularly intriguing because efficient export from the ER could also be mediated by motifs found in the cytoplasmic domain of Gurken. In type I transmembrane proteins such as ERGIC53 and Emp46, a doublet of phenylalanine and leucine, respectively, is

important for the exit from the ER (Barlowe, 2003; Bonifacino and Glick, 2004). Both doublets are found in Gurken cytoplasmic domain (aa251 sfpvLLmlss lyvlfaavfm lrnvpdyrrk qqqlhlh kqr FFvrc, our observation). The removal of the cytoplasmic domain of Gurken does not seem, though, to affect to a great extent the efficient exit of the truncated protein from the ER, perhaps because it can still interact with Cornichon. The role of the cytoplasmic domain could perhaps be unravelled in a weak *cornichon* mutant background.

BFA treatment of the WT eggchambers was expected to lead to full retention / retrieval of Gurken in the ER followed by its diffusion. However, many oocytes remained seemingly unaffected, suggesting that the binding of Gurken to its sorting receptor Cornichon locked Gurken at tER sites. When the drug treatment was performed in a weak allele of *cornichon*, Gurken could be observed diffusing in the ER, suggesting that the locking mechanism was impaired. This diffusion, however, was not as extensive as this observed in the strong *cornichon* mutant under non-treated conditions. This partial diffusion could represent this of the complex Cni^{CF5}/Gurken (two transmembrane proteins) instead of Gurken alone. Why, under BFA treatment, Cni^{CF5}/Gurken complex diffuses more readily than Cornichon/Gurken is still not understood and further work is needed to elucidate the molecular details of the BFA effect in oocytes.

Further work is needed to find out whether the polar synthesis and deposition other transmembrane proteins rely also on a pre-translational mechanism (through mRNA localization), alone or coupled to efficient protein sorting events from the ER.

Independence of tER-Golgi units: Implication for other polarized cells

All tER-Golgi units are able to work in synchrony for the transport of transmembrane proteins, of which the RNAs are not localized, such as Yolkless (Schonbaum et al., 2000). However, we have shown, here, that a subset of tER-Golgi units can be recruited to perform the specific task of transporting a given transmembrane / secreted protein. This suggests that the different tER-Golgi units within a single cell can function in an uncoupled / nonsynchronous / independent manner, even though the ER is continuous. The restricted localization of transcripts is a necessary cue for imposing this uncoupling, as it has been suggested in muscle heterokaryons and hybrid myotubes (Pavlath et al., 1989; Ralston and Hall, 1989), though it is not clear in these systems whether the ER is continuous.

We have here exemplified the functional uncoupling of the tER-Golgi units in *Drosophila* oocytes, and we propose that a similar mechanism could also take place for other types of highly polarized cells, such as neurons. This is suggested by series of observations, showing that RNA encoding transmembrane proteins specific for the dendrites are translated in the dendrites themselves, and not exclusively in the cell body (Mohr and Richter, 2003). It is also suggested by the immunofluorescence labeling of Golgi markers such as galactosyltransferase and GM130, in a dotty pattern along the dendrites (Horton and Ehlers, 2003), suggesting that perhaps Golgi-like structures could underlie this labeling. It is therefore possible that the mechanism we have identified here also occurs in neurons. mRNA encoding transmembrane/secreted proteins specific for the dendrites could be localized in these specialized domains and use dendritic Golgi-outposts to induce the local synthesis and transport of the proteins they encode.

Whether in mammalian cells, the multiple ER exit sites and the dozens of Golgi stacks making up the Golgi ribbon could also function in an uncoupled manner and respond to a restricted mRNA localization remains to be elucidated.

Acknowledgements
We wish to thank Trudi Schupbach for the *gurken* cDNA clone, the *squid*[1] allele, the transgenic stocks gΔTC4.1 and gΔC100, and advice on immunofluorescence. We thank Margaret Fuller for the dCOG5-GPF stocks; Ilan Davis for the *merlin* ts stock; Yves Bobinnec for the PDI-GFP stocks; Anne Ephrussi for the grk^{2B6} and grk^{2E12} stocks; Siegfried Roth for the cornichon alleles and Anthony Mahowald for Yolkless antibody. We thank Judith Klumperman, Vangelis Kondylis and Anne Ephrussi for critically reading the manuscript, and Elly van Donselaar and Adrian Oprins for help in electron microscopy and cryosectioning. We are grateful to the intellectual contribution of Ilan Davis, who is supported by a Senior Fellowship from the Wellcome Trust. The monoclonal antibody 1D12 developed by Trudi Schupbach was obtained from the Developmental studies Hybridoma Bank developed under auspices of the NICHD and maintained by The University of Iowa, Department of Biological Sciences, Iowa City, IA 52242. (http://www.uiowa.edu/~dshbwww/index.html). We acknowledge the use of Flybase (http://flybase.net) and Bloomington Stock Center (http://fly.bio.indiana.edu). BH is funded by a Nederlandse Organisatie voor Wetenschappelijk Onderzoek (NWO) Aspasia grant (015.001.129) to CR.

References

Altan-Bonnet,N., Sougrat,R., and Lippincott-Schwartz,J. (2004). Molecular basis for Golgi maintenance and biogenesis. Curr. Opin. Cell Biol. 16, 364-372.

Barlowe,C. (2003). Signals for COPII-dependent export from the ER: what's the ticket out? Trends Cell Biol. 13, 295-300.

Barlowe,C., Orci,L., Yeung,T., Hosobuchi,M., Hamamoto,S., Salama,N., Rexach,M.F., Ravazzola,M., Amherdt,M., and Schekman,R. (1994). COPII: a membrane coat formed by Sec proteins that drive vesicle budding from the endoplasmic reticulum. Cell 77, 895-907.

Bashirullah,A., Cooperstock,R.L., and Lipshitz,H.D. (1998). RNA localization in development. Annu. Rev. Biochem. 67, 335-394.

Bobinnec,Y., Marcaillou,C., Morin,X., and Debec,A. (2003). Dynamics of the endoplasmic reticulum during early development of Drosophila melanogaster. Cell Motil. Cytoskeleton 54, 217-225.

Boevink,P., Oparka,K., Santa,C.S., Martin,B., Betteridge,A., and Hawes,C. (1998). Stacks on tracks: the plant Golgi apparatus traffics on an actin/ER network. Plant J. 15, 441-447.

Bonifacino,J.S. and Glick,B.S. (2004). The mechanisms of vesicle budding and fusion. Cell 116, 153-166.

Colman,A., Besley,J., and Valle,G. (1982). Interactions of mouse immunoglobulin chains within Xenopus oocytes. J. Mol. Biol. 160, 459-474.

Ephrussi,A., Dickinson,L.K., and Lehmann,R. (1991). Oskar organizes the germ plasm and directs localization of the posterior determinant nanos. Cell 66, 37-50.

Farkas,R.M., Giansanti,M.G., Gatti,M., and Fuller,M.T. (2003). The Drosophila Cog5 homologue is required for cytokinesis, cell elongation, and assembly of specialized Golgi architecture during spermatogenesis. Mol. Biol. Cell 14, 190-200.

Ghiglione,C., Bach,E.A., Paraiso,Y., Carraway III,K.L., Noselli,S., and Perrimon,N. (2002). Mechanism of activation of the Drosophila EGF Receptor by the TGFalpha ligand Gurken during oogenesis. Development 129, 175-186.

Guichard,A., Roark,M., Ronshaugen,M., and Bier,E. (2000). brother of rhomboid, a rhomboid-related gene expressed during early Drosophila oogenesis, promotes EGF-R/MAPK signaling. Dev. Biol. 226, 255-266.

Horton,A.C. and Ehlers,M.D. (2003). Dual modes of endoplasmic reticulum-to-Golgi transport in dendrites revealed by live-cell imaging. J. Neurosci. 23, 6188-6199.

Ikonen,E. and Simons,K. (1998). Protein and lipid sorting from the trans-Golgi network to the plasma membrane in polarized cells. Semin. Cell Dev. Biol. 9, 503-509.

Juschke,C., Ferring,D., Jansen,R.P., and Seedorf,M. (2004). A novel transport pathway for a yeast plasma membrane protein encoded by a localized mRNA. Curr. Biol. 14, 406-411.

King,R.C. (1970). Ovarian development in Drosophila melanogaster. (New York: Academic Press).

Kondylis,V., Goulding,S.E., Dunne,J.C., and Rabouille,C. (2001). Biogenesis of Golgi stacks in imaginal discs of Drosophila melanogaster. Mol. Biol. Cell 12, 2308-2327.

Kondylis,V. and Rabouille,C. (2003). A novel role for dp115 in the organization of tER sites in Drosophila. J. Cell Biol. 162, 185-198.

Lee,S.K. and Hollenbeck,P.J. (2003). Organization and translation of mRNA in sympathetic axons. J. Cell Sci. 116, 4467-4478.

Liou,W., Geuze,H.J., and Slot,J.W. (1996). Improving structural integrity of cryosections for immunogold labeling. Histochem. Cell Biol. 106, 41-58.

Lippincott-Schwartz,J., Yuan,L.C., Bonifacino,J.S., and Klausner,R.D. (1989). Rapid redistribution of Golgi proteins into the ER in cells treated with brefeldin A: evidence for membrane cycling from Golgi to ER. Cell 56, 801-813.

Long,R.M., Singer,R.H., Meng,X., Gonzalez,I., Nasmyth,K., and Jansen,R.P. (1997). Mating type switching in yeast controlled by asymmetric localization of ASH1 mRNA. Science 277, 383-387.

MacDougall,N., Clark,A., MacDougall,E., and Davis,I. (2003). Drosophila gurken (TGFalpha) mRNA localizes as particles that move within the oocyte in two dynein-dependent steps. Dev. Cell 4, 307-319.

MacDougall,N., Lad,Y., Wilkie,G.S., Francis-Lang,H., Sullivan,W., and Davis,I. (2001). Merlin, the Drosophila homologue of neurofibromatosis-2, is specifically required in posterior follicle cells for axis formation in the oocyte. Development 128, 665-673.

Mellman,I. and Warren,G. (2000). The road taken: past and future foundations of membrane traffic. Cell 100, 99-112.

Mogelsvang,S., Gomez-Ospina,N., Soderholm,J., Glick,B.S., and Staehelin,L.A. (2003). Tomographic evidence for continuous turnover of Golgi cisternae in Pichia pastoris. Mol. Biol. Cell 14, 2277-2291.

Mohr,E. and Richter,D. (2003). Molecular determinants and physiological relevance of extrasomatic RNA localization in neurons. Front Neuroendocrinol. 24, 128-139.

Murthy,M. and Schwarz,T.L. (2004). The exocyst component Sec5 is required for membrane traffic and polarity in the Drosophila ovary. Development 131, 377-388.

Nehls,S., Snapp,E.L., Cole,N.B., Zaal,K.J., Kenworthy,A.K., Roberts,T.H., Ellenberg,J., Presley,J.F., Siggia,E., and Lippincott-Schwartz,J. (2000). Dynamics and retention of misfolded proteins in native ER membranes. Nat. Cell Biol. 2, 288-295.

Nelson,W.J. and Yeaman,C. (2001). Protein trafficking in the exocytic pathway of polarized epithelial cells. Trends Cell Biol. 11, 483-486.

Neuman-Silberberg,F.S. and Schupbach,T. (1993). The Drosophila dorsoventral patterning gene gurken produces a dorsally localized RNA and encodes a TGF alpha-like protein. Cell 75, 165-174.

Neuman-Silberberg,F.S. and Schupbach,T. (1996). The Drosophila TGF-alpha-like protein Gurken: expression and cellular localization during Drosophila oogenesis. Mech. Dev. 59, 105-113.

Norvell,A., Kelley,R.L., Wehr,K., and Schupbach,T. (1999). Specific isoforms of squid, a Drosophila hnRNP, perform distinct roles in Gurken localization during oogenesis. Genes Dev. 13, 864-876.

Pavlath,G.K., Rich,K., Webster,S.G., and Blau,H.M. (1989). Localization of muscle gene products in nuclear domains. Nature 337, 570-573.

Pickup,A.T. and Banerjee,U. (1999). The role of star in the production of an activated ligand for the EGF receptor signaling pathway. Dev. Biol. 205, 254-259.

Powers,J. and Barlowe,C. (1998). Transport of axl2p depends on erv14p, an ER-vesicle protein related to the Drosophila cornichon gene product. J. Cell Biol. 142, 1209-1222.

Powers,J. and Barlowe,C. (2002). Erv14p directs a transmembrane secretory protein into COPII-coated transport vesicles. Mol. Biol. Cell 13, 880-891.

Preisinger,C., Short,B., De,C., V, Bruyneel,E., Haas,A., Kopajtich,R., Gettemans,J., and Barr,F.A. (2004). YSK1 is activated by the Golgi matrix protein GM130 and plays a role in cell migration through its substrate 14-3-3zeta. J. Cell Biol. 164, 1009-1020.

Queenan,A.M., Barcelo,G., Van Buskirk,C., and Schupbach,T. (1999). The transmembrane region of Gurken is not required for biological activity, but is necessary for transport to the oocyte membrane in Drosophila. Mech. Dev. 89, 35-42.

Ralston,E. and Hall,Z.W. (1989). Intracellular and surface distribution of a membrane protein (CD8) derived from a single nucleus in multinucleated myotubes. J. Cell Biol. 109, 2345-2352.

Ripoche,J., Link,B., Yucel,J.K., Tokuyasu,K., and Malhotra,V. (1994). Location of Golgi membranes with reference to dividing nuclei in syncytial Drosophila embryos. Proc. Natl. Acad. Sci. U. S. A 91, 1878-1882.

Rossanese,O.W., Soderholm,J., Bevis,B.J., Sears,I.B., O'Connor,J., Williamson,E.K., and Glick,B.S. (1999). Golgi structure correlates with transitional endoplasmic reticulum organization in Pichia pastoris and Saccharomyces cerevisiae. J. Cell Biol. 145, 69-81.

Roth,S. (2003). The origin of dorsoventral polarity in Drosophila. Philos. Trans. R. Soc. Lond B Biol. Sci. 358, 1317-1329.

Roth,S., Neuman-Silberberg,F.S., Barcelo,G., and Schupbach,T. (1995). cornichon and the EGF receptor signaling process are necessary for both anterior-posterior and dorsal-ventral pattern formation in Drosophila. Cell 81, 967-978.

Saunders,C. and Cohen,R.S. (1999). The role of oocyte transcription, the 5'UTR, and translation repression and derepression in Drosophila gurken mRNA and protein localization. Mol. Cell 3, 43-54.

Schonbaum,C.P., Lee,S., and Mahowald,A.P. (1995). The Drosophila yolkless gene encodes a vitellogenin receptor belonging to the low density lipoprotein receptor superfamily. Proc. Natl. Acad. Sci. U. S. A 92, 1485-1489.

Schonbaum,C.P., Perrino,J.J., and Mahowald,A.P. (2000). Regulation of the vitellogenin receptor during Drosophila melanogaster oogenesis. Mol. Biol. Cell 11, 511-521.

Serano,T.L., Karlin-Mcginness,M., and Cohen,R.S. (1995). The role of fs(1)K10 in the localization of the mRNA of the TGF alpha homolog gurken within the Drosophila oocyte. Mech. Dev. 51, 183-192.

Simmonds,A.J., dosSantos,G., Livne-Bar,I., and Krause,H.M. (2001). Apical localization of wingless transcripts is required for wingless signaling. Cell 105, 197-207.

Slot,J.W., Geuze,H.J., Gigengack,S., Lienhard,G.E., and James,D.E. (1991). Immuno-localization of the insulin regulatable glucose transporter in brown adipose tissue of the rat. J. Cell Biol. 113, 123-135.

Takizawa,P.A., DeRisi,J.L., Wilhelm,J.E., and Vale,R.D. (2000). Plasma membrane compartmentalization in yeast by messenger RNA transport and a septin diffusion barrier. Science 290, 341-344.

Tautz,D. and Pfeifle,C. (1989). A non-radioactive in situ hybridization method for the localization of specific RNAs in Drosophila embryos reveals translational control of the segmentation gene hunchback. Chromosoma 98, 81-85.

Urban,S., Lee,J.R., and Freeman,M. (2002). A family of Rhomboid intramembrane proteases activates all Drosophila membrane-tethered EGF ligands. EMBO J. 21, 4277-4286.

van Eeden,F. and St Johnston,D. (1999). The polarisation of the anterior-posterior and dorsal-ventral axes during Drosophila oogenesis. Curr. Opin. Genet. Dev. 9, 396-404.

Whyte,J.R. and Munro,S. (2001). The Sec34/35 Golgi transport complex is related to the exocyst, defining a family of complexes involved in multiple steps of membrane traffic. Dev. Cell 1, 527-537.

CHAPTER 3

Ultrastructural localization of mRNAs by RNA *in situ* hybridization coupled to immuno-electron microscopy on ultrathin cryosections

Bram Herpers and Catherine Rabouille

University Medical Centre Utrecht, Department of Cell Biology and the Institute of Biomembranes, Heidelberglaan 100, 3584 CX Utrecht, The Netherlands

IN PREPARATION

Abstract
RNA *in situ* hybridization methods have revealed that some mRNAs exhibit a specific localization within a cell or tissue. To investigate what underlies mRNA localization at the ultrastructural level, we evaluated different previously published techniques and optimized these into a novel protocol. Here, we report the development of this technique which enables us to visualize mRNAs at the ultrastructural level, using a combination of RNA *in situ* hybridization and immuno-electron microscopy (ISH-IEM). This is based on protocols used to detect proteins on ultrathin cryosections of fixed materials after gelatin-embedding and ultracryomicrotomy. This technique allows the detection of endogenous mRNAs and the optimal preservation of cell ultrastructure by postfixing the sections with glutaraldehyde before the overnight incubation at 55°C, required for the hybridization. Addition of dextran sulphate to the hybridization buffer not only improves the detection efficiency, but also helps the maintenance of the ultrastructure. With this protocol double immuno-labeling of mRNA and proteins can be achieved. We applied this technique to investigate the asymmetric localization of the *gurken*, *oskar* and *bicoid* mRNAs in the *Drosophila* oocyte to establish the relationship between proteins and structural elements that mediate their maintenance. We propose that this ISH-IEM technique is applicable in other biological systems and will aid to identify structures underlying mRNA localization.

Introduction

Messenger RNAs (mRNAs) mediate the flow of information from DNA to protein. In eukaryotes, mRNAs are transcribed from genes encoded by the DNA in the nucleus before being exported to the cytoplasm. Here, mRNAs serve as blueprints for protein synthesis by ribosomes (Moore, 2005). Protein synthesis and therefore gene expression, can be regulated by controlling either the amount of transcript produced, or by regulating the translation of the transcripts.

Control of protein levels is important for proper functioning of the cell, especially when it performs a specialized function. For instance, the local control of protein expression in the dendrites contributes to synaptic plasticity. Similarly, local production of a protein can regulate developmental processes such as germ cell formation and body axis formation (St Johnston, 2005).

Local production of a protein is often preceded by the localization of the transcript encoding this protein (St Johnston, 2005). To understand the function of the localization of such mRNAs, how it is localized there and how its translation is regulated, it is important to understand what underlies the location of this given mRNA at the molecular level and to visualise it.

One technique that has allowed direct detection of mRNA in a cell or tissue is called *in situ* hybridization (ISH). It uses tagged antisense strands of nucleic acids (DNA or RNA probes) that specifically anneal/hybridise to their complementary nucleic acid sequences, either encoded by the DNA or mRNA in a cell. This is followed by the visualization of the probe using specific antibody to the tag (digoxigenin or biotin). This *in situ* hybridization technique is used in studies of gene mapping, gene expression, tumour genetics, microbial infections and RNA processing and transport (Speel, 1999). The location of genes on the chromosomes can provide insight in transcript production (Livak et al., 1978), while the detection of transcripts can be linked to protein expression (Ambrosio and Schedl, 1984). Furthermore, differences in transcript levels can point at the characteristics and function of a cell, not only for pathological (Loni and Green, 1973; Denijn et al., 1992), but also for developmental studies (St Johnston, 1995; Tomancak et al., 2002).

In situ hybridization studies revealed that mRNAs can be localized to a specific region within a cell. Examples range from *beta-actin* mRNA in neurons and fibroblasts (Lawrence and Singer, 1986), *ASH1* mRNA within the yeast bud (Long et al., 1997), *Vg1* mRNA at the vegetal pole of the *Xenopus* oocyte (Pondel and King, 1988) and *gurken*, *bicoid* and *oskar* mRNA in the *Drosophila* oocyte (Riechmann and Ephrussi, 2001). Although different models have been put forward to explain the asymmetric localization of mRNAs, these often depend on motor-mediated transport along the actin or microtubule cytoskeleton of the cell (Tekotte and Davis, 2002). In these cases, factors are bound to the transcript to function as adaptors for the transport machinery before the mRNA is delivered to its final destination, where it is anchored and translation can initiate (Wilhelm and Vale, 1993; St Johnston, 2005).

This intimate relation between mRNAs and RNA binding and adaptor proteins has been exploited to visualize these mRNA-protein complexes at the light-microscopy level. However, to achieve the fine resolution of localization and its relationship to the cytoskeleton and cell structure, ultrastructural analysis at the EM level is required.

Two different ISH approaches exist to visualize RNA on ultrathin EM sections. The pre-embedding ISH is based upon performing the hybridization of the probe to the cognate nucleic acid sequence before the tissue is strongly fixed and embedded for sectioning (Wolber

et al., 1989; Trembleau, 1993; Punnonen et al., 1999; Izumi et al., 2001; Kitazawa and Kitazawa, 2006). The advantage of this pre-embedding method is that the probe hybridization is not hampered by strong cross-linking fixatives. The disadvantage is that the tissue often needs to be permeabilized with proteases and detergents to allow the proper penetration of the probe in the thickness of the tissue, which affects its morphology and decreases further the resolution and preservation of the ultrastructure (Macville et al., 1996; Le Guellec, 1998).

Post-embedding ISH is the converse; the tissue is strongly fixed and embedded before the hybridization of the probe is performed. Because the fixation and embedding procedures are similar to normal preparations for EM, the morphology is more informative than pre-embedding ISH.

For successful post-embedding ISH, the tissues of interest need to be maintained in a hydrophilic environment, for the antisense probe to detect the mRNA. This is possible in resins like LR White and Lowicryl K4M (Le Guellec, 1998). So was elucidated the intracellular localization of *collagen I*, *fibronectin*, *growth hormone*, and *myoglobin* mRNA in kidney, brain, pituitary and muscle tissue (Le Guellec et al., 1992; Dorries et al., 1993; Mitsui et al., 1994; Yi et al., 1995). However, the strong fixation hampers the accessibility of the RNA in the tissue for the antisense probes, and these resins do not optimally conserve membrane structure (Voorhout et al., 1989). Furthermore, some proteolytic treatment on the tissue sections seems imperative to efficiently detect the RNAs (Macville et al., 1996), which further decrease structural information.

Ultrathin frozen sections from gelatine-embedded chemically fixed tissues and cells, however, have a superior morphology. Because the cells are fixed mildly and remain in an aqueous environment, immunoreactivity is retained. For many years, this has allowed the detailed and successful analysis of intracellular protein distributions by immuno-gold labeling on membrane-bound organelles, such as endoplasmic reticulum (ER), ER exit sites, Golgi, endosomes, and peroxisomes (Geuze et al., 1981; Geuze et al., 1982; Geuze et al., 1983; Herpers and Rabouille, 2004; Kondylis et al., 2005; Zeuschner et al., 2006). Here, we describe protocols that we have developed using a very similar approach to detect RNA on ultrathin frozen sections. The application of ISH on cryosections has been explored in a few reports (Jambou et al., 1995; Macville et al., 1996; Chevalier et al., 1997; van Minnen and Bergman, 2003; Taupin et al., 2006). These reports have convincingly shown the feasibility to detect mRNA on ultrathin frozen sections, and have been the basis of this investigation to develop a protocol to study the asymmetric localization of mRNAs together with proteins at the ultrastructural level.

As briefly mentioned above, three crucial mRNAs are asymmetrically localized in the *Drosophila* stage 9 oocyte. One of them, *gurken* mRNA, is very specifically localized near the oocyte nucleus at the dorsal-anterior corner. It locally encodes a protein of the TGF alpha family that is synthesized in the exocytic pathway and locally secreted to elicit a signaling cascade in the adjacent follicle cells covering the oocyte (Roth, 2003). We have shown that the organization of the exocytic pathway in stage 9 *Drosophila* oocyte is linked to the translation of such a localized RNA. Indeed, this exocytic pathway is not a single copy organelle as in mammalian cells but comprises 1000 tER-Golgi units that can function independently. These closest to the *gurken* mRNA are used to transport Grk protein to the nearest plasma membrane whatever the localization of the mRNA (Herpers and Rabouille, 2004). From this study, we made the hypothesis that *gurken* mRNA could be directly localized to the membrane compartments of the exocytic pathway.

To investigate this question, we developed protocols suitable to visualize both *gurken* mRNA and Gurken protein (that is specifically localized on the tER-Golgi units during its transport to the extracellular space) on the same cryosections. For this, the ultrastructural information, the immunoreactivity for the proteins, and the tissue accessibility of the antisense probe needed to be kept optimal. With these three demands in mind, we tested a number of different fixatives, incubation times, temperatures, compositions of the hybridization buffer and antibodies to detect the tagged antisense probe.

Here, we present this protocol that allows RNA detection by (direct) ISH on cryosections, which can be combined with protein immuno-labeling. We tested this protocol on *gurken* mRNA localized at the dorso-anterior corner of the *Drosophila* oocyte, *bicoid* mRNA localized at the anterior side, and *oskar* mRNA that localizes to the posterior pole of the oocyte (St Johnston, 2005; Steinhauer and Kalderon, 2006).

Materials and Methods

Tissue and fixation

Whole ovaries of wild type (OreR) *Drosophila melanogaster*, excised from anaesthetised fattened female flies in Ringer buffer, were immediately transferred to either of the three fixatives in 0.1M Phosphate buffer at pH7.4: 4% Paraformaldehyde (PFA); 2% PFA + 0.2% Glutaraldehyde (GA); and 2% PFA + 0.2% Acrolein. Acrolein is carcinogenic and has to be handled with extreme care. All three fixatives were applied for 4-6 hours at room temperature (RT). When 4% PFA was used, this was followed by an overnight incubation at 4°C. The fixative was removed and replaced by 1% PFA in 0.1M Phosphate buffer to store the fixed tissue for years.

Ultrathin and semi-thin cryo-sectioning

Ovaries were embedded in 12% gelatine as described previously (Herpers and Rabouille, 2004; Sommer et al., 2005). Ultrathin cryosections (60nm) were cut at -120°C, picked up with methylcellulose/sucrose (Herpers and Rabouille, 2004), and collected on nickel 50 mesh grids supporting a carbon coated formvar film. Only nickel grids are suitable for the ISH procedure as copper grids dissolve in the hybridization buffer (see below). Semi-thin cryosections (400nm) were cut at -90°C and collected on sterilized silane-coated glass object slides in an area marked and surrounded by wax.

Probe preparation

Sense and antisense probes were prepared from the full length cDNA of *gurken* (T. Schupbach). *oskar* probe was a gift of A. Ephrussi and *bicoid* probe a gift of I. Davis. Incorporation of digoxigenin (DIG)-UTP or biotin-UTP was performed according manufacturers recommendations (Roche).

Antibodies

We have used rabbit anti biotin (1:10,000, Rockland) to detect the biotinylated probe; sheep anti digoxigenin (DIG) Fab fragments coupled to Alkaline Phosphatase (DIG-AP, 1:1000, Roche) and sheep anti digoxigenin Fab fragments coupled to horse radish peroxidase (DIG-HRP, 1:1000, Roche) to detect the DIG labeled probe; and mouse anti Gurken (1D12, 1:30, DSHB). The bridging antibodies for sheep and mouse antibodies we used are rabbit anti sheep (1:750, Nordic), rabbit anti mouse (1:250, Dako), and for immunofluorescence, the AlexaFluor 488 goat anti rabbit (1:300, Molecular probes).

RNA *in situ* hybridization coupled to immunoelectron microscopy (ISH-IEM)

NB: To retain ultrastructure, permeabilizing agents like detergents and proteinase K incubations are not used. Instead, the antisense nucleotides will anneal to the mRNA exposed on the surface of the ultrathin frozen sections. For the protocol described here (which can be used for both ultrathin sections and for semi-thin sections, with adaptations described below) the best fixative to use is 4% PFA in 0.1M Phosphate buffer.

- **Pre-hybridization**
  The following steps were performed on 250µl drops on Parafilm:
  1. Wash the methylcellulose/sucrose mixture, with which the sections were collected, off by floating the grids with the sections-side on drops of diethylpyrocarbonate (DEPC)-treated PBS for 2x 10 minutes in an incubator at 37°C.
  2. Post-fix in 1% GA in PBS for 5 minutes at room temperature (RT).
  3. Rinse the fixative on 2 drops of PBS.
  4. Incubate for 15 minutes at 37°C in **pre-hybridization** buffer (50% deionised formamide, 2x SSC from a 20x stock (3M NaCl, 300mM sodium citrate) in DEPC treated water, pH6.5).
  5. Incubate further in pre-hybridization buffer on a hot plate at 55°C for 5 minutes.
  6. Meanwhile, denature the antisense probe (final dilution 0.5-1.0 µg/ml) by boiling in a water bath for 10 minutes in **hybridization** buffer (50% deionised formamide, 2x SSC, 10% dextran sulphate (w/v), 50µg/ml heparin and 100µg/ml *E. coli* tRNA in DEPC treated water, pH6.5). Use a final probe-concentration of 2µg/ml.
  7. Cool down the diluted probe on ice for at least 2 minutes.

NB: The temperature at which 50% of the RNA molecules are single-stranded, is called the melting temperature. This melting temperature (Tm) is linear with the %G and the %C in the RNA. Furthermore, the Tm is also dependent on the molar content of protons in the solution and the percentage of formamide in the buffer. This is summarized in the following equation: Tm= 81.5°C +16.6 log[Na^+] +0.41(%GC) - 0,63(%formamide) (Howley et al., 1979; Le Guellec, 1998). So when probes with a GC content of 45% are diluted in 2x SSC (330mM Na^+) and 50% formamide, the Tm is around 60°C. The annealing temperature of nucleotides is considered to be 5°C lower than the Tm, therefore 55°C has been used for hybridization. The Results section will elaborate on the use of dextran sulphate, heparin and tRNA in the hybridization buffer.

- **Hybridization and detection**
  The actual hybridization was performed in a humid environment constructed from a 9 cm Petri-dish with filter paper on the bottom soaked with 50% formamide in H_2O.
  8. Cut off the caps from eppendorf tubes and place these flat-size down on the filter paper.
  9. Load the caps with 150µl hybridization buffer containing the denatured probe.
  10. Place on hot plate at 55°C and transfer the pre-hybridized grids (step 5) onto the probe-containing hybridization buffer in the eppendorf caps.
  11. Cover the caps with a 5 cm Petri dish that are further surrounded by tissues soaked in 50% aqueous formamide, close the 9 cm Petri dish and incubate for 16 hours (overnight).
  12. Wash the unbound probe at 55°C 2x 5 minute with pre-hybridization buffer.
  13. After the second wash, leave to cool down to RT.
  14. Rinse in the pre-hybridization buffer at RT.
  15. Incubate the grids onto 5 drops of 0.15% glycin (w/v) in PBS in 10 minutes.
  16. Incubate the grids for 3 minutes in 1% BSA in PBS.
  17. Proceed with the immuno-labeling protocol using protein A gold conjugates (PAG) as described (Slot et al., 1991; Herpers and Rabouille, 2004).
      - Biotinylated probes were followed with rabbit anti biotin antibodies and then PAG.
      - DIG-labeled probes were detected by either sheep anti DIG-AP, followed by rabbit anti sheep and then PAG, or anti DIG-HRP, followed by rabbit anti sheep and then PAG. The DIG-HRP antibody, however, created artefacts in IEM (see Results).

<u>Double labeling of mRNA and protein</u>
Double labeling on ultrathin frozen sections is based on the sequential labeling method. After detection of the RNA using specific antibodies to the tag and protein A gold, another protein of choice can be detected using a different primary antibody and protein A gold of a different size as described in (Slot et al., 1991; Herpers and Rabouille, 2004)

Adaptations for (immuno-) fluorescent ISH (FISH) on semi-thin sections
ISH on semi-thin cryosections was essentially the same as for ISH on ultrathin cryosections, except that:

a. Washes were performed with drops within an area of 20mm by 20mm marked by a wax pen directly on the glass slides.
b. The post-fixation with 1% GA (step 2) was not applied and the fixative remaining on the sections after picking up was quenched by 2x 2 minute incubation with 1mg/ml $NaBH_4$ in PBS.
c. The probe detection can be performed with the same antibodies as for ultrathin sections, except that PAG is replaced by AlexaFluor 488 goat anti rabbit.
d. Simultaneous detection of the tagged probe and an antibody of choice is possible: make sure the two (or three) antibodies used are raised in different species. Detect then also with different secondary antibodies.
e. For imaging, the sections are mounted in Vectashield (Vectorlabs).

Controls
To check the specificity of the antisense probes, different controls were used. We omitted the antisense probe during the ISH, the primary antibody, or the secondary antibody (in the case of DIG-AP). Antibodies were also tested on sections not treated for ISH-IEM. We also checked the specificity of the *gurken* probe by using a sense probe produced from the *gurken* cDNA.

Results

The aim of developing the ISH-IEM protocol was to reach an optimal ultrastructural preservation with the highest signal to noise ratio for detecting endogenous RNA (that is, the highest specific labeling density). Different fixatives, hybridization times, temperatures and buffer were tested in a number of combinations using *gurken*, *bicoid* and *oskar* probes on *Drosophila* oocytes. This is summarized in Table 1. The final protocol is described in Materials and Methods.

Influence of different fixatives on the structural integrity after ISH-IEM
The ISH protocol was tested on three different fixation methods (see Materials and Methods). For this, we used in each test the same hybridization buffer for all three fixatives, and analyzed the preservation of the ultrastructure of the cryosections after overnight incubation. Consistently, the fixation of the oocytes in 2% PFA in combination with 0.2% Acrolein (Figure 4B (*bicoid*) and 5B (*oskar*)) or GA (Figure 5E-F (*oskar*)) was found the best to retain the ultrastructure under most conditions (see table 1). In contrast, under some conditions the ISH procedure damaged the ultrastructure of 4% PFA fixed oocytes (Figure 2 A, B, C (*gurken*)).

Although showing the least ultrastructural preservation, the 4% PFA fixed samples consistently resulted in more signal when compared to Acrolein or GA fixed oocyte sections (compare 5A to 5B for *oskar*). This result is explained by the fact that Acrolein and GA are strong cross-linking fixatives that prevent extraction of the cytoplasm during the procedure. This extraction by the buffer seems to be necessary for increasing the ability of the antisense probe to penetrate the sections and to bind to the mRNA in the tissue sections. This is possible in the fast but relatively weaker fixed 4% PFA samples, which yields an increased labeling.

The good signal to noise ratio in the 4% PFA fixed oocyte sections prompted us to overcome the loss of ultrastructure by the hybridization procedure. Therefore a post-fixation step with 1% GA for 5 minutes before the pre-hybridization was implemented. The resulting morphology was similar to ISH-IEM on sections of strongly fixed oocytes, together with a two to three fold higher labeling density of, for instance, *oskar* mRNA at the posterior pole (compare Figure 5A to 5B). Because of the increased yield in labeling density, we favour 4% PFA fixed oocyte sections for ISH-IEM.

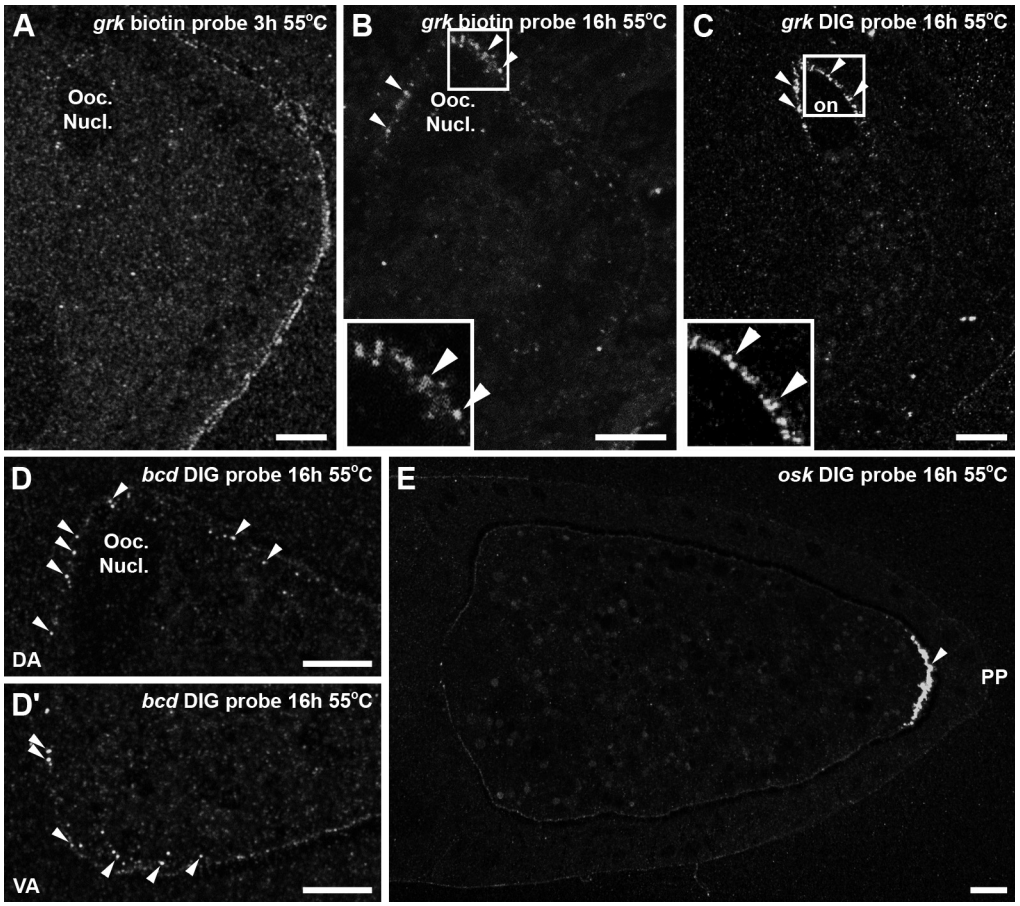

Figure 1: FISH on semi-thin sections requires overnight incubation.
(A-C) Semi-thin sections of stage 9 wild type oocytes incubated with a *gurken* (*grk*) probe at 55°C. **(A)** is incubated for 3 hours, **(B and C)** for 16 hours. **(A and B)** were incubated with a biotin labeled probe, visualized with rabbit anti biotin and Alexa 488 goat anti rabbit. **(C)** was incubated with a DIG-labeled *gurken* probe, visualized with sheep anti DIG-AP, rabbit anti sheep and Alexa 488 goat anti rabbit. Note the discrete dots (arrowheads) at the DA corner capping the oocyte nucleus (Ooc. Nucl./on) in **(B and C)**. Boxed areas show magnifications of *gurken* mRNA found in the dots at the DA corner.
(D and D') Semi-thin section of a stage 10 oocyte incubated with a DIG-labeled *bicoid* probe at 55°C for 16 hours. **(D)** shows labeling in spots (arrowheads) at the dorso-anterior (DA) corner, **(D')** at the ventral-anterior (VA) corner.
(E) *oskar* mRNA detected with a DIG-labeled *oskar* probe on semi-thin sections. Note the restriction of the signal to the posterior pole (PP) of this stage 10 oocyte (arrowhead).
Scale bars: 10µm.

⟶ **Figure 2: ISH-IEM on ultrathin sections is dependent on hybridization buffer composition.**
(A) Ultrathin frozen sections of a stage 9, 4% PFA fixed oocyte were directly hybridized at 55°C with a DIG-labeled *gurken* probe for 16 hours in condition B (see table 1) after washes in PBS. Detection with DIG-AP (10nm). Labeling was specifically found at the DA corner between the oocyte nucleus (Ooc. Nucl.) and the plasma membrane (PM). Arrows point at non-specific labeling in the yolk deposits.
(B) Similar to **(A)**, but with biotin-labeled *gurken* probe (biotin, 10nm). Note the labeling near or on an electron-dense structure (asterisk). Also note the extraction of the cytoplasm.
(C) Similar to **(B)**, but incubated under condition C (table 1) at 70°C and detection with 15nm PAG. Note the damaging effect of higher temperatures.
(D) Similar to **(C)**, but incubated at 55°C. Note that the addition of dextran sulphate prevents extraction of the cytoplasm, compared to **(C)**.
(E) Similar to **(D)**, but under condition D: post-fixed in 1% GA for five minutes before incubation.
(F) Non-treated sections incubated with anti DIG-HRP (15nm). It labels tER-Golgi units (G): this anti-DIG antibody is not useable for probe detection by IEM.
Cytoplasmic areas: asterisks. Scale bars: 200nm.

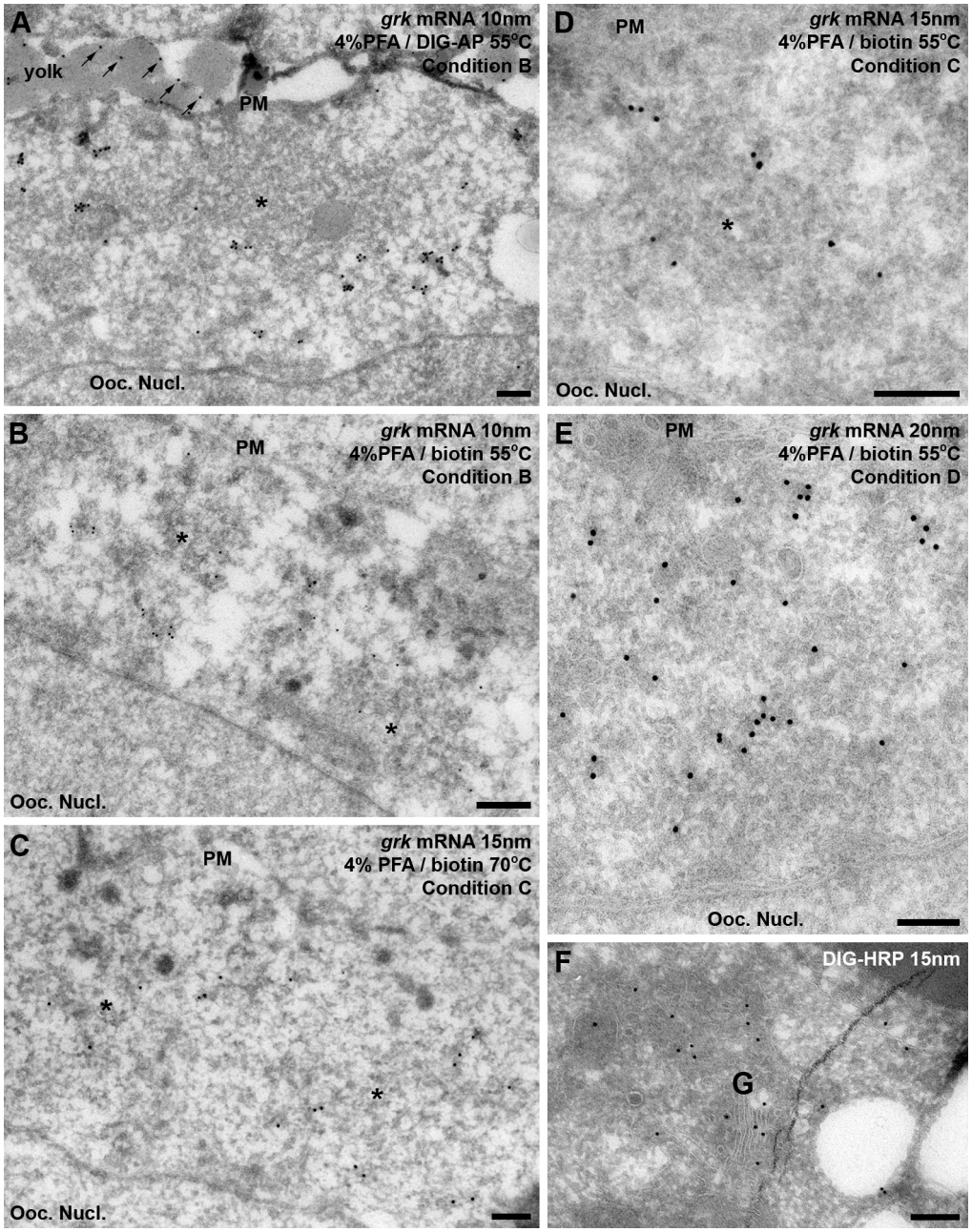

The composition of the hybridization buffer

The hybridization buffer functions to keep RNA molecules in a linearized state, allowing the antisense probe to bind the mRNA in the tissue by base-pairing. The temperature at which 50% of the RNA is single-stranded is dependent on the GC-content of the RNA itself, the amount of protons in the buffer and the percentage of formamide in the hybridization buffer (Howley et al., 1979; Le Guellec, 1998) (see Materials and Methods).

The efficiency with which a single-stranded RNA probe can anneal to the mRNA in the section also depends on the following reagents: heparin, transfer (t)RNA, salmon-sperm (ss)DNA, Denhardt's reagent and dextran sulphate. Heparin is used to reduce background in the signal (Singh and Jones, 1984), Denhardt's reagent (50x corresponds to 1% Ficoll 400, 1% polyvinylpyrrolidone and 1% bovine serum albumin) can be used to increase the efficiency of the hybridization (Denhardt, 1966). Dextran sulphate increases the binding of the probe to the target mRNA, speeds up the hybridization process and reduces background (Ku et al., 2004; Kubota et al., 2006). ssDNA and tRNA essentially play the same role in the hybridization buffer. They act to promote specific hybridization by reduction of non-specific absorption of the probe by the tissue.

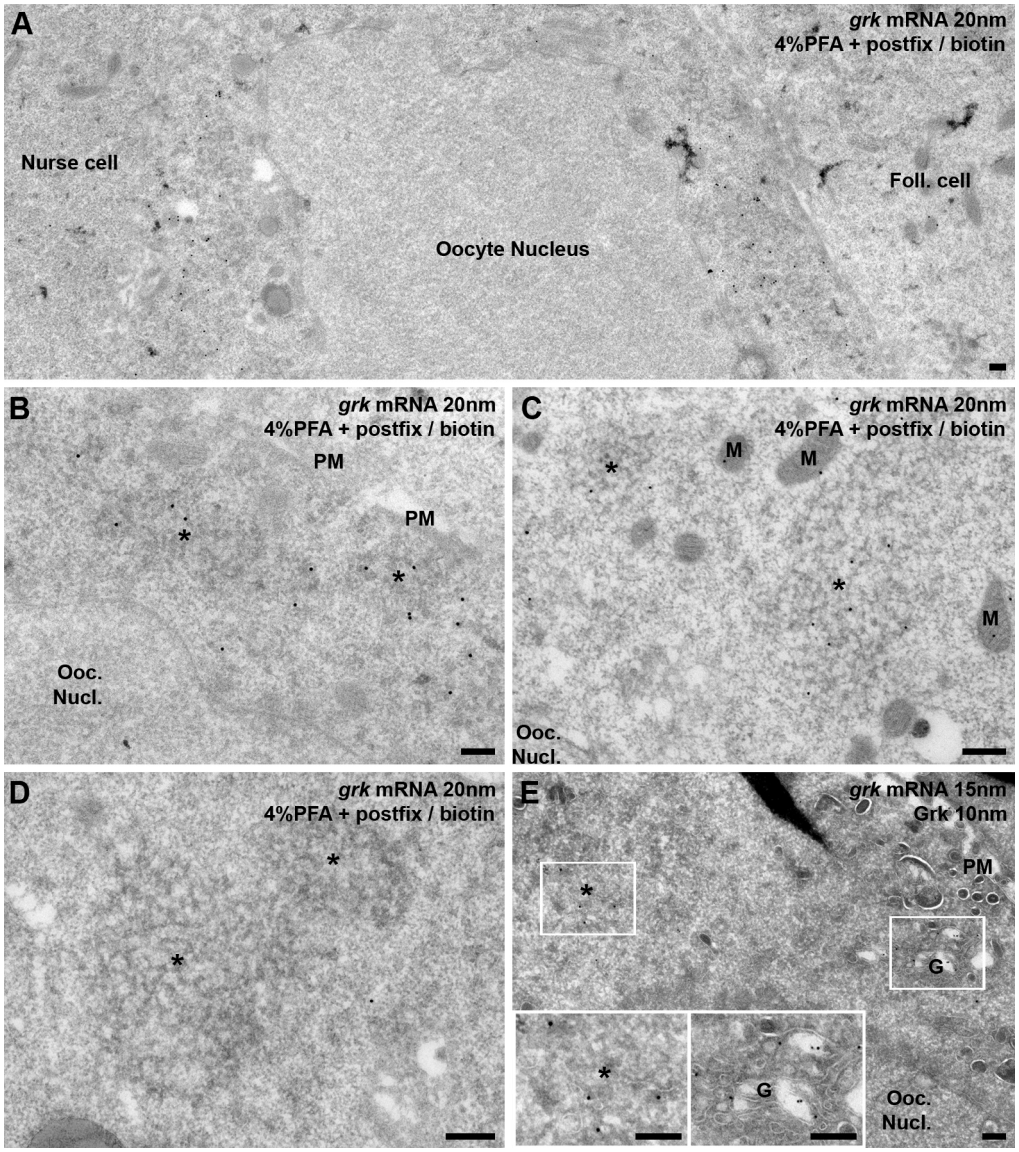

Table 1.

Fixative \ Condition	A at 55°C	B at 37°C	B at 55°C	B at 70°C	C at 37°C	C at 55°C	C at 70°C	D at 55°C
4% PFA	n(-+)	n(-)	r(+)	n(-+)	g(-+)	g(++)	r(-+)	v(++)
2% PFA + 0.2% GA	g(-)	v(-)	g(-+)	g(-+)	v(-)	v(+)	g(-+)	v(+)
2% PFA + 0.2% Ac	g(-)	v(-)	v(-+)	g(-+)	v(-)	v(+)	g(-+)	v(+)

A: Melt on 1% Gelatin in PBS, hybridize in 50% Formamide, 2x SSC, 50mM heparin, 100mM tRNA

B: Melt on PBS, hybridize in 50% Formamide, 2x SSC, 50µg/ml heparin, 100µg/ml tRNA

C: Melt on PBS, hybridize in 50% Formamide, 2x SSC, 50µg/ml heparin, 100µg/ml tRNA, 10% dextran sulphate

D: Melt on PBS, post fix, hybridize in 50% Formamide, 2x SSC, 50µg/ml heparin, 100µg/ml tRNA, 10% dextran sulphate

Table 1: Hybridization conditions, fixative and temperature
Three different fixatives were used to test four different buffers / conditions (A to D) at three different temperatures (37°C, 55°C and 70°C). The results were empirically categorized into morphology (not good (n), reasonable (r), good (g) and very good (v)) and signal to noise (not good (-), reasonable (-+), good (+) and very good (++)). Signal to noise ratios were based on the comparison with sections that were not hybridized with an RNA probe, or internally controlled by comparing the labeling in the oocyte to the follicle cells. These cells should not express *gurken*, *bicoid*, or *oskar* mRNA. In summary, post-fixation of the sections with 1% GA before hybridization in hybridization buffer containing dextran sulphate gives the best results for all three fixatives at 55°C.

For the ISH-IEM protocol we have developed, we found that the hybridization buffer comprising 50% formamide, 2x SSC, 100µg/ml tRNA, 50µg/ml heparin and 10% w/v dextran sulphate, gives the best results in terms of labeling when a full length antisense probe is used. The addition of dextran sulphate is essential in the hybridization buffer. Not only the non-specific labeling decreases, but the morphology of the ultrathin sections is also better preserved (table 1, compare Figure 2A, B to 2D, E for *gurken*). The presence of dextran sulphate in the hybridization buffer might prevent the evaporation of the water from the hybridization buffer during the overnight incubation at 55°C, keeping salt concentrations equal to the starting levels and thereby stabilizing the melting temperature of the RNAs. The prevention of an increased salt concentration might be the basis of the ultrastructural preservation, diminishing extraction by the buffer.

Hybridization time

We compared two different incubation times (3 and 16 hours) of the antisense probe with the tissue sections. We found that the incubation of 16 hours was better. This is exemplified in Figure 1A, showing a 400nm thick section of a stage 9 oocyte, incubated for 3 hours at 55°C in which no signal is detected. In contrast, sections incubated overnight at the same temperature

← **Figure 3: ISH-IEM on ultrathin frozen sections detects *gurken* in discrete cytoplasmic areas.**
(A) 60nm sections of a stage 9 wild type oocyte hybridized with a biotin-labeled *gurken* specific probe (20nm). Note that the signal is not found in the nucleus or in the neighbouring follicle (Foll.) or nurse cells, but exclusively in the cytoplasm of the DA corner.
(B) *gurken* mRNA is found inside electron dense areas (asterisks) of the cytoplasm between the oocyte nucleus (Ooc. Nucl.) and the plasma membrane (PM).
(C) Similar to **(B)**, only note here the occasional background labeling of biotin in mitochondria (M).
(D) On the same sections, no signal for *gurken* mRNA is found in those discrete cytoplasmic areas (here in the middle (asterisks)), other than in the DA corner.
(E) Gurken protein (10nm, in the tER-Golgi unit (G), right boxed area), does not colocalize with *gurken* mRNA (15nm) in the cytoplasmic areas (asterisk, left boxed area).
Scale bars: 200nm.

displayed a labeling pattern (Figure 1B,C for *gurken*) that is by all means very similar to this obtained in whole mount in situ hybridization (ISH) (Herpers and Rabouille, 2004). That is, a tight crescent next to the oocyte nucleus at the dorsal anterior corner. We also used this 16 hour incubation for ISH on ultrathin (60nm) sections with similar results.

Influence of hybridization temperature on the labeling density and structural integrity

Three hybridization temperatures (37°C, 55°C and 70°C) were tested. At 37°C the loss of ultrastructure was found to be minimal, but the signal to noise ratio was too low. It was necessary to incubate at higher temperatures under more stringent conditions to increase the specificity of the signal. 70°C was found too high for good ultrastructural preservation, and led to decrease in signal (Table 1, Figure 2C for *gurken*). However, at 55°C the stringency was sufficient to allow good signal to noise ratios while retaining adequate preservation of the ultrastructure (Figure 2D for *gurken*).

RNAse sensitivity and section storage

We tested our protocol by incubating the sections in 10μg/ml RNAse A in PBS for 20 minutes at 37°C, before post-fix and hybridization. This resulted only in background labeling and provides us with a control for the specificity of the reaction. Similar results were obtained when the grids were incubated on 1% gelatine in PBS to wash off the pick-up solution composed of methylcellulose/sucrose (see Materials and Methods) before the hybridization steps. This indicated the gelatine solution was contaminated with RNAse activity. It was therefore omitted and replaced by RNAse inactivated (diethylpyrocarbonate (DEPC) treated) PBS.

Cryosections of gelatine-embedded tissues can be stored under a drop of pick-up solution at 4°C for extended periods (Griffith and Posthuma, 2002). We tested the influence of longer storage on the detection of mRNA by ISH-IEM. No difference was found when sections were either processed for ISH-IEM directly after sectioning, or after a few months storage at 4°C.

Specificity of the antibodies

Two different tagged nucleotides, biotin-UTP and DIG-UTP, were used to make the antisense RNA probes. To detect these tags, three antibodies, one directed against biotin (rabbit anti biotin), and two against DIG (sheep anti DIG-AP and sheep anti DIG-HRP), were tested for their background on ultrathin cryo-sections, prior to ISH-IEM, that is, in the absence of RNA probe incubation.

The sheep anti DIG-HRP (used for its anti-DIG properties, not for the coupled HRP) showed a substantial non-specific labeling in Golgi membranes and was therefore not used further (Figure 2F). The sheep anti-DIG-AP antibody incubated sections were clean from background in the nucleus, the cytoplasm and membrane-compartments, only the yolk deposited by the follicle cells in the intercellular space between them and the oocyte appeared to label non-specifically (Figure 2A (*gurken*) (arrows), 5A (*oskar*)).

When incubated with the rabbit anti-biotin antibody, no background was found in the cytoplasm, nucleus or membrane-bound compartments, except the occasional background in mitochondria (M, Figure 3C (*gurken*)), a cross-reactivity reported previously (Chevalier et al., 1997). Therefore we concluded that both the anti DIG-AP and the anti biotin antibodies are potentially useful to specifically detect DIG-labeled and biotin-labeled probes in the ISH-IEM.

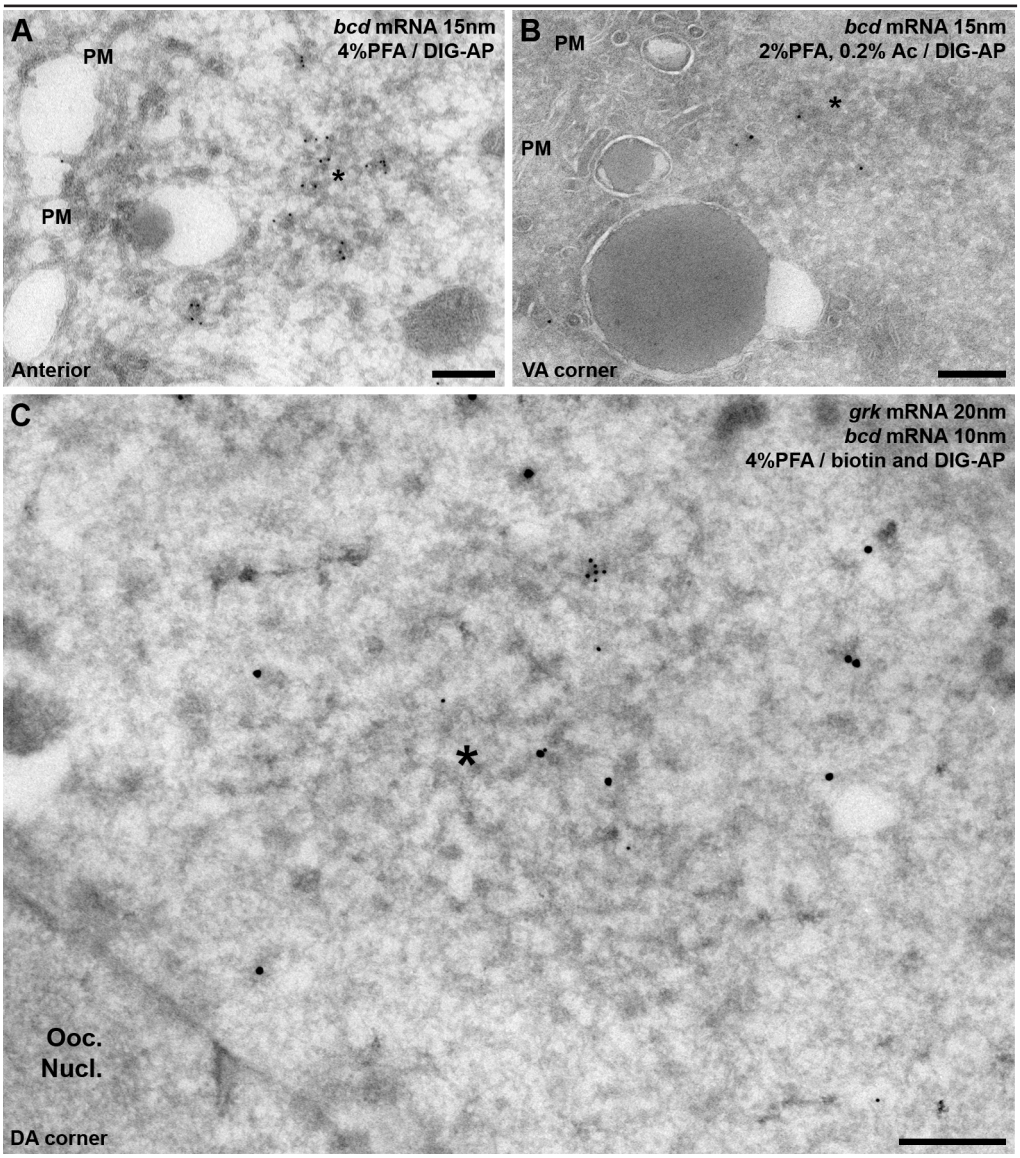

Figure 4: *bicoid* mRNA localizes in the same cytoplasmic areas as *gurken* mRNA.
(A) Ultrathin frozen section of a 4% PFA fixed oocyte *in situ* hybridized with a DIG-labeled *bicoid* (*bcd*) probe reveals *bicoid* mRNA (15nm) in discrete cytoplasmic areas at the anterior side. PM: plasma membrane facing the nurse cells.
(B) Similar to **(A)**: *bicoid* mRNA (15nm) is found in cytoplasmic areas, here at the ventral anterior corner. This oocyte was fixed in 2% PFA / 0.2% Acrolein: note the low amount of labeling.
(C) Double ISH with DIG-labeled *bicoid* mRNA (10nm) and biotin-labeled *gurken* mRNA (20nm) on 4% PFA fixed stage 9 oocyte sections. This shows that the discrete cytoplasmic areas can be occupied simultaneously by different mRNAs.
Cytoplasmic areas: asterisks. Scale bars: 200nm.

Detection of *gurken*, *bicoid* and *oskar* mRNA in the *Drosophila* oocyte by ISH-IEM

Using our final protocol (4% PFA fixed oocytes, incubated for 16 hours at 55°C in hybridization buffer with dextran sulphate added) without the post-fixation step on semi-thin sections, we found that *gurken* mRNA was specifically localized at the dorso-anterior (DA) corner, capping

the oocyte nucleus, whether a biotin-labeled (Figure 1B) or a DIG labeled (Figure 1C) probe was used, in agreement with whole mount ISH (Herpers and Rabouille, 2004), showing the specificity of the method. In addition, this new technique on semi-thin sections reveals that the mRNA was present in discrete dots (Figure 1B and C, insets).

To investigate the nature of these dots, we performed ISH-IEM on oocyte ultrathin cryosections, and we found that *gurken* mRNA indeed localizes in specific structures in the cytoplasm of at the dorso-anterior corner of the oocyte. These structures can be distinguished from the surrounding cytoplasm by the difference in electron-density (Figure 3B and C, asterisks) and fine morphology. These cytoplasmic areas were exclusively labeled at the DA corner where the oocyte nucleus resides (Figure 3A). This indicates a role for these cytoplasmic areas in *gurken* mRNA localization at the DA corner (Delanoue et al., 2006).

Intracellular Gurken protein is predominantly found in tER-Golgi units at the DA corner in stage 9-10 oocytes (Herpers and Rabouille, 2004), see introduction. Our initial question was to investigate whether *gurken* mRNA was anchored on the membrane of the exocytic pathway present at the dorsal-anterior corner. We therefore performed a double labeling for *gurken* RNA and Gurken protein as described in Materials and Methods. By FISH/ immunofluorescence on semi-thin sections, the mRNA and the protein did not colocalize (not shown).

Using ISH-IEM, we confirmed that the cytoplasmic areas containing *gurken* mRNA were not associated to the tER-Golgi units that were positive for Gurken (Figure 3E). The surrounding ER was sometimes labeled for *gurken* mRNA in line with the synthesis of the protein on this organelle (Herpers and Rabouille, 2004).

We also used the antisense *bicoid* RNA probes on semi-thin sections of oocytes, that yielded labeling along the anterior side, at the dorsal-anterior corner, and at the ventral-anterior corner, as expected. Interestingly, the labeling was also present in discrete dots similar to those found for *gurken* mRNA (Figure 1D and D'). By ISH-IEM we found that *bicoid* populates the same cytoplasmic areas we had characterized for *gurken* mRNA, at the dorsal-anterior corner, along the anterior pole and at the VA corner (Figure 4A and 4B). When *gurken* and *bicoid* mRNA were simultaneously hybridized with two different labeled probes on ultrathin cryosections, we found that *bicoid* and *gurken* can populate the same cytoplasmic areas at the DA corner (Figure 4C).

oskar mRNA, in contrast, is restricted to the posterior pole at stage 10 (Figure 1E). Since *gurken* and *bicoid* mRNA are both found in electron-dense cytoplasmic areas, we asked whether this was also the case for *oskar* mRNA. By ISH-IEM, *oskar* mRNA was restricted to the posterior pole, in the cytoplasm close to the endocytic profiles budding from the plasma membrane (Figure 5A and 5B), but not in the cytoplasmic areas we described for *gurken* and *bicoid* mRNA.

Oskar protein has been shown to localize in specialized structures called the polar granules (Ephrussi and Lehmann, 1992; Vanzo and Ephrussi, 2002). The polar granules are restricted to the oocyte posterior pole and are known to play a role in the formation of the germline in the future embryo (Williamson and Lehmann, 1996), recruiting germ cell specific factors. When Oskar protein and *oskar* mRNA were double labeled on oocyte ultrathin sections, they did not show colocalization (Figure 5C and 5D). We then tested whether *oskar* mRNA colocalized with the double stranded RNA binding protein Staufen, which is involved in *oskar* mRNA localization (St Johnston et al., 1992). We found that Staufen colocalizes with *oskar* mRNA in the cytoplasm at the posterior pole, and not in polar granules (Figure 5E and 5F).

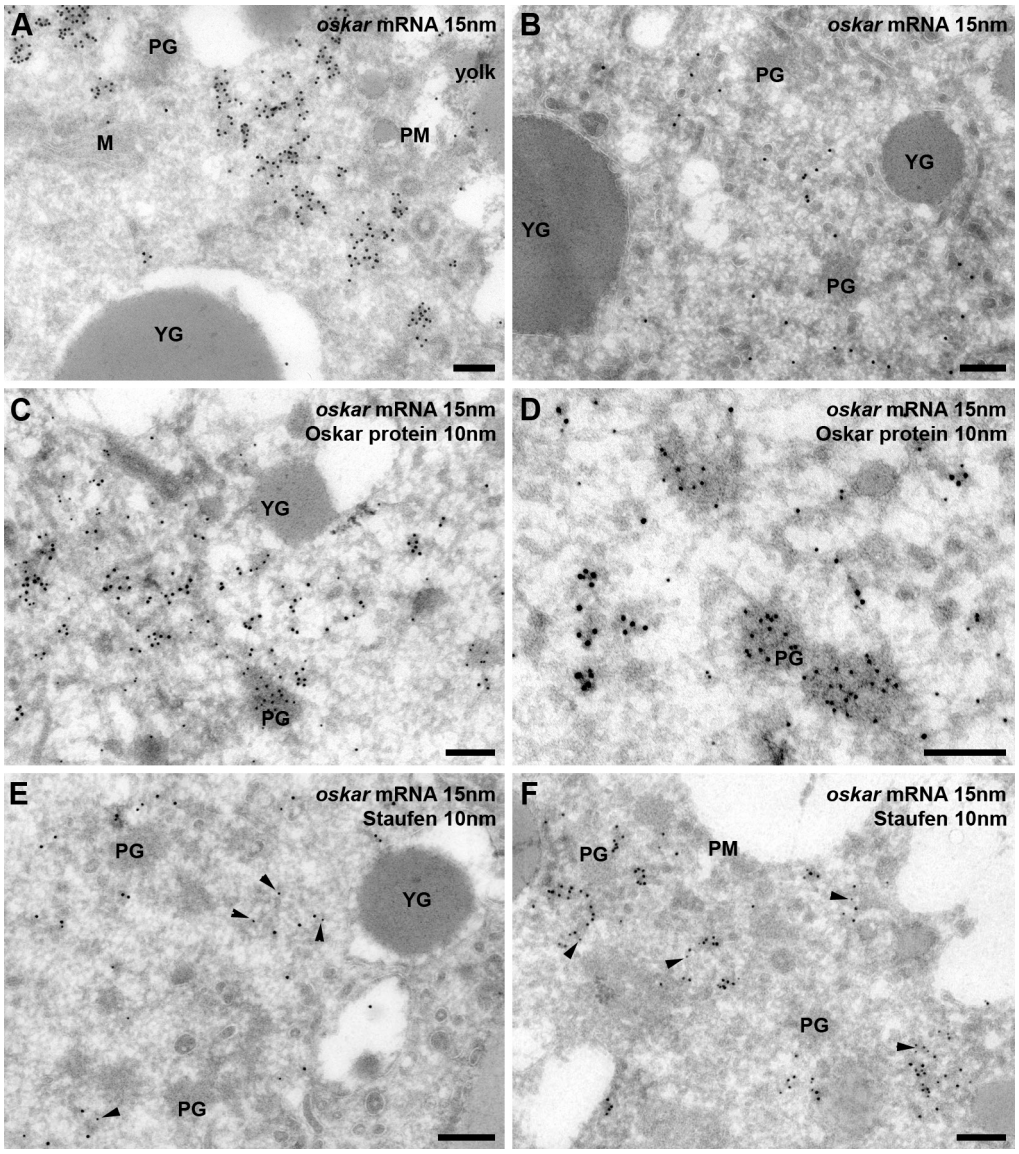

Figure 5: *oskar* mRNA colocalizes with Staufen in the cytoplasm, not in polar granules.
(A) Section of a stage 10 oocyte, 4% PFA fixed. This section was post-fixed in 1%GA after sectioning, before hybridization with DIG-labeled *oskar* probe at 55°C. Note that the *oskar* mRNA labeling (15nm) is restricted to the cytoplasm close to the plasma membrane (PM) at the posterior pole and not associated with a polar granule (PG).
(B) Endogenous *oskar* mRNA (15nm) detected with a DIG-probe at 55°C on 2%PFA / 0.2% Acrolein fixed oocyte sections. Note that the labeling is less than in **(A)**, but also restricted to the cytoplasm and not in polar granules.
(C and D) Double labeling of *oskar* mRNA (15nm) and Oskar protein (10nm) clearly shows separation of transcript and protein. Sections from a 4% PFA fixed oocyte.
(E and F) Double labeling of *oskar* mRNA (15nm) and the double-stranded RNA binding protein Staufen (10nm, some are marked by arrowheads) shows colocalization of oskar mRNA and Staufen. Sections from a 2% PFA / 0.2% GA fixed oocyte.
Scale bars: 200nm.

Discussion

We described here a novel post-embedding technique applicable for both semi-thin and ultrathin cryosections of fixed materials to specifically detect RNA. With this technique it is possible to analyze not only the intracellular localization of different mRNAs, but also to identify the structures involved in their localization. Because this technique allows retention of the immunoreactivity of proteins in the sections after hybridization, double-labelings are possible. This not only opens the possibility to identify cellular structures, but also the analysis of their functions, in term of transport and anchoring of mRNA, for instance.

This method does not use amplification steps such as silver-enhancement or precipitation reactions. Instead, the RNA is ultimately detected by protein A-gold gold leading to a rather low labeling efficiency. The labeling efficiency using proteinA gold is estimated to be between 0.1% and 10%, depending on factors such as the support material for embedding, section thickness and intrinsic properties of the antibodies (Griffiths and Hoppeler, 1986). Here, the RNA has to be detected first by the tagged antisense probe before the immuno-labeling procedures. We propose that the labeling efficiency is even more reduced.

This low labeling efficiency is a clear limitation of this technique, especially when the RNA is not very abundant. However, it could be used to monitor the different levels of expression of given RNAs. This indeed seems to be the case for the three mRNAs tested: *oskar* mRNA was the most abundant both by light and electron-microscopy. *gurken* and *bicoid* mRNA, however, showed lower labeling intensities by both techniques.

The retention of ultrastructure that we achieved is of special importance for the biological questions we had regarding the mRNA localization and anchoring, that is, to understand how the localization of transcripts in the *Drosophila* oocyte is controlled, what mechanisms regulate the anterior localization of *bicoid* mRNA, the restriction of *gurken* mRNA to the DA corner and the posterior localization of *oskar* mRNA and what mechanisms regulate their translation during development.

The localization, timing and degree of translation need to be controlled for proper development. The importance of this control is expressed by the many gene products identified to play a role in the localization and translation of these RNAs (St Johnston, 2005; Steinhauer and Kalderon, 2006).

Therefore it is important to have established a method with which it is possible to visualize proteins suspected to have a role in localization and translational control of mRNAs in the structures supporting their function. The finding that *gurken* mRNA and *bicoid* mRNA localize to the same cytoplasmic areas calls for further research into the nature and function of these areas. Combinations of ISH-IEM and antibody labeling, drug treatment, mutant analysis, as well as RNA injection and antibody injection experiments will shed light on the function of these structures and help identify proteins involved in mRNA localization and anchoring. In this perspective, we have used a combination of these to investigate *gurken* mRNA anchoring (Delanoue et al., 2006).

Last, the location of *oskar* mRNA at the posterior pole, seemingly not associated to polar granules, calls for interesting further studies. For instance, to understand how the translation of *oskar* mRNA is regulated and what proteins colocalize with this mRNA. Similarly interesting is how Oskar protein is able to mediate the localization of the *oskar* mRNA to the posterior pole (Rongo et al., 1995), while the RNA does not seem to be directly attached to the polar granules in which Oskar protein resides. Another topic for investigation is whether the *oskar* mRNA labeling

pattern, that colocalizes with Staufen, corresponds to the large (50S-80S) silencing particles, formed by the oligomerization of the translation regulator Bruno (Chekulaeva et al., 2006).

The development of this ISH technique on cryosections has also broader implications; it has opened doors for RNA biology to immuno-electron microscopy that provides a direct view on the location and underlying ultrastructure. In this perspective, live cell imaging results obtained by light microscopy, could be further investigated by EM to correlate functional data to structural insight (Oorschot et al., 2002).

This technique is also applicable to other RNA detection methods such as the use of MS2-GFP tags (expressing mRNAs with a specific MS2-recognition sequence) (Bertrand et al., 1998; Beach et al., 1999), molecular beacons (oligonucleotides with a fluorophore and a quencher that separate and thereby fluoresce upon binding to the target mRNA) (Bratu et al., 2003) or by RNA injection (*in vivo* injection assays with labeled synthetic RNAs) (MacDougall et al., 2003; Delanoue and Davis, 2005). For instance, by using fluorescent injected RNAs, specific events can be captured in time by fixation and further investigated by correlative immuno-EM. Although not tested, we predict that this technique would be applicable to other tissues and cells, not only for *Drosophila*. With the increasing amount of asymmetrically localized mRNAs identified in neurons, epithelial cells and oocytes (Mohr and Richter, 2003; Lopez and Jansen, 2004; St Johnston, 2005), in unicellular organisms like yeast, algae and amoeba (Han et al., 1997; Chartrand et al., 2001; Colon-Ramos et al., 2003; Gonsalvez et al., 2005), it will be interesting to investigate whether intracellular structures mediating RNA trafficking, anchoring, translation regulation and degradation share morphological features.

Acknowledgements
This work was supported by a Nederlandse Organisatie voor Wetenschappelijk Onderzoek (NWO) Aspasia grant (015.001.129) to C.R.

References

Ambrosio,L. and Schedl,P. (1984). Gene expression during Drosophila melanogaster oogenesis: analysis by in situ hybridization to tissue sections. Dev. Biol. 105, 80-92.

Beach,D.L., Salmon,E.D., and Bloom,K. (1999). Localization and anchoring of mRNA in budding yeast. Curr. Biol. 9, 569-578.

Bertrand,E., Chartrand,P., Schaefer,M., Shenoy,S.M., Singer,R.H., and Long,R.M. (1998). Localization of ASH1 mRNA particles in living yeast. Mol. Cell 2, 437-445.

Bratu,D.P., Cha,B.J., Mhlanga,M.M., Kramer,F.R., and Tyagi,S. (2003). Visualizing the distribution and transport of mRNAs in living cells. Proc. Natl. Acad. Sci. U. S. A 100, 13308-13313.

Chartrand,P., Singer,R.H., and Long,R.M. (2001). RNP localization and transport in yeast. Annu. Rev. Cell Dev. Biol. 17, 297-310.

Chekulaeva,M., Hentze,M.W., and Ephrussi,A. (2006). Bruno acts as a dual repressor of oskar translation, promoting mRNA oligomerization and formation of silencing particles. Cell 124, 521-533.

Chevalier,J., Yi,J., Michel,O., and Tang,X.M. (1997). Biotin and digoxigenin as labels for light and electron microscopy in situ hybridization probes: where do we stand? J. Histochem. Cytochem. 45, 481-491.

Colon-Ramos,D.A., Salisbury,J.L., Sanders,M.A., Shenoy,S.M., Singer,R.H., and Garcia-Blanco,M.A. (2003). Asymmetric distribution of nuclear pore complexes and the cytoplasmic localization of beta2-tubulin mRNA in Chlamydomonas reinhardtii. Dev. Cell 4, 941-952.

Delanoue,R. and Davis,I. (2005). Dynein anchors its mRNA cargo after apical transport in the Drosophila blastoderm embryo. Cell 122, 97-106.

Delanoue, R., Herpers, B., Soetaert, J., Rabouille, C., and Davis, I. (2006). Squid, Drosophila hnRNP-A, is required for Dynein to form static anchoring complexes with gurken mRNA. This thesis, Chapter 4.

Denhardt,D.T. (1966). A membrane-filter technique for the detection of complementary DNA. Biochem. Biophys. Res. Commun. 23, 641-646.

Denijn,M., Schuurman,H.J., Jacobse,K.C., and de Weger,R.A. (1992). In situ hybridization: a valuable tool in diagnostic pathology. APMIS 100, 669-681.

Dorries,U., Bartsch,U., Nolte,C., Roth,J., and Schachner,M. (1993). Adaptation of a non-radioactive in situ hybridization method to electron microscopy: detection of tenascin mRNAs in mouse cerebellum with digoxigenin-labelled probes and gold-labelled antibodies. Histochemistry 99, 251-262.

Ephrussi,A. and Lehmann,R. (1992). Induction of germ cell formation by oskar. Nature 358, 387-392.

Geuze,H.J., Slot,J.W., Strous,G.J., Lodish,H.F., and Schwartz,A.L. (1982). Immunocytochemical localization of the receptor for asialoglycoprotein in rat liver cells. J. Cell Biol. 92, 865-870.

Geuze,H.J., Slot,J.W., Strous,G.J., Lodish,H.F., and Schwartz,A.L. (1983). Intracellular site of asialoglycoprotein receptor-ligand uncoupling: double-label immunoelectron microscopy during receptor-mediated endocytosis. Cell 32, 277-287.

Geuze,H.J., Slot,J.W., van der Ley,P.A., and Scheffer,R.C. (1981). Use of colloidal gold particles in double-labeling immunoelectron microscopy of ultrathin frozen tissue sections. J. Cell Biol. 89, 653-665.

Gonsalvez,G.B., Urbinati,C.R., and Long,R.M. (2005). RNA localization in yeast: moving towards a mechanism. Biol. Cell 97, 75-86.

Griffith,J.M. and Posthuma,G. (2002). A reliable and convenient method to store ultrathin thawed cryosections prior to immunolabeling. J. Histochem. Cytochem. 50, 57-62.

Griffiths,G. and Hoppeler,H. (1986). Quantitation in immunocytochemistry: correlation of immunogold labeling to absolute number of membrane antigens. J. Histochem. Cytochem. 34, 1389-1398.

Han,J.W., Park,J.H., Kim,M., and Lee,J. (1997). mRNAs for microtubule proteins are specifically colocalized during the sequential formation of basal body, flagella, and cytoskeletal microtubules in the differentiation of Naegleria gruberi. J. Cell Biol. 137, 871-879.

Herpers,B. and Rabouille,C. (2004). mRNA localization and ER-based protein sorting mechanisms dictate the use of transitional endoplasmic reticulum-golgi units involved in gurken transport in Drosophila oocytes. Mol. Biol. Cell 15, 5306-5317.

Howley,P.M., Israel,M.A., Law,M.F., and Martin,M.A. (1979). A rapid method for detecting and mapping homology between heterologous DNAs. Evaluation of polyomavirus genomes. J. Biol. Chem. 254, 4876-4883.

Izumi,S., Shin,M., Hishikawa,Y., and Koji,T. (2001). Localization in situ of specific RNA by electron microscopy. Ital. J. Anat. Embryol. 106, 45-50.

Jambou,R., Hatin,I., and Jaureguiberry,G. (1995). Evidence by in situ hybridization for stage-specific expression of the ATP/ADP translocator mRNA in Plasmodium falciparum. Exp. Parasitol. 80, 568-571.

Kitazawa,S. and Kitazawa,R. (2006). In situ detection of specific gene expression during and immediately after transcription at electron microscopic level. J. Struct. Biol. 153, 64-72.

Kondylis,V., Spoorendonk,K.M., and Rabouille,C. (2005). dGRASP localization and function in the early exocytic pathway in Drosophila S2 cells. Mol. Biol. Cell 16, 4061-4072.

Ku,W.C., Lau,W.K., Tseng,Y.T., Tzeng,C.M., and Chiu,S.K. (2004). Dextran sulfate provides a quantitative and quick microarray hybridization reaction. Biochem. Biophys. Res. Commun. 315, 30-37.

Kubota,K., Ohashi,A., Imachi,H., and Harada,H. (2006). Visualization of mcr mRNA in a methanogen by fluorescence in situ hybridization with an oligonucleotide probe and two-pass tyramide signal amplification (two-pass TSA-FISH). J. Microbiol. Methods.

Lawrence,J.B. and Singer,R.H. (1986). Intracellular localization of messenger RNAs for cytoskeletal proteins. Cell 45, 407-415.

Le Guellec,D. (1998). Ultrastructural in situ hybridization: a review of technical aspects. Biol. Cell 90, 297-306.

Le Guellec,D., Trembleau,A., Pechoux,C., Gossard,F., and Morel,G. (1992). Ultrastructural non-radioactive in situ hybridization of GH mRNA in rat pituitary gland: pre-embedding vs ultra-thin frozen sections vs post-embedding. J. Histochem. Cytochem. 40, 979-986.

Livak,K.J., Freund,R., Schweber,M., Wensink,P.C., and Meselson,M. (1978). Sequence organization and transcription at two heat shock loci in Drosophila. Proc. Natl. Acad. Sci. U. S. A 75, 5613-5617.

Long,R.M., Singer,R.H., Meng,X., Gonzalez,I., Nasmyth,K., and Jansen,R.P. (1997). Mating type switching in yeast controlled by asymmetric localization of ASH1 mRNA. Science 277, 383-387.

Loni,M.C. and Green,M. (1973). Detection of viral DNA sequences in adenovirus-transformed cells by in situ hybridization. J. Virol. 12, 1288-1292.

Lopez,d.H. and Jansen,R.P. (2004). mRNA localization and the cytoskeleton. Curr. Opin. Cell Biol. 16, 80-85.

MacDougall,N., Clark,A., MacDougall,E., and Davis,I. (2003). Drosophila gurken (TGFalpha) mRNA localizes as particles that move within the oocyte in two dynein-dependent steps. Dev. Cell 4, 307-319.

Macville,M.V., Van Dorp,A.G., Dirks,R.W., Fransen,J.A., and Raap,A.K. (1996). Evaluation of pepsin treatment for electron microscopic RNA in situ hybridization on ultra-thin cryosections of cultured cells. Histochem. Cell Biol. 105, 139-145.

Mitsui,T., Kawai,H., Naruo,T., and Saito,S. (1994). Ultrastructural localization of myoglobin mRNA in human skeletal muscle. Histochemistry 101, 99-104.

Mohr,E. and Richter,D. (2003). Molecular determinants and physiological relevance of extrasomatic RNA localization in neurons. Front Neuroendocrinol. 24, 128-139.

Moore,M.J. (2005). From birth to death: the complex lives of eukaryotic mRNAs. Science 309, 1514-1518.

Oorschot,V., de Wit,H., Annaert,W.G., and Klumperman,J. (2002). A novel flat-embedding method to prepare ultrathin cryosections from cultured cells in their in situ orientation. J. Histochem. Cytochem. 50, 1067-1080.

Pondel,M.D. and King,M.L. (1988). Localized maternal mRNA related to transforming growth factor beta mRNA is concentrated in a cytokeratin-enriched fraction from Xenopus oocytes. Proc. Natl. Acad. Sci. U. S. A 85, 7612-7616.

Punnonen,E.L., Fages,C., Wartiovaara,J., and Rauvala,H. (1999). Ultrastructural localization of beta-actin and amphoterin mRNA in cultured cells: application of tyramide signal amplification and comparison of detection methods. J. Histochem. Cytochem. 47, 99-112.

Riechmann,V. and Ephrussi,A. (2001). Axis formation during Drosophila oogenesis. Curr. Opin. Genet. Dev. 11, 374-383.

Rongo,C., Gavis,E.R., and Lehmann,R. (1995). Localization of oskar RNA regulates oskar translation and requires Oskar protein. Development 121, 2737-2746.

Roth,S. (2003). The origin of dorsoventral polarity in Drosophila. Philos. Trans. R. Soc. Lond B Biol. Sci. 358, 1317-1329.

Singh,L. and Jones,K.W. (1984). The use of heparin as a simple cost-effective means of controlling background in nucleic acid hybridization procedures. Nucleic Acids Res. 12, 5627-5638.

Slot,J.W., Geuze,H.J., Gigengack,S., Lienhard,G.E., and James,D.E. (1991). Immuno-localization of the insulin regulatable glucose transporter in brown adipose tissue of the rat. J. Cell Biol. 113, 123-135.

Speel,E.J. (1999). Robert Feulgen Prize Lecture 1999. Detection and amplification systems for sensitive, multiple-target DNA and RNA in situ hybridization: looking inside cells with a spectrum of colors. Histochem. Cell Biol. 112, 89-113.

St Johnston,D. (1995). The intracellular localization of messenger RNAs. Cell 81, 161-170.

St Johnston,D. (2005). Moving messages: the intracellular localization of mRNAs. Nat. Rev. Mol. Cell Biol. 6, 363-375.

St Johnston,D., Brown,N.H., Gall,J.G., and Jantsch,M. (1992). A conserved double-stranded RNA-binding domain. Proc. Natl. Acad. Sci. U. S. A 89, 10979-10983.

Steinhauer,J. and Kalderon,D. (2006). Microtubule polarity and axis formation in the Drosophila oocyte. Dev. Dyn. 235, 1455-1468.

Taupin,V., Metenier,G., Delbac,F., Vivares,C.P., and Prensier,G. (2006). Expression of two cell wall proteins during the intracellular development of Encephalitozoon cuniculi : an immunocytochemical and in situ hybridization study with ultrathin frozen sections. Parasitology 132, 815-825.

Tekotte,H. and Davis,I. (2002). Intracellular mRNA localization: motors move messages. Trends Genet. 18, 636-642.

Tomancak,P., Beaton,A., Weiszmann,R., Kwan,E., Shu,S., Lewis,S.E., Richards,S., Ashburner,M., Hartenstein,V.,

Celniker,S.E., and Rubin,G.M. (2002). Systematic determination of patterns of gene expression during Drosophila embryogenesis. Genome Biol. 3, RESEARCH0088.

Trembleau,A. (1993). Detection of mRNA in electronic microscopy: in situ hybridization of a biotin-labeled oligonucleotide prior to embedding. Pathol. Biol. (Paris) 41, 194-197.

van Minnen,J. and Bergman,J.J. (2003). Stimulus-dependent translocation of egg-laying hormone encoding mRNA into the axonal compartment of the neuroendocrine caudodorsal cells. Invert. Neurosci. 5, 1-7.

Vanzo,N.F. and Ephrussi,A. (2002). Oskar anchoring restricts pole plasm formation to the posterior of the Drosophila oocyte. Development 129, 3705-3714.

Voorhout,W.F., Leunissen-Bijvelt,J.J., Van Der Krift,T.P., and Verkleij,A.J. (1989). The application of cryo-ultramicrotomy and freeze-substitution in immuno-gold labelling of hybrid proteins in Escherichia coli. A comparison. Scanning Microsc. Suppl 3, 47-55.

Wilhelm,J.E. and Vale,R.D. (1993). RNA on the move: the mRNA localization pathway. J. Cell Biol. 123, 269-274.

Williamson,A. and Lehmann,R. (1996). Germ cell development in Drosophila. Annu. Rev. Cell Dev. Biol. 12, 365-391.

Wolber,R.A., Beals,T.F., and Maassab,H.F. (1989). Ultrastructural localization of herpes simplex virus RNA by in situ hybridization. J. Histochem. Cytochem. 37, 97-104.

Yi,J., Michel,O., Sassy-Prigent,C., and Chevalier,J. (1995). Electron microscopic location of mRNA in the rat kidney: improved post-embedding in situ hybridization. J. Histochem. Cytochem. 43, 801-809.

Zeuschner,D., Geerts,W.J., van Donselaar,E., Humbel,B.M., Slot,J.W., Koster,A.J., and Klumperman,J. (2006). Immuno-electron tomography of ER exit sites reveals the existence of free COPII-coated transport carriers. Nat. Cell Biol. 8, 377-383.

CHAPTER 4

Drosophila Squid hnRNP is required for Dynein to form static anchoring complexes with *gurken*/TGF-alpha mRNA

Renald Delanoue[1,3@], Bram Herpers[2@], Jan Soetaert[1], Catherine Rabouille[2] and Ilan Davis[1]

1. Wellcome Trust Centre for Cell Biology, Michael Swann building, University of Edinburgh, Mayfield Road, Edinburgh EH9 3JR, UK
2. University Medical Centre Utrecht, Department of Cell Biology and the Institute of Biomembranes, Heidelberglaan 100, 3584 CX Utrecht, The Netherlands
3. Current address: Centre de Biochimie, Parc Valrose, Faculté des Sciences, 06108 NICE cedex 2, France

@ The first two authors contributed equally to this work (joint first authors in alphabetic order)

SUBMITTED FOR PUBLICATION

Summary

In *Drosophila* oocytes, *gurken* mRNA is transported by Dynein to form the primary embryonic axes. We show that *gurken* transcripts are transported directly by Dynein in EM-dense particles on microtubules. These particles are not associated with vesicles or membrane-bound and contain many copies of *gurken* mRNA, Dynein and Squid/hnRNP. At their dorso-anterior destination, transport particles assemble into large EM-dense cytoplasmic anchoring complexes, within which *gurken* transcripts are statically anchored by Dynein. Squid is required for transport of *gurken* mRNA into these structures and for its static anchoring by Dynein. In *squid* mutants, *gurken* mRNA remains in transport particles that are in continuous anterior flux. Inhibiting Squid function after *gurken* mRNA is localized leads to loss of anchoring and the conversion of sponge bodies into transport particles. We propose a general principle for RNA anchoring, involving molecular motors acting as static anchors in large anchoring complexes facilitated by RNA binding proteins.

Introduction

mRNA localization directs the biosynthesis of proteins to specific sub-cellular compartments in all major model systems, such as yeast, *Drosophila* and a number of vertebrate models (St Johnston, 2005). In *Drosophila*, well known examples include the apical localization of pair-rule transcripts (Davis and Ish-Horowicz, 1991; Wilkie and Davis, 2001) that concentrates the transcription factors they encode into adjacent nuclei, ensuring fidelity of embryonic patterning (Bullock et al., 2004). *wingless (wg)* mRNA is also apically localized in order to concentrate the WNT signal it encodes to apical membranes (Simmonds et al., 2001). There are also many localized transcripts in *Drosophila* oocytes that contribute to patterning by targeting proteins to the same site. The best characterized of these are localized to three key sites. At the posterior pole, *oskar (osk)* and *nanos (nos*) are responsible for setting up the posterior pattern and the pole plasm that defines the germ line; *bicoid (bcd)* mRNA encodes the anterior morphogen; and *gurken (grk)* encodes a secreted TGF-α signal and is localized at two different times in oogenesis, first posteriorly, then dorso-anteriorly. The Grk signal is targeted to the same locations, thus initiating the antero-posterior and dorso-ventral axes of the oocyte and future embryo (Neuman-Silberberg and Schupbach, 1993; Gonzalez-Reyes et al., 1995).

mRNA localization occurs by several distinct mechanisms, including selective degradation (Bashirullah et al., 1999), diffusion followed by anchoring (Glotzer et al., 1997; Forrest and Gavis, 2003) or continual active transport (Weil et al., 2006), amongst other forms of delivery by molecular motors (Tekotte and Davis, 2002). The best characterized case of a motor that transports RNA is MyosinV, which transports *ASH1* mRNA along actin microfilaments to the bud in *S. cerevisiae* (Jansen et al., 1996; Sil and Herskowitz, 1996; Bertrand et al., 1998). Members of the Kinesin family of plus end directed molecular motors, have also been shown to be required for the transport of mRNAs. Notably, Kinesin I (Kin I) transports *osk* mRNA to the posterior of the *Drosophila* oocytes (Brendza et al., 2000; Cha et al., 2002; Palacios and St Johnston, 2002). The minus end directed microtubule (MT) motor, cytoplasmic Dynein (Dynein) is required for the transport of a number of mRNA cargoes to the minus ends of MTs (Van de Bor and Davis, 2004). Examples include pair-rule and *wg* mRNAs in *Drosophila* blastoderm embryos, as well as *grk* mRNA ((Wilkie and Davis, 2001; MacDougall et al., 2003), and probably *bcd* mRNA in the oocyte (Cha et al., 2001; Januschke et al., 2002; Schnorrer et al., 2000).

grk mRNA is also probably transported by Dynein from the nurse cells to the oocyte as *grk* transcription by the nurse cells is sufficient for proper axis formation (Caceres and Nilson, 2005). Once in the oocyte, *grk* RNA is transported to the posterior in early stages, and in later stages transported in two Dynein dependent steps, first to the anterior and then to the dorso-anterior corner (MacDougall et al., 2003). However, in none of these cases of Dynein transport, is it known whether transport occurs by direct association of the mRNA cargo with the transporting motor, or indirectly by hitchhiking on a transport vesicle or along a membrane bound compartment such as the Endoplasmic Reticulum (ER), as previously postulated for *Xenopus* Vg1 (Deshler et al., 1997).

Once at its final destination, mRNA must be kept localized, a process that could occur by a number of possible mechanisms (Delanoue and Davis, 2005), including anchoring or continuous active transport. Actin dependent tethering has been favoured as a means of anchoring mRNA. However, F-actin is not required for anchoring of the apically localized pair-rule transcripts in blastoderm embryos. Instead, apical transcripts are tethered in a MT and Dynein dependent

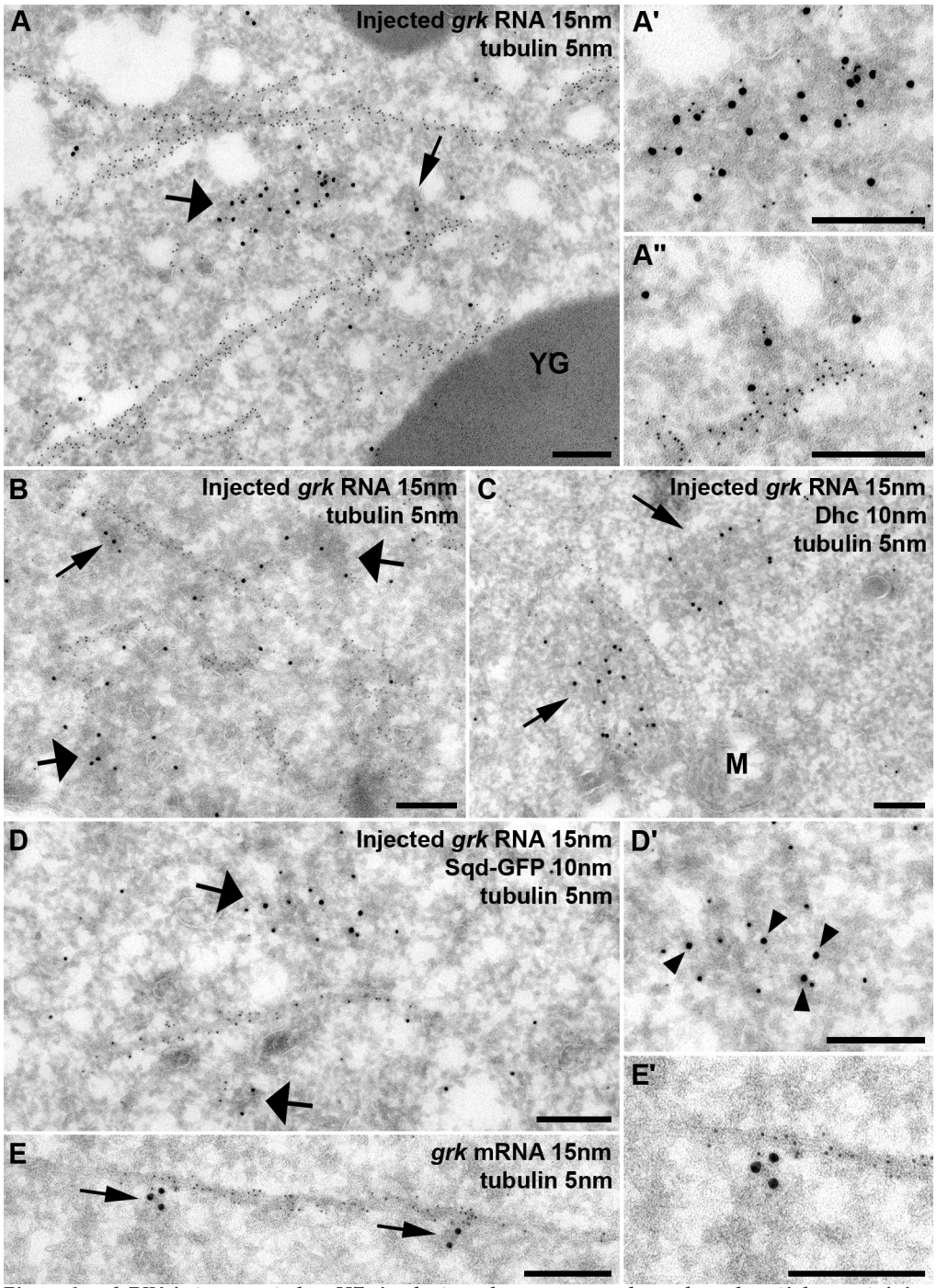

Figure 1. *grk* RNA is transported on MTs in electron dense non-membrane bound particles containing Dynein and Sqd.
(A-B) Wild type oocyte injected with biotinylated *grk* RNA and fixed after 20 min. *grk* RNA (15nm) is found in electron dense transport particles ranging from 70 to 500nm that are either on MTs (thin arrows), or near them (thick arrows) marked by αtubulin (5nm).

(C) Transport particles labeled for *grk* RNA (15nm), Dynein heavy chain (10nm) and MTs (5nm).
(D-D') Biotinylated *grk* RNA (15 nm, small arrowheads) injected into a SqdGFP (10nm), which is found in transport particles on MTs (5nm).
(E-E') Endogenous *grk* mRNA in stage 9 wild type oocytes (15nm) detected in transport particles associated with MTs (5nm). Yolk granules (YG), mitochondria (M).
Scale bars: 200nm.
In this and all subsequent figures "*grk* mRNA" refers to the endogenous transcript and "*grk* RNA" to the injected RNA.

manner, independently of the ATPase activity of the motor and the Dynein cofactors Bicaudal D (BicD) and Egalitarian (Egl), which are required for transport (Delanoue and Davis, 2005). It is not currently known how *grk* mRNA is maintained at its final site of localization, nor whether any specialized structure or membrane bound organelles are involved.

Some factors have been identified that are involved in *grk* mRNA localization (Van Buskirk and Schupbach, 2002; Goodrich et al., 2004), of which the best studied is Squid (Sqd), a *Drosophila* hnRNP (Norvell et al., 1999). Like other hnRNPs, Squid probably binds to many RNAs in addition to *grk* in the oocyte and has many basic cellular functions. However, the *Drosophila squid* null phenotype has a specific defect in the second step of *grk* mRNA transport rather than a more severe defect expected from an essential cellular factor (Norvell et al., 1999; MacDougall et al., 2003). It remains unclear whether Sqd is also required for anchoring.

Here, we address these questions by imaging and perturbing the movement and anchoring of *grk* RNA in living cells, in combination with immuno-EM techniques we have developed to co-visualize *grk* mRNA, the Dynein motor complex and Sqd. We first show that multiple molecules of *grk* mRNA are transported together in electron-dense particles we term "transport particles". These are found in close association with MTs and contain components of the Dynein motor complex and Sqd. Transport particles are not membrane-bound nor associated specifically with membrane, demonstrating that Dynein directly transports *grk* mRNA on MTs, presumably through a protein linker. We show that, at the dorso-anterior destination, *grk* RNA is statically anchored together with components of the Dynein complex and Sqd in large EM-dense structures, previously described as sponge bodies (Wilsch-Brauninger et al., 1997). Like apical anchoring in the embryo (Delanoue and Davis, 2005), *grk* mRNA anchoring by Dynein does not require the motor cofactor, Egl, required for Dynein dependent transport. We also found that, in addition to its role in the second step of *grk* mRNA transport, Sqd is required for *grk* anchoring and efficient formation and maintenance of anchoring complexes. We propose that Sqd is required for *grk* mRNA transport particles to become incorporated or converted into sponge bodies at the dorso-anterior corner. We suggest that Sqd is required for static anchoring of *grk* by Dynein, perhaps by promoting its switch from a motor to an anchor during the formation of the sponge bodies.

Results

grk RNA is transported along MTs in transport particles containing Dynein and Sqd

The transport of *grk* RNA by Dynein could either be achieved by association with Dynein on MTs, or indirectly by hitchhiking on another Dynein dependent transport process, such as vesicular transport. To distinguish definitively between these possibilities, we used immuno-EM methods on cryo-sections to co-detect *grk* mRNA with MTs and Dynein motor components. We first studied the transport intermediates of injected biotinylated *grk* RNA in the centre of early stage 9 oocytes. 20 minutes after the injection, we fixed, recovered and processed the egg chambers for immuno-EM using methods we established for good membrane preservation of this tissue (Herpers and Rabouille, 2004). We found that injected *grk* RNA particles co-assemble

in non-membrane bound electron dense particles (Figure 1A-D') that vary in size from 70 to 500nm. These particles are not consistently or specifically in close proximity to membrane bound organelles, such as Endoplasmic Reticulum (ER), or vesicles. Many particles are either adjacent to MTs or closer than 100 nm from the nearest MT (Figure 1, thin arrow), although some particles are located at larger distances from MTs (Figure 1, thick arrow). We estimated crudely from the density of gold particles and efficiency of labeling, that transport particles contain 100 to 2000 injected RNA molecules or 20-100 endogenous transcripts (see suppl. experimental procedures).

We found that injected *grk* RNA co-localizes with Dynein motor complex components: Dynein heavy chain (Dhc), (Figure 1C), BicD and Egl (Suppl. Figure 1A and B), indicating that there are likely to be many Dynein motors as well as RNA molecules in each EM-dense particle. Furthermore, GFP tagged Squid (SqdGFP) is also present in *grk* RNA transport particles (Figure 1D-D'). We conclude that injected *grk* RNA is transported directly on MTs by the Dynein motor in electron dense RNP particles, containing many *grk* RNA molecules, Dynein motor complexes and transacting factors, which we refer to as *grk* RNA "transport particles".

To investigate whether endogenous *grk* mRNA, like injected RNA, can be detected in transport particles, we improved methods of *in situ* hydridization on ultrathin cryo-sections followed by immuno electron microscopy (ISH-IEM) that allow detection of the relatively low abundance of *grk* transcript (see experimental procedures). We found that *grk* RNA localizes within EM-dense particles similar in appearance to transport particles (Figure 1E-E').

grk RNA is anchored at the DA corner in sponge bodies

To determine the fate of transport particles once they arrive at their dorso-anterior destination, we studied at the ultra-structural level, the localization of endogenous *grk* RNA in stage 9 oocytes. At the dorso-anterior corner, endogenous *grk* mRNA is localized within large cytoplasmic structures whose ultrastructure is different in appearance from transport particles (Figure 2B-C and Suppl. Figure 2). Sectioning plastic embedded wild type oocytes, revealed that are similar in appearance to previously described sponge bodies that contain the Exu protein (Figure 2A, (Wilsch-Brauninger et al., 1997)). We find sponge bodies throughout the oocyte cytoplasm, but *grk* mRNA is only present in those located in the dorso-anterior corner. Sponge bodies are not membrane bound, can be as large as 2.5μm and consist of electron dense material forming interconnected strands of 60-90nm wide that are inter-digitated by cytoplasm and ER tubules, thus giving them a sponge-like appearance. They are often flanked by MTs (Figure 2A) and, like the transport particles, contain Dhc (Figure 2D, Suppl. Figure 3C and D), as well as BicD and Egl

→ **Figure 2. *grk* RNA is localized with Dynein in dorso-anterior sponge bodies.**
(also see suppl. Figure 2, highlights the same structures in pseudo-colours)
(A-A') Sections of Spurr embedded wild type stage 9 oocytes showing large electron dense sponge bodies (asterisks) often flanked by MTs (rows of small arrowheads) at the dorso-anterior corner **(A)**. Square indicates the area shown at high magnification showing difference in morphology between sponge bodies and the surrounding cytoplasm **(A')**.
(B-B') Endogenous *grk* mRNA is detected specifically at the dorso-anterior corner (20nm) in sponge bodies (asterisk) **(B)**. The squared area is shown at high magnification illustrating the similarity to the plastic section **(A')** and showing the gold labeled RNA. The thin line marks the oocyte plasma membrane (PM in **B**).
(C-C') Low magnification view of the dorsal-anterior corner of a stage 9 oocyte showing the endogenous *grk* mRNA both in sponge bodies (asterisks) and in transport particles in the vicinity (arrowheads). The squared area is shown at high magnification **(C')**.
(D-D') The sponge bodies (asterisks) where the endogenous *grk* mRNA (15nm) is found are also positive for Dhc (10nm, arrowheads) **(D)**. The square indicates the area shown at high magnification **(D')**.
(E-E') Dhc (10nm) and injected biotinylated *grk* RNA (15nm) in sponge bodies in a wild type stage 9 oocyte, 60min after injection. MTs (5nm). The squared area in **(E)** is shown at high magnification **(E')**. Mitochondria (M); Oocyte nucleus (Ooc nucl); Plasma membrane (PM). Asterisks indicate the sponge bodies.
Scale bars: 200nm.

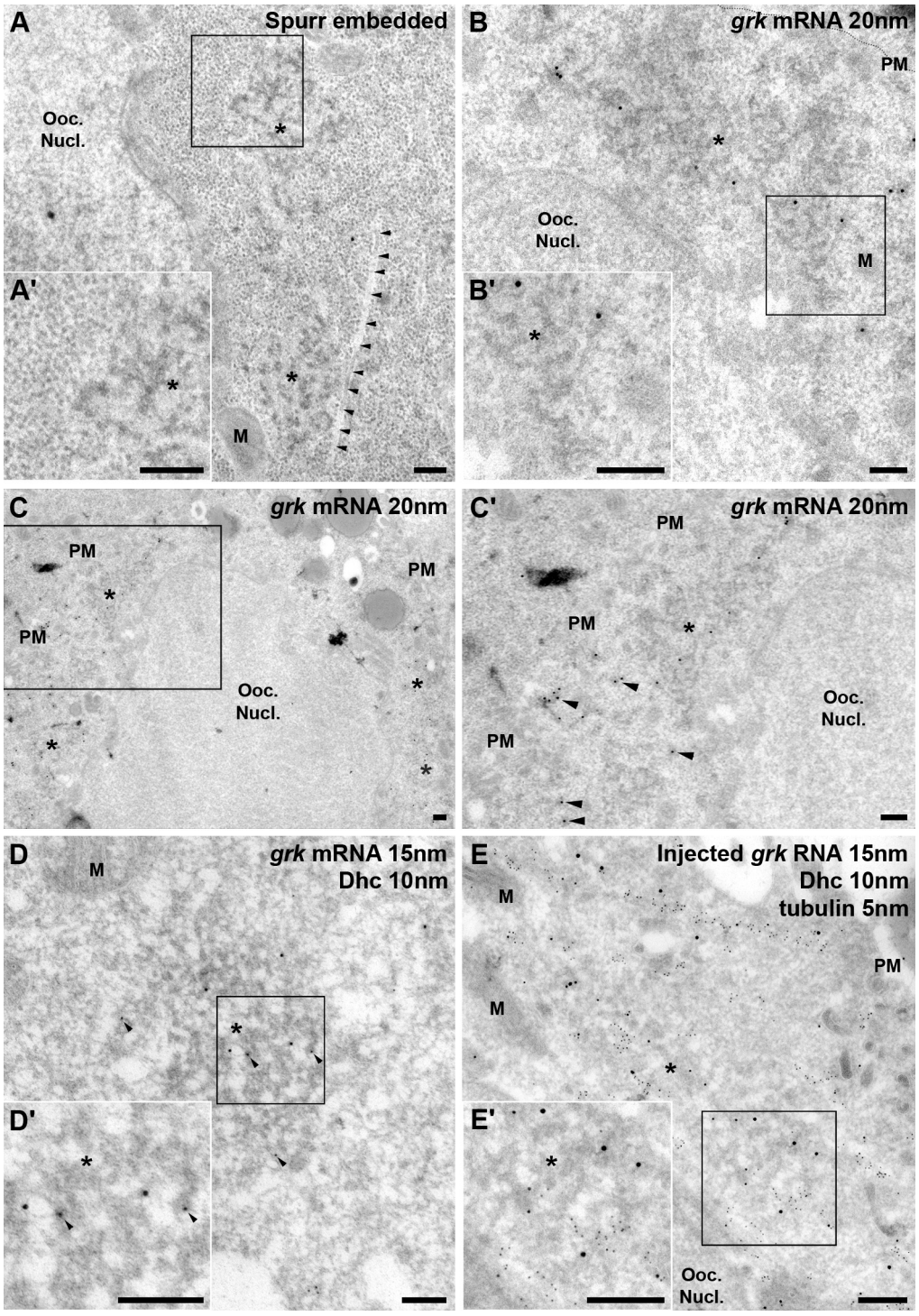
A
Spurr embedded
Ooc.
Nucl.
A'
M
B
grk mRNA 20nm
PM
Ooc.
Nucl.
M
B'
C
grk mRNA 20nm
PM
PM
PM
Ooc.
Nucl.
C'
grk mRNA 20nm
PM
PM
PM
Ooc.
Nucl.
D
M
grk mRNA 15nm
Dhc 10nm
D'
E
Injected grk RNA 15nm
Dhc 10nm
tubulin 5nm
M
M
PM
E'
Ooc.
Nucl.

(Suppl. Figure 3C). Injected *grk* RNA also localizes to sponge bodies at the dorso-anterior corner together with Dhc (Figure 2E), BicD and Egl (Suppl. Figure 3A and B), and sponge bodies size and number is increased in the dorso-anterior corner by injecting *grk* RNA (data not shown). We conclude that the Dynein rich *grk* RNA transport particles are delivered to the final site of localization at the dorso-anterior corner where the RNA in some way becomes anchored together with other components of the particle within sponge bodies (Figure 2C).

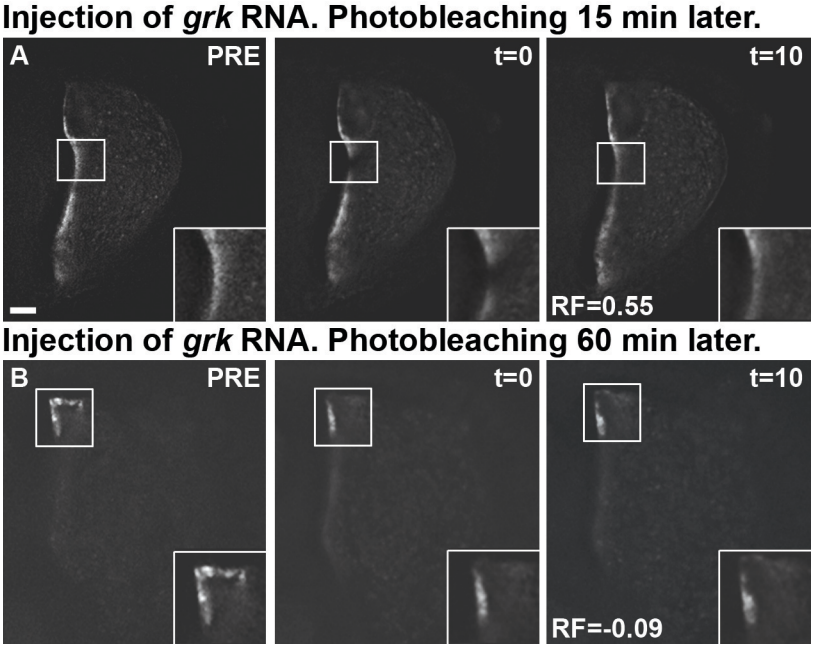

Figure 3. Injected *grk* RNA is statically anchored at the dorso-anterior corner.
(A) FRAP experiment in a living oocyte with AlexaFluor488 labeled *grk* RNA in mid transport (15 min after injection). At t=0 min, the region of the anteriorly localized *grk* RNA shown by the white square, is bleached. A partial recovery of the signal is observed (recovery fraction, RF=0.55) 10 min after bleaching (t=10min).
(B) FRAP experiment of living oocyte showing AlexaFluor488 labeled *grk* RNA fully localized at the dorso-anterior corner (60 min after injection). At t=0, region of *grk* RNA shown by the white square is bleached and does not recover (RF=-0.09) 10 min later (t=10min). Insets show higher magnifications of the bleached areas. PRE: pre-photobleaching. Scale bar: 10µm.

grk RNA anchoring is static and requires intact MT and Dynein but not Egl

We next investigated the mechanism by which *grk* RNA is kept within the sponge bodies once it arrives at the dorso-anterior corner. The presence of Dynein motor components with endogenous and injected *grk* RNA at the site of localization (above) suggests that the transcript could be anchored at the dorso-anterior by the Dynein motor, in a similar manner to pair-rule transcript anchoring at the apical cytoplasm of the blastoderm embryo (Delanoue and Davis, 2005). Alternatively, *grk* RNA could be continuously transported to the dorso-anterior by the Dynein motor, a model that predicts a continuous flow of RNA particles moving in and out the sponge bodies. To distinguish between static anchoring and continuous transport of *grk* RNA, we carried out Fluorescence Recovery After Photo-bleaching (FRAP) experiments on fully localized injected *grk* RNA in wild type egg chambers. We found that photo-bleached *grk* RNA that has completed only the first stage of transport and is temporarily localized at the anterior of the oocyte, recovers (Figure 3A). In contrast, photo-bleached *grk* RNA fails to recover at the dorso-anterior corner (Figure 3B). We conclude that *grk* RNA is not anchored at the anterior

after completion of the first step of its localization, but is statically anchored once it arrives at the dorso-anterior corner.

We then investigated further the mechanism of static anchoring at the dorso-anterior corner. We first co-visualized the RNA with F-actin and MT at the site of localization by immuno-fluorescence. We found that *grk* RNA co-localizes with MTs (Figure 4A and 4C) but not with F-actin (Suppl. Figure 4A). We then inhibited F-actin polymerization with Latrunculin A and found that it had no effect on the localization of either endogenous or injected *grk* RNA (Suppl. Figure 4B-F). In contrast, depolymerizing MTs with Colcemid disrupted the localization of injected *grk* RNA (Figure 4D) and partly disrupts the localization of endogenous *grk* mRNA (Figure 4B). Control experiments showed that depolymerizing MTs did not lead to a loss of the sponge bodies (data not shown). We conclude that MTs and not F-actin are required for static anchoring of *grk* mRNA.

To test whether Dynein itself is required for anchoring *grk* RNA at the dorso-anterior, we injected an inhibitory Dynein heavy chain antibody into stage 9 egg chambers, 60 minutes after injection of *grk* RNA. We found that perturbing Dynein function, leads to a rapid loss of *grk* RNA anchoring, 3-5 minutes after injection of anti-Dhc antibody (Figure 4E). Similar results were obtained with endogenous *grk* RNA (Figure 4G and G'). Control experiments showed that MTs are intact after the injection (Figure 4E) and injection of rabbit serum or IgG did not affect *grk* RNA anchoring (Suppl. Figure 5D and E). In contrast to the effects of anti-Dhc antibody, injection of anti-Egl antibodies did not lead to a loss of anchoring of neither injected nor endogenous *grk* RNA (Figure 4F and H). Given that Egl is required for active Dynein motility and transport of *grk* RNA (Suppl. Figure 5A-C), these results suggest that Dynein is required to statically anchor *grk* mRNA at the dorso-anterior corner.

A static anchoring role for Dynein predicts that the motor complex is recruited together with *grk* RNA to the site of anchoring. We tested this prediction by visualizing components of the Dynein motor complex after injection of *grk* RNA and found that Dhc (Figure 4I-K), Egl (Figure 4L-N) and BicD (data not shown) are all significantly enriched at the site of localization of the injected *grk* RNA, compared with uninjected controls (Figures 4I and 4L). Control injections of unlocalized *hunchback (hb)* RNA did not lead to any enrichment of Dynein motor components (Suppl. Figure 5F-H). We conclude that dynein is required to statically anchor *grk* mRNA at the dorso-anterior corner.

Sqd is involved in converting Dynein from a motor to a static anchor

The movement of *grk* mRNA to its site of anchoring has been shown previously to require two steps, the second being Sqd dependent (see introduction). To determine whether Sqd is present with *grk* RNA after completion of transport, we co-visualized *grk* RNA and Sqd by cryo-immuno-EM in wild type egg chambers. We found that SqdGFP co-localizes with endogenous *grk* RNA in sponge bodies at the dorso-anterior corner (Figure 5B), raising the possibility that Sqd could be transported to these structures through its association with *grk* RNA. We tested this idea by injecting *grk* RNA and investigating whether this causes a further enrichment of SqdGFP at the same site. We found that injection of *grk* RNA into transgenic flies expressing SqdGFP leads to a strong enrichment of SqdGFP at the dorso-anterior corner (Figure 5A). SqdGFP is found in sponge bodies (Figure 5C) together with Dhc, BicD and Egl in un-injected controls (Suppl. Figure 6A). We conclude that Sqd is at least partly recruited to the dorso-anterior corner through its association with *grk* mRNA.

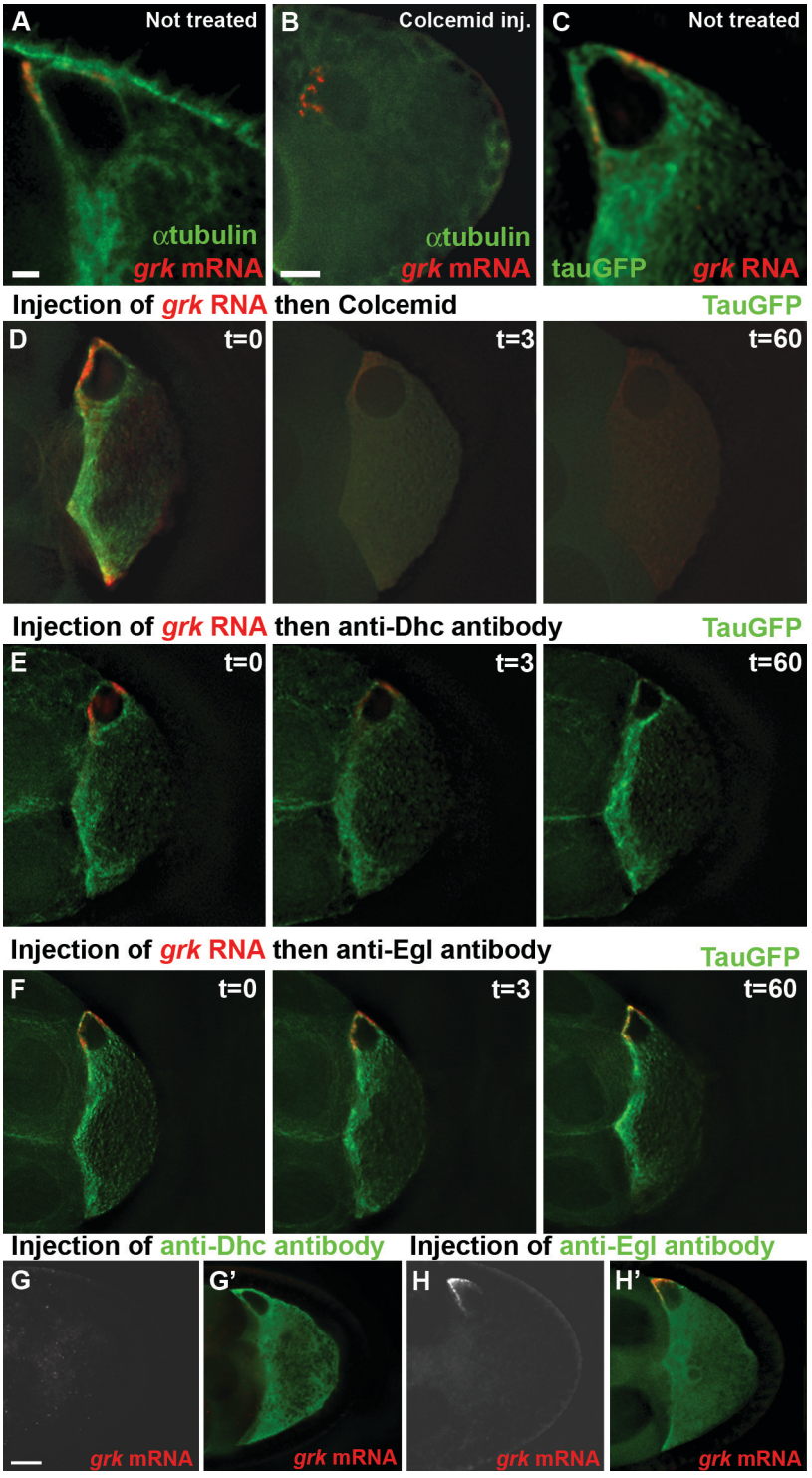
A
Not treated
αtubulin
grk mRNA
B
Colcemid inj.
αtubulin
grk mRNA
C
Not treated
tauGFP
grk RNA
Injection of grk RNA then Colcemid
TauGFP
D
t=0
t=3
t=60
Injection of grk RNA then anti-Dhc antibody
TauGFP
E
t=0
t=3
t=60
Injection of grk RNA then anti-Egl antibody
TauGFP
F
t=0
t=3
t=60
Injection of anti-Dhc antibody
Injection of anti-Egl antibody
G
grk mRNA
G'
grk mRNA
H
grk mRNA
H'
grk mRNA

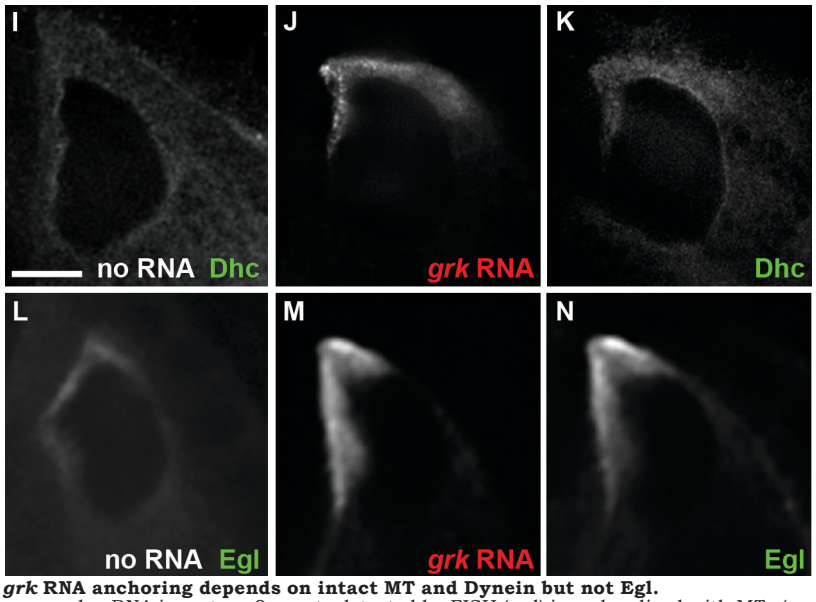

Figure 4. *grk* RNA anchoring depends on intact MT and Dynein but not Egl.
(A) Endogenous *grk* mRNA in a stage 9 oocyte detected by FISH (red) is co-localized with MTs (green).
(B) A stage 9 egg chamber treated for 45-60 min with Colcemid leading to a severe, but incomplete, delocalization of endogenous *grk* mRNA detected by FISH (red). MTs (green) are depolymerized.
(C) AlexaFluor546 labeled *grk* RNA (red) 45 min after injection into a stage 9 oocyte expressing tauGFP (marking the MTs network, green) co-localizes with MTs.
(D) AlexaFluor546 labeled *grk* RNA (red) localized at the dorso-anterior corner in a stage 9 oocyte expressing tauGFP, looses its localization upon Colcemid injection at t=0 min. The anchoring of injected *grk* RNA at the cap is altered after few minutes (t=3 min), and at t=60 min, is no longer detected at the dorso-anterior corner.
(E) AlexaFluor546 labeled *grk* RNA (red) localized at the dorso-anterior corner in a stage 9 oocyte expressing tauGFP looses its localization upon anti-Dhc antibody injection at t=0 min. The anchoring of injected *grk* RNA at the cap is altered after a few minutes (t=3min), and at t=60 min, no injected RNA is detected at the dorso-anterior corner.
(F) AlexaFluor546 labeled *grk* RNA (red) localized at the dorso-anterior corner in a stage 9 oocyte expressing tauGFP is unaffected upon anti-Egl antibody injection at t=0 min. *grk* RNA anchoring at the cap remains at t=3min and at t=60 min.
(G) Anchoring of endogenous *grk* mRNA (red) is disrupted by injection of anti-Dhc antibody, detected with an anti-mouse AlexaFluor488 (green) (G'), 45-60min after injection.
(H) Anchoring of endogenous *grk* mRNA (red) is not disrupted by injection of anti-Egl antibody, detected with an anti-rabbit AlexaFluor488 (green) (H'), 45-60min after injection.
(I-N) Dhc **(I)** and Egl **(L)** are slightly enriched at the dorso-anterior corner in uninjected oocytes. Injection of AlexaFluor546 *grk* RNA in a stage 9 oocyte leads to a large increase in detectable Dhc **(K)** and Egl **(N)**, colocalized with *grk* RNA at the dorso-anterior corner **(J and M)**. Scale bars: 10µm.

To study in more detail the role of Sqd in *grk* mRNA localization, we first show that intact microtubules but not F-actin are required for the anterior localization of injected and endogenous *grk* RNA localization in *sqd* null mutant egg chambers (Suppl. Figure 6B-E). We then disrupted Dhc function by injecting inhibitory antibodies into *sqd* mutant oocyte pre-injected with *grk* RNA. The results show that the anterior localization of injected *grk* RNA is disrupted by injection of anti-Dhc (Figure 5D). In control experiments, we injected rabbit antiserum, which had no effect (Suppl. Figure 5F and G). We also showed that the endogenous *grk* mRNA localization at the anterior in *sqd* mutants is Dhc dependent (Figure 5E). We conclude that in the absence of Sqd, *grk* mRNA localization at the anterior requires Dynein.

In a *sqd* mutant, Dynein could either be required for statically anchoring the RNA at the anterior on MTs, or to continuously transport the RNA anteriorly on MTs. To distinguish between these two possibilities, we carried out FRAP experiments. The results show that injected fluorescent *grk* RNA that accumulates at the anterior pole of *sqd* mutants recovers after photo-bleaching, showing that in the absence of Sqd, *grk* RNA is in continuous flux at the

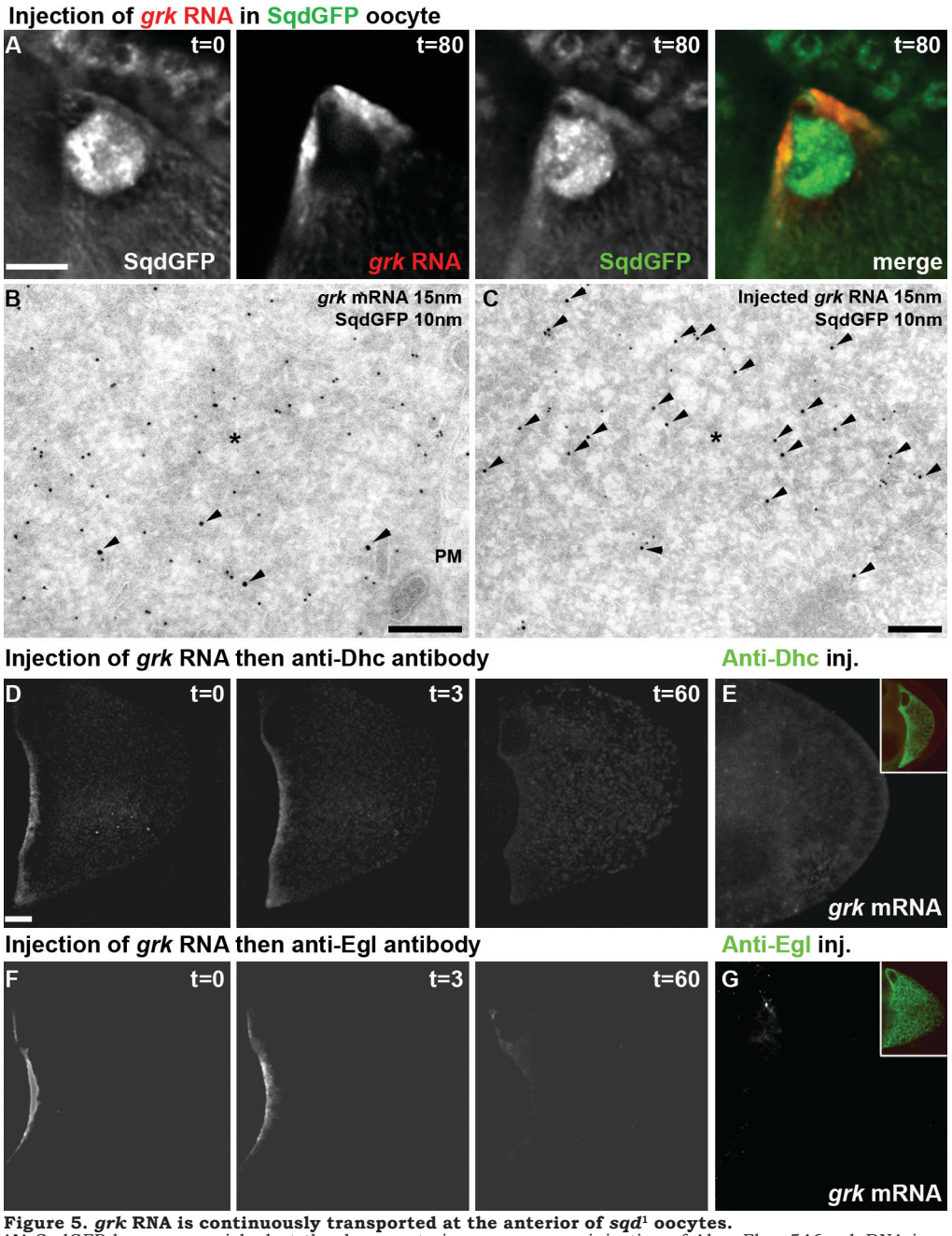

Figure 5. *grk* RNA is continuously transported at the anterior of *sqd*[1] oocytes.
(A) SqdGFP becomes enriched at the dorso-anterior corner upon injection of AlexaFluor546 *grk* RNA in a stage 9 oocyte. At t=0, SqdGFP is mostly in the nucleus. At t=80min, SqdGFP is enriched at the dorso-anterior corner with *grk* RNA (merge).
(B) Endogenous *grk* mRNA (15nm, arrowheads) co-localizes with SqdGFP (10nm) in sponge bodies (asterisks) in SqdGFP oocytes.
(C) SqdGFP also co-localizes with biotinylated injected *grk* RNA (15nm, arrowheads) in sponge bodies (asterisks).
(D) The anterior localization of injected AlexaFluor546 *grk* RNA (red) in a stage 9 *sqd*[1] mutant oocyte (t=0 min) is disrupted 60min after anti-Dhc antibody injection.

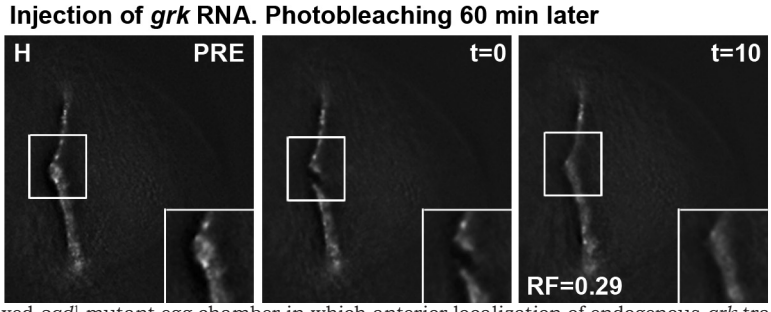

(E) Fixed *sqd*[1] mutant egg chamber in which anterior localization of endogenous *grk* transcripts (not shown) was disrupted by injection of anti-Dhc antibody (45-60 min after antibody injection). Inset shows injected anti-Dhc antibody detected by AlexaFluor488 anti-mouse antibody (green).
(F) The anterior localization of injected AlexaFluor546 *grk* RNA (red) in a stage 9 *sqd*[1] mutant oocyte (t=0 min) is disrupted 60min after anti-Egl antibody injection.
(G) Fixed *sqd*[1] mutant egg chamber in which anterior localization of endogenous *grk* mRNA (not shown) is disrupted by injection of anti-Egl antibody (45-60 min after injection of antibody). Inset shows anti-Egl antibody detected by AlexaFluor488 anti-Rabbit (green).
(H) FRAP experiment in living *sqd*[1] mutant oocyte showing anterior localization of AlexaFluor488 *grk* RNA (60 min after injection) immediately before the photobleaching (PRE). Insets show higher magnifications of the bleached areas. In contrast to wild type (Figure 3), the signal partly recovered 10 min after the bleaching, (RF=0.29). Scale bars: 10μm.

anterior (Figure 5H). In contrast, FRAP experiments also showed that the very small amount of *grk* RNA that is localized at the dorso-anterior corner in *sqd* mutant oocytes, is statically anchored (data not shown). We also found that injection of anti-Egl antibody disrupts both injected and endogenous *grk* transcript maintenance at the anterior pole in *sqd* mutants (Figure 5F and G), demonstrating that these transcripts are maintained at the anterior using continuous active transport requiring the motor activity of Dynein. Control rabbit serum injection showed no effect (Suppl. Figure 6D). Finally, we showed in *sqd* mutants, that the sponge bodies appear similar in shape and number to those in wild type oocytes (Suppl. Figure 3D). Interestingly, we found that in the absence of *sqd* function, the vast majority of *grk* RNA localized abnormally at the anterior in transport particles (Figure 6A). However, a very small proportion of the RNA remained in sponge bodies at the dorsal-anterior corner (Suppl. Figure 1E). These transport particles also contain Dynein (Figure 6B), BicD and Egl (Suppl. Figure 1C and 1D). We conclude that Sqd is required for the movement of transport particles from the anterior to the dorso-anterior corner and propose that Sqd is also required for Dynein to change from a motor to a static anchor.

Sqd is required for the dynamic conversion of transport particles into sponge bodies

To determine whether Sqd is required for anchoring *grk* RNA, we inactivated *Sqd* after *grk* RNA was fully anchored at the dorso-anterior corner. We first tried to inhibit Sqd function with anti-Sqd monoclonal antibodies, but these only showed very weak effects. As an alternative approach, we injected *grk* RNA into SqdGFP oocytes, allowed the RNA to become fully localized for 60 min, after which an inactivating anti-GFP antibody was injected. We found that within 15 min, injected *grk* RNA became detached from its site of anchoring in the dorso-anterior corner (Figure 6C). Furthermore, ultra-structural analysis revealed that in such cases, the *grk* RNA is found in transport particles rather than in sponge bodies in such egg chambers (Figure 6D and D'). Control injections of the anti-GFP antibody into wild type oocytes, in which *grk* RNA was pre-localized, showed no effect on *grk* RNA anchoring (Figure 6E). Moreover, injection of the anti-GFP antibody prior *grk* RNA leads to an accumulation of *grk* RNA along the anterior side, confirming that the inhibition of SqdGFP function with the anti-GFP antibody resembles the

sqd mutant, by disrupting the second step of *grk* RNA transport (Figure 6F). Finally, when we injected a large excess of *grk* RNA into *sqd* mutant oocytes, we also observed a conversion of sponge bodies into transport particles containing *grk* RNA.

To test whether Sqd is also required for the anchoring of endogenous *grk* mRNA, we injected anti-GFP antibody into SqdGFP egg chambers, fixed and recovered them 15 minutes after the injection and processed them for *in situ* hybridization. The results show that, like the injected RNA, the anchoring of endogenous *grk* mRNA is disrupted rapidly after inhibiting Sqd function (Figure 6G) and some of the RNA was found in particles resembling endogenous transport particles that also contain Dynein (Figure 6H). We conclude that Sqd is involved in regulating a dynamic equilibrium between transport particles and anchoring bodies and promotes the assembly or transformation of transport particles into sponge bodies. We suggest that Sqd is required for initiation and maintenance of static anchoring of *grk* RNA by Dynein and promotes its switch from a motor to an anchor concomitant with the formation of anchoring complexes in sponge bodies.

Discussion

Here, we have analyzed the molecular mechanism of *grk* mRNA transport and anchoring in the *Drosophila* oocyte using a number of novel methods, combining live cell imaging of oocytes with immuno-electron microscopy to co-visualize *grk* RNA and transacting factors. We show that *grk* mRNA is transported in particles containing many individual RNA molecules assembled with numerous molecules of Dynein motor components. Transport particles are often in close association with MTs and not consistently associated with membranes or vesicles. This validates that RNA particles are transported directly by motors on MTs. Once delivered to its final destination, *grk* mRNA is anchored by Dynein in EM dense structures previously described as sponge bodies. This anchoring by Dynein is static as it does not involve Egl, a cofactor of the motor required for active cargo transport. The anchoring of *grk* mRNA in sponge bodies also requires the hnRNP homologue, Sqd, required for *grk* mRNA transport. We show that Sqd is also required for the transition of *grk* mRNA transport particles to anchoring complexes, during which Dynein switches from a motor to an anchor. We propose a general principle for transport and anchoring of mRNA by molecular motors that involves assembly into large transport particles whose structure changes when they arrive at the final destination to form large EM dense anchoring complexes.

⟶ **Figure 6: Sqd is required for the dynamic conversion of sponge bodies into transport particles.**
(A-B) In *sqd*[1] mutant, biotinylated injected *grk* RNA (15nm) is found along the anterior side (within 5µm from the anterior plasma membrane) in transport particles that contain Dhc (10nm, B) along MTs (rows of small arrowheads). Small arrows point to Dhc in transport particles.
(C) SqdGFP oocyte injected with AlexaFluor546 *grk* RNA, which became fully anchored after 60 min. GFP antibody was injected (t=0), leading to the loss of *grk* RNA anchoring after 20 minutes.
(D-D') The same experiment that was described in C was performed by injecting biotinylated *grk* RNA. After processing this sample for immunolocalization, *grk* RNA (15nm) was found along the anterior side in particles that have the exact same feature as the particles described in A and B, and are also positive for Dhc (10nm, small arrows).
(E) Wild type oocyte injected with AlexaFluor546 *grk* RNA, which became anchored after 50 min. GFP antibody was then injected at t=0. Localization of *grk* RNA is unaffected and remains at the dorso-anterior corner.
(F) SqdGFP oocyte injected first with the anti-GFP antibody followed by the AlexaFluor546 *grk* RNA at t=0. *grk* RNA fails to reach the dorso-anterior corner and localizes at the anterior after 60 minutes (similar to *sqd*[1] mutant).
(G-G') Anchoring of endogenous *grk* mRNA (red) is disrupted by injection of anti-GFP antibody in a SqdGFP oocyte, 15min after injection **(G')**. *grk* mRNA anchoring at the dorso-anterior corner is lost and the RNA is found along the anterior side.
(H) The SqdGFP oocytes injected with anti-GFP antibody were processed for ISH-IEM to detect endogenous *grk* mRNA (15nm) that was found along the anterior side and partly in particles (arrows) that are also positive for Dhc (10nm, arrowheads).
Oocyte nucleus (Ooc Nucl); Mitochondria (M); Plasma membrane (PM).
Scale bars: 10µm in (C,E,F and G) and 200nm in (A,B,D,D' and H).

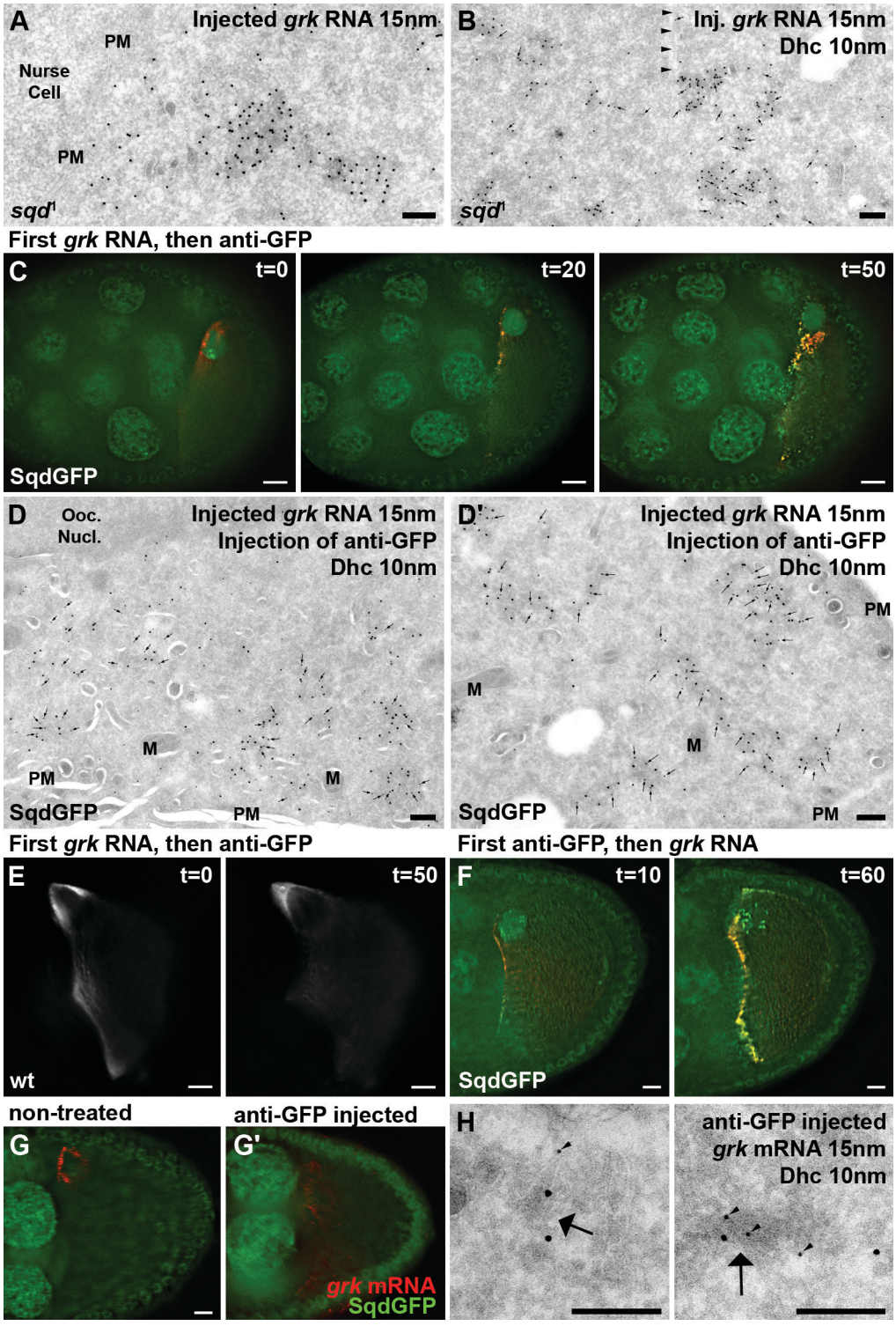
A
Injected grk RNA 15nm
PM
Nurse Cell
PM
sqd1
B
Inj. grk RNA 15nm
Dhc 10nm
sqd1
First grk RNA, then anti-GFP
C
t=0
t=20
t=50
SqdGFP
D
Ooc. Nucl.
Injected grk RNA 15nm
Injection of anti-GFP
Dhc 10nm
M
PM
M
SqdGFP
PM
D'
Injected grk RNA 15nm
Injection of anti-GFP
Dhc 10nm
PM
M
M
SqdGFP
PM
First grk RNA, then anti-GFP
First anti-GFP, then grk RNA
E
t=0
t=50
wt
F
t=10
t=60
SqdGFP
non-treated
anti-GFP injected
G
G'
grk mRNA
SqdGFP
H
anti-GFP injected
grk mRNA 15nm
Dhc 10nm

The use of EM methods to covisualize multiple components at the ultra-structural level has allowed us to show definitively that *grk* mRNA is present in numerous copies within transport particles, together with multiple molecules of Dynein on MTs. Our work provides compelling evidence that *grk* is transported by Dynein on MTs within RNP complexes, which presumably include a cargo-motor linker, whose identity is not yet known, but may involve Sqd in some manner. We have shown that *grk* mRNA is also present in many copies in its final site of anchoring at the dorso-anterior corner, together with the same components present in the transport particles. At this site *grk* mRNA is statically anchored in structures, which are distinct in appearance from transport particles and from the few other RNA granules, whose morphology is known (see below). However, the structures we describe in the dorso-anterior corner are very similar in morphology to sponge bodies, previously described as containing Exu. Sponge bodies have been hypothesized to be RNA transport intermediates from the nurse cells to the oocyte. Although we have found Exu-GFP in these *grk* anchoring structures, we have identified them in the oocyte as functioning in anchoring rather than transport, and containing Sqd and components of the Dynein complex.

Transport particles and sponge bodies are related to RNA particles or granules that have been proposed or suspected in many organisms and tissues and have been given a diversity of names, including germinal granules, P-bodies, and neuronal granules (St Johnston, 2005; Anderson and Kedersha, 2006). Such particles have a huge diversity of size, composition, and ultrastructural morphology, reflecting their wide range of probable functions in transport, storage, translational control and processing. Nevertheless, it seems likely that the transport particles we have identified are related to *bcd* and *osk* mRNA granules (Chekulaeva et al., 2006; Tekotte and Davis, 2006), as well as to neuronal RNA granules (St Johnston, 2005). The primary function of the sponge bodies seems to be in RNA anchoring, but it is not known whether they are also involved in translational control, degradation and storage.

We argue that sponge bodies containing *grk* mRNA are dynamic structures that are assembled by components that are delivered by *grk* transport particles. First, some transport particles containing endogenous *grk* RNA are detected on MTs near the dorso-anterior corner. Second, injection of a large excess of *grk* RNA leads to an increase in the size and number of sponge bodies. Third, disrupting Sqd function in the presence of a large excess of *grk* RNA leads to sponge bodies disassembling into transport particles. This suggests an active role for Sqd in promoting the conversion of transport particles into anchoring structures by facilitating their re-organization into anchoring complexes.

In general, the injection assay we use for *grk* localization recapitulates faithfully the transport of the endogenous transcript. Injected *grk* RNA localizes to the same type of anchoring structures as the endogenous *grk* transcript, and its second step of localization also depends on Sqd (MacDougall et al., 2003). However, our study reveals subtle differences between the anchoring of injected and endogenous transcript. Depolymerising MTs causes a complete loss of anchoring of injected *grk* RNA, but a partial loss of anchoring of endogenous transcript.

→ Figure 7. Model for the mechanism of transport and anchoring of *grk* RNA in the oocyte.
Transport particles containing *grk* mRNA molecules, dynein and Sqd travel on MTs toward the dorso-anterior corner in a Dhc and Egl dependent manner. At the dorso-anterior corner, *grk* RNA is anchored in sponge bodies containing the same components. Anchoring depends on MTs and Dhc, but not on Egl. Sqd is involved in the switch of Dynein from a motor to an anchor and in the transformation of transport particles into sponge bodies. The higher density of MTs near the nucleus in the DA corner would ensure the concentration of transport particles that can self associate and associate with pre-existing SB components to form an EM dense mess that tethers the RNA. The model proposes that in sponge bodies, Dynein is not always bound to MTs, but nevertheless remaining bound to *grk* mRNA.

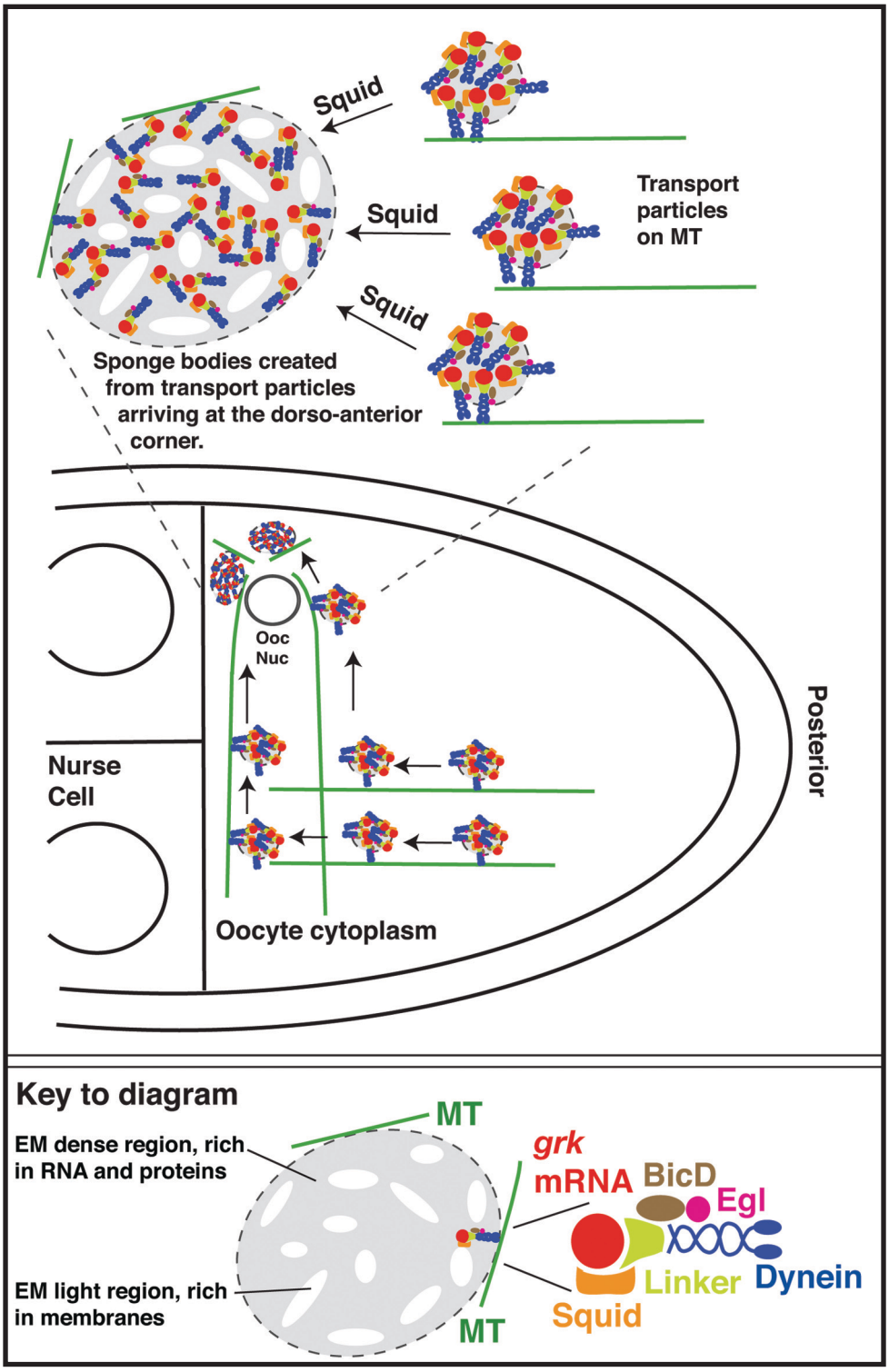
Squid
Squid
Squid
Transport particles on MT
Sponge bodies created from transport particles arriving at the dorso-anterior corner.
Ooc Nuc
Nurse Cell
Posterior
Oocyte cytoplasm
Key to diagram
EM dense region, rich in RNA and proteins
EM light region, rich in membranes
MT
MT
grk mRNA
BicD
Egl
Linker
Dynein
Squid

In addition, injecting a large excess of *grk* RNA causes an increase in the size and number of sponge bodies at the dorso-anterior corner. Injection of *grk* RNA also causes the conversion of sponge bodies into transport particles in the absence of Sqd function, while endogenous RNA is largely in sponge bodies at the anterior in *sqd* mutants. We interpret these differences as indicating that when the *grk* mRNA anchoring system is saturated, the new sponge bodies that are formed are more labile than existing sponge bodies. This could either be because of a lack of sufficient time for sponge bodies to mature fully from injected *grk* RNA, or due to the absence of some limiting constituent that is saturated by an excess of *grk* RNA.

However, our data show that both injected *grk* RNA and endogenous *grk* mRNA are anchored statically by Dynein in sponge bodies together with Sqd, BicD and Egl. Anchoring requires Sqd and Dynein, but not Egl, which is required for active transport of *grk*. *grk* RNA is therefore anchored by a similar mechanism to pair-rule and *wg* transcripts in the syncitial blastoderm embryo. In the embryo and oocyte, we propose that when the Dynein motor complex reaches its final destination, the motor becomes a static anchor that no longer depends on the transport activity of the motor. The Dynein motor consists of multiple complexes, including Dhc, Dynein intermediate chain, Dynein light chain and several other sub-complexes and associated factors such as Dynactin (Pfister et al., 2006). In vitro studies have shown that the MT-binding domain of Dhc is distinct from the force generating ATPase domain. It is easy to imagine how such a large protein can associate with many other cellular factors, including MTs, thus forming a large and immobile anchoring complex.

In contrast to the transport particles, which are often in close association with MTs, sponge bodies are usually only flanked by MTs. Interestingly, disassembling MTs does not lead to a change in their structure and only leads to a partial loss of endogenous *grk* RNA anchoring. Therefore, we propose the following model for *grk* mRNA anchoring (Figure 7). *grk* RNA is transported within transport particles to the dorso-anterior corner and becomes incorporated into sponge bodies. During this transformation, the Dynein complex switches from an active motor to a static anchor. Sqd is involved in this switch, and together with Dynein promotes the formation of a dense and immobile network of RNP anchoring complexes. MTs flank the sponge bodies, but are not required for their maintenance nor directly for anchoring most *grk* RNA, except when a large excess of *grk* RNA is present. Why anchoring only occurs in the sponge bodies that are at the dorso-anterior corner is not yet understood.

It is also unclear to what extent other transcripts in the oocyte are anchored by sponge bodies with distinct functions. Although our work clearly points to distinct specialized functions for the Dynein motor, both in delivering distinct cargo to distinct destinations and in functioning as a static anchor, the molecular basis of these distinct functions is unclear. While Sqd is clearly involved in these processes in the case of *grk* mRNA, equivalent RNA binding proteins involved in anchoring have not been identified yet for other transcripts. It is also likely, that distinct populations of MTs play a role in the choice of anchoring site. In addition, the cargo itself may influence the behaviour of the motor (Bullock et al., 2004). Future experiments will have to resolve these questions and to determine whether a similar mechanism of static anchoring in sponge body like structures is operating in early stages when *grk* mRNA is localized at the posterior of the oocyte. The EM methods we have established will play a key role in such studies and in determining how general our model for cargo anchoring is in *Drosophila* and other model systems.

Experimental procedures

Fly strains

Stocks were raised on standard cornmeal-agar medium at 25°C. The wild type strain was Oregon R (OrR), for functional loss of Sqd we used the mutant Sqd^1 (T. Schüpbach) or SqdGFP (A. Debec). An *nlsGFP* strain containing four copies of the *nlsGFP* transgene (*yw; nlsGFPM; nlsGFPN*) (Davis et al., 1995) was used to visualize nuclei. TauGFP (D. St Johnston) flies were used to visualize MTs.

Injection of RNA and inhibitors

RNA was transcribed *in vitro* using T7, T3 or SP6 polymerase with UTP-AlexaFluor 546, UTP-AlexaFluor 488 or UTP-Biotin (Wilkie and Davis, 2001). Ovaries were dissected and separated into individual ovarioles directly onto coverslips in Series 95 halocarbon oil (KMZ Chemicals Ltd) and injected with labelled *grk* RNA using Femtotip needles (Eppendorf). RNA was injected at a concentration of 250-500 ng/ml, Colcemid (Sigma) at 1 mg/ml and LatrunculinA (Sigma) at 20mM. Anti-Dhc (D. Sharp), anti-Egl (R. Lehmann), anti-GFP (G6539 Sigma, containing 25mg/ml total protein, 5.8mg/ml IgG), anti-Sqd (T. Schüpbach), IgG and Rabbit serum were injected at the same concentration (20mg/ml). Each experiment was repeated with at least two different batches of RNA in a total of at least 12 and on average 25 egg chambers (Suppl. Table 1).

Antibodies

To detect the biotinylated RNA, we used AlexaFluor546-coupled Avidin (Molecular Probes) or the polyclonal rabbit anti-Biotin (Rockland) at 1:10,000 for IEM. We used anti-αtubulin-FITC (Sigma, 1:1,000), monoclonal anti-αtubulin B512 (Sigma) at 1:5000 for IEM; rabbit polyclonal anti-Dhc, PEP1 (T. Hays) at 1:100 and 1:300 for IEM), rabbit polyclonal anti-Egl (R. Lehmann), 1:4,000 and 1:300 for IEM), monoclonal anti-BicD 1B11 (B. Suter), at 1:20; and clones 2G10 and 4C2 at 1:20 for IEM; rabbit polyclonal anti-GFP A6455, (Molecular probes) at 1:200 and FITC-Phalloidin to label F-actin. For IEM, rabbit polyconal antibodies are detected directly with ProteinA gold conjugates (Dept. of Cell Biology, Utrecht, The Netherlands). Mouse monoclonals were detected with rabbit anti mouse (Dako, 1/250) followed by ProteinA gold conjugates.

Immuno-fluorescence and RNA fluorescence in situ hybridization (FISH)

Injected oocytes were fixed for 20min or 1 hour in 4% Paraformaldehyde, PFA (Polysciences) added directly on top of the egg chambers in halocarbon oil. Fixed oocytes were then recovered with glass pipettes into glass multi-well plates and fixative and oil washed away with PBS. Post-fixation was performed with 4% paraformaldehyde for 20 min, followed by several washes with PBT (PBS+0.1%Tween). After fixation, ovaries were immuno-labelled and processed for FISH as described previously (Wilkie et al., 1999) using fluorescent tyramide detection (NEN LifeSciences) and mounted in Vectashield (Vector). The Digoxigenin labelled antisense probes were prepared from a full length *grk* cDNA (T. Schüpbach).

4-D Imaging and deconvolution

Imaging was performed on a widefield DeltaVision microscope (Applied Precision, Olympus IX70 and with a Roper Coolsnap HQ) with 20X/0.75NA and 100X/1.4NA objectives and then deconvolved using SoftWorks (Applied Precision) based on Sedat/Agard algorithms (Parton

and Davis, 2005). Up to 25 egg chambers were imaged in parallel (Davis, 2000; Parton and Davis, 2004). Photo–bleaching experiments used a 488 nm laser with 10 iterations at the maximum intensity and measurement of the recovery of the fluorescence initiated 1s later. Images were analysed using SoftWorks (Applied Precision).

Detection of injected grk RNA by Immuno Electron Microscopy (IEM)

Egg chambers were injected in Series 95 halocarbon oil and left for either 20 min for transport studies, or for 45-60min for anchoring studies. Fixation was performed for a minimum of 3 hours using 2% EM grade PFA and 0.2% glutaraldehyde (GA) in 0.1M phosphate buffer at pH7.4, before being transferred and stored in 1% PFA in the same buffer at 4°C. Single stage 9 oocytes were embedded in blocks of 12% gelatin that were infused in 2.3M sucrose and frozen in liquid nitrogen. 60nm ultrathin sections were cut and collected on carbon coated-formvar copper grids as previously described (Herpers and Rabouille, 2004). The injected RNA was detected using polyclonal rabbit anti-biotin antibodies followed by ProteinA gold conjugates.

grk mRNA ISH-IEM

Egg chambers were fixed overnight in 4% PFA or 3h in 2% PFA and 0.2% GA in 0.1M phosphate buffer at pH7.4. 60nm sections were retrieved on carbon coated-formvar nickel grids on a drop of sucrose/methylcellulose mixture that was washed off by floating the grids 3 times for 5 minutes on drops of PBS at 37°C. The sections were post-fixed in 1% glutaraldehyde in PBS and washed another 3 times in PBS. Pre-hybridization was performed at 37°C in 50% Formamide, 2xSSC in DEPC treated H_2O for 15 min. Biotinylated *grk* RNA probes were made according to the manufacturer's specifications (Roche) and was denatured by 10 minutes boiling in hybridization buffer and then cooled on ice. Hybridization buffer is pre-hybridization buffer supplemented with 10% Dextran Sulphate (Sigma), 100 μg/ml tRNA and 50 μg/ml Heparin. Hybridization was performed in a humid chamber at 55°C by floating the grids on the denatured probe at 0.5 to 1 μg/ml for 16 hours. The unbound probe was washed off by 3 washes of prehybridization buffer followed by the IEM labelling protocol described above. The grids were incubated with anti-biotin antibodies followed by ProteinA gold conjugates.

Acknowledgements

We thank the Davis and Rabouille's lab as well as David Tollervey for helpful discussions, and Robin Allshire, Edele Marston and Veronique van de Bor for their critical comments on the manuscript. We thank Carine Meignin for proposing to use an anti-GFP antibody to inhibit SqdGFP and Richard Parton for help and advice with light microscopy. This work was supported by a Wellcome Trust senior research fellowship (067413) to I.D., a Marie Curie fellowship to R.D. B.H. is funded by a Nederlandse Organisatie voor Wetenschappelijk Onderzoek (NWO) Aspasia grant (015.001.129) to C.R.

References

Anderson,P. and Kedersha,N. (2006). RNA granules. J. Cell Biol. 172, 803-808.

Bashirullah,A., Halsell,S.R., Cooperstock,R.L., Kloc,M., Karaiskakis,A., Fisher,W.W., Fu,W., Hamilton,J.K., Etkin,L.D., and Lipshitz,H.D. (1999). Joint action of two RNA degradation pathways controls the timing of maternal transcript elimination at the midblastula transition in Drosophila melanogaster. EMBO J. 18, 2610-2620.

Bertrand,E., Chartrand,P., Schaefer,M., Shenoy,S.M., Singer,R.H., and Long,R.M. (1998). Localization of ASH1 mRNA particles in living yeast. Mol. Cell 2, 437-445.

Brendza,R.P., Serbus,L.R., Duffy,J.B., and Saxton,W.M. (2000). A function for kinesin I in the posterior transport of oskar mRNA and Staufen protein. Science 289, 2120-2122.

Bullock,S.L., Stauber,M., Prell,A., Hughes,J.R., Ish-Horowicz,D., and Schmidt-Ott,U. (2004). Differential cytoplasmic mRNA localisation adjusts pair-rule transcription factor activity to cytoarchitecture in dipteran evolution. Development 131, 4251-4261.

Caceres,L. and Nilson,L.A. (2005). Production of gurken in the nurse cells is sufficient for axis determination in the Drosophila oocyte. Development 132, 2345-2353.

Cha,B.J., Koppetsch,B.S., and Theurkauf,W.E. (2001). In vivo analysis of Drosophila bicoid mRNA localization reveals a novel microtubule-dependent axis specification pathway. Cell 106, 35-46.

Cha,B.J., Serbus,L.R., Koppetsch,B.S., and Theurkauf,W.E. (2002). Kinesin I-dependent cortical exclusion restricts pole plasm to the oocyte posterior. Nat. Cell Biol. 4, 592-598.

Chekulaeva,M., Hentze,M.W., and Ephrussi,A. (2006). Bruno acts as a dual repressor of oskar translation, promoting mRNA oligomerization and formation of silencing particles. Cell 124, 521-533.

Davis,I. (2000). Visualising Fluorescence in Drosophila - optimal detection in thick specimens. In Protein Localization by Fluorescence Microscopy: A Practical Approach, V.J.Allen, ed. (Oxford: OUP), pp. 131-162.

Davis,I., Girdham,C.H., and O'Farrell,P.H. (1995). A nuclear GFP that marks nuclei in living Drosophila embryos; maternal supply overcomes a delay in the appearance of zygotic fluorescence. Dev. Biol. 170, 726-729.

Davis,I. and Ish-Horowicz,D. (1991). Apical localization of pair-rule transcripts requires 3' sequences and limits protein diffusion in the Drosophila blastoderm embryo. Cell 67, 927-940.

Delanoue,R. and Davis,I. (2005). Dynein anchors its mRNA cargo after apical transport in the Drosophila blastoderm embryo. Cell 122, 97-106.

Deshler,J.O., Highett,M.I., and Schnapp,B.J. (1997). Localization of Xenopus Vg1 mRNA by Vera protein and the endoplasmic reticulum. Science 276, 1128-1131.

Forrest,K.M. and Gavis,E.R. (2003). Live imaging of endogenous RNA reveals a diffusion and entrapment mechanism for nanos mRNA localization in Drosophila. Curr. Biol. 13, 1159-1168.

Glotzer,J.B., Saffrich,R., Glotzer,M., and Ephrussi,A. (1997). Cytoplasmic flows localize injected oskar RNA in Drosophila oocytes. Curr. Biol. 7, 326-337.

Gonzalez-Reyes,A., Elliott,H., and St Johnston,D. (1995). Polarization of both major body axes in Drosophila by gurken-torpedo signalling. Nature 375, 654-658.

Goodrich,J.S., Clouse,K.N., and Schupbach,T. (2004). Hrb27C, Sqd and Otu cooperatively regulate gurken RNA localization and mediate nurse cell chromosome dispersion in Drosophila oogenesis. Development 131, 1949-1958.

Herpers,B. and Rabouille,C. (2004). mRNA localization and ER-based protein sorting mechanisms dictate the use of transitional endoplasmic reticulum-golgi units involved in gurken transport in Drosophila oocytes. Mol. Biol. Cell 15, 5306-5317.

Jansen,R.P., Dowzer,C., Michaelis,C., Galova,M., and Nasmyth,K. (1996). Mother cell-specific HO expression in budding yeast depends on the unconventional myosin myo4p and other cytoplasmic proteins. Cell 84, 687-697.

Januschke,J., Gervais,L., Dass,S., Kaltschmidt,J.A., Lopez-Schier,H., St Johnston,D., Brand,A.H., Roth,S., and Guichet,A. (2002). Polar transport in the Drosophila oocyte requires Dynein and Kinesin I cooperation. Curr. Biol. 12, 1971-1981.

MacDougall,N., Clark,A., MacDougall,E., and Davis,I. (2003). Drosophila gurken (TGFalpha) mRNA localizes as particles that move within the oocyte in two dynein-dependent steps. Dev. Cell 4, 307-319.

Neuman-Silberberg,F.S. and Schupbach,T. (1993). The Drosophila dorsoventral patterning gene gurken produces a dorsally localized RNA and encodes a TGF alpha-like protein. Cell 75, 165-174.

Norvell,A., Kelley,R.L., Wehr,K., and Schupbach,T. (1999). Specific isoforms of squid, a Drosophila hnRNP, perform distinct roles in Gurken localization during oogenesis. Genes Dev. 13, 864-876.

Palacios,I.M. and St Johnston,D. (2002). Kinesin light chain-independent function of the Kinesin heavy chain in cytoplasmic streaming and posterior localisation in the Drosophila oocyte. Development 129, 5473-5485.

Parton,R. and Davis,I. (2004). Time-lapse Cinematography in Living Drosophila Tissues. In Live Cell Imaging: A Laboratory Manual, D.Spector and R.Goldman, eds. (NY: Cold Spring Harbor Laboratory Press), pp.

385-409.
Parton,R. and Davis,I. (2005). Deconvolution: Lifting the fog. In Cell Biology, a laboratory handbook, J.Celis, ed. (Cambridge: Academic Press).
Pfister,K.K., Shah,P.R., Hummerich,H., Russ,A., Cotton,J., Annuar,A.A., King,S.M., and Fisher,E.M. (2006). Genetic analysis of the cytoplasmic dynein subunit families. PLoS. Genet. 2, e1.
Schnorrer,F., Bohmann,K., and Nusslein-Volhard,C. (2000). The molecular motor dynein is involved in targeting swallow and bicoid RNA to the anterior pole of Drosophila oocytes. Nat. Cell Biol. 2, 185-190.
Sil,A. and Herskowitz,I. (1996). Identification of asymmetrically localized determinant, Ash1p, required for lineage-specific transcription of the yeast HO gene. Cell 84, 711-722.
Simmonds,A.J., dosSantos,G., Livne-Bar,I., and Krause,H.M. (2001). Apical localization of wingless transcripts is required for wingless signaling. Cell 105, 197-207.
St Johnston,D. (2005). Moving messages: the intracellular localization of mRNAs. Nat. Rev. Mol. Cell Biol. 6, 363-375.
Tekotte,H. and Davis,I. (2002). Intracellular mRNA localization: motors move messages. Trends Genet. 18, 636-642.
Tekotte,H. and Davis,I. (2006). Bruno: a double turn-off for Oskar. Dev. Cell 10, 280-281.
Van Buskirk,C. and Schupbach,T. (2002). Half pint regulates alternative splice site selection in Drosophila. Dev. Cell 2, 343-353.
Van de Bor,V. and Davis,I. (2004). mRNA localisation gets more complex. Curr. Opin. Cell Biol. 16, 300-307.
Weil,T.T., Forrest,K.M., and Gavis,E.R. (2006). Localization of bicoid mRNA in Late Oocytes Is Maintained by Continual Active Transport. Dev. Cell 11, 251-262.
Wilkie,G.S. and Davis,I. (2001). Drosophila wingless and pair-rule transcripts localize apically by dynein-mediated transport of RNA particles. Cell 105, 209-219.
Wilkie,G.S., Shermoen,A.W., O'Farrell,P.H., and Davis,I. (1999). Transcribed genes are localized according to chromosomal position within polarized Drosophila embryonic nuclei. Curr. Biol. 9, 1263-1266.
Wilsch-Brauninger,M., Schwarz,H., and Nusslein-Volhard,C. (1997). A sponge-like structure involved in the association and transport of maternal products during Drosophila oogenesis. J. Cell Biol. 139, 817-829.

Supplementary Material

Supplementary Experimental Procedures

Sample preparation for EM analysis

Oocytes were embedded in Spurr as previously described (Herpers and Rabouille, 2004). Images were captured on a Jeol EX1200 electron microscope.

Estimation of the number of RNA molecules in transport particles

The area of individual transport particles was estimated using the classical stereological point hit method with a grid of 0.4 cm on pictures printed at the magnification of 10 to 12,000 (final magnification 40 to 60,000) (Herpers and Rabouille, 2004). The number of gold particles in each transport particle was divided by the estimated area. To estimate the number of gold particles per unit volume, the transport particles were modelled as a sphere and the thickness of the sections was taken into account (60nm). We estimate that about 10 biotins are incorporated per RNA molecule and that the labelling efficiency is 1 to 5%. We observed a density ranging from 72 to 250 gold particles labeling the biotin in the RNA per μm^2 of particle section and estimated that a transport particle contains on average between 100 and 2,000 RNA molecules. An estimate of the volume of RNA/dynein complex from structural and biophysical information is in general agreement with these measurements, suggesting that a transport particle could contain between 600 and 10,000 RNA molecules with 100% packing (Graeme Ball personal communication).

Supplementary Table 1.

Statistics for injection experiments

Number of egg chambers and percent localized in secondary injections following *grk* RNA pre-injections into the oocyte. The symbols and abbreviations used are the same as those used in the figures and the text.

***grk* RNA pre-injection**

Secondary inj.	Time after 1st inj. (min)	RNA localization	Localized (%)	Partially delocalized (%)	De-localized (%)	n
LatrunculinA 20mM (in *nlsGFP* oocytes)	45-60	cap	93.5	5	2.5	40
LatrunculinA 20mM (in *sqd*^{1} oocytes)	45-60	anterior	100	0	0	22
Colcemid 1mg/ml (in *tauGFP* oocytes)	45-60	cap	3.7	29.6	66.7	27
Colcemid 1mg/ml (in Or^{R} oocytes)	45-60	cap	0	89.2	10.8	28
Colcemid 1mg/ml (in *sqd*^{1} oocytes)	45-60	anterior	0	83.3	16.7	42
Anti-Dhc (in *tauGFP* oocytes)	45-60	cap	11	18	71	72
Anti-Dhc (in *sqd*^{1} oocytes)	45-60	anterior	0	16.6	83.4	12
Anti-Egl (in *tauGFP* oocytes)	45-60	cap	100	0	0	20
Anti-Egl (in *tauGFP* oocytes)	15-20	anterior	0	0	100	15
Anti-Egl (in *sqd*^{1} oocytes)	45-60	anterior	0	11.7	88.3	17
Rabbit Serum (in *tauGFP* oocytes)	45-60	cap	100	0	0	16
Rabbit Serum (in *tauGFP* oocytes)	15-20	anterior	100 (at the cap)	0	0	12
Rabbit Serum (in *sqd*^{1} oocytes)	45-60	anterior	72.3	27.7	0	18
Immunoglobulin G (IgG) (in *tauGFP* oocytes)	45-60	anterior	100	0	0	23
IgG (in *sqd*^{1} oocytes)	45-60	anterior	86.7	13.3	0	15

Table 1: Statistics (percentage localized and numbers analyzed) for the injection experiments.

The symbols used are the same as those used in the figures and the text. Supplementary Table 1 describes the statistics for secondary injection following grk *RNA pre injection in oocytes.*

Supplementary Figures.

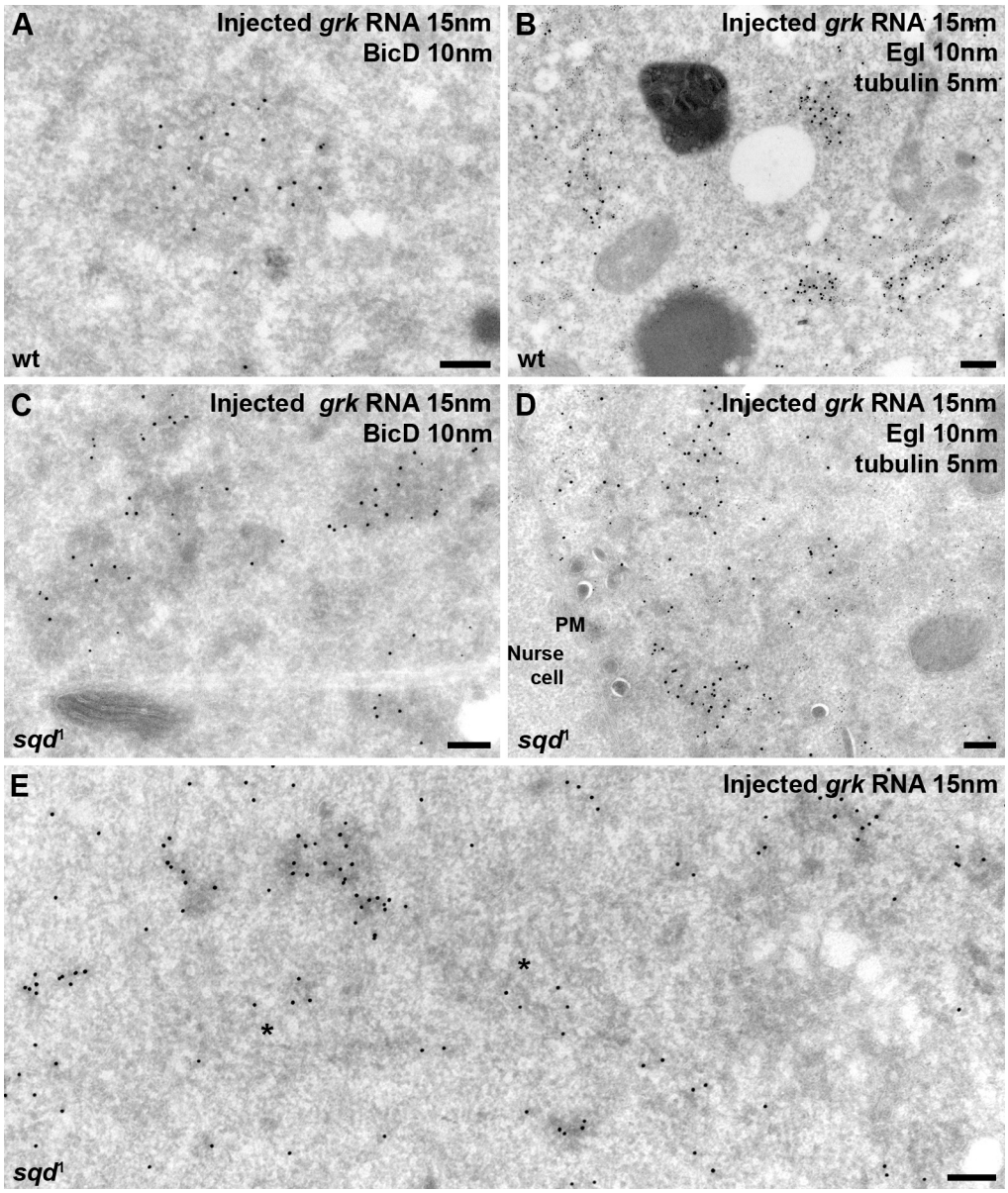

Supplementary Figure 1. Transport particles contain BicD and Egl in wild type and *sqd*^{1} mutant.
(A-B) Wild type egg chamber 20 min after injection of biotinylated *grk* RNA (15nm gold). *grk* RNA in found in electron dense transport particles together with BicD, 10nm, **(A)** and Egl, 10nm **(B)**.
(C-D) *sqd*^{1} mutant egg chamber 60 min after injection of biotinylated *grk* RNA (15nm) which is found along the anterior in transport particles that contain BicD, 10nm **(C)** and Egl, 10nm **(D)** along MTs (5nm).
(E) *sqd*^{1} mutant oocyte injected with biotinylated *grk* RNA. RNA is mostly found in transport particles but also to a lesser extent in sponge bodies (asterisks).
Scale bars: 200nm.

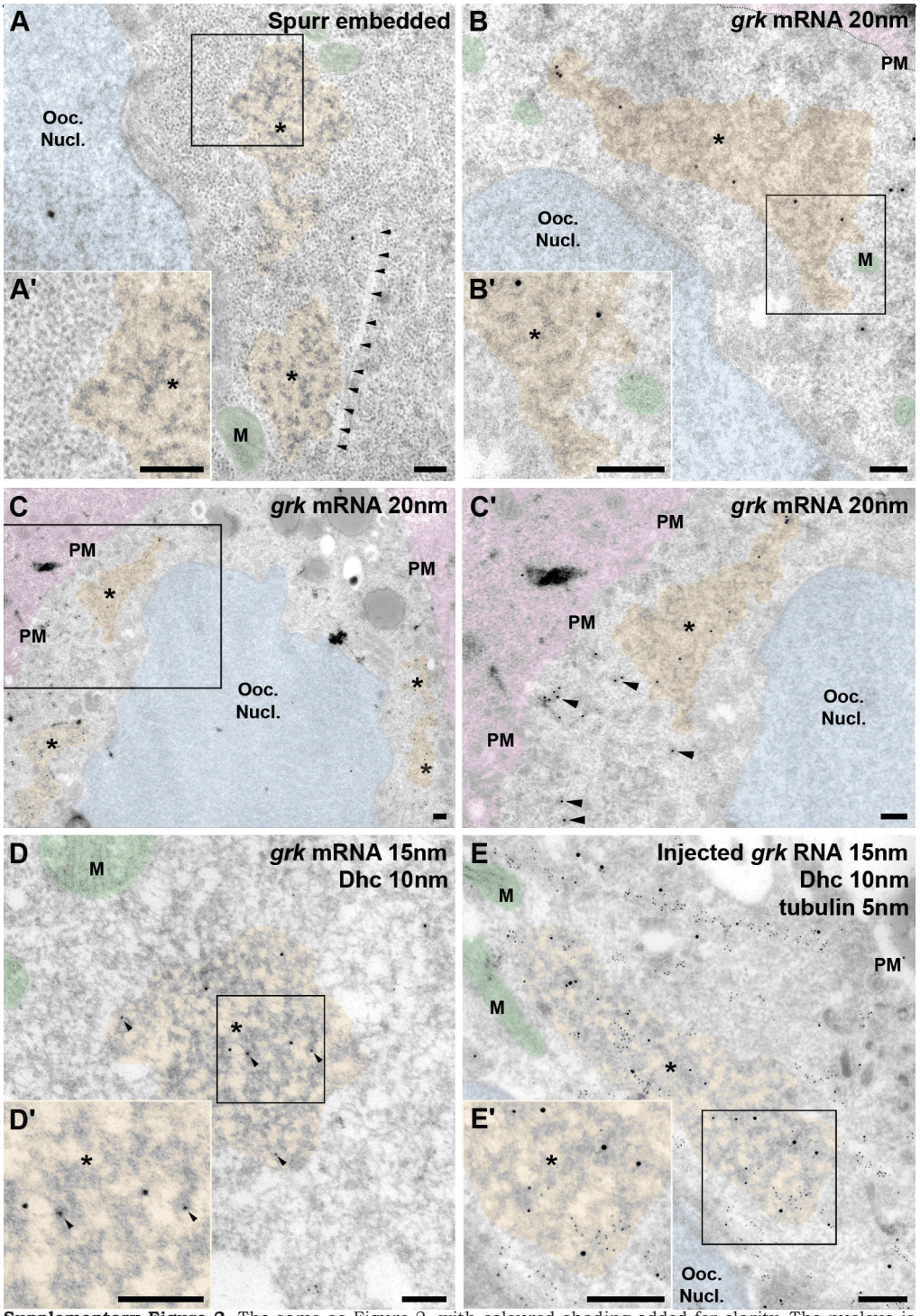

Supplementary Figure 2. The same as Figure 2, with coloured shading added for clarity. The nucleus is coloured in blue, the mitochondria in green and the sponge bodies in orange. Cells adjacent to the oocyte are coloured in pink.

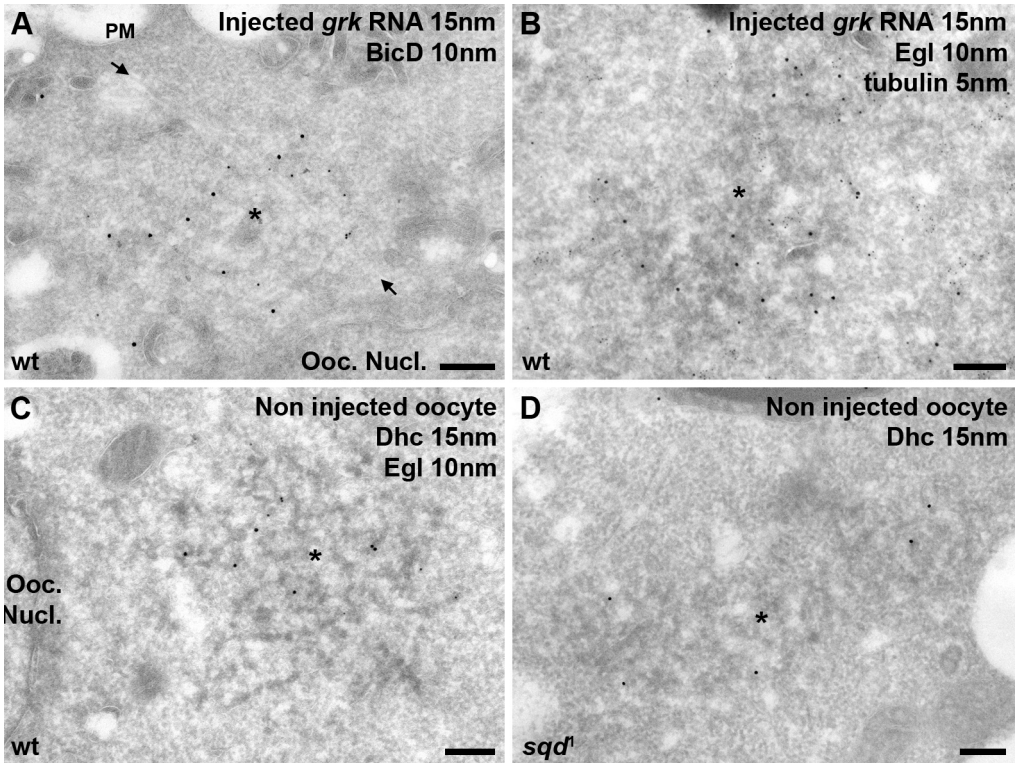

Supplementary Figure 3. Dhc, Egl and BicD in sponge bodies in wild type and *sqd*^{1} mutant.
(A-B) Wild type oocyte injected with biotinylated *grk* RNA. After 60 min grk RNA (15nm) is found in sponge bodies together with BicD, 10nm **(A)** and Egl, 10nm **(B)**.
(C) Uninjected wild type oocyte, showing that Dhc and Egl are also present at the dorso-anterior corner in sponge bodies.
(D) In an uninjected *sqd*^{1} mutant oocyte, sponge bodies are also present and contain Dhc.
Scale bars: 200nm.

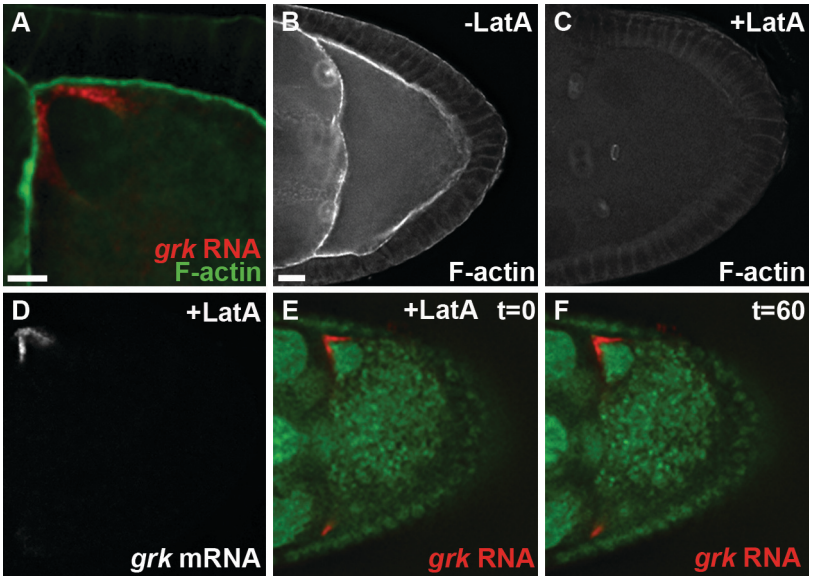

Supplementary Figure 4. F-actin is not required for *grk* RNA anchoring.
(A) Injected AlexaFluor546 *grk* RNA (red) does not co-localize with the cortical actin detected by Phalloidin-FITC (green) at the dorso-anterior cap in stage 9 oocyte.
(B-C) F-Actin organization in a non-injected **(B)** or Latrunculin A **(C)** stage 9 oocyte detected by Phalloidin AlexaFluor546. Latrunculin A was injected at 20 mM for 30 min prior fixation to depolymerize F-actin.
(D) A stage 9 oocyte injected with Latrunculin A and fixed 45-60 min after injection. Anchoring of endogenous *grk* mRNA (red) is unaffected.
(E and F) Two time points from a time lapse movie of a stage 9 oocyte expressing the nuclear marker, nlsGFP fusion protein (green), and pre-injected (60 min before t=0) with AlexaFluor546 *grk* RNA (red). *grk* remains fully localized at the dorso-anterior corner 60 min after injection of Latrunculin A.
Scale bars: 5µm in (A), 10µm in (B-F).

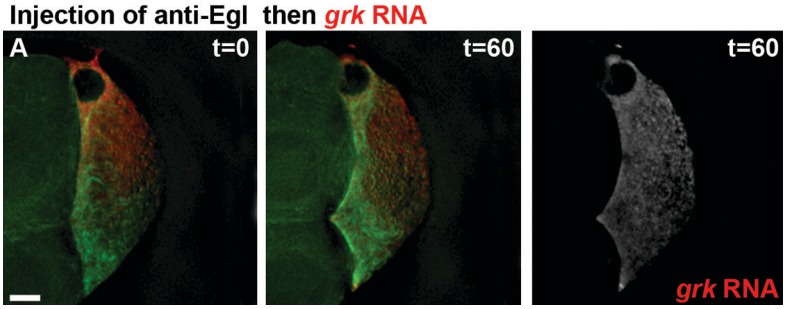

Supplementary Figure 5. Anti-Egl antibody injection inhibits active transport.
(A) Wild type oocyte pre-injected with anti-Egl antibodies, 5 min before injection of *grk* RNA, showing complete disruption of *grk* RNA transport.
(B) Wild type oocyte pre-injected with AlexaFluor546 *grk* RNA 10 min before injection of anti-Egl antibody (t=0). *grk* RNA is initially partly localized at the anterior, but no further localization to the dorso-anterior corner occurs after anti-Egl antibody injection and at t=60 *grk* RNA is unlocalized.
(C) Control experiment with rabbit serum under very similar conditions to **(B)**. Rabbit serum showed no effect on *grk* RNA localization.
(D-E) Control for the Dhc antibody injections. Rabbit serum **(D)** and rabbit IgG **(E)** have no effect on the localization of anchored injected *grk* RNA in wild type oocyte, nor on tauGFP distribution (green).
(F-H) Control for the *grk* RNA injection experiments. *hb* RNA **(F)** injection does not lead to an increase of Dhc **(G)** or BicD **(H)** at the DA corner, when compared to Figure 4.
Scale bars: 10µm in (A-E), 5µm in (F-H).

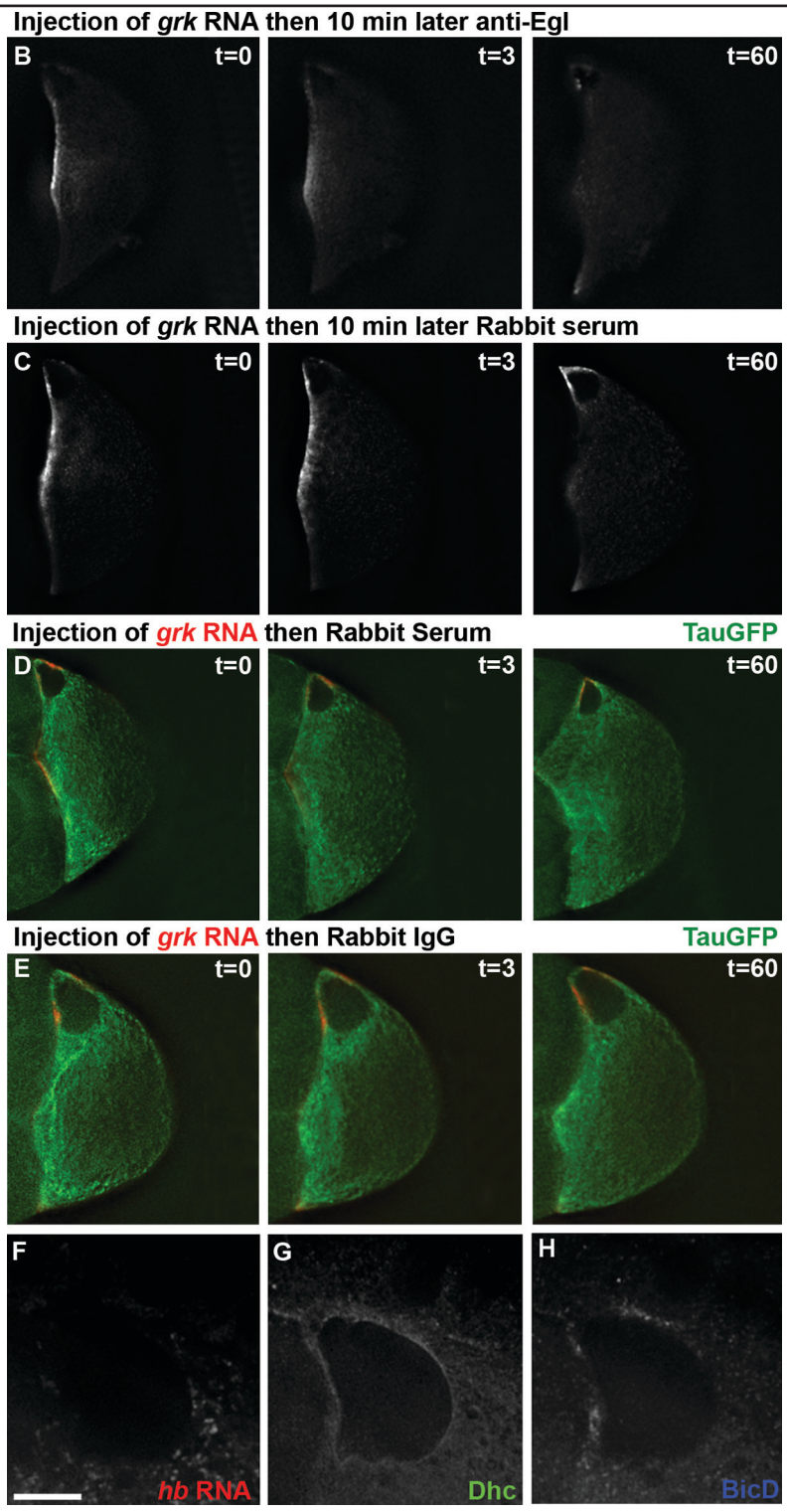
Injection of grk RNA then 10 min later anti-Egl
B
t=0
t=3
t=60
Injection of grk RNA then 10 min later Rabbit serum
C
t=0
t=3
t=60
Injection of grk RNA then Rabbit Serum
TauGFP
D
t=0
t=3
t=60
Injection of grk RNA then Rabbit IgG
TauGFP
E
t=0
t=3
t=60
F
hb RNA
G
Dhc
H
BicD

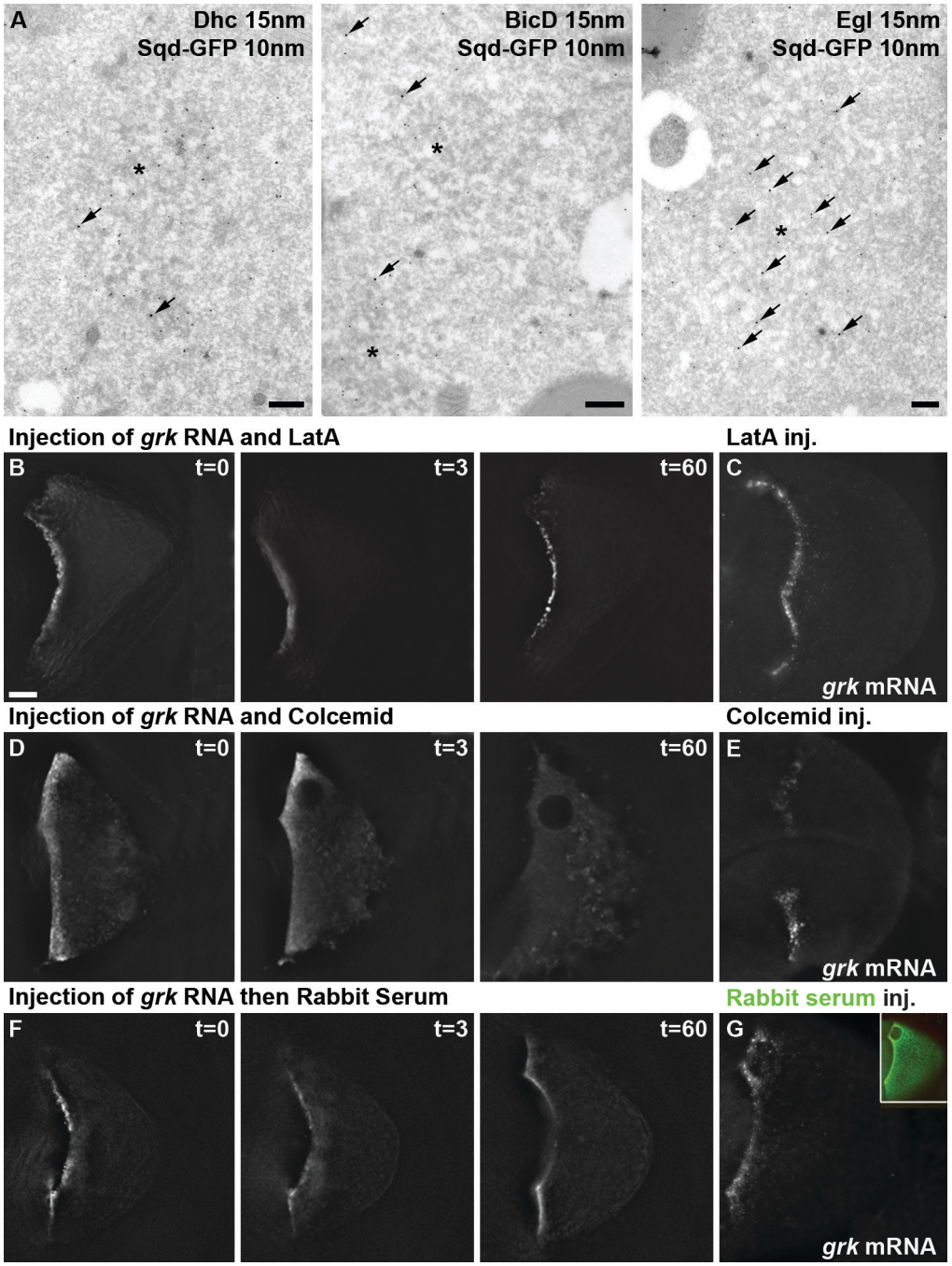
A
Dhc 15nm
Sqd-GFP 10nm
BicD 15nm
Sqd-GFP 10nm
Egl 15nm
Sqd-GFP 10nm
Injection of grk RNA and LatA
LatA inj.
B
t=0
t=3
t=60
C
grk mRNA
Injection of grk RNA and Colcemid
Colcemid inj.
D
t=0
t=3
t=60
E
grk mRNA
Injection of grk RNA then Rabbit Serum
Rabbit serum inj.
F
t=0
t=3
t=60
G
grk mRNA

Supplementary Figure 6. Sqd co-localizes with BicD and Egl in sponge bodies and anterior *grk* mRNA localization in sqd mutants is MT, not actin dependent.
(A) SqdGFP (10nm) co-localizes with Dhc(15nm), BicD (15nm) and Egl (15nm) in sponge bodies.
(B) Latrunculin A has no effect on the localization of injected *grk* RNA in *sqd*^{1} mutants. Time points from a time lapse movie of a *sqd*^{1} oocyte, pre-injected with AlexaFluor546 *grk* RNA (red) localized along the anterior pole. At t=0 min (45-60 min after injection of RNA), Latrunculin A (20mM) was injected. After 60 min, F-actin removal does not affect maintenance of injected *grk* RNA at the anterior pole.
(C) Endogenous *grk* mRNA in a *sqd*^{1} oocyte injected with Latrunculin A 45-60 min prior to fixation. Latrunculin A has no effect on *grk* mRNA localization at the anterior.
(D) Effect of Colcemid on the localization of injected *grk* RNA in *sqd*^{1} mutant. Time points from a time lapse movie of a *sqd*^{1} oocyte pre-injected with AlexaFluor546 *grk* RNA (red) localized along the anterior. Colcemid (1mg/ml) was injected at t=0 min (45-60 min after RNA injection). At t=60 min, depolymerization of MTs disrupts completely the anterior localization of *grk* RNA.
(E) Endogenous *grk* mRNA in a *sqd*^{1} oocyte injected with Colcemid and fixed 45-60 min after injection. Depolymerizing MTs causes a partial disruption of *grk* mRNA localization.
(F) Control rabbit antibody injected into a stage 9 *sqd*^{1} mutant oocyte. The anterior localization of pre-injected AlexaFluor546 labeled *grk* RNA is unaffected up to t=60 min.
(G) Control injection of Normal Rabbit Serum 45-60 min prior to fixation has no effect on endogenous *grk* mRNA localization. Inset shows the injected Rabbit Serum detected with an AlexaFluor488 anti-Rabbit (green). Scale bars: 200nm in (A), 10µm in (B-G).

CHAPTER 5

Dynein transports its own RNA into P-bodies and maintains their structure

Bram Herpers[1], Jan Soetaert[2], Renald Delanoue[3], Ilan Davis[2] and Catherine Rabouille[1]

1. University Medical Centre Utrecht, Department of Cell Biology and the Institute of Biomembranes, Heidelberglaan 100, The Netherlands
2. Wellcome Trust Centre for Cell Biology, Michael Swann building, University of Edinburgh, Mayfield Road, Edinburgh EH9 3JR, UK
3. Centre de Biochimie, Parc Valrose, Faculté des Sciences, 06108 NICE cedex 2, France

IN PREPARATION

Dynein is required for both active transport and static anchoring of localized transcripts in *Drosophila*. Here we show that mRNAs encoding components of the Dynein motor are themselves transported and anchored by Dynein in large cytoplasmic ribonucleoprotein-rich structures that are translationally silent and are the *Drosophila* equivalent of yeast P-bodies. Furthermore, Dynein is also required for their structural integrity. We propose that the formation of P-bodies involves Dynein switching from an active motor to a structural crosslinker that assembles large ribonuclear anchoring complexes.

Dynein is the major molecular motor in the cell that is involved in the transport of many cytoplasmic cargoes to the minus ends of microtubules. One type of its cargo are localized transcripts such as the pair rules mRNAs in the syncitial *Drosophila* embryos (Bullock and Ish-Horowicz, 2001; Wilkie and Davis, 2001) and *gurken* mRNA in the Drosophila oocyte (Januschke et al., 2002; MacDougall et al., 2003). Dynein is a large multi-component molecular machine that is able to generate net unidirectional movement through the ATPase activity of its largest subunit, Dynein heavy chain (Dhc). The processivity of Dynein is regulated by the interaction with dynactin (Schroer, 2004) and the motor cofactors Bicaudal D (BicD) and Egalitarian (Egl) (Claussen and Suter, 2005; Bullock et al., 2006), an interaction that is required for Dynein motility *in vivo*. With the many complexes that regulate its activity identified, it is easy to imagine how such a large molecular machine could perform other cytoplasmic functions besides cargo transport along microtubules. In this perspective, Dynein has been recently shown to be involved in the static anchoring its mRNA cargo (Delanoue and Davis, 2005), independently of its motor activity. However, the study of the non-motile functions of molecular motors in general is still in its infancy.

Using a combination of live cell imaging and ultrastructural localization of proteins and RNAs, we found that components of the Dynein motor are localized within the oocyte in cytoplasmic structures, similar to the previously described large Exuperantia-positive non-membrane bound sponge bodies (Wilsch-Brauninger et al., 1997). These structures that we confirmed to be sponge bodies (fig. S1) are present throughout the oocyte and concentrate Dhc (Fig. 1, A and C) approximately 3 times over the surrounding cytoplasm (Table 1), BicD (Fig. 1B) and Egl (Fig. 1C).

The sponge bodies were proposed to contain *bicoid* mRNA (Wilsch-Brauninger et al., 1997), suggesting that they could be a class of RNA granules. RNA granules have been identified in many tissues and organisms and their function ranges from RNA transport to storage to translation regulation, including repression and decay (Anderson and Kedersha, 2006). We therefore tested whether sponge bodies are also involved in translation regulation.

Inhibition of translation through the polysome-destabilizing drug puromycin had no effect on the sponge bodies or its contents (not shown). Using immuno-electron microscopy (IEM) on ultrathin frozen sections of Drosophila oocytes, we found that sponge bodies were depleted of ribosomes (Fig. 1D). The hnRNP Squid (visualized using the fly strain SqdGFP (Norvell et al., 2005)) that functions in translational control was found to concentrate in all the sponge bodies that are found throughout the oocyte (Fig. 1, B, C and E). We further localized Orb (Castagnetti and Ephrussi, 2003), the *Drosophila* homologue of CPEB, a translation regulator that inhibits translation in its non-phosphorylated form (Piccioni et al., 2005) and we found it enriched in the sponge bodies (Fig. 1F). Finally, Bruno, a well-known translational repressor (Kim-Ha et al., 1995; Webster et al., 1997) is also a component of the sponge bodies, both in the middle of the oocyte (Fig. 1G) and at the dorso-anterior corner (Fig. 1H).

Me31B, an RNA helicase that can be involved in translational repression and RNA decay, has also been localized in sponge bodies (Nakamura et al., 2001). In addition, Me31B has been shown to be part of a ribonucleoprotein complex involved in the control of mRNA translation, comprising the RNA binding proteins Yps and Tra1, the eukaryotic initiation factor 4E binding protein Cup, (Wilhelm et al., 2005; Decker and Parker, 2006), and the RNA localization factor Exu (Wilhelm et al., 2000), the original marker of sponge bodies (Wilsch-

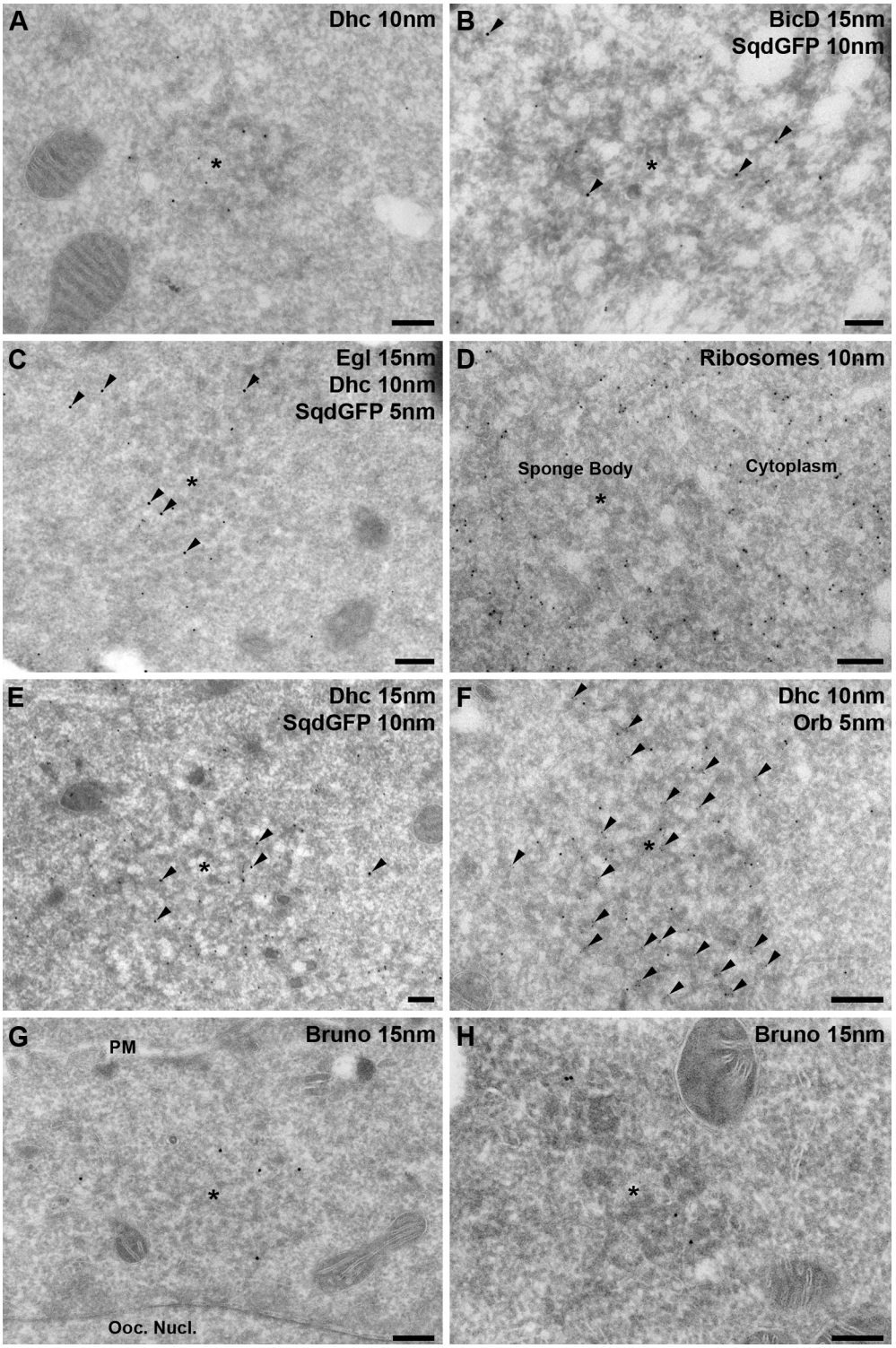
A
Dhc 10nm
B
BicD 15nm
SqdGFP 10nm
C
Egl 15nm
Dhc 10nm
SqdGFP 5nm
D
Ribosomes 10nm
Sponge Body
Cytoplasm
E
Dhc 15nm
SqdGFP 10nm
F
Dhc 10nm
Orb 5nm
G
Bruno 15nm
PM
Ooc. Nucl.
H
Bruno 15nm

Figure 1. Dynein is concentrated in sponge bodies, the oocyte P-bodies.
We use immuno-electron microscopy (IEM) on ultrathin frozen sections of a stage 9 wild type or SqdGFP expressing oocytes (Norvell et al., 2005) to localize **(A)** Dhc (rabbit polyclonal anti-Dhc (PEP1, T. Hays, 1/300, followed by 10nm proteinA gold (PAG) from the Dept. of Cell Biology, UMC Utrecht, Utrecht, The Netherlands); **(B)** BicD (clone 4C2, B. Suter, 1/20, Rabbit anti mouse; 15nm PAG, arrowheads) and SqdGFP (rabbit polyclonal anti-GFP A6455, Molecular probes, 1/200; 10nm); **(C)** Egl (rabbit polyclonal anti-Egl, R. Lehmann, 1/300, PAG 15nm, arrowheads), Dhc (10nm) and SqdGFP (5nm); **(D)** Ribosomes (Human anti ribosome, J. van Minnen, 1/300, rabbit anti human, PAG 10nm); **(E)** SqdGFP (10nm) and Dhc (15nm, arrowheads); **(F)** The *Drosophila* homologue of CPEB (Orb) (DSHB, 1/20; 5nm, arrowheads) and Dhc (10nm); **(G-H)** The translational repressor Bruno (rat anti Bruno, A. Ephrussi, 1/3000, Rabbit anti rat; 15nm) at the dorso-anterior corner **(G)** between the oocyte nucleus (Ooc. Nucl.) and the plasma membrane (PM) facing the follicle cells and **(H)** in the middle of the oocyte. Processing and labeling protocols are previously described in (Herpers and Rabouille, 2004). Imaging was performed on a Jeol EX1200 electron microscope. Asterisks: sponge bodies. Scale bars: 200nm

Brauninger et al., 1997) (fig. S1B). These proteins co-localize and co-immunoprecipitate with the *Drosophila* decapping enzyme dDcp1, required for mRNA decay, but also involved in mRNA regulation (Lin et al., 2006).

This strongly suggests that the sponge bodies are specific cytoplasmic structures that do not support active translation but act either as storage sites for translationally repressed mRNAs, or as sites for RNA degradation, in a manner reminiscent of the biology of the eukaryotic processing bodies (P-bodies) (Sheth and Parker, 2003; Brengues et al., 2005; Coller and Parker, 2005). P-bodies are RNA containing cytoplasmic structures depleted from ribosomes (Anderson and Kedersha, 2006), but contain a series of proteins, such as the homologue of Me31B (the yeast Dhh1 and the mammalian p54/rck), CPEB, decapping enzymes (Dcp1 and Dcp2), and Tra1 homologues (a protein from the Scd6 family) (Weston and Sommerville, 2006). The P-bodies are thought to store RNAs which are either to be degraded, repressed or eventually allowed to re-enter translation (Brengues et al., 2005). We propose that sponge bodies are the oocyte P-bodies. Taken together, these results show that in the *Drosophila* oocyte, components of the Dynein motor complex are concentrated in P-bodies.

To determine what function the Dynein complex could have in these structures, we inactivated the Dynein complex in stage 9 *Drosophila* oocytes by injecting anti-Dhc antibodies that we have previously shown to inhibit Dhc function (Wilkie and Davis, 2001; MacDougall et al., 2003; Delanoue and Davis, 2005). Using electron microscopy techniques, we found that the oocyte P-bodies then lost their structural integrity. Proteins that are typically concentrated in these structures, such as Dhc itself (Fig. 2, A and B), and SqdGFP (Fig. 2B) display a diffuse distribution in the cytoplasm, suggesting that loss of function of the Dynein complex led to the loss of P-bodies and their structural integrity, thus identifying a novel function for this complex.

To test whether the Dynein complex exerts this structural role by constantly transporting components involved in the P-body integrity, we compromised the motor activity of Dynein by inactivating its cofactor Egl. So far, all the dynein mediated transport steps we have studied in *Drosophila* have been greatly reduced or inhibited upon Egl inactivation (Delanoue and Davis, 2005). This inactivation of Egl had no effect on the P-body integrity, as assessed by morphology and by the distribution of the SqdGFP that remain concentrated in these structures (Fig. 2C). This not only suggests that the Dhc antibody injection does not create an artefact, but also that the structural role of Dynein does not require its motor activity.

Furthermore, Dynein has previously been suggested to play a role in MT organization (Vorobjev et al., 2001; Malikov et al., 2004). We tested whether the inactivation of Dynein has not indirectly led to the impairment of the P-body structure by affecting the microtubule cytoskeleton, especially at the dorso-anterior corner where it is the most abundant. First, we

found that the microtubules that normally flank the P-bodies were unaffected by the injection of anti-Dhc antibodies (Fig. 2, A and B). Second, the depolymerization of the microtubules by Colcemid treatment did not affect the oocyte P-body integrity or the distribution of SqdGFP (Fig. 2D). Taken together, these results show that Dynein, independently from its motor activity, is required for the structural integrity of the oocyte P-bodies in which it is concentrated.

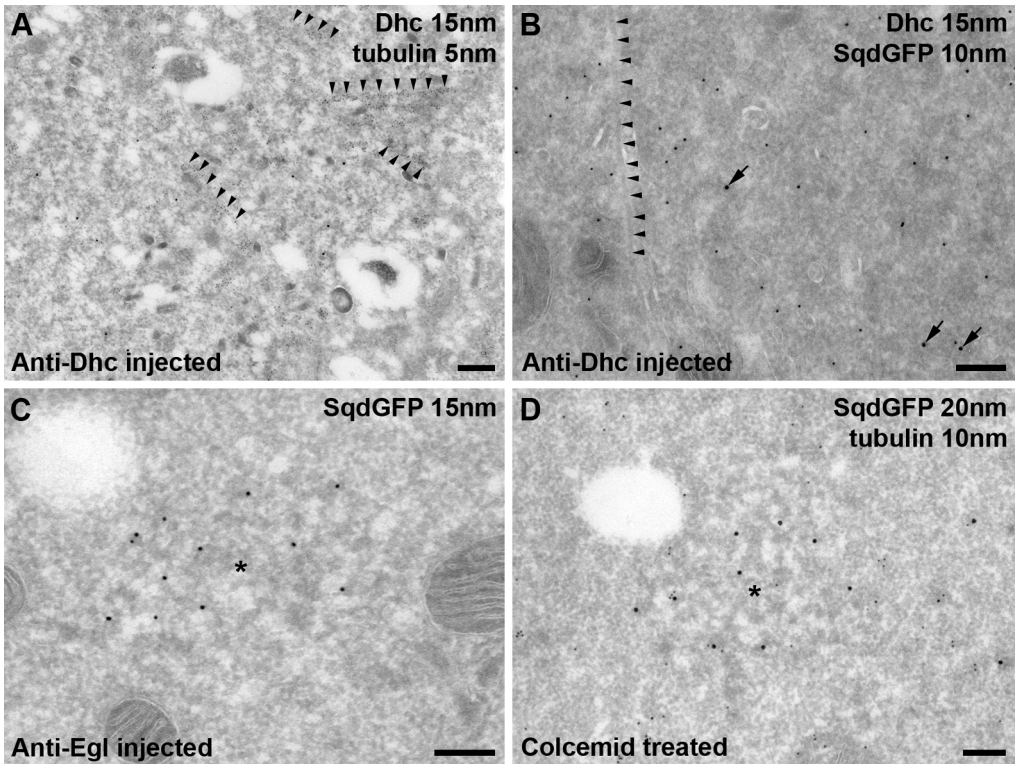

Figure 2: Dhc is required for the structural integrity of the oocyte P-bodies.
(A) Wild-type ovaries separated as described in (MacDougall et al., 2003) were injected with anti-Dhc antibodies (Gift from D.Sharp, 20mg/ml) for 10 minutes before fixation. This resulted in the disruption of the P-bodies without affecting the microtubules (monoclonal anti αtubulin antibody, clone B512, Sigma, 1/5000; 5nm, rows of arrowheads), and the redistribution of Dhc (detected with the Dhc antibody PEP1; 15nm). **(B)** Same as **(A)**, but in SqdGFP oocyte. SqdGFP (10nm) is also dispersed in the cytoplasm due to the disruption of the P-bodies. Dhc (15nm, arrows).The row of small arrowheads indicates an intact microtubule. **(C)** Inhibition of Egl by anti-Egl antibody injection (Gift from R. Lehmann; 20mg/ml; Delanoue et al, 2006) does not affect the P-body structure where SqdGFP (15nm) stays concentrated. (D) Colcemid treatment of the oocytes (Sigma; 1 mg/ml) leads to the depolymerization of the microtubules (10nm) but does not affect the ultrastructure of the P-bodies (SqdGFP, 20nm). Asterisks: sponge bodies. Scale bars: 200nm.

To understand how Dynein is required in the P-body structure, we asked how it becomes concentrated there. The yeast P-bodies have been shown to depend on RNA for their formation (Teixeira et al., 2005). Furthermore, Dynein has been shown to transport many cargoes in a diversity of tissues (King, 2000; Pfister et al., 2006), including mRNAs in the *Drosophila* oocyte (MacDougall et al., 2003). We therefore made the hypothesis that Dynein is delivered to the P-bodies by mediating mRNA transport, upon which it remains and acts as a structural component. To test this, we needed to show that the oocyte P-bodies are RNA containing structures, and identify oocyte P-body mRNAs that could be used as markers.

Using RNA *in situ* hybridization on whole stage 9 oocytes, we first localized the

endogenous *dhc* mRNA. We found it concentrated in bright foci throughout the oocyte (Fig. 3A, arrows) with a slight concentration at the dorso-anterior corner. Using a method of RNA *in situ* hybridization coupled to IEM on ultrathin frozen sections (ISH-IEM) that we have recently developed to localize endogenous mRNAs at the ultrastructural level (Delanoue et al., 2006), we found that these bright foci correspond to the P-bodies, in which *dhc* mRNA is enriched 5 fold when compared to the surrounding cytoplasm, including those at the dorso-anterior corner (Fig. 3B, Table 1). The fact that the mRNA is slightly more concentrated at the dorso-anterior corner simply reflects the fact that P-bodies are two times more abundant there than in the rest of the oocyte (Table 1). We also localized endogenous *bicD* mRNA that displayed a similar pattern, although it localizes more strongly to the anterior side of the oocyte and the foci in the middle of the oocyte were less bright (Fig. 3C). By ISH-IEM, we also found that *bicD* mRNA was localized to P-bodies together with Dhc (Fig. 3D). These data show that, as proposed, the oocyte P-bodies contain mRNAs, such as *dhc* and *bicD*.

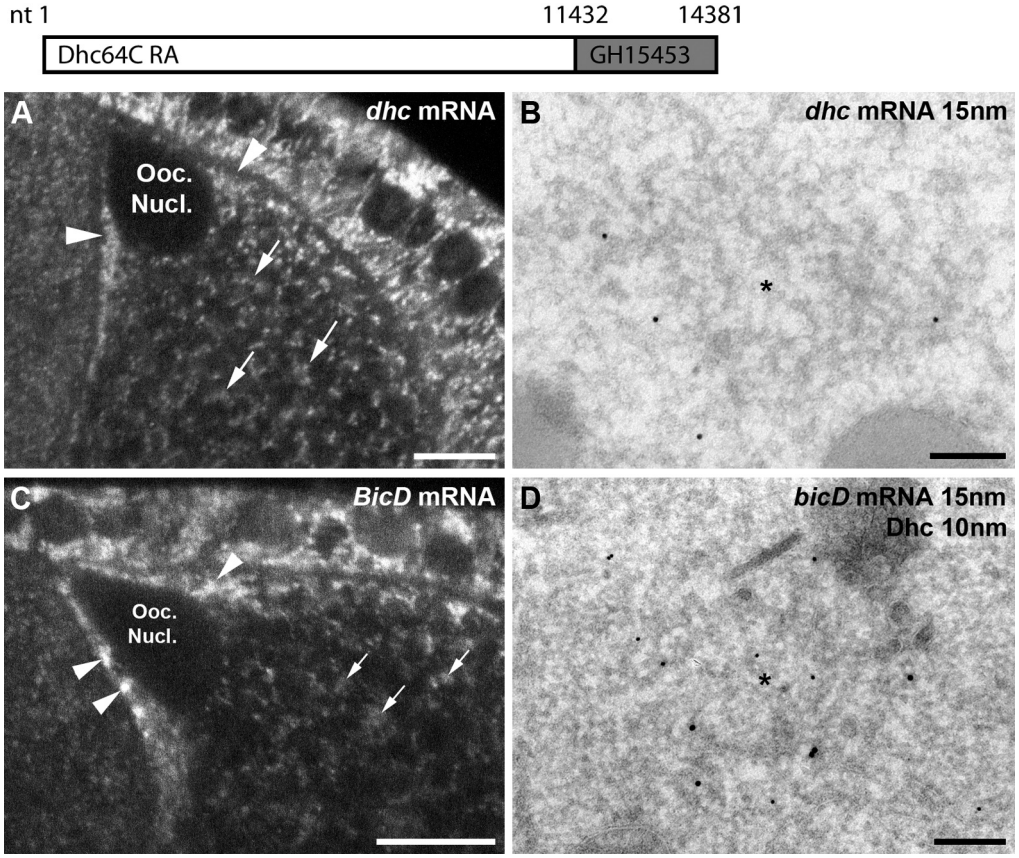

Figure 3. *dhc* and *bicD* mRNAs are concentrated in P-bodies.
(A) FISH of *dhc* mRNA using a *dhc* antisense probe prepared from the Drosophila Gene Collection (DGC) cDNA clone GH15453 that represents the last 3000 nucleotides of the sequence encoding Dhc64C-RA. *dhc* mRNA is found around the oocyte nucleus (Ooc. Nucl., arrowheads) and in discrete areas of the cytoplasm (some are marked by arrows). **(B)** ISH-IEM of *dhc* mRNA on frozen sections of chemically fixed stage 9 oocytes (using a biotin labeled RNA probe detected by anti-biotin antibody (Rockland, 1/10,000) and PAG (15nm) (as described in (Delanoue et al., 2006)) that is found in the oocyte P-bodies. **(C)** FISH of *bicD* mRNA using an antisense probe made from the full length DGC cDNA clone LD17129, that is found around the oocyte nucleus (arrowheads), at the ventral-anterior corner (not shown) and in discrete areas of the cytoplasm (some are marked by arrows). **(D)** ISH-IEM of *bicD* mRNA (15nm), this is also found in P-bodies throughout the oocyte, together with Dhc (10nm). Asterisks: sponge bodies. Scale bars: 10µm (A and C), 200nm (B and D).

To test whether the transport of these mRNA to the oocyte P-bodies requires Dynein, we used the *in vivo* localization assay based on the injection of *in vitro* synthesized fluorescently labeled RNAs in the *Drosophila* oocyte, which has been used previously to study *gurken* RNA transport to the dorso-anterior corner (MacDougall et al., 2003). However, unlike *gurken*, *dhc* RNA does not move over long distances. Wherever it is injected in the oocyte, it gets trapped into the nearest SqdGFP positive spots (Fig. 4, A and B) that are likely to be the P-bodies (Fig. 1D). This was confirmed by analyzing the distribution of injected biotinylated *dhc* RNA by IEM. We found that it localizes almost exclusively to P-bodies near or at the site of injection (Fig. 4C) together with Dhc (Fig. 4D), reflecting the localization of the endogenous transcripts. When *bicD* RNA is injected using the same assay, it localizes along the anterior of the oocyte, where it colocalizes with SqdGFP in P-bodies (Fig. 4, E and F), in a pattern reminiscent of the endogenous *bicD* mRNA (Nakamura et al., 2001).

The delivery of *dhc* RNA to P-bodies is very specific. First, the P-bodies located away from the site of injection were negative for the injected *dhc* RNA (not shown). Second, the property of localizing into the nearest sponge bodies is also specific for *dhc* RNA. When injected at the centre of the oocyte, *bicD* RNA ultimately reaches the anterior side (Fig. 4E) and *gurken* RNA the dorso-anterior corner (MacDougall et al., 2003). Third, the property of *dhc* and *bicD* RNA to be delivered to P-bodies is also specific. Injected *hunchback* RNA (Fig. 4G) and injected *gurken* RNA lacking the localization signal (thus failing to localize to the dorso-anterior corner) (Fig. 4H), localized randomly in the oocyte cytoplasm, but not in the P-bodies.

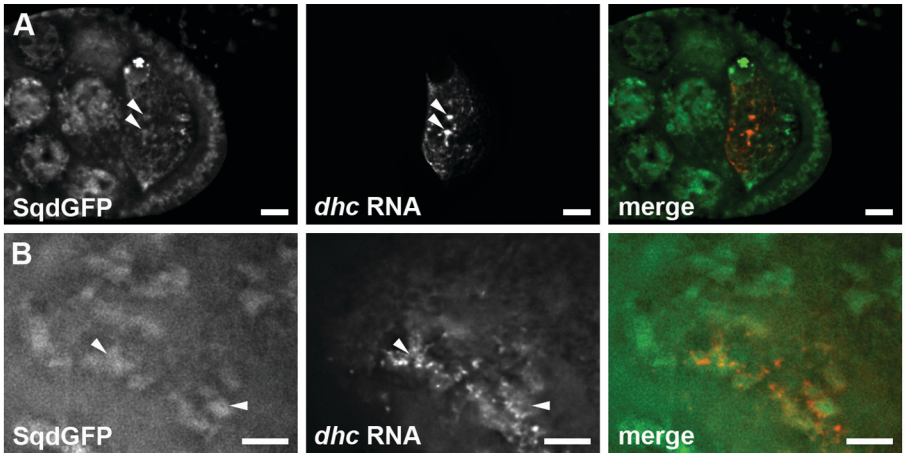

Figure 4: Dynein mediates the transport of its own RNA to P-bodies.
(A-B) *In vivo* injection in SqdGFP oocytes (green) of AlexaFluor546 labeled *dhc* RNA (red) *in vitro* transcribed from the GH15453 clone using UTP-Alexa 546 (Wilkie and Davis, 2001) at the concentration of 250-500 ng/µl. The injected dhc RNA is not transported further than the site of injection and accumulates in SqdGFP positive areas (arrowheads). **(C-D)** Oocytes injected with biotin-labeled *dhc* RNA (from UTP-biotin) were processed for IEM (Delanoue et al., 2006) and the *dhc* RNA (anti-biotin,15nm, arrowheads) is found in P-bodies together with SqdGFP (10nm, **C**) and Dhc (10nm, **D**). Microtubules were labeled with αtubulin (5nm). **(E)** AlexaFluor546 labeled *bicD* RNA (red) was injected into SqdGFP oocytes (green). After 60 minutes, the RNA has accumulated at the anterior of the injected oocyte where it colocalizes with SqdGFP (merge). Nuclei were stained with DAPI (blue). **(F)** Biotinylated *bicD* RNA injected SqdGFP oocyte (15nm) colocalizes with SqdGFP (10nm) in the oocyte P-bodies. **(G-H)** injected AlexaFluor546 labeled *hunchback* (*hb*) RNA **(G)** and *gurken* mRNA lacking its localization sequence (grkDeltaGLS, 15nm, arrowheads, **H**) do not localize or concentrate in SqdGFP positive areas (**G'** shows the magnification of the boxed area in which some SqdGFP positive areas are marked by arrowheads). **(I)** Inactivation of Egl by injection of inhibitory anti-Egl antibodies (as in Fig. 2C) 10 min before the *dhc* RNA injection makes *dhc* RNA (arrowheads) incompetent to enter the P-bodies, marked with SqdGFP (10nm). Imaging was performed on a widefield DeltaVision microscope (Applied Precision, Olympus IX70 and Roper Coolsnap HQ). Images were acquired with 20X/0.75NA or 100X/1.4NA and then deconvolved. Each experiment was repeated with at least two different batches of RNA in a total of 40 oocytes. Asterisks: sponge bodies. Scale bars: 10µm (A, E and G), 5µm (B) and 200nm (C,D,F,H,I).

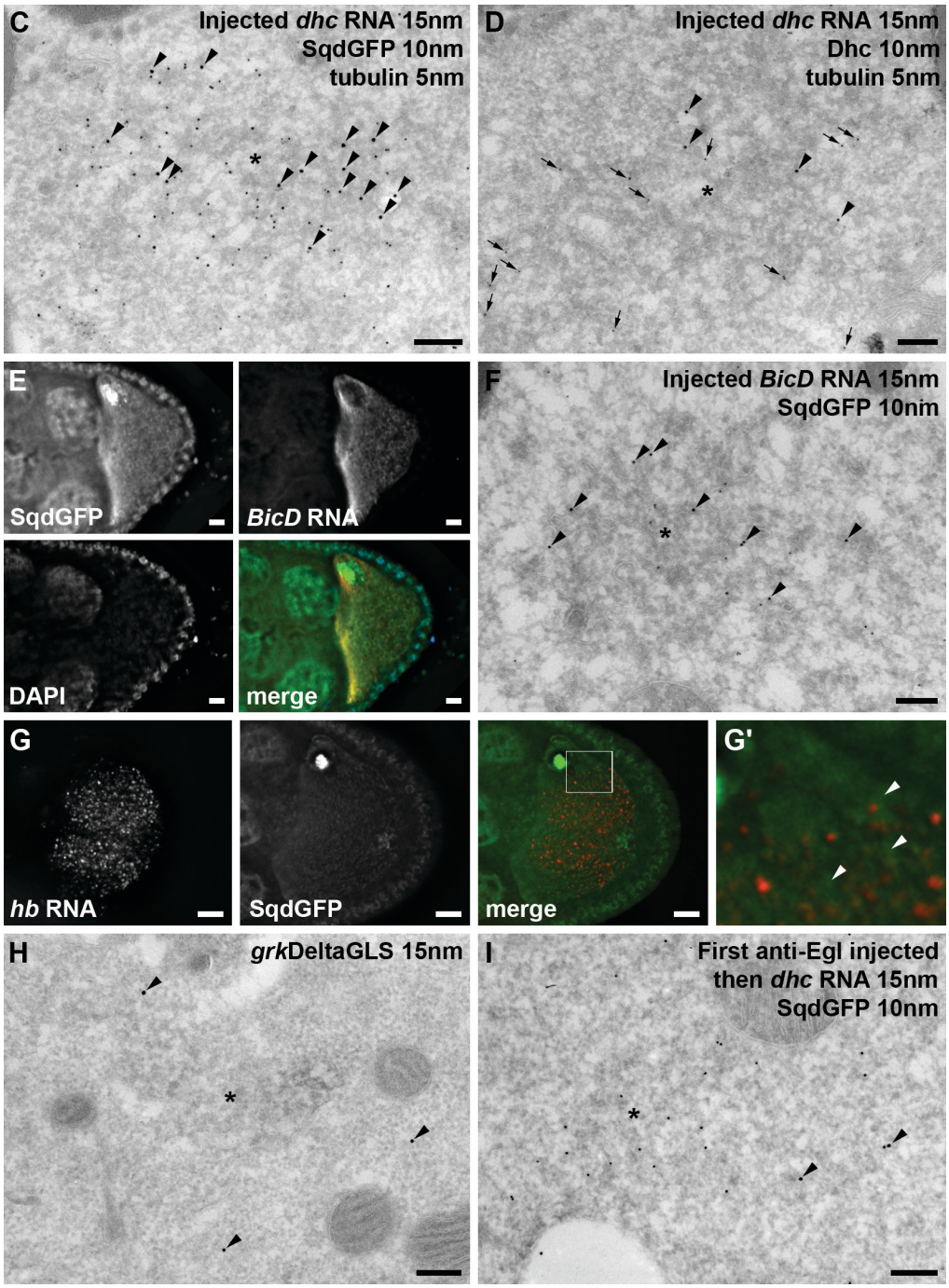
C
Injected dhc RNA 15nm
SqdGFP 10nm
tubulin 5nm
D
Injected dhc RNA 15nm
Dhc 10nm
tubulin 5nm
E
SqdGFP
BicD RNA
DAPI
merge
F
Injected BicD RNA 15nm
SqdGFP 10nm
G
hb RNA
SqdGFP
merge
G'
H
grkDeltaGLS 15nm
I
First anti-Egl injected
then dhc RNA 15nm
SqdGFP 10nm

We last tested whether the transport of *dhc* RNA to P-bodies required the dynein motor. We inhibited the function of the Dynein motor complex by inactivating the subunit Egl, 10 minutes before the injection of *dhc* RNA, and assessed the localization of *dhc* RNA. We found that the *dhc* RNA fails to localize in the P-bodies and remains non-localized in the cytoplasm (Fig. 4I), showing that the motor activity of the Dynein complex is required for the transport of *dhc* RNA to P-bodies.

Taken together, we have identified a novel role for the Dynein complex. We show that it is required for the structural integrity of the oocyte P-bodies, to which it is delivered and concentrated upon transport of its own RNA.

The targeting of mRNA to eukaryotic P-bodies has been shown to be mostly due to change in environmental conditions, such as stress (Teixeira et al., 2005), and glucose deprivation in yeast leads to the targeting of a number of mRNAs (such as *MFA2*, *RPL41*, *PGK1* and *CYH2*) to P-bodies (Brengues et al., 2005). Targeted mRNAs are then either stored, translationally repressed, degraded, or allowed to re-enter translation (Brengues et al., 2005). Based on the localization of proteins involved in these functions, we have postulated that the oocyte structures in which we found Dynein to be concentrated, the sponge bodies, were the equivalent of the oocyte P-bodies. We have further identified two mRNAs, *dhc* and *bicD*, that are delivered to, and concentrated in, the oocyte P-bodies. Although not all the known P-body markers have been localized in the oocyte P-bodies (including those involved in RNA decay), and that stress does not seem involved in the recruitment of *dhc* and *bicD* mRNAs to these structures, the oocyte P-bodies share many resemblances with the eukaryotic P-bodies and are here shedding light on novel aspects of their formation and maintenance.

Although the fate of *dhc* and *bicD* mRNAs in the oocyte P-bodies is not fully understood, their delivery and concentration into the oocyte P-bodies is specific, and probably relies on cis-acting elements. These are predicted to be present in the RNA sequences we used for the injection experiments, since they mimic perfectly the final localization of the endogenous transcript. In particular, *dhc* RNA was synthesized from the last 3' quarter of its full length sequence (including the 3'UTR), suggesting that this is where the information conferring P-body localization is situated. The lack of homology between this sequence and the one used for synthesizing *bicD* RNA suggests that the P-body targeting elements are probably contained in secondary structures, as it has been shown before for other localized RNAs (Van de Bor and Davis, 2004).

These targeting elements are likely to recruit trans-acting factors, including a transport machinery to be targeted to the P-bodies. Yet, the two RNAs exhibit different characteristics of transport. *dhc* RNA travels very short distances and accumulates in the nearest P-bodies, whereas *bicD* RNA is transported to P-bodies at the anterior side. This suggests that the cargo itself can modulate the specificity of movement and localization, as it has already been shown for *hairy* mRNA in the *Drosophila* embryo (Bullock et al., 2003) and *ASH1* mRNA in yeast (Kruse et al., 2002). Alternatively, these two mRNAs might recruit different trans-acting factors that might specify their differential delivery, perhaps by targeting to specific classes of P-bodies, though we have no morphological evidence so far to categorize any distinct pools.

One of the factors mediating the transport and localization of *dhc* mRNA to P-bodies is Dynein itself. Therefore, in addition to being identified as novel Dynein cargo, *dhc* RNA is also shown to require its translation product for its localization. A same principle has already

been shown for the localization of *oskar* mRNA at the posterior pole of the oocyte that requires the presence of Oskar protein (Kim-Ha et al., 1991; Rongo et al., 1995; Braat et al., 2004), and the targeting of *RPS28a* mRNA to yeast P-bodies, that required the RPS28a protein (Coller and Parker, 2004).

Dynein also mediates *gurken* mRNA transport to the dorso-anterior corner of stage 9 oocyte where the minus end of microtubules are concentrated (Januschke et al., 2006). However, the transport of *dhc* RNA does not show any directionality and might seem independent of anterior concentration of the microtubule minus ends. Nevertheless, we cannot exclude that short microtubules are present and used for this very small transport step for which the processivity of the Dynein motor could be modified to move short instead of long distances. It is also possible that Dynein acts as a chaperone for the *dhc* RNA, independently of the microtubule minus end.

In addition to its motor activity that is required to transport *dhc* RNA to P-bodies, Dynein is shown here to be required for their structural integrity. One possibility is that Dynein continuously transports and delivers structural components to the P-bodies, but we have shown that the structural role is not linked to its transport activity. Dynein could then transport one structural component and remain in a complex with it, in such a way that inactivation of Dhc also inactivates this component. Alternatively, Dynein itself could act as a structural component. This complex contains multiple subunits, including Dhc, a very large protein that in addition to microtubule binding and ATPase activity, could also be engaged in protein-protein interactions. It has already been shown that it can switch from a motor to an anchor in the *Drosophila* embryo (Delanoue and Davis, 2005). We propose that in the oocyte, this switch could occur upon arrival to P-bodies, perhaps by changing its conformation thus allowing interactions with P-bodies components, such as the hnRNP Squid and the translational regulators, and acting as a crosslinker contributing to the P-body structure.

This process is likely to trap the mRNAs that Dynein delivers and thereby anchor them to the structure it builds. This suggests that Dynein mediated transport is automatically followed by Dynein mediated anchoring in P-bodies, which brings a new light on RNA anchoring. It remains to be seen whether all the mRNAs transported by Dynein are anchored in P-bodies. Some might not be anchored at all, or anchored on different structures that have yet to be identified. Conversely, whether all components of the oocyte P-bodies are localized by Dynein transport/chaperoning is also not known.

The fact that this Dynein mediated RNA anchoring takes place in P-bodies strengthens the coupling between anchoring and translation regulation, including repression. The RNA targeted and stored in P-bodies are deadenylated, which is both a step preceding decapping (Coller and Parker, 2004) and a method to prevent translation (Piccioni et al., 2005). Indeed, short poly(A)-tailed mRNAs cannot circularize and trigger translation initiation. Furthermore, although some are ultimately degraded, many of the stored and repressed mRNAs are ultimately translated and therefore protected against degradation. This could be achieved by hnRNP, similar to the way that hnRNP-A1 binds to the 3' UTR of *CYP2A5* mRNA and protects it from degradation (Glisovic et al., 2003). It is not known whether *dhc* and *bicD* mRNAs are indeed deadenylated, but Squid, that is concentrated in the oocyte P-bodies, could play a role in their protection.

So far, P-bodies have not been shown to support protein synthesis, but RNAs are known to leave the P-bodies to the ribosome-rich cytoplasm in order to initiate their translation (Brengues et al., 2005). A similar movement out of the oocyte P-bodies is likely to occur for *dhc* and *bicD* RNAs to allow the synthesis of the corresponding protein, that are very active in the cytoplasm. Both RNAs are mostly found in the P-bodies, arguing against the possibility that Dhc and BicD are synthesized from a putative cytoplasmic pool. This also argues against the fact that the RNA pool found in the P-bodies is destined to degradation.

RNAs can leave the P-bodies as single RNA molecules or comprised within small particles. Alternatively, the P-bodies themselves could disassemble, perhaps by degrading or inactivating Dynein, and release the mRNAs away from the translational repressors, that could also ultimately be degraded. P-bodies are therefore structures whose dynamics regulate the fine balance between RNA anchoring and repression, and RNA release and translation.

We have shown here that the oocyte P-bodies contain Bruno that is involved in the translational repression of *gurken* mRNA by binding specific sequences in the transcript (Norvell et al., 1999; Filardo and Ephrussi, 2003). We have recently shown that Dynein is also involved in the static anchoring of *gurken* mRNA at its final destination in the large structures we have here identified as P-bodies (Delanoue et al., 2006). It means that *gurken* RNA also is likely to be repressed while anchored. However, and as for *dhc* and *bicD* RNA, Gurken protein is translated and transported in the exocytic pathway to the extracellular space at the dorso-anterior corner (Herpers and Rabouille, 2004), suggesting that *gurken* mRNA is protected from degradation and allowed to enter translation by moving to an ER membrane outside the P-bodies.

Altogether, this work provides, through Dynein, a novel link between transport, anchoring and translation regulation. Whether Dynein also recruits the translational repressors in the P-bodies, whether it is involved in the structural maintenance of P-bodies in other cells, or other RNA granules, will have to be clarified in the near future.

Acknowledgements
We thank the Davis and Rabouille's lab as well as David Tollervey for helpful discussions. We thank Richard Parton for help and advice with light microscopy. This work was supported by a Wellcome Trust senior research fellowship (067413) to I.D., a Marie Curie fellowship to R.D. B.H. is funded by a Nederlandse Organisatie voor Wetenschappelijk Onderzoek (NWO) Aspasia grant (015.001.129) to C.R.

Table 1: Concentration of Dhc and *dhc* mRNA in P-bodies

	Oocyte*	DA corner
Density of P-bodies in cytoplasm	7±1.0%	14±2.0%
Concentration of Dhc in P-bodies (gold/µm2)	4.8±1.1	4.8±0.9
Density of Dhc in cytoplasm (gold/µm2)	1.4±0.3	1.4±0.3
Concentration of *dhc* mRNA in P-bodies (gold/µm2)	4.3±2.8	4.5±3.2
Density of *dhc* mRNA in cytoplasm (gold/µm2)	0.5±0.4	0.7±0.6

The surface of sponge bodies was estimated using the stereological point hit method with a grid of 1.0 cm on random pictures printed at the magnification of 10k or 12k (Herpers and Rabouille, 2004). The density is defined by the number of gold particles corresponding to Dhc or *dhc* mRNA divided by the surface, either the sponge bodies or surrounding cytoplasm and is expressed at number of gold/µm2. Oocyte* corresponds to any region of the oocyte except the DA corner.

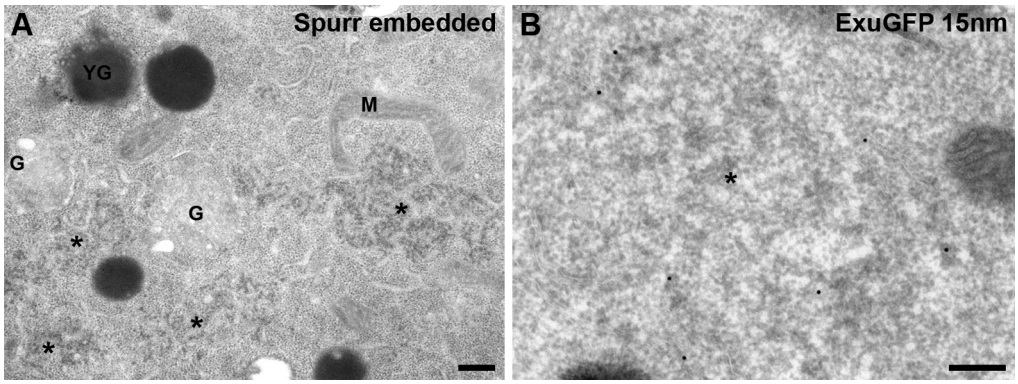

Supplementary Figure 1: Sponge body characterization.
(A) Oocyte embedded in the plastic resin Spurr (Herpers and Rabouille, 2004) clearly reveals the difference with the sponge bodies (asterisks) and the surrounding cytoplasm. G: tER-Golgi units; M: Mitochondria; YG: yolk granules. **(B)** Sponge bodies (asterisk) also contain ExuGFP (15nm). Scale bars: 200nm.

References

Anderson,P. and Kedersha,N. (2006). RNA granules. J. Cell Biol. 172, 803-808.

Braat,A.K., Yan,N., Arn,E., Harrison,D., and Macdonald,P.M. (2004). Localization-dependent oskar protein accumulation; control after the initiation of translation. Dev. Cell 7, 125-131.

Brengues,M., Teixeira,D., and Parker,R. (2005). Movement of eukaryotic mRNAs between polysomes and cytoplasmic processing bodies. Science 310, 486-489.

Bullock,S.L. and Ish-Horowicz,D. (2001). Conserved signals and machinery for RNA transport in Drosophila oogenesis and embryogenesis. Nature 414, 611-616.

Bullock,S.L., Nicol,A., Gross,S.P., and Zicha,D. (2006). Guidance of bidirectional motor complexes by mRNA cargoes through control of dynein number and activity. Curr. Biol. 16, 1447-1452.

Bullock,S.L., Zicha,D., and Ish-Horowicz,D. (2003). The Drosophila hairy RNA localization signal modulates the kinetics of cytoplasmic mRNA transport. EMBO J. 22, 2484-2494.

Castagnetti,S. and Ephrussi,A. (2003). Orb and a long poly(A) tail are required for efficient oskar translation at the posterior pole of the Drosophila oocyte. Development 130, 835-843.

Claussen,M. and Suter,B. (2005). BicD-dependent localization processes: from Drosophilia development to human cell biology. Ann. Anat. 187, 539-553.

Coller,J. and Parker,R. (2004). Eukaryotic mRNA decapping. Annu. Rev. Biochem. 73, 861-890.

Coller,J. and Parker,R. (2005). General translational repression by activators of mRNA decapping. Cell 122, 875-886.

Decker,C.J. and Parker,R. (2006). CAR-1 and trailer hitch: driving mRNP granule function at the ER? J. Cell Biol. 173, 159-163.

Delanoue,R. and Davis,I. (2005). Dynein anchors its mRNA cargo after apical transport in the Drosophila blastoderm embryo. Cell 122, 97-106.

Delanoue, R., Herpers, B., Soetaert, J., Rabouille, C., and Davis, I. (2006) Drosophila Squid hnRNP is required for Dynein to form static anchoring complexes with gurken/TGF-alpha mRNA. Submitted. This thesis, Chapter 4.

Filardo,P. and Ephrussi,A. (2003). Bruno regulates gurken during Drosophila oogenesis. Mech. Dev. 120, 289-297.

Glisovic,T., Ben David,Y., Lang,M.A., and Raffalli-Mathieu,F. (2003). Interplay between hnRNP A1 and a cis-acting element in the 3' UTR of CYP2A5 mRNA is central for high expression of the gene. FEBS Lett. 535, 147-152.

Herpers,B. and Rabouille,C. (2004). mRNA localization and ER-based protein sorting mechanisms dictate the use of transitional endoplasmic reticulum-golgi units involved in gurken transport in Drosophila oocytes. Mol. Biol. Cell 15, 5306-5317.

Januschke,J., Gervais,L., Dass,S., Kaltschmidt,J.A., Lopez-Schier,H., St Johnston,D., Brand,A.H., Roth,S., and Guichet,A. (2002). Polar transport in the Drosophila oocyte requires Dynein and Kinesin I cooperation. Curr. Biol. 12, 1971-1981.

Januschke,J., Gervais,L., Gillet,L., Keryer,G., Bornens,M., and Guichet,A. (2006). The centrosome-nucleus complex and microtubule organization in the Drosophila oocyte. Development 133, 129-139.

Kim-Ha,J., Kerr,K., and Macdonald,P.M. (1995). Translational regulation of oskar mRNA by bruno, an ovarian RNA-binding protein, is essential. Cell 81, 403-412.

Kim-Ha,J., Smith,J.L., and Macdonald,P.M. (1991). oskar mRNA is localized to the posterior pole of the Drosophila oocyte. Cell 66, 23-35.

King,S.M. (2000). The dynein microtubule motor. Biochim. Biophys. Acta 1496, 60-75.

Kruse,C., Jaedicke,A., Beaudouin,J., Bohl,F., Ferring,D., Guttler,T., Ellenberg,J., and Jansen,R.P. (2002). Ribonucleoprotein-dependent localization of the yeast class V myosin Myo4p. J. Cell Biol. 159, 971-982.

Lin,M.D., Fan,S.J., Hsu,W.S., and Chou,T.B. (2006). Drosophila decapping protein 1, dDcp1, is a component of the oskar mRNP complex and directs its posterior localization in the oocyte. Dev. Cell 10, 601-613.

MacDougall,N., Clark,A., MacDougall,E., and Davis,I. (2003). Drosophila gurken (TGFalpha) mRNA localizes as particles that move within the oocyte in two dynein-dependent steps. Dev. Cell 4, 307-319.

Malikov,V., Kashina,A., and Rodionov,V. (2004). Cytoplasmic dynein nucleates microtubules to organize them into radial arrays in vivo. Mol. Biol. Cell 15, 2742-2749.

Nakamura,A., Amikura,R., Hanyu,K., and Kobayashi,S. (2001). Me31B silences translation of oocyte-localizing RNAs through the formation of cytoplasmic RNP complex during Drosophila oogenesis. Development 128, 3233-3242.

Norvell,A., Debec,A., Finch,D., Gibson,L., and Thoma,B. (2005). Squid is required for efficient posterior localization of oskar mRNA during Drosophila oogenesis. Dev. Genes Evol. 215, 340-349.

Norvell,A., Kelley,R.L., Wehr,K., and Schupbach,T. (1999). Specific isoforms of squid, a Drosophila hnRNP, perform distinct roles in Gurken localization during oogenesis. Genes Dev. 13, 864-876.

Pfister,K.K., Shah,P.R., Hummerich,H., Russ,A., Cotton,J., Annuar,A.A., King,S.M., and Fisher,E.M. (2006). Genetic analysis of the cytoplasmic dynein subunit families. PLoS. Genet. 2, e1.

Piccioni,F., Zappavigna,V., and Verrotti,A.C. (2005). Translational regulation during oogenesis and early development: the cap-poly(A) tail relationship. C. R. Biol. 328, 863-881.

Rongo,C., Gavis,E.R., and Lehmann,R. (1995). Localization of oskar RNA regulates oskar translation and requires Oskar protein. Development 121, 2737-2746.

Schroer,T.A. (2004). Dynactin. Annu. Rev. Cell Dev. Biol. 20, 759-779.

Sheth,U. and Parker,R. (2003). Decapping and decay of messenger RNA occur in cytoplasmic processing bodies. Science 300, 805-808.

Teixeira,D., Sheth,U., Valencia-Sanchez,M.A., Brengues,M., and Parker,R. (2005). Processing bodies require RNA for assembly and contain nontranslating mRNAs. RNA. 11, 371-382.

Van de Bor,V. and Davis,I. (2004). mRNA localisation gets more complex. Curr. Opin. Cell Biol. 16, 300-307.

Vorobjev,I., Malikov,V., and Rodionov,V. (2001). Self-organization of a radial microtubule array by dynein-dependent nucleation of microtubules. Proc. Natl. Acad. Sci. U. S. A 98, 10160-10165.

Webster,P.J., Liang,L., Berg,C.A., Lasko,P., and Macdonald,P.M. (1997). Translational repressor bruno plays multiple roles in development and is widely conserved. Genes Dev. 11, 2510-2521.

Weston,A. and Sommerville,J. (2006). Xp54 and related (DDX6-like) RNA helicases: roles in messenger RNP assembly, translation regulation and RNA degradation. Nucleic Acids Res. 34, 3082-3094.

Wilhelm,J.E., Buszczak,M., and Sayles,S. (2005). Efficient protein trafficking requires trailer hitch, a component of a ribonucleoprotein complex localized to the ER in Drosophila. Dev. Cell 9, 675-685.

Wilhelm,J.E., Mansfield,J., Hom-Booher,N., Wang,S., Turck,C.W., Hazelrigg,T., and Vale,R.D. (2000). Isolation of a ribonucleoprotein complex involved in mRNA localization in Drosophila oocytes. J. Cell Biol. 148, 427-440.

Wilkie,G.S. and Davis,I. (2001). Drosophila wingless and pair-rule transcripts localize apically by dynein-mediated transport of RNA particles. Cell 105, 209-219.

Wilsch-Brauninger,M., Schwarz,H., and Nusslein-Volhard,C. (1997). A sponge-like structure involved in the association and transport of maternal products during Drosophila oogenesis. J. Cell Biol. 139, 817-829.

CHAPTER 6

Summarizing Discussion

Summarizing Discussion

The establishment of the primary body axes of the future embryo depends on the asymmetric secretion of Gurken by the *Drosophila* oocyte. Gurken encodes a TGF-alpha like peptide that is specifically secreted at two time points during oogenesis. At stage 6-7 in oogenesis, the oocyte sets up the anterior-posterior axis by secreting Gurken towards the posterior follicle cells. At stage 8-10, Gurken is secreted at the region capping the oocyte nucleus, the dorso-anterior (DA) corner. This local deposition of Gurken creates a dorsal-ventral axis.

The local synthesis and secretion of Gurken occurs where its asymmetrically localized mRNA resides. The mechanisms underlying the asymmetric secretion of Gurken protein and the asymmetric localization of *gurken* mRNA have been the topic of this thesis, in which we examined two fundamental aspects of the oocyte biology.

1. The relationship between the restricted Gurken secretion and *gurken* mRNA localization, or how a transmembrane protein can acquire asymmetric distribution through mRNA localization. This has led us to study the organization of the exocytic pathway in the oocyte and the sorting and transport of Gurken in relation to the localization of its mRNA.

2. The mechanisms underlying the asymmetric localization of *gurken* mRNA.

Here I summarize and discuss the results we gathered during this investigation.

The exocytic pathway in the oocyte comprises one thousand tER-Golgi units that function independently from one another

The first important result we obtained was that the exocytic pathway in the *Drosophila* oocyte comprises about one thousand tER-Golgi units, distinct functional units composed of an ER exit site closely opposed by a Golgi stack, that are spread randomly throughout the oocyte. Furthermore, these tER-Golgi units can function independently of one another and be used differentially. Only a subset of them, those located at the DA corner, transports and sorts Gurken to the extracellular space, while all tER-Golgi units transport other transmembrane proteins, such as Yolkless (**chapter 2**). This is a novel notion that is likely to be extended to other cell types, such as neurons. In these cells, local delivery of transmembrane proteins to the plasma membrane in the synaptic region of the dendrites is likely to occur through a local exocytic system that functions independently of the exocytic pathway in the cell body (Horton and Ehlers, 2003).

The restricted secretion of Gurken is regulated by two mechanisms

The restricted secretion of Gurken was found to depend on two different sorting mechanisms: on the post-translational sorting of the newly synthesized Gurken protein in the early exocytic pathway, and on pre-translational sorting in the cytoplasm through the asymmetric localization of *gurken* mRNA.

Efficient intracellular sorting and transport in the early exocytic pathway (**chapter 2**)

The transport of Gurken has been found to be restricted to only a subset of the tER-Golgi units after synthesis in the ER, a single lumen organelle that pervades the entire cell. This led us to investigate what would prevent diffusion in the ER. It became clear that Gurken is efficiently sorted, just after its synthesis in the ER, by the presence of two different regions in its amino acid sequence: its transmembrane domain and its luminal domain proximal to the transmembrane domain.

Gurken is synthesized as a transmembrane protein, but is cleaved by Rhomboid-2 just after synthesis in the ER to release the bioactive luminal peptide (Bokel et al., 2006). Although still not completely understood, this luminal peptide, when it is expressed solely, is not sorted properly and diffuses in the ER. This suggests that the transmembrane domain of Gurken facilitates its interaction with a second sorting mechanism.

This comprises the interaction of the proximal domain of Gurken with the cargo receptor Cornichon, which is expressed in all the tER-Golgi units on the oocyte (Bokel et al., 2006). Cornichon is the *Drosophila* homologue of Erv14p. This is a cargo receptor specific for Axl2p in yeast, a protein that also exhibits a polarized deposition and it is packaged into COPII coated vesicles (Powers and Barlowe, 2002). Interestingly, the *cornichon* mutant and Gurken transgene lacking the transmembrane domain phenocopy each other (Queenan et al., 1999; Bokel et al., 2006).

A pre-translational sorting mechanism: *gurken* mRNA localization dictates the differential use of the tER-Golgi units (**chapter 2**)

In addition to this, we found that the localization of the *gurken* mRNA is crucial to determine which tER-Golgi units are used to sort and transport Gurken. In the wild-type oocyte, *gurken* mRNA is located at the DA corner and only the tER-Golgi units at this location transport Gurken. Mutants in which *gurken* mRNA is mislocalized (e.g. along the anterior side in *squid*, or at the posterior pole in *merlin* mutants) show Gurken transport in tER-Golgi units located in those areas (that is along the anterior in the *squid* mutant).

We conclude that the localization of *gurken* mRNA dictates the restricted secretion of Gurken protein by integrating local synthesis and utilization of the scattered exocytic pathway. Sorting of transmembrane/secreted proteins to distinct plasma membrane domains can therefore be established by a pre-translational mechanism, in addition to post-translational sorting in the tER sites, or the sorting mechanisms at the trans Golgi network (TGN) (Rodriguez-Boulan and Musch, 2005). For Gurken, sorting at the TGN has not been elucidated.

A similar way of achieving restricted protein deposition might also occur in other cell systems. Neurons, for instance, actively localize mRNAs to the distal ends of the dendrites to control synaptic plasticity. Some of the localized mRNAs encode transmembrane proteins; this suggests that pre-translational sorting mechanisms also precede local transmembrane /secreted protein deposition in neurons next to sorting at the TGN. For this a small, but functional secretory system should exist to sustain local secretion (Grigston et al., 2005).

***gurken* mRNA does not colocalize with Gurken protein**

Because of the strict link we found between the use of the tER-Golgi units and the localization of *gurken* mRNA, we made the hypothesis that *gurken* mRNA could be localized on, or very near the membrane of the tER-Golgi units.

For this, we had to develop a protocol that allows the detection of endogenous mRNA at the ultrastructural level. This technique makes use of antisense RNA probes that are directly hybridized to the RNA in the cryosections of the oocytes (**chapter 3**). This *in situ* hybridization combined with immuno-electron microscopy (ISH-IEM) technique has also been very useful to detect many endogenous RNAs such as *bicoid* and *oskar* (**chapter 3**) as well as *dhc* mRNA (**chapter 5**).

This successful detection of endogenous *gurken* mRNA has, however, made it clear that our initial hypothesis was wrong and that *gurken* mRNA is not localized near or on the tER-Golgi units (**chapter 3**).

***gurken* mRNA localization occurs in two steps: transport and anchoring. The first step is mediated by Transport Particles (chapter 4)**

However the ISH-IEM technique showed no direct physical relation between *gurken* mRNA and the exocytic pathway, the *gurken* mRNA localization process and the molecular mechanisms underlying this are crucial to the pre-translational sorting mechanism. *gurken* mRNA transport

has mostly been studied by *in vivo* injection assays that either use fluorescently labeled or biotinylated (for immuno-electron microscopy) *in vitro* synthesized *gurken* RNA. These recapitulate many of the steps known to occur in the localization of the endogenous *gurken* mRNA. The endogenous *gurken* mRNA has also been investigated by electron microscopy, by the application of the novel technique mentioned above (**chapter 3**).

The transport of *gurken* RNA is mediated by electron-dense particles that we called transport particles. The injected mRNA is found in transport particles of a size between 70nm and 500nm, the endogenous mRNA in particles between 50 and 200nm. They are not membrane-bound and contain many RNA molecules, estimated to be from 100 to 2000 for the injected *gurken* RNA and 20 to 100 for the endogenous transcripts.

Furthermore, they are often found in close proximity of microtubules, and contain the ATPase unit of the Dynein motor complex, Dynein heavy chain (Dhc), the cofactors of the Dynein complex Egl and BicD, and the *gurken* mRNA binding protein Squid (**chapter 4**). Functional experiments have shown that Dynein is involved in *gurken* mRNA transport. The transport particles do not specifically associate to membranes; they are therefore likely to be directly transported along microtubules by this motor. This is the first time that this direct movement is ever shown.

A similar type of particles has also been described in neurons (neuronal granules) that are large complexes of different mRNAs, motors and RNA binding proteins (Krichevsky and Kosik, 2001; Kanai et al., 2004). These granules depend on an intact microtubule network for directed transport, similar to *gurken* mRNA in the oocyte.

Translational repression in transport particles

During the transport phase, the *gurken* mRNA must be kept silent to prevent premature Gurken production. Analogous to neuronal granules that function to transport mRNAs into dendrites, the transport particles must be regulating translation. The first clue is given by the presence of Squid, the *Drosophila* hnRNP-A1 homologue. hnRNP-A1 has recently been implicated to be a regulator for cap-independent translation of transcripts (Bonnal et al., 2005). Furthermore, transport particles contain the translation regulator Orb, the *Drosophila* CPEB homologue. The presence of other components involved in translational control such as ribosomes and the repressor Bruno, will be investigated.

Many of the factors that are found to influence *oskar* mRNA localization (Steinhauer and Kalderon, 2006) could theoretically be tested for their function in *gurken* mRNA transport. This could be done using microscopy techniques, which we have used here so successfully, but also biochemically through the purification of *gurken* mRNA transport particles coupled to mass spectrometry. This will shed light on the additional function of the RNA transport particles.

Microtubules and Dynein are not only important for transport, but also for the second step in *gurken* mRNA localization: the anchoring (chapter 4)

The final location of the *gurken* mRNA is the DA corner of the oocyte, where it is statically anchored. Functional experiments have shown that this anchoring depends on microtubules and Dhc, but not on the other subunits of the motor complex, Egl and BicD. These results indicate a loss of the processing activity of the Dynein motor complex upon delivery of the cargo at its destination. This notion is furthermore supported by the finding that Dynein accumulates together with the *gurken* mRNA at the DA corner after transport.

This is in many aspects similar to what was found in *Drosophila* embryos where Dynein accumulates apically upon localization of pair-rule transcripts, and their apical maintenance remains microtubule and Dynein dependent. The embryo data supported a model in which Dynein turns from a motor into a stable anchor upon delivery of the injected pair-rule transcripts at the end of the microtubules at the apical side by loosing its processing activity (Delanoue and Davis, 2005). To some extent, this model is also applicable to the oocyte, with the difference that the mRNA moves towards the DA corner in transport particles and finally accumulates and anchors there in a different larger cytoplasmic structure (see final model below).

Anchoring of *gurken* mRNA occurs in RNA rich cytoplasmic structures called sponge bodies (chapter 4)

Electron microscopic analysis has revealed that *gurken* mRNA is localized in large cytoplasmic structures, the sponge bodies, where it colocalizes with Dhc, Egl, BicD and Squid, the same factors found in transport particles. But these areas of the cytoplasm were structurally different, as they are composed of electron-dense strands that seem interdigitated by electron-translucent ER-like tubules. Sponge bodies have been described before and proposed to contain RNAs (Wilsch-Brauninger et al., 1997) but we have shown it here directly for the first time.

However, the fact that sponge bodies and transport particles share many components suggests that sponge bodies could be formed by the transport particles that could undergo a structural change upon arrival at the destination, to become sponge bodies. This would be accompanied by the switch of Dynein from a motor to an anchor.

Squid regulates the balance between transport particles and sponge bodies and the switch in the Dynein activity (chapter 4)

We propose that the hnRNP Squid (RNA binding protein) mediates both the conversion of transport particles into sponge bodies and vice versa. The evidence for this is that injection of *gurken* RNA in a *squid* mutant leads to the complete conversion of the sponge bodies into *gurken* RNA positive transport particles. In wild-type oocytes, the same injection leads to complete anchoring of *gurken* RNA in sponge bodies at the DA corner. Furthermore, these transport particles in the *squid* mutant are localized along the anterior but they are not anchored. Rather, they are continuously transported, suggesting that Dynein, though present and functional, cannot undergo its functional switch. And last, inactivation of endogenous Squid after full

anchoring leads to the conversion of the sponge bodies into transport particles.

This is the first record of a structural change of RNA containing structures and this identifies a novel role for Squid, which was initially thought to be a factor that controlled the second transport step of *gurken* mRNA from anterior to dorso-anterior (Norvell et al., 1999). In addition to the role in nucleoplasmic shuttling of mRNAs and regulation of translation, an hnRNP protein is now also involved in the anchoring of the RNA it binds. Whether this is also the case for other RNA binding proteins remains to be elucidated.

Dynein heavy chain (Dhc) is essential for the structural integrity of the sponge bodies (chapter 5)

Dhc is a component of the sponge bodies at the DA corner where it accumulates and colocalizes with *gurken* mRNA. Furthermore, the injection of *gurken* RNA drives the enrichment of Dhc at the DA corner and the formation of more sponge bodies at this location, suggesting that Dhc could contribute to the formation of the sponge bodies.

This is shown by inactivating Dhc using injections of inhibitory antibodies. Under these conditions, the sponge bodies completely disappear, suggesting that Dhc is required for their structural integrity. This is a novel role for Dhc because not only it switches from a motor to an anchor; it is also required for the building of the anchoring structure. Dhc is a large molecule with multiple domains and many different interacting proteins that influence its functionality. Through this, and the Squid-induced switch, it is possible that these interactions promote the formation of a large immobile network.

Dhc transports and anchors its own RNA in the sponge bodies throughout the oocyte where it acts as a structural component (chapter 5)

The role of Dynein is therefore not limited to the sponge bodies at the DA corner of the oocyte. Dhc is concentrated in all the sponge bodies throughout the oocyte and its inactivation leads to the disappearance of all these sponge bodies, revealing a much broader role.

Dhc arrives in sponge bodies by transporting transcripts, *gurken* mRNA to the DA corner and its own (*dhc* mRNA) to the sponge bodies throughout the oocyte. This has been recapitulated using RNA injection assays and inactivation of Dynein by antibodies. Once in the sponge bodies, Dhc remains localized there and acts as a structural component.

Because its own RNA is anchored in the structure that Dhc builds, it is tempting to suggest that it can be translated directly there. There could therefore be two pools of Dhc, one synthesized in the cytoplasm involved in the transport and the anchoring of RNAs, and one that would be synthesized directly in the sponge bodies involved in their structural integrity.

However, we find that translation must be repressed in the sponge bodies, since we found these to contain no ribosomes, whereas Orb and Bruno are enriched in there. This renders the sponge bodies translation-silent and probably involved in translational repression. It is therefore likely that there is only one Dhc pool with multiple functions, which comes from RNA transport processes rather than local translation in the sponge bodies.

Sponge bodies are the *Drosophila* P-bodies (chapter 5)

Sponge bodies might serve as mRNA storage compartments, and thereby regulate mRNA translation. The storage function is supported by the fact that puromycin treatment, that destabilizes transcript-ribosome complexes, does not influence sponge body morphology or the presence of *gurken* mRNA in the sponge bodies. Second, *bicoid* mRNA localizes in sponge bodies at the anterior side and is not translated until after fertilization (many hours later). Third, as we have seen above, the sponge bodies do not contain ribosomes but contain the translational repressor Bruno, the RNA helicase Me31B (Nakamura et al., 2001) and the translation regulator Orb. These facts point at a role in RNA storage and translational regulation and have significant implications on the view on anchoring: anchoring is not just a stable end-point for mRNAs, but also a way of local control on translation.

Local control over translation is also exhibited by P-bodies. These cytoplasmic structures that have been described in yeast and mammalian cells, also contain mRNAs, but not ribosomes, and actually require RNA for their assembly (Teixeira et al., 2005). Our observation that the accumulation of injected *gurken* RNA leads to the formation of more sponge bodies at the DA corner, indicates that P-bodies and sponge bodies share similarities.

These similarities are widespread; P-bodies are not only known to be able to function as RNA storage compartments, but sponge bodies and P-bodies also contain similar components. First of all, the human homologue of the sponge body component Me31B, p54/rck, is a well-described component of P-bodies (Cougot et al., 2004). Me31B is biochemically shown to be part of an RNAse sensitive ribonucleoprotein complex that further consists of at least the proteins Cup, Yps and Tra1 (Wilhelm et al., 2005), proteins that show homology with described P-body components (Weston and Sommerville, 2006). Cup resembles eIF4E-transporter (Wilhelm et al., 2003) that mediates the targeting of RNAs to the P-bodies (Andrei et al., 2005). Cup physically interacts with Bruno to regulate *oskar* mRNA translation and Bruno mediates the oligomerization of mRNPs in large "silencing" particles (Chekulaeva et al., 2006). Silencing is a known feature of P-bodies (Anderson and Kedersha, 2006) and very interestingly, we have localized Bruno in sponge bodies. Me31B, Cup, Yps and Tra1 proteins furthermore colocalize and coimmunoprecipitate with the sponge body component Exu (Wilhelm et al., 2000) and the *Drosophila* decapping enzyme dDcp1 (Lin et al., 2006). Dcp1 is a core enzyme for the function of P-bodies, mRNA decapping, which is not only involved in translation repression, but also RNA degradation (Sheth and Parker, 2003; Anderson and Kedersha, 2006).

Whether RNA degradation occurs in the sponge bodies is yet to be tested, by for instance immuno-labeling for the 5'-3' exonuclease Xrn1, Dcp2 or the proteins that enhance the decapping process, such as the Edc proteins or Lsm proteins. With the findings described above and the data from these tests, the similarity of sponge bodies and P-bodies will be definite.

However, these oocyte P-bodies (sponge bodies) might be a specialized type of P-bodies, focused on RNA storage and translation regulation. Our data indicate that the mRNAs present in the sponge bodies are translationally regulated, particularly *gurken* mRNA, as Squid and Bruno are negative regulators of its translation (Norvell et al., 1999; Steinhauer and Kalderon,

2006). However, while *gurken* mRNA is anchored in the oocyte P-bodies at stage 9 of oogenesis, Gurken protein is translated and transported in the exocytic pathway.

This indicates that the translation of the anchored and stored *gurken* mRNA can be activated. In yeast P-bodies, mRNAs re-entering translation need to move out of the P-bodies into the cytoplasm to sustain translation initiation (Brengues et al., 2005). Analogous to the P-bodies, the *gurken* mRNA is hypothesized to leave the sponge bodies to sustain translation on the ribosome rich ER outside the sponge bodies. The same mechanism could apply to *dhc* mRNA except that its synthesis takes place in the cytoplasm. What regulates this movement of RNA molecules out to the cytoplasm and whether this occurs in particles is unknown.

Nevertheless, the similarities in function, behaviour and composition between the sponge bodies and P-bodies strongly suggests them to be related structures, at least in terms of RNA storage, and suggests that mRNA regulating mechanisms are widespread and used extensively in different cells, tissues and organisms.

The anchoring model

Summarizing our findings, we can draw a model for *gurken* mRNA anchoring, which requires Dynein and Squid. The Dynein-mediated arrival of *gurken* mRNA positive transport particles at the DA corner drives the formation of the sponge bodies to anchor the mRNA at this location. This anchoring is possible through two events:

I. a functional switch of Dhc from an active motor into a static anchor, imposed by Squid, which renders the cofactors Egl and BicD no longer essential;
II. a structural change of Dhc that is accompanied by Dynein becoming a structural component of the sponge bodies.

This structural change can be envisaged by a change in conformation of the Dynein complex, which allows the oligomerization of RNPs into the sponge bodies, possibly by other components associated with Dynein.

This same oligomerization and coalescence into sponge bodies occurs similarly elsewhere in the oocyte, for instance by the anchoring of *dhc* mRNA and most likely many other mRNAs. This could be a general mechanism of anchoring mRNAs that require Dynein for their localization. In fact, Dynein mediated transport could be considered coupled to Dynein mediated anchoring since it is a structural component of the anchoring structures and it is exclusively delivered to sponge bodies by transport of mRNAs.

While present and anchored in the sponge bodies, the mRNAs are translationally repressed, *gurken* most likely by Squid, Bruno and Orb. To allow their translation initiation, the mRNAs move out to the cytoplasm, either as single molecules or as particles, and engage in translation. *gurken* mRNA in that case is targeted to the ER and thereby leads to Gurken synthesis followed by sorting and transport through the tER-Golgi units. *dhc* mRNA is translated presumably in the cytoplasm into the Dhc protein, which assembles into the Dynein motor complex with its associated factors to engage in transport processes, in particular this of *dhc* and *gurken* mRNA.

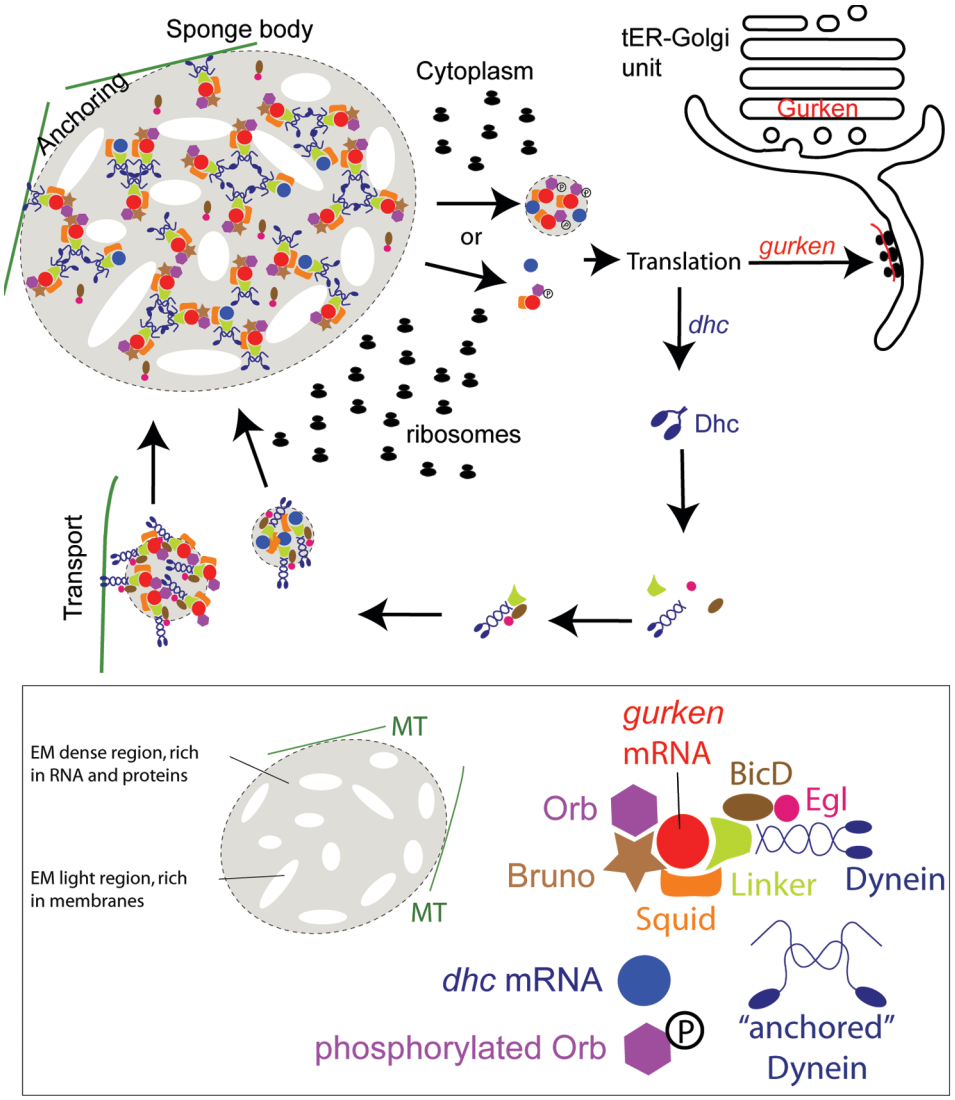

mRNA anchoring model.
Some mRNAs are transported in transport particles along microtubules to their destination. While being transported, these mRNAs, such as *gurken* mRNA, are translationally silent, possibly regulated by Squid and Orb. The transport process itself that may target many mRNAs, including *dhc* mRNA, is mediated by Dynein and its associated cofactors BicD and Egl that forms a complex which is connected via an unknown linker to the Squid bound mRNA. At the destination, the transport particle undergoes a change and becomes an anchoring structure where the mRNAs can be stored. This change is regulated by Squid, which facilitates a functional and structural change of Dynein. Dynein turns from a motor to an anchor that contributes to the structural integrity of the sponge bodies. This is possibly due to a conformational change of Dynein into an "anchored" Dynein state, which may crosslink with itself or other sponge body components to contribute to the sponge body structure. Once in the sponge bodies, the mRNA remains associated with Dynein, but the cofactors BicD and Egl dissociate from the complex through the conformational change. In the sponge bodies, the mRNAs are translationally regulated, *gurken* mRNA by at least Bruno and Orb. But when translation is required, the mRNA will move out to the cytoplasm where the ribosomes can initiate the translation. Whether this is by the release of single RNA molecules or occurs in particles is unknown. The translation of *gurken* mRNA may be preceded by the phosphorylation of Orb, which allows the formation of a translation initiation complex. The first resulting amino acids of the Gurken protein target it to the ER, from where it is sorted efficiently after complete synthesis into the tER-Golgi units that will direct it to the plasma membrane. The translation of *dhc* mRNA in the cytoplasm results into the Dhc protein, which may then assemble into the Dynein motor complex and engage in new transport processes or contribute to the sponge body structure.

Injected RNAs are a good model for endogenous RNAs but not in every single aspect

Injected *gurken* RNA has been a precious tool to dissect molecularly many aspects of its transport and anchoring. In many respects, it has mimicked the endogenous mRNA. The injected RNAs use similar transport particles and anchoring structures localized at the same locations within the oocyte and Dynein and Squid are required for the anchoring of both.

However, some discrepancies exist. First, microtubule depolymerization does not lead to a complete loss of endogenous *gurken* mRNA from the DA corner. Second, injection of *gurken* RNA in *squid* mutant oocytes leads to the complete conversion of sponge bodies into transport particles at the anterior side, whereas the endogenous *gurken* mRNA was anchored along the anterior side in sponge bodies rather than in transport particles.

This indicates that the injection of exogenous RNA molecules might disturb the transport particle-sponge body balance in the cell. This might also be due to additional factors *gurken* mRNA could have picked up in the nurse cells during its synthesis in their nucleus, which might reinforce aspects of its endogenous anchoring. These factors would not be bound to the injected RNA. *oskar* RNA, for instance, needs to bind Magoh and Y14 in the nurse cells nucleus to get properly localized at the posterior pole (St Johnston, 2005). *gurken* RNA that has been injected in the nurse cells is finally fully localized in the oocyte (Clark and Davis, submitted). It would be interesting to look at this in *squid* mutants.

Although these slight differences might lead to inconsistencies, the possibility of using injected RNA creates immense possibilities to study the localization and anchoring processes in time and to mimic situations that are hard to catch in the gradually developing oocyte. In this sense, the use of inducible MS2-GFP would be another great technology to develop at the EM level to study the transcription, nuclear translocation, transport and other intracellular fates of mRNAs.

Conclusion

Besides transport and sorting through the exocytic pathway, asymmetric distribution of transmembrane proteins can be achieved by mRNA localization processes. On its way to its destination, these mRNAs are highly regulated by intrinsic properties and the proteins that recognize these properties. The assembly of RNA and protein complexes results in different kinds of RNA granules with different functions that determine the fate of the mRNAs. By electron microscopy and *in vivo* injection experiments we have been able to visualize the different RNA granules involved in *gurken* mRNA localization. The next challenge is to understand what determines their function and how this can regulate mRNA localization, storage, translation initiation and at the end of the life of an mRNA, degradation.

References

Anderson,P. and Kedersha,N. (2006). RNA granules. J. Cell Biol. 172, 803-808.

Andrei,M.A., Ingelfinger,D., Heintzmann,R., Achsel,T., Rivera-Pomar,R., and Luhrmann,R. (2005). A role for eIF4E and eIF4E-transporter in targeting mRNPs to mammalian processing bodies. RNA. 11, 717-727.

Bokel,C., Dass,S., Wilsch-Brauninger,M., and Roth,S. (2006). Drosophila Cornichon acts as cargo receptor for ER export of the TGFalpha-like growth factor Gurken. Development 133, 459-470.

Bonnal,S., Pileur,F., Orsini,C., Parker,F., Pujol,F., Prats,A.C., and Vagner,S. (2005). Heterogeneous nuclear ribonucleoprotein A1 is a novel internal ribosome entry site trans-acting factor that modulates alternative initiation of translation of the fibroblast growth factor 2 mRNA. J. Biol. Chem. 280, 4144-4153.

Brengues,M., Teixeira,D., and Parker,R. (2005). Movement of eukaryotic mRNAs between polysomes and cytoplasmic processing bodies. Science 310, 486-489.

Chekulaeva,M., Hentze,M.W., and Ephrussi,A. (2006). Bruno acts as a dual repressor of oskar translation, promoting mRNA oligomerization and formation of silencing particles. Cell 124, 521-533.

Clark, A. and Davis, I. A Dynein dependent shortcut delivers axis determination transcripts rapidly into the Drosophila oocyte. Submitted.

Cougot,N., Babajko,S., and Seraphin,B. (2004). Cytoplasmic foci are sites of mRNA decay in human cells. J. Cell Biol. 165, 31-40.

Delanoue,R. and Davis,I. (2005). Dynein anchors its mRNA cargo after apical transport in the Drosophila blastoderm embryo. Cell 122, 97-106.

Grigston,J.C., VanDongen,H.M., McNamara,J.O., III, and VanDongen,A.M. (2005). Translation of an integral membrane protein in distal dendrites of hippocampal neurons. Eur. J. Neurosci. 21, 1457-1468.

Horton,A.C. and Ehlers,M.D. (2003). Dual modes of endoplasmic reticulum-to-Golgi transport in dendrites revealed by live-cell imaging. J. Neurosci. 23, 6188-6199.

Kanai,Y., Dohmae,N., and Hirokawa,N. (2004). Kinesin transports RNA: isolation and characterization of an RNA-transporting granule. Neuron 43, 513-525.

Krichevsky,A.M. and Kosik,K.S. (2001). Neuronal RNA granules: a link between RNA localization and stimulation-dependent translation. Neuron 32, 683-696.

Lin,M.D., Fan,S.J., Hsu,W.S., and Chou,T.B. (2006). Drosophila decapping protein 1, dDcp1, is a component of the oskar mRNP complex and directs its posterior localization in the oocyte. Dev. Cell 10, 601-613.

Nakamura,A., Amikura,R., Hanyu,K., and Kobayashi,S. (2001). Me31B silences translation of oocyte-localizing RNAs through the formation of cytoplasmic RNP complex during Drosophila oogenesis. Development 128, 3233-3242.

Norvell,A., Kelley,R.L., Wehr,K., and Schupbach,T. (1999). Specific isoforms of squid, a Drosophila hnRNP, perform distinct roles in Gurken localization during oogenesis. Genes Dev. 13, 864-876.

Powers,J. and Barlowe,C. (2002). Erv14p directs a transmembrane secretory protein into COPII-coated transport vesicles. Mol. Biol. Cell 13, 880-891.

Queenan,A.M., Barcelo,G., Van Buskirk,C., and Schupbach,T. (1999). The transmembrane region of Gurken is not required for biological activity, but is necessary for transport to the oocyte membrane in Drosophila. Mech. Dev. 89, 35-42.

Rodriguez-Boulan,E. and Musch,A. (2005). Protein sorting in the Golgi complex: shifting paradigms. Biochim. Biophys. Acta 1744, 455-464.

Sheth,U. and Parker,R. (2003). Decapping and decay of messenger RNA occur in cytoplasmic processing bodies. Science 300, 805-808.

St Johnston,D. (2005). Moving messages: the intracellular localization of mRNAs. Nat. Rev. Mol. Cell Biol. 6, 363-375.

Steinhauer,J. and Kalderon,D. (2006). Microtubule polarity and axis formation in the Drosophila oocyte. Dev. Dyn. 235, 1455-1468.

Teixeira,D., Sheth,U., Valencia-Sanchez,M.A., Brengues,M., and Parker,R. (2005). Processing bodies require RNA for assembly and contain nontranslating mRNAs. RNA. 11, 371-382.

Weston,A. and Sommerville,J. (2006). Xp54 and related (DDX6-like) RNA helicases: roles in messenger RNP assembly, translation regulation and RNA degradation. Nucleic Acids Res. 34, 3082-3094.

Wilhelm,J.E., Buszczak,M., and Sayles,S. (2005). Efficient protein trafficking requires trailer hitch, a component of a ribonucleoprotein complex localized to the ER in Drosophila. Dev. Cell 9, 675-685.

Wilhelm,J.E., Hilton,M., Amos,Q., and Henzel,W.J. (2003). Cup is an eIF4E binding protein required for both the translational repression of oskar and the recruitment of Barentsz. J. Cell Biol. 163, 1197-1204.

Wilhelm,J.E., Mansfield,J., Hom-Booher,N., Wang,S., Turck,C.W., Hazelrigg,T., and Vale,R.D. (2000). Isolation of a ribonucleoprotein complex involved in mRNA localization in Drosophila oocytes. J. Cell Biol. 148, 427-440.

Wilsch-Brauninger,M., Schwarz,H., and Nusslein-Volhard,C. (1997). A sponge-like structure involved in the association and transport of maternal products during Drosophila oogenesis. J. Cell Biol. 139, 817-829.

Nederlandse Samenvatting
en
Dankwoord

Nederlandse samenvatting

De aanleg van de lichaamsassen in de fruitvlieg *Drosophila melanogaster* wordt gedreven door de asymmetrische expressie van een eiwit Gurken. Dit eiwit is een transmembraan eiwit dat uitgescheiden wordt door de oocyt, de zich ontwikkelende eicel. Deze ontwikkeling vindt plaats in een ei-kamer, die opgebouwd is uit de oocyt en 15 voedende cellen, de nurse cellen, en deze 16 cellen worden omgeven door een enkele laag epitheelcellen, de follikel cellen. Doordat Gurken in de twee keer dat het uitgescheiden wordt maar door een paar follikel cellen 'gezien' wordt, is het mogelijk vroeg in de ontwikkeling zowel de anterior-posterior (voor- en achterzijde) as als de dorsaal-ventraal (rug- en buik zijde) as aan te leggen.

De beperkte expressie van het Gurken eiwit wordt altijd vooraf gegaan door de asymmetrische lokalisatie van het *gurken* mRNA. Polariteit van cellen en weefsels is meestal het resultaat van asymmetrische lokalisatie van eiwitten en andere intracellulaire factoren. Een vaak gebruikt principe om asymmetrie te creëren in de verdeling van cytoplasmatische eiwitten, is de asymmetrische lokalisatie van hun corresponderend mRNA. Door lokaal het eiwit the synthetiseren verzekert de cel zich van een lokale aanwezigheid van dat eiwit. Een dergelijk principe lijkt ook aan de grondslag te liggen van de asymmetrische Gurken synthese.

Echter, Gurken is een transmembraan eiwit en transmembrane eiwitten kunnen alleen via een systeem van membranen en blaasjes gesorteerd worden naar bepaalde regionen in of buiten een cel. Dit systeem, het uitscheidingssysteem, bestaat uit het endoplasmatisch reticulum (ER), waar transmembrane en lumenale eiwitten het systeem door synthese binnenkomen, uit plaatsen waar deze eiwitten het ER kunnen verlaten (ER exit sites) en het Golgi apparaat. In dit Golgi apparaat, dat bestaat uit een opeenstapeling van platte cisternen, worden de transmembrane eiwitten gemodificeerd tot hun uiteindelijke functionele vorm. Aan het eind van het Golgi apparaat, de trans zijde, ligt het trans Golgi netwerk (TGN), dat functioneert als een sorteer station voor eiwitten met verschillende bestemmingen zoals lysosomen, endosomen en het plasma membraan en de extracellulaire matrix. Dit TGN is in staat om transmembrane eiwitten asymmetrisch te sorteren naar beperkte regionen van de cel. Aangezien Gurken een dergelijk eiwit is, is transport door dit systeem vereist.

In dit proefschrift zijn twee aspecten die leiden tot de asymmetrische lokalisatie van Gurken aan bod gekomen. Het eerste aspect is de relatie tussen Gurken eiwit synthese en *gurken* mRNA lokalisatie, ofwel hoe een transmembraan eiwit een asymmetrisch verdeeld kan worden door mRNA lokalisatie, wat leidde tot het bestuderen van de organisatie van het uitscheidingssysteem in de oocyt en het transport van Gurken door dit systeem. Het tweede aspect zijn de mechanismen die gebruikt worden om *gurken* mRNA te lokaliseren.

In **hoofdstuk 2** is de relatie tussen mRNA lokalisatie en Gurken eiwit transport naar de ruimte tussen de oocyt en de aangrenzende follikel cellen aan bod gekomen. Hierin hebben we aangetoond dat de organisatie van het uitscheidingssysteem lijkt op dat van de *Drosophila* S2 cellen, namelijk dat het opgedeeld is in meerdere tER-Golgi units, eenheden van een ER exit site en een Golgi apparaatje. We vonden in een stadium 9 oocyt duizend van die tER-Golgi units geheel verspreid over de oocyt, dus niet slechts in de dorsaal-anterior (DA) hoek waar Gurken tot expressie komt, maar overal. Dit betekende dat de beperkte uitscheiding van Gurken niet bepaald wordt door de organisatie van het uitscheidingssysteem zelf.

We vonden wel dat het transport van Gurken door dit systeem gereguleerd is door een efficiënt sorteer systeem, dat tweeledig is. Allereerst een eigenschap van Gurken zelf: Gurken wordt aanvankelijk geproduceerd als een transmembraan eiwit, dus met een transmembraan domein, maar dit domein is niet aanwezig in het uiteindelijk uitgescheiden peptide. Derhalve, dit domein moet eraf geknipt worden op weg naar het plasma membraan. We testten de functie van dit domein door een Gurken eiwit tot expressie te laten komen die dit domein niet bevat. We vonden dat zonder het transmembrane domein dit Gurken eiwit dan niet in de tER-Golgi units geraakte in de DA hoek, maar dat het zich totaal verspreidde in het ER door de gehele cel. Dit betekent dat het transmembraan domein nodig is om de verspreiding door de oocyt te voorkomen en verder door het secretiesysteem te gaan.

Het tweede aspect dat de beperkte secretie van Gurken mogelijk maakt is de aanwezigheid van een specifieke ER cargo receptor voor Gurken. Dit eiwit, Cornichon, bleek nodig om Gurken efficiënt te verzamelen in de ER exit sites. Zonder dit eiwit kan het Gurken eiwit zich vrij verspreiden in het ER door de gehele oocyt. Deze twee eigenschappen, het transmembrane domein en het binden van de cargo receptor Cornichon, zijn later in directe link gebracht met elkaar: het zojuist geproduceerde Gurken, dus nog met het transmembrane domein, wordt al in het ER gebonden door Cornichon, aan de lumenale kant, maar dicht bij het transmembrane domein. Voordat Gurken dan ook daadwerkelijk de ER exit site in gesorteerd wordt, wordt het transmembrane domein reeds eraf geknipt, waarna het peptide via het Golgi naar het plasma membraan getransporteerd wordt zonder verdere sortering in het TGN.

Maar naast een efficiënt sorteer systeem dat plaats vindt nadat het eiwit gesynthetiseerd is, is nog een sorteer systeem nodig om Gurken secretie te beperken. Dit systeem functioneert voordat het eiwit geproduceerd wordt, het is namelijk de lokalisatie van het *gurken* mRNA. Dit mRNA wordt, zoals al eerder genoemd, gelokaliseerd in de DA hoek, waar het Gurken eiwit tot expressie moet komen. Om aan te tonen dat mRNA lokalisatie ten grondslag ligt aan de correcte expressie van Gurken hebben we mutanten geanalyseerd waarin het *gurken* mRNA op een verkeerde plek ligt. Deze zijn bijvoorbeeld *squid* en *merlin* mutante oocyten, waarin het mRNA respectievelijk aan de voorzijde of aan de achterzijde van de oocyt komt te liggen. We vonden Gurken eiwit in deze mutanten dan ook respectievelijk in de tER-Golgi units aan de voorzijde en aan de achterzijde, plaatsen waar in wildtype oocyten het Gurken eiwit niet gevonden wordt. Dit betekent dat *gurken* mRNA lokalisatie in de oocyt van belang is om de lichaamsassen aan te kunnen leggen.

De vraag die overbleef na hoofdstuk 2, was of het *gurken* mRNA in directe relatie stond met het gebruik van de tER-Golgi units. Met andere woorden, is er een directe co-lokalisatie tussen het mRNA en de tER-Golgi units? Om deze vraag te beantwoorden was het ontwikkelen van een protocol nodig waarin zowel het endogene *gurken* mRNA gevisualiseerd kon worden, evenals het Gurken eiwit. Dit resulteerde in een protocol van directe *in situ* hybridisatie op ultradunne vriescoupes voor immuno-elektronen microscopie (ISH-IEM) en is beschreven in **hoofdstuk 3**. Dit protocol maakt het mogelijk om niet alleen de lokalisatie van verschillende mRNAs te analyseren, of de structuren te identificeren waar het mRNA zich in bevindt, maar ook mRNA en eiwit tegelijkertijd in dezelfde coupe te visualiseren. We gebruikten dit protocol niet alleen om de intracellulaire lokalisatie van *bicoid* en *oskar* mRNA te bestuderen samen met de structuren en eiwitten waarmee deze mRNAs geassocieerd zijn, maar ook voor *gurken* mRNA. Het bleek dat het *gurken* mRNA zich in cytoplasmatische structuren bevindt die niet in direct contact staan met de tER-Golgi units die Gurken eiwit bevatten.

In een eerdere studie is gebleken dat de lokalisatie van *gurken* mRNA in twee stappen plaats vindt. Deze stappen zijn afhankelijk van microtubuli en de moleculaire motor Dynein, die zich specifiek naar het minus eind van de microtubuli beweegt. Als *gurken* RNA geïnjecteerd wordt in een stadium 9 oocyt, verzamelt het mRNA zich eerst aan de voorkant voordat het verder gelokaliseerd wordt naar de DA hoek. Deze lokalisatie bleek plaats te vinden in partikels. In **hoofdstuk 4** hebben we deze partikels geanalyseerd met behulp van elektronen microscopie. Deze elektronendichte partikels waren ongeveer 300nm in diameter, lagen vaak in de buurt van microtubuli en bleken tot in de duizend mRNA moleculen te bevatten. Deze partikels hadden geen membraan er omheen en waren niet consistent geassocieerd met het ER, wat betekent dat dit gespecialiseerde cytoplasmatische structuren zijn die het transport van *gurken* mRNA voor hun rekening nemen, en daarom hebben we ze transport partikels genoemd.

Verdere analyse van de transport partikels toonde aan dat deze de Dynein motor bevatten, we vonden namelijk de grote subunit Dhc en de transport co-factors Egl en BicD samen met het *gurken* RNA in de transport partikels. Daarnaast vonden we er ook het *gurken* mRNA bindende eiwit Squid in, en zoals hierboven aangegeven, is dit eiwit van belang om *gurken* mRNA correct naar de DA hoek te transporteren.

Eenmaal in de DA hoek, is het *gurken* mRNA niet meer te vinden in transport partikels, maar in grote (tot 2,5µm) cytoplasmatische structuren die ook verrijkt zijn met de componenten van het Dynein motor complex en met Squid. Deze cytoplasmatische gebieden zijn eerder beschreven als "sponge bodies", structuren met een sponsachtig uiterlijk door het elektrondichte materiaal afgewisseld met lichte ER-achtige buisjes. We vonden niet alleen het endogene *gurken* mRNA in die sponge bodies, maar ook het geïnjecteerde en volledig gelokaliseerde *gurken* RNA. Dit betekent dat de transport partikels omvormen als ze hun bestemming bereikt hebben, in het geval van *gurken* mRNA in de DA hoek, en deze omvorming draagt bij tot de formatie van of coagulatie tot sponge bodies.

We vonden dat deze formatie van sponge bodies niet gebeurde in oocyten die het Squid eiwit missen. Als *gurken* RNA geïnjecteerd werd in deze oocyten, verzamelde het zich aan de voorzijde, maar niet in sponge bodies, maar in transport partikels. Dit wees erop dat Squid een rol kon spelen in de omvorming van de transport partikels naar de sponge bodies. Deze rol werd duidelijk door Squid eiwit te blokkeren nadat het *gurken* mRNA volledig verankerd was in de DA hoek in de sponge bodies van wildtype oocyten. Dit leverde een exacte kopie van het fenotype van de geïnjecteerde Squid mutant. We concludeerden daarom dat Squid de staat van transport en verankering reguleert.

Zoals hierboven vermeld, waren ook de componenten van de Dynein motor, Dhc, BicD en Egl aanwezig in de sponge bodies. We vonden dat deze componenten rijker aanwezig waren in de DA hoek van *gurken* geïnjecteerde oocyten, wat erop wijst dat het transport van het mRNA en de accumulatie van transport partikels en de formatie van sponge bodies gepaard gaat met de verankering van het *gurken* mRNA. We testten de functie van deze componenten voor hun rol in de verankering. Uit eerder werk is gebleken dat de motor componenten vereist zijn tijdens het transport van het mRNA. In **hoofdstuk 4** toonden we aan dat Egl en BicD niet meer vereist zijn als het mRNA verankerd is. Dhc daarentegen blijft vereist voor de verankering, evenals de microtubuli. Dit wees op een vergelijkbaar verankeringmechanisme in de oocyt als in het embryo van *Drosophila*: Dynein verandert van een actieve motor in een stabiel anker aan het eind van de microtubuli door het verlies van zijn motor functie. We hebben in de oocyt aangetoond dat dit gepaard gaat met de omvorming van transport partikels naar de verankeringstructuren,

de sponge bodies.

De rol voor Dhc in de sponge bodies en hun rol in verankering van mRNAs werd verder bestudeerd in **hoofdstuk 5**. Hierin hebben we aangetoond dat de sponge bodies overeenkomsten vertonen met processing (P-) bodies die te vinden zijn in gist en zoogdiercellen. P-bodies staan bekend om hun functie in de regulatie van mRNAs; niet alleen van hun translatie, maar ook van hun aanwezigheid: in P-bodies kunnen mRNAs specifiek afgebroken worden. Voor de translatie regulatie functie worden de P-bodies gebruikt als opslagplaatsen voor mRNAs. Een dergelijke rol voor mRNA opslag lijkt ook toepasbaar voor de sponge bodies.

In de sponge bodies vonden we namelijk, naast Squid die een beschermende en translatie regulerende rol kan spelen, ook de translatie onderdrukker Bruno en de translatie regulator Orb. Dit wijst erop dat mRNAs opgeslagen kunnen worden in de sponge bodies zonder dat ze actief getransleerd worden, net als mRNAs inactief opgeslagen worden in P-bodies. De vergelijking met P-bodies gaat verder: in de oocyt zijn een aantal eiwitten beschreven die ook in P-bodies gevonden worden, deze eiwitten maken deel uit van een RNA-eiwit complex dat een vergelijkbare intracellulaire verdeling heeft als de sponge bodies. Dit wijst erop dat de sponge bodies de P-bodies zijn in de *Drosophila* oocyt.

De aanwezigheid van Dhc in deze P-bodies van de oocyt bleek bij nader onderzoek niet alleen het resultaat te zijn van RNA transport processen, dus niet alleen van *gurken* mRNA transport naar P-bodies in de DA hoek, of transport van *dhc* mRNA zelf naar P-bodies door de gehele oocyt, maar Dhc bleek ook een andere rol te spelen in deze P-bodies. Inactivatie van Dhc met behulp van inhiberende antilichaam injecties zorgde er namelijk voor dat alle P-bodies uit elkaar vielen, waardoor hun inhoud verspreid werd door de oocyt, met als gevolg dat de verankering van mRNAs niet behouden kon worden. Deze gegevens hebben inzicht gegeven in een nieuwe link tussen mRNA transport, verankering en translatie regulatie.

Dankwoord

Wat zijn vier jaar toch snel voorbij. Maar wat kan een mens allemaal in zo'n korte tijd bewerkstelligen! Zo pasten al mijn bezittingen in hun geheel achter in een niet al te grote auto toen ik vanuit Oxford terug naar Nederland keerde, nu woon ik, drie adressen later, samen met mijn lieve vriendin Manon in een fantastisch eigen huis. Alles wat er in die vier jaar gebeurd is, zou ik bij lange na niet zo helder voor de geest kunnen halen als mijn fotobestandenlijst niet met zesduizend toegenomen zou zijn. En daar zitten niet eens de duizenden plaatjes bij van de ultradunne plakjes fruitvlieg die mij zoveel hebben verteld, dat ik dit boekje heb kunnen schrijven.

Dat ik deze herinneringen en deze kennis heb mogen opdoen, daarvoor zou ik graag de volgende mensen in het bijzonder willen bedanken:

Allereerst Dr. Catherine Rabouille, ik wil je graag heel erg bedanken voor alles wat je me geleerd hebt, je hebt altijd ingezien welke persoonlijke ontwikkeling ik nodig had en hebt me altijd gestimuleerd om mezelf te overtreffen. Ik vind het een eer om met jou samen te hebben gewerkt aan dit project, je begeleiding was altijd doorspekt met kritische vragen, interessante ideeën en welgemeende interesse voor alle uithoeken van het onderzoek. Ik denk dat je kwaliteiten zich uitermate uiten in het feit dat je groep gegroeid is van drie toen ik begon naar een huidig aantal van acht onderzoekers!

Daarnaast Prof. Dr. Judith Klumperman, als hoofd van de "Morfologie" kant van Celbiologie heb je mijn vorderingen door de jaren heen in de gaten gehouden en heb je richting gegeven waar die even niet helemaal duidelijk was in dit project. Bedankt voor alle mogelijkheden tot kennisontwikkeling in dit lab en ik wens je een goed welverdiend sabbatical toe.

Also Prof. Ilan Davis, you always have been a great intellectual support for this project, I think that our collaboration has been wonderful. Your ideas and the merger of injection techniques and electron microscopy have opened doors to insights into the biology of the fruit fly that no-one could have imagined, but we managed to image it!

This collaboration could not have taken off so smoothly without the expertise of Dr. Rénald Delanoue. I appreciate all the work you have done for this project and the quality of the specimens which you managed to maintain constant during your devotion to this project. I wish you and Véro all the best with Mellie in France.

En dan ook zijn opvolger, Jan Soetaert. Ik wil je heel erg bedanken voor al je tijd die je in dit project hebt gestoken, ook al zou je je graag in het I-factor project willen storten. Ik wil je ook bedanken voor de gezellige tijd samen, je gastvrijheid en de zo gekoesterde Duvelkes. Also Carine Meignin, thank you very much for your hospitality and ideas.

De Rabouille groep verdient ook een speciaal bedankje. Ten eerste Dr. Vangelis Kondylis, die ik altijd een briljant wetenschapper heb gevonden, met een fanatieke voorliefde voor het Eurovisie Songfestival. Ik wens je een fantastische carrière toe. Hans Schotman, jij ook bedankt voor de

discussies over vliegenwerk, in situ's en het me op de hoogte houden van alle gebeurtenissen op en rondom het lab. Natuurlijk ook bedankt dat je mijn paranimf wilde zijn. Dr. Adriaan Oprins, ook al ben je ondertussen alweer een hele poos niet meer werkzaam in de groep van je vrouw Catherine, jouw hulp wordt ook zeer gewaardeerd. Dr. Gert de Voer, ik heb jou alvast deze titel gegeven omdat ik weet hoeveel tijd en moeite jij steekt in alles wat je doet en ik wens je nog veel succes toe met je werk en ook met jouw promotie. Despina Xanthakis, heel erg bedankt voor je zorg op het lab, niet alleen voor de vliegen, maar ook voor een goede sfeer. Dr. Viorica Ivan and Leena Karhinen, although we haven't worked together for long in the Rabouille group, many thanks for your support.

Mijn EM kennis zou niet van de grond zijn gekomen zonder jouw vakkundigheid, Elly van Donselaar, heel erg bedankt voor je persoonlijke begeleiding in de eerste maanden. Janice Griffith, Viola Oorschot, Suzanne van Dijk en Corlinda ten Brink, ik waardeer jullie vak- en technische kennis heel erg en ik weet zeker dat jullie een goede steun zijn geweest voor mijn werk. Ook zonder jullie, Marc van Peski en René Scriwanek, zou dit proefschrift niet tot stand kunnen zijn gekomen. George Posthuma, bedankt voor de kritische vragen en technische ondersteuning.

Ook alle andere mensen van morfologie, met Dagmar Zeuschner voorop, maar ook Harry Heijnen, Ann de Mazière, Hezder van Nispen, Vincent Schoonderwoert, Muriel Mari, Fulvio Reggiori, Carolien van Rijnsoever, Arjan de Jong en Eline van Meel, bedankt voor de discussies tijdens werkbesprekingen en lunch.

Ik wil ook graag Prof. Dr. Hans Geuze en Dr. Jan Willem Slot heel erg bedanken voor jullie support en het is een eer van jullie de Memo-prijs in handen te hebben mogen nemen.

Aan "de andere kant" van Celbiologie, Biochemie, zou ik allereerst Prof. Dr. Ger Strous en Dr. Peter van der Sluijs willen bedanken voor de discussies bij de werkbesprekingen en de gastvrijheid bij jullie thuis. En ook Dr. Madelon Maurice, bedankt voor je interesse en heel veel succes met de wingdiscs en je onderzoeksgroep. Ik mag natuurlijk ook niet Peter van Kerkhof en Carin Zwartjes vergeten te bedanken en alle studenten die kwamen en gingen en soms ook terug keerden bij Celbiologie. Maar in het bijzonder zou ik de AiO's van Biochemie willen bedanken, zonder jullie, Maaike Neeft, Marnix Wieffer, Claudia Fila, Monique van den Eijnden, Joyce Putters, Nicoline Schaap, Thijs van Vlijmen en Ioana Popa en verder natuurlijk ook Hezder en Hans S., zouden borrels, kerstdiners en lange avonden in de kroeg nooit zo gezellig zijn geweest.

Langer dan de vier jaar in Utrecht, eigenlijk sinds ik me kan heugen, word ik al gesteund door mijn familie, mijn ouders Jo en Marianne en mijn broer Robert. Ik vind jullie geweldige mensen en geniet er altijd van als we weer eens heerlijk Limburgs kunnen praten. Ik wil jullie heel erg bedanken voor jullie support, interesse, begrip en gezelligheid door de jaren heen, ik hoop nog vele jaren met jullie te delen. Ik wil natuurlijk ook de rest van mijn familie bedanken, niet alleen voor de gezelligheid, maar ook al die stukken vlaai die ik door de jaren heen aangeboden heb gekregen op verjaardagen en andere feesten. Het is altijd weer genieten.

Sinds meer dan drie jaar ben ik ook blij met de gastvrijheid van Harry en Carla Oude Nijhuis en de broer van Manon, Niels, ik wil jullie bedanken voor de gezelligheid en de ontspannende vakantie in Zwitserland op het moment dat ik even tot over mijn oren in de papierwinkel zat die een proefschrift schrijven oplevert.

Natuurlijk wil ik ook vrienden, vriendinnen en partners bedanken voor hun gezelligheid. Joyce van der Vegt, heel veel succes met je opleiding tot neuroloog, Dick Makkink, Giel Jansen en Marja, Christiaan Nijboer en Marieke, Arjan Kappert en Anke, en Monique Kappert, ik weet zeker dat het jullie goed zal gaan in de toekomst en ik hoop dat we nog vele gezellige tijden zullen kennen.

Tot slot wil ik mijn lieve vriendin Manon bedanken, voor de ondersteuning door de jaren heen, de lieve woorden en het vertrouwen. Je ging me voor met het maken van een proefschrift en wist daardoor exact wat er mij allemaal te wachten stond. Jouw ervaringen hebben mij enorm geholpen. Ik ben trots op je en ik hoop dat we na dit bizarre jaar samen een bijzonder mooie toekomst tegemoet gaan!

Bram

Curriculum Vitae and Publications

Curriculum Vitae

Bram Hubertus Anne Herpers werd geboren op 4 april 1979 te Urmond, Nederland. Na het behalen van zijn VWO diploma aan het College Sittard te Sittard in 1997 studeerde hij Biologie aan Wageningen Universiteit. Tijdens deze studie deed hij in zijn eerste zes maanden stage onderzoek aan wortel en wortelknol ontwikkeling in *Arabidopsis thaliana* (zandraket) en de vlinderbloemigen *Medicago trunculata* en *Lotus japonica* in het laboratorium voor Moleculaire Biologie van Wageningen Universiteit onder begeleiding van Dr. Henk Franssen. Tijdens zijn tweede stage deed hij een jaar onderzoek aan genexpressie in de fruitvlieg *Drosophila melanogaster* onder begeleiding van Dr. Marcel van den Heuvel aan het MRC Functional Genetics Unit (MRC-FGU) te Oxford, Groot-Brittannië. Bram behaalde zijn Masters diploma in Biologie in juni 2002 en werkte tot en met oktober 2002 in het MRC-FGU. In november 2002 begon hij als assistent in opleiding (AiO) aan een door NWO-gesubsidieerd onderzoeksproject bij de afdeling Celbiologie in het Cell Microscopy Center van het Universitair Medisch Centrum Utrecht onder begeleiding van Dr. Catherine Rabouille en Prof. Dr. Judith Klumperman. Dit onderzoek heeft uiteindelijk geresulteerd in dit proefschrift.

Bram Hubertus Anne Herpers was born in Urmond, the Netherlands, on April 4th, 1979. After finishing high school at *College Sittard* in Sittard in 1997, he studied Biology at Wageningen University. During his studies he participated in two research projects. The first six months project was devoted to root and root nodule development in *Arabidopsis thaliana* (thale cress) and the fabaceae *Medicago trunculata* and *Lotus japonica* in the Laboratory of Molecular Biology of Wageningen University under supervision of Dr. Henk Franssen. During his second, one year project he researched gene expression in the fruit fly *Drosophila melanogaster* under supervision of Dr. Marcel van den Heuvel at the MRC Functional Genetics Unit (MRC-FGU) in Oxford, United Kingdom. Bram obtained his Masters in Biology in June 2002 and continued working at the MRC-FGU until October 2002. In November 2002 he started working as a PhD student on a NWO-financed research project at the Department of Cell Biology, in the Cell Microscopy Center in the University Medical Center Utrecht under supervision of Dr. Catherine Rabouille and Prof. Dr. Judith Klumperman. This research is described in this dissertation.

Publications

Vargas,J.D., **Herpers,B**., McKie,A.T., Gledhill,S., McDonnell,J., van den Heuvel,M., Davies,K.E., and Ponting,C.P. (2003). Stromal cell-derived receptor 2 and cytochrome b561 are functional ferric reductases. Biochim. Biophys. Acta *1651*, 116-123.

Herpers,B. and Rabouille,C. (2004). mRNA localization and ER-based protein sorting mechanisms dictate the use of transitional endoplasmic reticulum-golgi units involved in gurken transport in Drosophila oocytes. Mol. Biol. Cell *15*, 5306-5317.

Dawber,R.J., Hebbes,S., **Herpers,B**., Docquier,F., and van den Heuvel,M. (2005). Differential range and activity of various forms of the Hedgehog protein. BMC. Dev. Biol. *5*, 21.

Kondylis, V., **Herpers, B**., Xanthakis, D., Friggi-Grelin, F., and Rabouille, C. The Golgi comprises a paired stack that is separated at G2 by modulation of the actin cytoskeleton through Abi and Scar/WAVE. Manuscript in revision for Dev. Cell.

Delanoue, R., **Herpers, B**., Soetaert, J., Rabouille, C., and Davis, I. Drosophila Squid hnRNP is required for Dynein to form static anchoring complexes with gurken/TGF-alpha mRNA. Manuscript in revision for Cell.